UNIVERSIDAD
DE LA REPUBLICA
URUGUAY

FACULTAD DE
CIENCIAS
UDELAR fcien.edu.uy

PEDECIBA

cap

Critical Phenomena: Non-Perturbative Renormalization Group and Conformal Invariance

Gonzalo Héctor De Polsi Astapenco

Critical Phenomena: Non-Perturbative Renormalization Group and Conformal Invariance

Gonzalo Héctor De Polsi Astapenco

Tesis de Doctorado presentada al Programa de Posgrado de Pedeciba Física, Facultad de Ciencias de la Universidad de la República, como parte de los requisitos necesarios para la obtención del título de Doctor en Pedeciba Física.

Directores:
    Nicolás Wschebor
    Matthieu Tissier

Montevideo – Uruguay

Febrero de 2020

INTEGRANTES DEL TRIBUNAL DE DEFENSA DE TESIS

_____

Yan Levin

_____

Alessandro Codello

_____

Matilde Martínez

_____

Rodolfo Gambini

_____

Matthieu Tissier

Montevideo – Uruguay

Febrero de 2020

iv

A la memoria de mi tio Ariel

Agradecimientos

Para empezar quisiera agradecer a las instituciones PEDECIBA, CSIC, CAP, LIA y la Embajada de Francia en Uruguay que financiaron e hicieron posible la realización de esta tesis. También agradezco a los Institutos de Física de la Facultad de Ciencias y de la Facultad de Ingeniería por atender a las necesidades de locación y tiempo que esta tesis exigió.

Agradezco enormemente a mis tutores Nicolás y Matthieu por toda la experiencia y tiempo que compartieron conmigo. El aprendizaje tuvo lugar tanto en el plano profesional como en el personal. En particular, agradezco cómo me hicieron sentir al trabajar con ellos y haber podido formar parte de ese grupo de trabajo. Los dos tienen una dinámica de trabajo que valoro mucho y resulta un placer verlos trabajar juntos.

Quiero agradecer a mis "Colegas del Café" con los que compartí diariamente almuerzos y tardes con amenos sobremesas. Entre ellos incluyo a Daniel, Raúl y Marcela. También agradezco a todo mi grupo de investigación por generar tan lindo ambiente de trabajo.

No quiero dejar de agradecer a algunos personas que conocí hace ya mucho tiempo en el ámbito académico y que aprecio mucho. A Jimena, siempre dispuesta a ayudar y atenta a lo que uno pueda precisar tanto en lo administrativo como en lo personal. A Nico y Rodri que me sufren y aguantan en la oficina hace ya varios años (¡y vamos por más!).

Sobran motivos por los cuales estoy agradecido con toda mi familia. En particular agradezco a mi círculo más cercano: Carli, Javo, Má y Pá. Siempre presentes y acompañándome en todas mis empresas: ¡Muchísimas gracias!

Por último, quiero agradecer de forma especial a un subgrupo de mi familia. Sofi e Isma: Es un cliché, pero no me alcanzan las palabras para agradecerles lo suficiente. Sofi, por todo el cariño y apoyo incondicional que me diste, así como por todo el sacrificio que hiciste a lo largo de esta travesía, sin el cual esto no hubiese sido posible. Isma, porque me llenás de alegría cada día desde que entraste a mi vida. A los dos, los amo.

ABSTRACT

The critical phenomena exhibit many interesting properties, such as being scale invariant at long distances. As a consequence, the properties depending on the long distances regime of the system behave in power laws. However, given the intrinsic complexity of the these kind of phenomena, their analytical treatment represents a formidable task. The non-perturbative renormalization group (NPRG) method is especially adapted for addressing these kind of phenomena. It is also observed that, on top scale invariance, many systems exhibit in their long distance physics conformal invariance (i.e. invariance under transformations which preserve angles). This thesis explores the properties of the NPRG when treating critical phenomena with an emphasis in conformal invariance. We do it so, mostly, within an approximation scheme specially powerful in this framework, the derivative expansion (DE). Three main contributions can be identified as unpinning from this thesis.

First, we implement the DE approximation scheme within the NPRG framework to an unprecedented order for the $O(N)$ models, which describe the critical behaviour of many systems such as Helium-4 fluid-superfluid transition, isotropic ferromagnets and many more. While doing so, we achieved two objectives. On one hand we computed some physical quantities which are in agreement with the best result of the literature or even yielded the most accurate results of the literature. Additionally, we discuss about the convergence properties of the method, for which high orders of its approximation have been implemented in just one other model.

Second, we study the presence of conformal invariance, within the NPRG framework, in the critical regime of $O(N)$ models. This is done by exploiting an existent sufficient condition for conformal invariance to be realized. This study yields strong indications, in some physically relevant cases ($O(2)$, $O(3)$ and $O(4)$ models) with a more rigorous character, that $O(N)$ models exhibit conformal invariance at their critical regime, for all non-negative values of N.

Third, we exploit the fact that conformal invariance imposes extra constraints on a physical system, on top of the constraints that scale invariance

imposes. We do this by using one such constraint within the derivative expansion of the NPRG for the $O(1)$ model. This allows us to better understand the behaviour of the DE and to discuss a criterion for computing physical quantities in this approximation scheme. This criterion is potentially extensible to other models.

RESUMEN

Los fenómenos críticos tienen muchas propiedades interesantes, como ser invariantes de escala en el régimen de distancias grandes. Esto se traduce en un comportamiento en leyes de potencia de sus propiedades que dependen de dicho régimen. Sin embargo, la complejidad inherente a estos fenómenos presenta grandes desafíos que dificultan su tratamiento analítico. El grupo de renormalización no perturbativo (NPRG) es un método especialmente adecuado para el tratamiento de este tipo de fenómenos. Otro aspecto que se observa en estos fenómenos, además de la invariancia de escala, es que muchos sistemas exhiben, además, invariancia conforme (es decir, invariancia ante transformaciones que conservan los ángulos). En esta tesis se exploran las propiedades del NPRG en el estudio de los fenómenos críticos, con un énfasis en la invariancia conforme. Este estudio es realizado, principalmente, en el marco de un esquema de aproximación, denominado desarrollo en gradientes (DE), que resulta muy potente al ser aplicado en el marco del NPRG. De esta tesis se deprenden tres contribuciones.

En primer lugar, implementamos el DE dentro del NPRG a un orden aún no explorado para los modelos $O(N)$. Estos modelos describen el régimen crítico de mucho sistemas físicos de interés como lo son la transición fluido-superfluido del Helio-4 o la transición paramagnética-ferromagnética de imanes isótropos, entre otros. Al hacerlo logramos dos objetivos. Por un lado, calculamos algunas propiedades físicas que están en acuerdo con los resultados más precisos de la literatura y qué en varios casos son los más precisos. Por otro lado, discutimos las propiedades de convergencia del método DE para el cual hay un único otro modelo en el que se han implementados órdenes altos de la aproximación.

En segundo lugar, estudiamos, en el marco del NPRG, la presencia de invariancia conforme en el régimen crítico de los modelos $O(N)$. Para ello, hacemos uso de una condición suficiente para la realización de invariancia conforme. Los resultados de este estudio dieron fuertes indicios, y con un carácter más riguroso en algunos casos físicamente relevantes ($O(2)$, $O(3)$ y $O(4)$), de

qué todos los modelos $O(N)$, con valores de N no negativos, presentan invariancia conforme en su régimen crítico.

En tercer y último lugar, utilizamos el hecho de que la invariancia conforme impone más restricciones, sobre un sistema físico, de lo que impone la invariancia por dilataciones. Estudiamos una de estas restricciones para el modelo $O(1)$ utilizando el DE. Esto nos permite entender mejor el comportamiento del esquema de aproximación y nos lleva a discutir un nuevo criterio para el cálculo de propiedades físicas dentro de dicho esquema. Asimismo, este nuevo criterio es potencialmente aplicable a muchos otros modelos.

Palabras Claves:

Fenómenos Críticos,   Grupo de Renormalización,   Invariancia Conforme, Mecánica Estadística.

Contents

Introduction

In many cases, the components of a system are weakly interacting and they can be regarded, to a reasonable extent, as independent or at least their interactions can be treated with relatively simplicity and accuracy. A canonical example of such a system is the diluted gas which, in a first approximation, can be regarded as an ideal gas with reasonable accuracy. Moreover, the interactions present in a real gas can be treated as corrections with perturbative methods without much difficulty.

However, the situation is radically different when the interactions between the degrees of freedom are important and each of them effectively interact with a macroscopic part of the system. In these kind of systems, the approach must be different and, as a general rule, their treatment is still an open problem. A typical case of this kind of problem is the one of a second order phase transition, also denominated as critical phenomena. In such case the distance to which a certain part of the system influence another grows to the size of the whole system. This behaviour is typically accompanied with a power law dependence of some of its properties with, for instance, the temperature. This is a typical footprint of scale invariance. A common example of a second order phase transition occurs in the liquid-gas phase transition of a pure substance at its critical point. In Fig.1 we show the phase diagram of pure water (taken from [1]). At the black curves separating different phases, a phase transition takes place. In particular, the red circles point out our everyday experience of boiling or freezing water. These are examples of first order phase transitions and are characterized by a *jump* in the density from one phase to the other. However, as can be appreciated, there is an endpoint in the curve separating the liquid and vapour phase, at a temperature $T_c = 647K$ and a pressure of $P_c = 22,1 \times 10^6 Pa$. This point, called *critical point*, is where the second order phase transition occurs and, in fact, the densities of the two phases are identical there. Because of this, second order phase transitions are also called *continuous phase transition*.
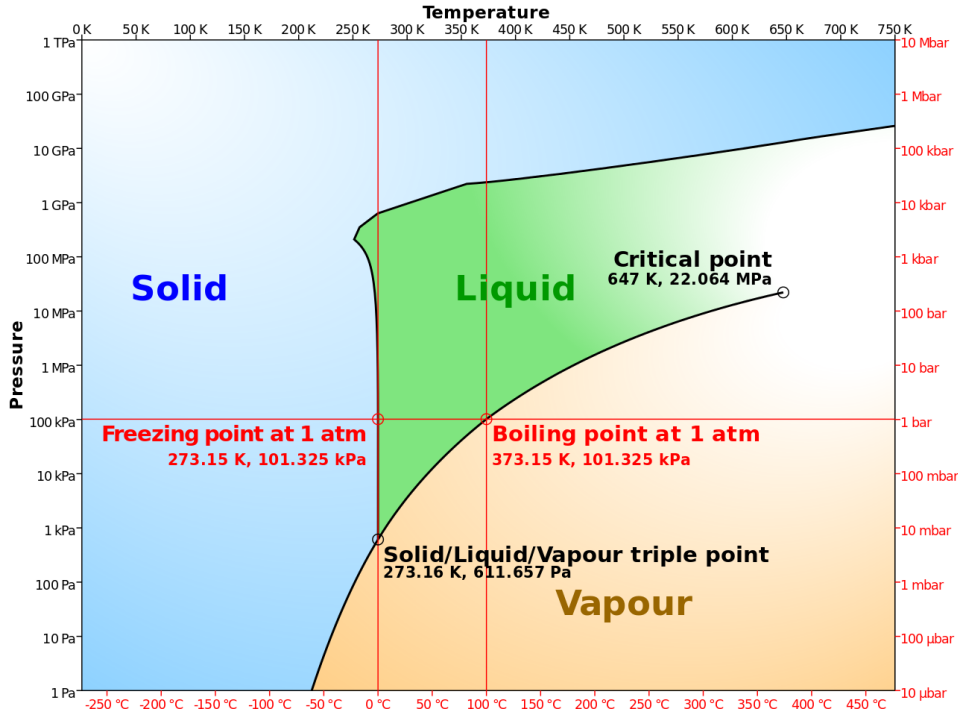
Figure 1: Phase diagram for the pure water, taken from [1].

Due to the complexity of critical phenomena, the problem is hard to address theoretically and raised many questions that demanded an explanation from the viewpoint of the underlying physics. One of such questions was to understand the phenomenon of universality. Universality refers to the fact that systems which seemed, in principle, nothing alike such as an uniaxial magnet and a saturated liquid-gas sample, exhibit at their critical point an identical power law behaviour for some of their properties. For example, for temperatures $T < T_c$, where T_c is the critical temperature, the difference of density of the two phases ρ_l and ρ_g for the liquid and gas, respectively, goes as $\rho_l - \rho_g \propto (T_c - T)^\beta$, with the value of β being exactly the same for many different substances. The universal quantity β, is an example of a *critical exponent*. Systems exhibiting the same critical behaviour are said to belong to the same *universality class*, which is the case for different pure substances at their the liquid-gas phase transition and, also for, uniaxial magnets. In Fig.2, taken from [2], the phase diagram of an uniaxial magnet is shown, where the critical point of the system is at the point $H = 0$ and $T = T_N$ (where the N stands for Néel).

A general approach for treating these kind of systems, called *renormalization group*, was developed in the 70's [3, 4]. This approach consists in a general framework for addressing this problem and, moreover, it provided a natural
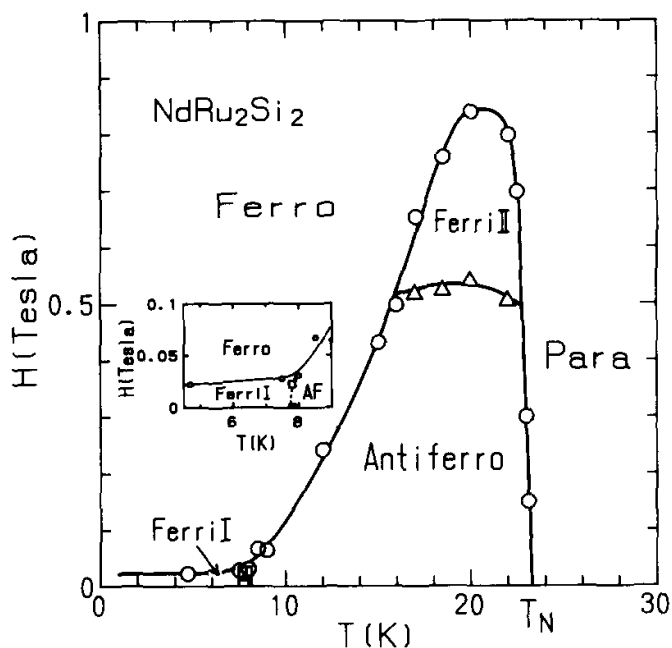
Figure 2: Phase diagram for magnet $NdRu_2Si_2$, taken from [2].

explanation for the phenomenon of universality. The underlying idea of the approach consists in building effective theories, which still describes in the same manner the long distances physics. This is done by successively replacing groups of particles by a single one with the effective properties of the whole group. In the 90's a modern version of the renormalization group was developed under the name of *non-perturbative renormalization group* [5, 6, 7, 8, 9, 10]. One of the biggest advantages of this new method is that it is much better suited for approximations. It consists in adding to the energy a term dependent on a scale that effectively freezes slow modes up to that scale. Then, by varying the scale of the regulator, it interpolates the central object of the framework, called *effective action*, between the Hamiltonian and the Gibbs free energy. The result of this procedure is an exact evolution equation for the effective action that takes the form of a functional differential equation.

Because of the complexity of the exact evolution, in general, one must perform approximations on top of the evolution equation in order to be able to use it for studying the system properties. One of the most used approximation schemes within the non perturbative renormalization group is called the *derivative expansion*. The reason why it is one of the most used approximations within the non perturbative renormalization group, is that, unlike other approximations, it does not rely on small interactions. This make the derivative expansion a powerful technique with a wide range of applicability. This

method consists in taking an ansatz for the effective action with up to a given number of derivatives. Then, the order $\mathcal{O}(\partial^s)$ consists in taking into account s derivatives. Although the derivative expansion can be implemented within other frameworks, it is best suited for the non-perturbative renormalization group, see for example [11], and up to recently it was not clear why it yielded such good results, due to the apparent lack of a small expansion parameter. However, this situation was elucidated in a recent study of its convergence properties in the universality class of the liquid-gas second order phase transition [12], where the approximation scheme was pushed up to order $\mathcal{O}(\partial^6)$. In a nutshell, any approximation scheme introduces a spurious dependence on the regulator which is non-physical and, in order for the derivative expansion to have good convergence properties, a criterion referred as *principle of minimal sensitivity* must be employed [13]. This criterion consists in reducing the dependence of the results on the regulator as much as possible. Although reasonable, this criterion still lacks of a rigorous argument.

Parallel to the development of the renormalization group, another method for treating the critical properties of systems was developed in the 70's. This was known under the name of *conformal bootstrap* and it was based on a conjecture which stated that systems at their criticality not only presented scale invariance but rather the full conformal group (this is, transformations which conserve angles). Of course, both scale and conformal invariance are valid in the regime of large distances compared with a typical microscopic scale. This is, if we implement a scale transformation of the system at criticality, the microscopic details are not invariant. However, quantities that depend only on the long distance physics are, indeed, invariant under the scale transformation. This conjecture stated that the same was true regarding all conformal transformations.

The conformal bootstrap method benefited from the fact that invariance under general conformal transformations is far more restrictive than mere invariance under scale transformations. Indeed, invariance under conformal transformations was particularly powerful in two dimensional systems but, it was not until recently that it was figured out how to take advantage of it to treat the three dimensional case. A breakthrough in this matter took place in 2012, where the conformal bootstrap method was able to compute, with unprecedented accuracy, critical quantities of the three dimensional liquid-gas universality class [14].

The aim of this thesis is twofold. On one hand, we study properties of

the non perturbative renormalization group method and, in particular, the convergence properties of the derivative expansion in the case of a family of models, named $O(N)$ models. They describe the critical regime of many physical systems such as: a transition on dilute solutions of polymers ($N = 0$); liquid-gas phase transition and also the Ising model phase transition ($N = 1$); fluid-superfluid phase transition of Helium-4 ($N = 2$), also known as the λ transition, and paramagnetic-ferromagnetic phase transition in isotropic ferromagnets ($N = 3$), among others. While doing so, we pushed the derivative expansion up to order $\mathcal{O}(\partial^4)$ for the $O(N)$ models, which has never been done before, and propose a general method for improved estimates of quantities and their respective error bars, within this approximation scheme, which can be applied in many other models. On top of this, part of the motivation for this study was to shed some light in a long-standing controversy regarding the precise value of the critical exponent α, associated to the specific heat, in the Helium-4 fluid-superfluid transition. The most precise experiments [15] and theoretical estimates, due to a Monte Carlo simulation [16], were in disagreement beyond error bars. We expect that the order $\mathcal{O}(\partial^4)$ of the derivative expansion for $O(N)$ models would discriminate between these two situations. Up to last year the conformal bootstrap, which establishes rigorous bounds, was not able to discriminate between the two estimates [17]. However, this situation changed simultaneously, and independently, with our work [18], when we, both, the conformal bootstrap [19] and us, were able to take a stand in the dispute. Both, our results and the conformal Bootstrap confirm Monte Carlo over experiments.

We remark that although Monte Carlo simulations are a tool whose spectrum of applicability is very broad, it is a method which relies on strong computation capabilities. To give perspective, the most precise estimations in the case of the $O(2)$ model [20] demanded 10^2 years of CPU time. Also, the conformal bootstrap method is a very powerful technique with established rigorous bounds but, contrary with Monte Carlo, its range of applicability is very narrow, being restricted only to the critical regime of systems. On top of this, the recent estimations of the $O(2)$ model in [19] demanded, also, roughly 10^2 years of CPU time. In this respect, the computation power demanded by the derivative expansion of the non perturbative renormalization group in our calculation of the $O(2)$ model take a couple of hours in a personal laptop. However, in order to do so there is a need to develop substantial symbolic programming for deriving the governing equations, although still doable in a personal computer.

Deriving the flow equations at hand, however, is more than a week of human work. One last point to mention in favour of the non perturbative renormalization group is that, although in this thesis we focused on critical properties, its application scope is also much wider than the conformal bootstrap, allowing for the computation of non-universal quantities such as, for example, critical temperatures [21, 22] or phase diagrams [23, 24, 25, 26] for a large variety of systems either in or out of equilibrium.

A second topic studied in this thesis is conformal invariance within the framework of the non perturbative renormalization group. In [27] a sufficient condition for the presence of conformal invariance was presented, altogether with a proof of its realization for the liquid-gas universality class. In this article, a discussion of conformal invariance in the non perturbative renormalization group formalism was developed. In view of this sufficient condition we study the realization of conformal invariance in the critical regime of a large family of theories, the $O(N)$ models. The outcome is that we prove, in the physically interesting cases $O(2)$, $O(3)$ and $O(4)$, and give strong indications, for any other non-negative value of N, that conformal invariance is indeed realized [28]. Subsequently, we managed to deduce an equation, within the non perturbative renormalization group, which combines the information coming from scale and (special) conformal invariance.

As a related but independent result, we were able to use conformal invariance in order to obtain concrete results regarding the derivative expansion of the non-perturbative renormalization group applied to the liquid-gas universality class. In this new work, which shortly will be sent for publication [29], we try to constrain the critical properties by using conformal invariance in non perturbative renormalization group. This result corresponds to the first use, as far as we know, of conformal invariance within the non perturbative renormalization group for a concrete calculation. Moreover, this allows us to give a more rigorous argument to the use of the principle of minimal sensitivity. We found that the principle of minimal sensitivity, at order $\mathcal{O}(\partial^4)$ of the derivative expansion, is not only reasonable but, when applied to the computation of the critical exponent η (which in some way can be interpreted as applying the criterion to the solution of the non-perturbative renormalization group equation), it coincides with the condition where conformal invariance is best satisfied [29].

This thesis is organized as follows. A brief introduction to the field of statistical mechanics and to the physics of critical phenomena is given in Chapter 1.

Chapter 2 presents the ideas of Wilson's renormalization group and introduces its modern implementation: the non-perturbative renormalization group. We present in Chapter 3 the implementation of the derivative expansion approximation scheme up to order $\mathcal{O}(\partial^4)$ to compute critical exponents η, ν and ω of $O(N)$ models. While doing so, we propose a general method that can be applied to the estimation of quantities and their error within the derivative expansion for many models. We continue, in Chapter 4, with a discussion of scale and conformal invariance within the non perturbative renormalization group. We discuss a sufficient condition for the presence of conformal invariance once dilatation invariance is realized. Afterwards we assume conformal invariance as given and address how can it be used for studying the properties of a system and features of the non perturbative renormalization group itself. In Chapter 5 we study the presence of conformal invariance in the $O(N)$ models by means of three approximation schemes, namely the ϵ-expansion, the large-N approximation and the derivative expansion at order $\mathcal{O}(\partial^3)$. Furthermore, we give a proof for the realization of conformal invariance in the critical regime of $O(2)$, $O(3)$ and $O(4)$ models. We compute the only extra constraint that conformal invariance imposes (with respect to scale invariance) at order $\mathcal{O}(\partial^4)$ of the derivative expansion in the critical regime of a ϕ^4 model in Chapter 6. This allows for the introduction of a new criterion in order to obtain good convergence properties with the derivative expansion. Finally, conclusions and perspectives are presented in Chapter 7.

Chapter 1

Critical Phenomena

In nature, there are many systems whose microscopic components or degrees of freedom are so numerous that one can not study them by integrating fundamental laws. In such situations, the interest is often on the macroscopic properties of the system which are determined by an average of microscopic fluctuations of its components. The field of statistical mechanics was developed to study this type of systems by constructing the link between the microscopic and the observed macroscopic world. Statistical mechanics has become a platform for studying almost any macroscopic system (or more generally, systems with a large number of degrees of freedom). In particular, it is standard for the treatment of systems exhibiting phase transitions, a phenomena that is inherent to large, or macroscopic, systems.

In this chapter we present, first, a short introduction to the concepts of statistical mechanics and, in particular, its application for the study of phase transitions. After that, we present a qualitative description of continuous phase transitions (often denominated critical phenomena) in the case of the liquid-gas or ferromagnetic-paramagnetic phase transition. We end this section with a discussion of Landau theory of phase transitions and its limits. This will be used, in Chapter 2, as a basis for introducing the renormalization group formalism.

1.1 Statistical Mechanics and Phase Transitions

The history of statistical mechanics may trace its beginnings to the kinetic theory of gases and to the work of Daniel Bernoulli [30], who proposed that

the pressure of a gas emerged in terms of the continuous collisions from the gas molecules into the wall. Nowadays, statistical mechanics has become a framework which is applied to the study almost any macroscopic system (from simple gases to complex networks).

When the constituents of a systems are extremely numerous, we can not even think of giving a detailed description of the system for two reasons. On one hand, even if we know exactly the microscopic theory governing the dynamics of the particles we would need to solve them, which is already unthinkable in practice. On the other hand, to even start solving the equation, we would need to measure with, astonishing precision, the initial condition of each particle.[1] We call the configuration of given positions and velocities of each particle, as well as their internal state, a *microscopic state*. Of course, this is if we are working at a classical level, otherwise we describe a microscopic state by specifying all the quantum numbers of the system.

Since we are neither able to describe a microscopic state nor its evolution, what we can really do, instead, is to specify the macroscopic state, or the thermodynamic properties, of the system. This is, *temperature*, *pressure*, *magnetization*, etc. The aim of statistical mechanics is, then, to infer the macroscopic states from the microscopic ones. Given the astonishing number of constituents, to accomplish this task, statistic or probabilistic methods are compulsory.

The approach of statistical mechanics is, then, to regard any macroscopic quantity of the system as a suitable average over the microscopic states of the system. Take for example, the pressure of a gas, which originates in the colissions of the particles with the container, but since the motion of particles is erratic there is an intrinsic fluctuation. However, given the huge amount of collisions that take place at a small time window, and the fact that the measurement device *registers* an average of collisions during that time window, the reasonable thing to do is to consider averaged quantities. This measurement process is schematically depicted in Fig.1.1. The problem then boils down to finding a suitable probability distribution for the microscopic states, subject to external macroscopic constraints, and afterwards to compute the physical, or macroscopic, properties of the system from that distribution.

---

[1]Measuring the positions and velocities of particles with extremely high precision would not be enough since the system would, most certainly, be highly chaotic and the least error lead to diametrically different, quantitative, behaviour at later times. Moreover, to avoid such a problem we would need to update constantly our highly accurate measurements of particles.
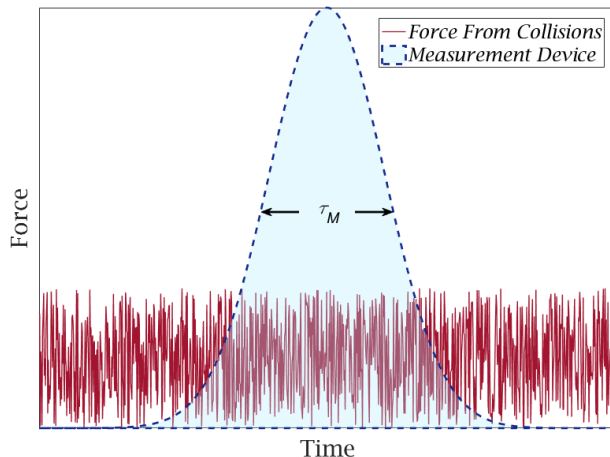
Figure 1.1: Schematic representation of a pressure measurement process with characteristic time τ_M.

We can think of this probability distribution as an infinite number of frozen (non-evolving) copies of the system each in definite microscopic states, where the fraction of copies on a given microscopic state is equal to the probability of that state within the probability distribution. In the literature, this collection of copies of the system is referred as an *ensemble*, and average over those ensembles are referred to as *ensemble average* [31].

The question arising is, then, how can we assign a probability distribution to microscopic states, in such a way that time averages over microscopic fluctuations can be interpreted as an ensemble average. The hypothesis that the time average of a quantity is equivalent to the ensemble average is the famous *ergodic hypothesis* [32]. Even if the hypothesis is true for a given system (which in any case, needs to be proven), one must further require that during the time τ_M in which the measure is performed, the system wanders efficiently through different microscopic states. In any case, the necessity of ergodic hypothesis is not settled and there are arguments in favour of dispense with it for equilibrium statistical mechanics, see [33, 34].

The external macroscopic constraints to which a system is subject will affect the specific probability distribution that must be used in order to compute the physical quantities. For example, if the system is isolated from the surroundings and in equilibrium, the energy would be constant and no exchange of particles will take place with the outer universe. This case corresponds to what is usually called as the *microcanonical ensemble*. If we know, or assume, the energy of the system to be E with an error ΔE, the distribution probabil-

ity in this ensemble consists in equal probability for states whose energy lies within a narrow band $E - \Delta E$ and $E + \Delta E$ and vanishing probability fo all other states. This is known as the *postulate of equal a priori probabilities.*

A common physical situation is that of a system in thermal equilibrium with the environment, which does not interchange particles with it. In this case, it is not reasonable to consider all states of the system as having equal probability. However, the universe (i.e. the system plus its surroundings) is isolated from everything else and therefore, its microscopic states are equally likely to be realized. After some algebra, this leads to the probability of a microscopic state *of the system r* with energy E_r, to be given by *Boltzmann distribution* [31]

$$P_r = \frac{e^{-\beta E_r}}{\mathcal{Z}}, \tag{1.1}$$

where $\beta = 1/k_B T$ is called the statistical temperature, k_B is the Boltzmann constant, T is the absolute temperature and $\mathcal{Z}$ is the partition function of the system and the central object of this ensemble. This ensemble is probably the most used one, although it depends in the particular system under study, and is denominated as *canonical ensemble.*[1] All along this thesis we will consider systems at equilibrium with a thermal bath, and employ the Boltzmann probability distribution.

The importance of the partition function is due to the fact that all thermodynamic quantities can be extracted from it by some manipulation. For example, the average energy of the system with this probability measure is:

$$U \equiv \langle E \rangle = \sum_r E_r P_r = -\frac{1}{\beta} \left(\frac{\partial \log(\mathcal{Z})}{\partial \beta} \right)_V. \tag{1.2}$$

The volume is the previous equation is held fixed because, otherwise, the energy levels of microscopic states would change.

The quantity $F = -\beta^{-1} \log\left(\mathcal{Z}\right)$ is the thermodynamic potential known as *Helmholtz free energy* of the system. These are the standard definitions for the partition function and the Helmholtz free energy. However, at this point we remark that in the remaining of the thesis a slightly different definition for these two objects will be used. In particular, we will omit β factors (in fact, we will use β for another quantity) and define the Helmholtz free energy with an opposite sign. However, for the present chapter we keep the standard

---

[1]Another useful ensemble is the *grand canonical ensemble*, which corresponds to the case where the system is in thermal and diffusive equilibrium with the environment [31] (this is, it can exchange energy and particles with the surroundings).

notation.

In general, for a system with $\mathcal{N}$ particles, the fluctuations of properties decays as $1/\sqrt{\mathcal{N}}$ and therefore, they can be ignored in the *thermodynamic limit* $\mathcal{N} \to \infty$. We remark that the thermodynamic properties are retrieved once the thermodynamic limit is taken. In many materials or systems, when varying some control parameter, as the temperature, one observes qualitative changes in some of its properties for certain values of the control parameter. For example, the density of a substance (say water) drops drastically in a boiling process and the spontaneous magnetization of a magnetic material (such as a Ni magnet) decreases abruptly when heating it above the Curie temperature. These changes are what is called a phase transition. This can only occur in the thermodynamic limit since finite sums of smooth functions (as the Boltzmann distribution) of the external parameters can never lead to a discontinuous behaviour [35, 36].

We will make a distinction between a first order phase transition and a second order, or continuous, phase transition. The former is characterized by a discontinuity in the first derivative of the Helmholtz free energy of the system with respect to an external parameter, for example the pressure or temperature. This means that we must give a finite amount of energy (*latent heat*) to make the system undergo the change. A continuous phase transition, as its name states, consists in a qualitative change in the behaviour of the properties of the system from one phase to the other, but the Helmholtz free energy of the system and its first derivative, as well as many other quantities, remain continuous at the transition (there is no latent heat). However, higher derivatives of the Helmholtz free energy exhibit discontinuities.

A typical example of phase transitions is the case of the liquid-gas phase transition of, for instance, water. When we heat it on a jar or cool it inside a freezer, we witness the change of state of water. These are examples of first order phase transition. Indeed, when boiling or freezing water the change is not along the whole sample but, rather, small amounts of substance changes its state while the rest remains in the liquid phase until, eventually, the whole system is either in gaseous or solid state. This slow change is due to the latent heat, because the heat provided to, or taken from, water is used to convert one small part of the sample to another state, but it is not enough energy to convert the whole system. This is our experience but, at odds with it, at temperature $T \simeq 647K$ and pressure $P \simeq 22MPa$, water undergoes a continuous phase transition. Beyond this point of the phase diagram, see Fig.1, the liquid and

gaseous phase become indistinguishable from each other.

We start by discussing the first model that captured some physics of the liquid-gas phase transition, namely the *van der Waals* model for fluids. This model was introduced by Johannes van der Waals in his thesis [37] and due to his works on the subject he was awarded with the Nobel prize in 1910.

The equation of state for the van der Waals gas, which can be deduced within statistical mechanical methods with various approximations (for example, with a *virial expansion*), takes the form:

$$\left(P + \frac{a}{v^2}\right)(v - b) = RT, \tag{1.3}$$

where P is the pressure, v the specific volume, T the temperature and a, b and R are constants (in fact, R is the ideal gas universal constant). This equation resembles a bit the equation of state of an ideal gas ($Pv = RT$) and by comparison it is easy to understand the meaning of the a and b constants. First, notice that b reduces the available volume for the molecules to be in. This can be interpreted as the hard-core repulsion of molecules. Second, the term with a constitutes an effective reduction of the pressure in the van der Waals gas, with respect to an ideal gas for the same effective volume and temperature, which originates from attractive forces between molecules at moderate distances.

This equation, with improved corrections, recovers quite well the typical isotherms of a real gas. At a given value of T and P the equation can be satisfied with up to three different values of v. This, in principle, may seems strange but it needs to be understood in the following way. Whenever three solutions exist, this means that the real isotherm is not this one, but it must be corrected by the equal areas rule of Maxwell [38]. In Fig.1.2 (taken from [31]) the isotherms given by van der Waals expression are depicted schematically, altogether with Maxwell's correction (which correspond to the horizontal lines). In the figure we can also appreciate a value of temperature T_c above which there is only one solution to Eq.(1.3). The critical point shown in this figure corresponds to the critical point of Fig.1. Below this point there exists a region which is delimite by a *coexistence curve* and isotherms are horizontal in that region. The region under the coexistence curve corresponds to the first order phase transition (this is, the line separating liquid from vapour phase in Fig.1) and in this region the liquid and gaseous phases coexist.

The critical point for this model is not hard to compute and corresponds to the values $P_c = a/27b^2$, $v_c = 3b$ and $T_c = 8a/27br$. Let us rewrite the equation

6
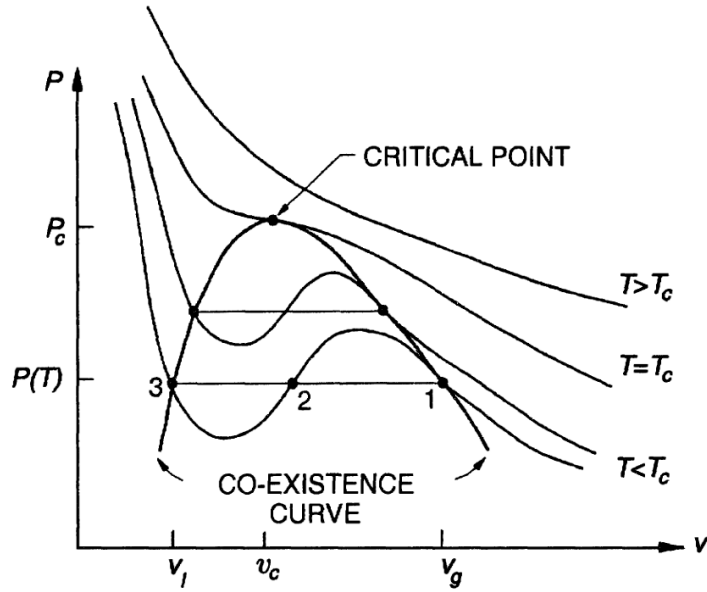
Figure 1.2: Representation of typical van der Waals isotherms in a $P-v$ diagram. Maxwell equal area rule is used for correcting isotherm under the coexistent curve. Figure taken from [31].

in terms of relative values $\bar{P} \equiv P/P_c$, $\bar{v} \equiv v/v_c$ and $\bar{T} \equiv T/T_c$, which yields

$$\bar{P} = \frac{8\bar{T}}{3\bar{v}-1} - \frac{3}{\bar{v}^2}. \tag{1.4}$$

This simple model allows us to study the behaviour around the critical point. For example, start at a temperature below the critical one $\bar{T} < \bar{T}_c = 1$ and look for the two stable solutions $\bar{v}_l$ and $\bar{v}_g$ in the coexistence curve. These are:

$$\bar{P} = \frac{8\bar{T}}{3\bar{v}_l-1} - \frac{3}{\bar{v}_l^2} = \frac{8\bar{T}}{3\bar{v}_g-1} - \frac{3}{\bar{v}_g^2}. \tag{1.5}$$

We can solve this equation for $\bar{T}$ which yields

$$\bar{T} = \frac{(3\bar{v}_l-1)(3\bar{v}_g-1)(\bar{v}_l+\bar{v}_g)}{8\bar{v}_l^2\bar{v}_g^2}$$

and, of course, it is symmetric in the interchange $\bar{v}_l \leftrightarrow \bar{v}_g$ as well as it yields $\bar{T} \to 1$ when $\bar{v}_l, \bar{v}_g \to \bar{v}_c = 1$. The interesting thing to notice is that we can do a Taylor expansion for the behaviour around the critical point. In particular, we can rewrite it in terms of the molar densities $\bar{\rho}_l = v_l^{-1}$ and $\bar{\rho}_g = v_g^{-1}$ which yields simply:

$$\bar{T} = \frac{(\bar{\rho}_l-3)(\bar{\rho}_g-3)(\bar{\rho}_l+\bar{\rho}_g)}{8}. \tag{1.6}$$

7

This means that expanding around the critical value $\bar{\rho}_c = 1$ as $\bar{\rho}_l = 1 + \Delta\bar{\rho}/2$ and $\bar{\rho}_g = 1 - \Delta\bar{\rho}/2$ (this is because close to the critical point the coexistence curve is symmetric) yields

$$\frac{T_c - T}{T_c} = 1 - \bar{T} = \frac{(\Delta\tilde{\rho})^2}{16} + \mathcal{O}((\Delta\tilde{\rho})^2) = \frac{(\Delta\rho)^2}{16\rho_c} + \mathcal{O}((\Delta\rho)^2), \tag{1.7}$$

or simply

$$\Delta\rho \propto (T_c - T)^\beta, \tag{1.8}$$

with $\beta = 1/2$. The exponent β is what we call a *critical exponent*. This means that $\Delta\rho$ is continuous but its derivative diverges at $T = T_c$. Of course, the behaviour of $\Delta\rho$ as we approach T_c from above is just vanishing since there is no notion of $\Delta\rho$, there is only one phase. It so happens that near a second order phase transition many different systems behave identically, in the sense that the have the same critical exponents.[1] This identical behaviour is what is referred as *universality* in the realm of critical phenomena. Systems which behave identically in their critical regime are, consequently, said to belong to the same *universality class*. In the next section we will discuss another system which is in the same universality class as the critical point of fluids.

Before going to discuss critical phenomena more in detail in the next section, we present two more critical exponents in the van der Waals fluid and compare to the measured values of a real gas.

For instance, one can consider the critical isotherm for whose critical point satisfy $\partial P/\partial v = \partial^2 P/\partial v^2 = 0$. This immediately means that:

$$P = P_c + \mathcal{C}(v - v_c)^\delta, \tag{1.9}$$

where $\mathcal{C}$ is some constant and $\delta = 3$. This exponent δ is another critical exponent. Lastly, we can compute the isothermal bulk modulus $\kappa_T \equiv -v^{-1}(\partial v/\partial P)_T$ at temperatures close to the critical one. Of course, $\partial P/\partial v$ vanishes at the critical temperature and in fact a Taylor expansion shows that it behaves as $\propto T - T_c + \mathcal{O}((T - T_c)^2)$, which means that the isothermal bulk modulus behaves as:

$$\kappa_T \propto (T - T_c)^{-\gamma}, \tag{1.10}$$

with $\gamma = 1$ being the last critical exponent that we consider within this exam-

---

[1]In fact, universality concerns a large family of physical quantities including critical exponents but not only.

ple. Finally, we remark that for a real fluid the values for the critical exponents differ from the ones we just computed, within the van der Waals model, and are:

$$\beta \simeq 0.3264, \tag{1.11}$$

$$\delta \simeq 4.7898, \tag{1.12}$$

$$\gamma \simeq 1.2371. \tag{1.13}$$

The discrepancy of the values obtained here, for the critical exponents, with the real ones originates from fluctuations which are not taken into account when deducing van der Waals equation. In fact, the obtained critical exponents in the van der Waals model are what is known as mean-field values.

1.2   Critical Phenomena

Critical phenomena can be consider one of the frontiers of statistical mechanics, since it still present many challenges for physicists. For example, computing accurately critical exponents is hard even for the simplest systems. An accurate treatment of a generic system at its second order phase transition is not know.

Let us discuss the Ising model from the viewpoint of statistical mechanics. Although it may look simple, captures many of the features that appear in a continuous phase transition. Moreover, its transition is in the same universality class as real fluids at their critical point. This model is related to the paramagnetic-ferromagnetic phase transition and it was proposed by Wilhelm Lenz in 1920 [39]. The model takes the name from a Lenz's student, Ernst Ising who studied the model a few years later as part of his PhD thesis [40].

The Ising model consists in modelling a magnet as a set of *classical spins* $\{S_i\}$, which can take the values ± 1, in a d dimensional lattice. The spins can interact with first neighbours in the lattice (denoted $\langle i, j \rangle$) with a Hamiltonian given by:

$$H = -J \sum_{\langle i,j \rangle} S_i S_j - \sum_i B S_i, \tag{1.14}$$

where J is a constant and B is an external magnetic field. This system exhibits a second order phase transitions for dimensions $d \geq 2$. Ising studied the one dimensional case and given that he did not find any transition, he considered that this model was unsuccessful in describing the ferromagnetic transition. In dimension $d = 2$ this model was solved by Onsager at $B = 0$. However, in dimension $d = 3$ the model has not yet been solved neither at $B = 0$ nor

$B \neq 0$.

The model in general dimension can be solved within the mean field approximation. This approximation consists in replacing interactions of spins by an average molecular value. For example, for the spin S_i we replace the interactions with its neighbours $\sum_{j/\langle i,j \rangle} S_i S_j$, by an average field M and we write instead $\sum_i q S_i M$ where q is half the number of first neighbours (because the energy is associated to pairs and, otherwise, we would count twice the contribution from a given interaction). The average field M is fixed by imposing a self-consistency condition $M = \langle S_i \rangle$. This replacement allows for the computation of the partition function which reads

$$\mathcal{Z} = \left[2\cosh\left(\frac{qJM + B}{k_B T} \right) \right]^{\mathcal{N}}, \qquad (1.15)$$

where $\mathcal{N}$ is the total number of spins and from which the magnetization can be computed directly as $\langle S_i \rangle = k_B T \left(\partial \log \left(\mathcal{Z} \right) / \partial B \right) / \mathcal{N}$, where we are assuming a translational invariant system. This yields:

$$\langle S_i \rangle = \tanh\left(\frac{qJM + B}{k_B T} \right). \qquad (1.16)$$

Imposing the self-consistency condition shows that the magnetization may be different from zero, even though we set $B = 0$, if $T < T_c \equiv qJ/k_B$. This is evident from:

$$\frac{qJM + B}{k_B T} = \tanh^{-1}(M) \simeq M + \frac{M^3}{3}, \qquad (1.17)$$

or rewriting

$$B \simeq k_B T \left(\frac{T - T_c}{T} M + \frac{M^3}{3} \right). \qquad (1.18)$$

This equation can be solved for M around the critical temperature T_c, with $B = 0$, and yields:

$$M \propto (T_c - T)^{\beta}, \qquad (1.19)$$

where $\beta = 1/2$ is the same critical exponent we found previously for the relation between density difference and the temperature. We can also compute the critical isotherm which relates M and B at $T = T_c$. This gives

$$B \propto M^{\delta}, \qquad (1.20)$$

with $\delta = 3$ as before. Finally, we can compute the susceptibility $\chi \equiv$

$\partial M/\partial B|_{B=0}$ which behaves as

$$\chi \propto (T - T_c)^{-\gamma}, \tag{1.21}$$

where $\gamma = 1$. In all three cases, we recovered the same critical exponents as in the van der Waals case.

Another implementation of the mean field approximation is the Landau theory of continuous phase transitions. Instead of considering discrete variables like the spins S_i, we consider continuous variables φ_i whose statistical average (i.e. the order parameter) is zero in the disordered phase (high temperature or symmetric phase) and non-zero in the ordered phase (low temperature or broken phase), in analogy with the previously discussed case, we consider the Hamiltonian (in absence of an external magnetic field) as invariant under parity $H(\varphi) = H(-\varphi)$. In presence of a magnetic field term $B\varphi$, the Hamiltonian exhibits an absolute minimum. Landau approximation consists in neglecting the contribution from all other states different from the one that minimizes the Hamiltonian (this is just the saddle-point approximation applied to this scenario) and, in analogy to the Ising model, we consider it as a polynomial in the order parameter. Since close to criticality the order parameter will be close to zero, we keep just a few terms in a polynomial expansion. On top of this, we add one last term to the Hamiltonian that amounts for the interactions between nearest neighbours. We write this term as $\frac{1}{2} \sum_\mu \sum_i (\partial_\mu \varphi_i)^2$, where $\partial_\mu \varphi_i$ stands for a discretization of a derivative on the lattice, as it is, for example,

$$\partial_\mu \varphi_i = \frac{\varphi(\vec{x}_i + a\hat{e}_\mu) - \varphi(\vec{x}_i - a\hat{e}_\mu)}{2a},$$

where a is the lattice spacing, $\hat{e}_\mu$ is a unit vector in the direction μ and $\varphi(\vec{x}_i)$ is the value of the *continuous spin* at the $\vec{x}_i$ position of the lattice which was rewritten in order to differentiate between directions. In this way, the interaction term expanded is

$$\frac{1}{2}(\partial_\mu \varphi_i)^2 = \frac{\varphi^2(\vec{x}_i + a\hat{e}_\mu) + \varphi^2(\vec{x}_i - a\hat{e}_\mu)}{2} - \varphi(\vec{x}_i + a\hat{e}_\mu)\varphi(\vec{x}_i - a\hat{e}_\mu), \tag{1.22}$$

which makes clear it favours homogeneous configurations of the variable φ.

Landau aimed at giving an unified description of all second order phase transitions. However, his approximation was too crude and neglected all fluctuations. Since the fluctuations are neglected, a criterion introduced by Vitali Guínzburg [41], called *Guínzburg criterion*, can be employed in order to es-

tablish up to what point Landau theory describes correctly the physics of the continuous phase transition. This is done by calculating a first correction to the Landau theory by considering some fluctuations and, then, computing the ratio, r_{GC}, of these fluctuations to the order parameter. The criterion is then implemented by saying that if $r_{GC} \ll 1$, fluctuations can be neglected and the theory is accurately described by Landau theory. With these ingredients into account, we will write down the continuous, at odds with the lattice presentation so far, version of the Guínzburg-Landau Hamiltonian:

$$H_{GL}[\varphi] = \int_x \left\{ \frac{1}{2}(\partial_\mu \varphi)^2 + \frac{r}{2}\varphi^2 + \frac{u}{4!}\varphi^4 \right\}, \qquad (1.23)$$

where the parameters r and u are regular functions of the temperature. The partition function is a functional integral which takes the form:[1]

$$\mathcal{Z}[B] = \int \mathscr{D}\varphi \, e^{-\frac{1}{k_B T}\left[H_{GL}[\varphi] - \int_x B(x)\varphi(x) \right]}. \qquad (1.24)$$

We point out that in order for this hamiltonian to reproduce the critical behaviour of the previously studied case, see below, in the mean field, or Landau theory, r must vanish at the critical temperature, see Eq.(1.29) below compared to Eq.(1.18). This Hamiltonian, although it may seems too simple to describe a realistic fluid, already encloses all critical properties of the liquid-gas second order phase transition or the ferromagnetic-paramagnetic phase transition of an uniaxial ferromagnet.[2] This is due to universality and will be justified within the *renormalization group* in Chapter 2 (in fact, explaining this property was one of the biggest achievement of the renormalization group).

Landau approximated all contributions in Eq.(1.24) by the contribution from the minimum of the exponent which satisfies

$$B(x) = \left. \frac{\delta H_{GL}}{\delta \varphi(x)} \right|_{\varphi = \varphi_0}, \qquad (1.25)$$

and yield the Helmholtz free energy:

$$F = -k_B T \log(\mathcal{Z}) \simeq H[\varphi_0] - \int_x B(x)\varphi_0(x). \qquad (1.26)$$

---

[1] It is clear that a lot of mathematically rigurous statements about the limit $a \to 0$ involved in the continuum formulation, Eq.(1.23) and Eq.(1.24), were swept under the rug.

[2] Let us note, however, that the common examples of physically realistic uniaxial magnets exhibit antiferromagnetism just below the critical temperature instead of ferromagnetism.

The magnetization is obtained by deriving the Helmholtz free energy with respect to the magnetic field:

$$M(x) = -\frac{\delta F}{\delta B(x)} = \varphi_0(x).$$

We can further compute the Gibbs free energy $\Gamma[M]$ by performing a Legendre transform, which yields

$$\Gamma[M] \equiv F + \int_x B(x)M(x) = H_{GL}[M]. \tag{1.27}$$

From this, one can recover the mean field results we described before, however, let us go differently. We introduce the correlation function $G_c(x, y)$ as:

$$G_c(x, y) \equiv \langle \varphi(x)\varphi(y) \rangle - \langle \varphi(x) \rangle \langle \varphi(y) \rangle. \tag{1.28}$$

This is nothing but $k_B T(\delta M(x)/\delta B(y))$. We can write an equation for G_c in the following way. Given that:

$$B(x) = \frac{\delta\Gamma}{\delta M(x)} = -\Delta M(x) + rM(x) + \frac{u}{6}M(x)^3, \tag{1.29}$$

we apply a functional derivative with respect to $B(y)$ to obtain:

$$\delta(x - y) = \frac{1}{k_B T}\left[-\Delta + r + \frac{u}{2}M(x)^2\right]G_c(x, y). \tag{1.30}$$

Now, if we consider an uniform external field B, $G_c(x, y)$ is just depend on the difference $x - y$ and $M(x)$ would be x-independent, for which we will just write M.

Performing a Fourier transform of this equation allows for a simple solution to the Fourier transform $\tilde{G}_c(q)$ of $G_c(x)$:

$$\tilde{G}_c(q) = \frac{k_B T}{q^2 + r + \frac{u}{2}M^2}. \tag{1.31}$$

One can then return to direct space to obtain $G_c(x - y)$ at $d = 3$:

$$\tilde{G}_c(x - y) = \frac{k_B T}{4\pi|x - y|}e^{-\frac{|x-y|}{\xi}}, \tag{1.32}$$

where ξ is called the *correlation length* since it describes distances up to which the system exhibit some amount of correlation, and takes the values $\xi = r$

13

if $T > T_c$ (since $M = 0$ for $B = 0$) and $\xi = r + uM^2/2$ if $T < T_c$. At zero magnetic field ($B = 0$) and close to criticality, but with $T < T_c$, the magnetization is $M = \sqrt{-6r/u}$.

Since r and u are analytic functions of the temperature, and the transition takes place at $T = T_c$, where $M = 0$, is only reasonable to expect that r vanishes linearly at the critical temperature and we write $r \simeq (T - T_c)r_0$ when T is near T_c. This shows that the correlation length diverges, when approaching the critical temperature from above and below as:

$$\xi \propto |T - T_c|^{-\nu}, \tag{1.33}$$

with $\nu = 1/2$. This is another example of critical exponent.

With this definition of correlation length we go back to Eq.(1.31) and rewrite it, at zero magnetic field, as:

$$\tilde{G}_c(q) = \frac{1}{q^2} \frac{k_B T}{1 + \frac{1}{\xi^2 q^2}}. \tag{1.34}$$

It happens that experiments show that this function $G_c(q)$ behaves near criticality as:

$$G_c(q) = \frac{1}{q^{2-\eta}} f(\xi q), \tag{1.35}$$

where η, called the *anomalous dimension*, is another example of a critical exponent. In this case, we see that within Landau approximation (as well as for mean field theory) $\eta = 0$.

Let us now analyse Guínzburg criterion. In order to do so, we recall that the magnetization at zero external field and, of course, below the critical temperature (but close) is $M^2 = 6r_0(T_c - T)/u$. Since the magnetization is, roughly, the same through a volume V whose linear dimension is of order $\mathcal{O}(\xi)$, we can compute the squared magnetic moment which is

$$\mathcal{M}^2 = \frac{6r_0(T_c - T)V^2}{u}.$$

The mean-square fluctuation can be computed integrating the correlation function over the same volume $V \propto \xi^d$ for x and y:

$$(\Delta\mathcal{M})^2 \equiv \int_{x,y} \left\{ \langle \varphi(x)\varphi(y) \rangle - \langle \varphi(x) \rangle \langle \varphi(y) \rangle \right\} = V \int_x G(x). \tag{1.36}$$

14

We can compute crudely this integral rather easily to get:

$$(\Delta\mathcal{M})^2 \propto \xi^2. \tag{1.37}$$

Considering now the ratio of the fluctuations to the order parameter yield:

$$\frac{(\Delta\mathcal{M})^2}{\mathcal{M}^2} \simeq \frac{\Omega_d u r_0^{\frac{d-4}{2}}}{6}(T_c - T)^{\frac{d-4}{2}}, \tag{1.38}$$

which shows that, at least within this crude approximation, if $d > 4$ fluctuations vanish as we approach the critical temperature, and Landau approximation accurately describes the critical behaviour. In the situation $d < 4$ it is clear that neglecting fluctuations is not a good idea, and there is no reason to believe that Landau approximation would yield accurate results. Of course, we could consider a temperature close, but not too much, to the critical temperature T_c for which fluctuations can still be ignored but this would not permit to compute critical exponents.

We present, now, a list of typical critical exponents, within ferromagnetic variable, which characterize the behaviour of physical quantities at criticality:

$$\begin{array}{lll}
\text{Order parameter} & M \propto (T_c - T)^\beta & (T < T_c), \\
\text{Specific heat} & C \propto |T - T_c|^{-\alpha} & (T \neq T_c), \\
\text{Susceptibility} & \chi \propto |T - T_c|^{-\gamma} & (T \neq T_c), \\
\text{Correlation length} & \xi \propto |T - T_c|^{-\nu} & (T \neq T_c), \\
\text{Critical isotherm} & B \propto M^\delta & (T = T_c), \\
\text{Correlation function} & \tilde{G}_c \propto q^{-2+\eta} & (T = T_c).
\end{array} \tag{1.39}$$

To end this chapter, let us remark that it was an experimental finding that these critical exponents exhibit certain scaling relations which hold for many system. This was an astonishing fact whose explanation was another striking success of the renormalization group formalism that we introduce in Chapter 2.

Chapter 2

Renormalization Group and Non-Perturbative Renormalization Group

In nature there are many systems which are composed of a very large number of degrees of freedom, macroscopic materials being one example of this. Each molecule's coordinate constitutes a degree of freedom. In general and recalling the discussion in Chapter 1, when the components of the system interact weakly (i.e. when the correlation length of the system is small with respect to a characteristic length determined by interactions, say a few characteristic intermolecular spacings or in a lattice a few lattice steps), the system can be regarded as a big number of independent components (at least in a first approximation) and in general these kind of systems can be studied with high precision. A typical example of this situation is the diluted gas which behaves in a first approximation as an ideal gas [42, 43, 44]. When the correlation length is large, the interactions can no longer be ignored and another approach is required (see however the case of the case of $d > 4$ in Chapter 1). In critical phenomena (for example, the critical point of a phase diagram) there is a large, macroscopic, number of degrees of freedom which are correlated and attemps to compute the partition function or thermodynamic properties are plagued with mathematical difficulties such as infrared divergences. The renormalization group (RG) ideas were introduced to circumvent these problems by progressively reducing the number of effective degrees of freedom.

2.1 Wilson's Renormalization Group

The ideas of the renormalization group trace back to the 30's,[1] with Landau's hydrodynamical approach to critical phenomena. The basic idea was to introduce mesoscopic variables, such as a density $\rho(x)$ in hydrodynamics, which plays the role of an average over the microscopic degrees freedom. This eliminates microscopic fluctuations and reduces the effective number of degrees of freedom. Although the ideas of the renormalization group share some similarities with Landau's theory, the later gives the same results for universal properties as mean field theory [45, 46, 47].

Kadanoff in 1966[2] [52] achieved a breakthrough by discussing how to successively reduce the number of degrees of freedom and recovering some known or conjetured results on the scaling behavior of the Ising model [39, 40]. Later on, Wilson put the pieces together and was astute enough to implement these ideas properly. He provided a big insight in the understanding of critical phenomena and how phase transitions took place [3, 4]. This worth him the Nobel prize in 1982.[3]

The aspects of Wilson's RG (or Kadanoff-Wilson's RG) are best expressed and understood using the example of a spin lattice. The ingredients to reduce the degrees of freedom consist in a coarse-graining of the system, followed by a rescaling of the system size that can be reinterpreted as renormalization of the parameters of the theory. This procedure ends up in a set of equations describing a dynamical system flow (in fact, it is customary to call this flow the *RG flow* and the set of equations the *RG flow equations*).

2.1.1 Coarse-Graining

The basic step is the coarse-graining of the system. To give a precise example, consider the planar lattice of Fig. 2.1 with lattice spacing a and with spins S_i in each node. For simplicity, let us assume that S_i takes the values $+1$ or

---

[1]It probably trace back even further, the *no man's an island* theorem applies.

[2]Parallel to Kadanoff and Wilson's, but not independent, there was a development of the renormalization group ideas in the context of quantum field theories by Callan and Symanzik, see [48, 49]. Prior to these developments and also in the context of quantum field theories, there was a different formulation of the renormalization group ideas by Stückelberg and Petermann and also by Gell-Mann and Low [50, 51]. In quantum field theory the field, say $\phi(x)$, at each point in space represent a different degree of freedom, and so it's in the same foot regarding the number of degrees of freedom as in statistical mechanics.

[3]See [53] for his Nobel lecture.

−1. Now divide it in blocks of spins (labeled by α), say of side length $3a$[1].
The coarse-graining consists schematically in replacing these 9 spins S_i^α inside
block α by just one new spin $\tilde{S}_\alpha$ (this is what Kadanoff proposed in [52] in a
handwaving manner [2]). Of course, to do this one needs to asign a value to this
new spin $\tilde{S}_\alpha$, say

$$\tilde{S}_\alpha = f(S_i^\alpha), \tag{2.1}$$

where f is a function that assign a representative value to a certain configuration
of the block. It is clear that if we choose f to be the average of the spins in the
block then, when the coarse-grained is applied over and over, the $\tilde{S}_\alpha$'s start
taking more and more values between -1 and 1, and the "spin" starts looking
like a continuous variable.
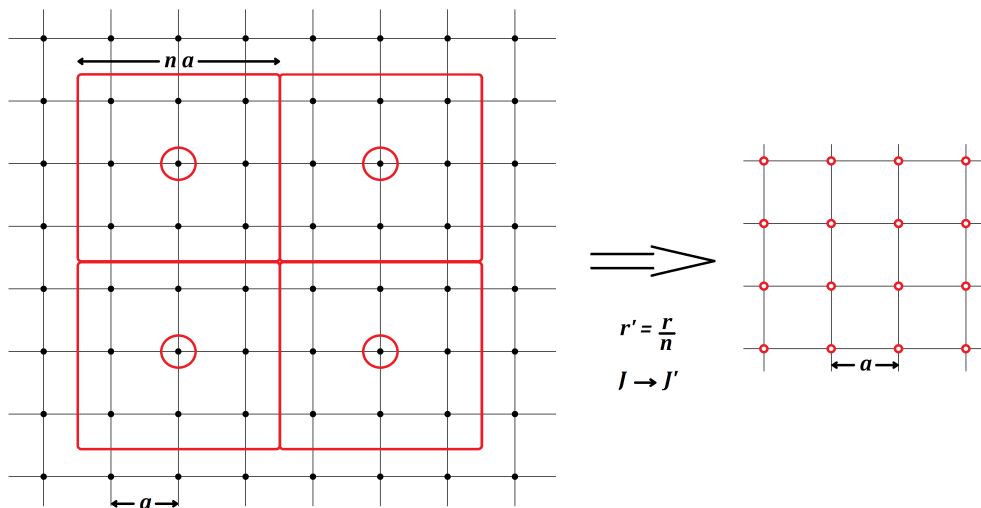
Figure 2.1: Ilustration of a renormalization group step.

With this prescription, given a state of the whole system (i.e. a specific
configuration of every spin in the lattice) labeled by r, the new Boltzmann
factor given by the blocks configuration $\{\tilde{S}_\alpha\}_r$ is obtained by summing the
internal fluctuations of the block which yields the same state:

$$e^{-H'[\{\tilde{S}\}_r]} = \sum_{\{S\}} \prod_\alpha \delta\big(\tilde{S}_\alpha - f(S_i^\alpha)\big) e^{-H[\{S\}_r]} \tag{2.2}$$

Here, there are a few things to comment. First, the $\beta = \frac{1}{k_B T}$ factor has
been absorbed in the definitions of the H's. Additionally, this serves as a

---

[1]The size of the blocks for the coarse-graining are evidently arbitrary. In fact it is useful
to extend this notion of block size to $a + \delta a$ with δa an infinitesimal, see below.

[2]Kadanoff motivation for this was that since the correlation length of the system near
a critical point is very large (in comparison with lattice spacing), one can replace each spin
block by an averaged quantity without much loss.

definition for H''s and, in fact, $H'[\{\tilde{S}\}_r]$ does not need to have the same form as the previous Hamiltonian but rather a general form compatible with the symmetries of the system. It's better to consider from scratch a generalization of $H[\{S\}_r]$ to $\hat{H}[\mathbf{J}, \{S\}_r]$, where $\mathbf{J}$ is a tensor parameter which encodes the full dependence on any possible term compatible with the symmetries. Consider for instance the Ising Hamiltonian

$$H_{Ising}[\{S\}_r] = -J \sum_{\langle i,j \rangle} S_i S_j, \tag{2.3}$$

where $\langle i,j \rangle$ represents nearest neighbours. Since the symmetry is $\mathbb{Z}_2$, the extended Hamiltonian $\hat{H}[\mathbf{J}, \{S\}_r]$ takes the form:

$$
\begin{aligned}
\hat{H}[\mathbf{J}, \{S\}_r] = \; & J_{00} + J_{11} \sum_{\langle i,j \rangle} S_i S_j + J_{12} \sum_{\langle\langle i,j \rangle\rangle} S_i S_j + J_{13} \sum_{\langle\langle\langle i,j \rangle\rangle\rangle} S_i S_j + \cdots \\
& + J_{21} \sum_{\langle i,j,k,l \rangle} S_i S_j S_k S_l + \cdots \\
& \vdots
\end{aligned}
\tag{2.4}
$$

where J_{00} is a spin-independent term, in general J_{ij} is the jth distinct possible term with $2i$ powers of S's and $\langle\langle i,j \rangle\rangle$ represent next-nearest neighbours, $\langle\langle\langle i,j \rangle\rangle\rangle$ next-next-nearest neighbours, $\langle i,j,k,l \rangle$ stands for four spin interaction displayed in a square, etc. The Ising Hamiltonian Eq.(2.3) corresponds to take $J_{11} = -J$ and every other $J_{ij} = 0$.

If instead of starting with $H_{Ising}[\{S\}_r]$, the Hamiltonian $\hat{H}[\mathbf{J}, \{S\}_r]$ is considered then, after the coarse-graining, the *form* of the Hamiltonian would remain the same, but with a different tensor $\mathbf{J}$, and so Eq.(2.2) can be rewritten as:

$$e^{-\hat{H}[\mathbf{J}', \{\tilde{S}\}_r]} = \sum_{\{S\}} \prod_\alpha \delta\big(\tilde{S}_\alpha - f(S_i^\alpha)\big) e^{-\hat{H}[\mathbf{J}, \{S\}_r]}. \tag{2.5}$$

It is simple to see that these two Boltzmann factors lead, when summed over $\sum_{\{\tilde{S}\}_r}$, to the same partition function $\mathcal{Z}$. Indeed, summing over all configurations $\{\tilde{S}\}_r$, defines for the *left hand side* of Eq.(2.5) the new partition function $\tilde{\mathcal{Z}}$,

$$\tilde{\mathcal{Z}} = \sum_{\{\tilde{S}\}_r} e^{-\hat{H}[\mathbf{J}', \{\tilde{S}\}_r]}.$$

On the *right hand side* we have that

$$\sum_{\{\tilde{S}\}_r} \sum_{\{S\}} \prod_\alpha \delta\big(\tilde{S}_\alpha - f(S_i^\alpha)\big) e^{-\hat{H}[\mathbf{J},\{S\}_r]} =$$

$$\sum_{\{S\}} \left[\sum_{\{\tilde{S}\}_r} \prod_\alpha \delta\big(\tilde{S}_\alpha - f(S_i^\alpha)\big) \right] e^{-\hat{H}[\mathbf{J},\{S\}_r]} = \sum_{\{S\}} e^{-\hat{H}[\mathbf{J},\{S\}_r]} = \mathcal{Z},$$

$$(2.6)$$

where the factor inside square brackets is just 1.

The term independent of spins, J_{00} in the tensor $\mathbf{J}$, can be dropped if one is interested in correlation functions because it does not affect any. However, notice that it does indeed affect the partition function (and therefore the Helmholtz free energy).

2.1.2 Rescaling and Renormalizing the System

This coarse-graining does not have an impact on the long range physics. However, since the spins are now separated by na a redimensionalization of the system is required, where n is the side of the spin blocks in terms of numbers of spin. This implies rescaling $na \to a$.

To continue with the example, the simplest thing to do is to take the f function in Eq.(2.1) to be proportional to the average and so:

$$\tilde{S}_\alpha = \frac{n^{d_\phi}}{n^d} \sum_{i \in \alpha} S_i^\alpha, \tag{2.7}$$

where d is the dimension of the lattice. In the example considered in Fig. 2.1, there are 3 spins in the side so $n = 3$ and since it is a bidimensional lattice then $d = 2$. The factor n^{d_ϕ}, which will be fixed later on, corresponds to the last step of the RG procedure, and it means that when these transformations are done in the system, the spins, as the lattice, also deforms with it. This factor accounts for this deformation. Of course, in general n is to be taken not large (otherwise we face the same problem of a big number of degrees of freedom interaction as in the original problem).

With this in mind, the correlation function in the transformed system can be written as:

$$\langle \tilde{S}_\alpha \tilde{S}_\beta \rangle = \frac{1}{\mathcal{Z}} \sum_{\{\tilde{S}\}} \tilde{S}_\alpha \tilde{S}_\beta e^{-\breve{H} - \hat{H}[\mathbf{J}', \{\tilde{S}_\alpha\}_r]}$$

$$= \frac{1}{\mathcal{Z}} \sum_{\{S\}} \frac{n^{2d_\phi}}{n^{2d}} \left(\sum_{i \in \alpha} S_i \right) \left(\sum_{j \in \beta} S_j \right) e^{-\hat{H}[\mathbf{J}, \{S\}_r]} \qquad (2.8)$$

$$= \frac{n^{2d_\phi}}{n^{2d}} \sum_{i \in \alpha} \sum_{j \in \beta} \sum_{\{S\}} S_i S_j e^{-\hat{H}[\mathbf{J}, \{S\}_r]} = \frac{n^{2d_\phi}}{n^{2d}} \sum_{i \in \alpha} \sum_{j \in \beta} \langle S_i S_j \rangle,$$

where it was used Eq.(2.5) and Eq.(2.7). Now, If the correlation length is much larger than the lattice's step (i.e. $\xi \gg na$), then S_i^α and S_j^β vary slowly (and can be regarded as constants inside blocks α and β). If on top this, the separation of blocks α and β is much larger than the lattice step na (i.e. $|\vec{r}_\alpha - \vec{r}_\beta| \gg na$), Eq.(2.8) then implies that one can establish a relation between the correlation functions,

$$\langle \tilde{S}_\alpha \tilde{S}_\beta \rangle = n^{2d_\phi} \langle S_i S_j \rangle. \qquad (2.9)$$

2.1.3 Renormalization Group Flows, Critical Surface and Fixed Points

One step of the renormalization group integrates out microscopic fluctuations. The procedure is to be repeated over and over, and with it the system parameters, $\mathbf{J}$, describe an orbit on some parameter space. In principle there are many possible type of attractors, which drives the trajectories, for a generic dynamical system: fixed points, cycles, strange attractors (related to chaotic behaviour), among others. In 2-dimensions, there is a well established result by Alexander Zamolodchikov[54], known as *c-theorem*, which states that upon reasonable hypotesis, a monotonically decreasing function exists along the RG flow (this is, monotonically decreasing with the length scale). A similar result exists in 4-dimensions[1], known as the *a-theorem*, due to John Cardy [55]. This seems to imply that the RG flow is dissipative and no chaotic or cyclic behaviour are allowed [2]. In any case, the main interest here is the case of an isolated fixed point as will be clear in further discussions.

Iterating the RG procedure makes physical distances smaller, when mea-

---

[1]In fact, the result holds in even dimensional space.
[2]However, there has been some work done where limit cycles are found. We do not discuss here, whether this is an artifact of the approximation scheme used or are indeed physical realizable, see [56, 57].

sured in units of the (running) lattice spacing. This is simple to understand since, in the previous example, if spins were correlated initially roughly up to three lattice steps then after just one iteration, the block spins correlate, roughly, up to one lattice spacing.

Now consider the initial couplings $\mathbf{J}_0$ as function of the temperature $\mathbf{J}_0(T)$. This dependence in temperature is partly due to the fact that the temperature and Boltzmann constant were reabsorbed into the couplings, but moreover, at the microscopic level, parameters may also depend on the temperature (see Chapter 1). The set $\mathbf{J}_0(T)$ can be viewed as a curve $\mathcal{C}_\Lambda$ in the parameter space where the RG flow lives and any point in this line is to represent the microscopic Hamiltonian or initial condition of the RG equations.[1]

This curve has a particular point at the critical temperature T_c as we discuss below. Since the correlation length diverges at T_c, iterating over and over does not modify this feature: the correlation length still diverges. This implies that when $T = T_c$ the flow is restricted to an hypersurface. This hypersurface is of codimension one if the system under consideration is critical, altough it could be of codimension higher than one if the system is multicrital (i.e. if one needs to fine-tune more than one control parameter[2]). This hypersurface is called *critical surface* or *critical manifold*. If the system is outside this surface, the correlation length is finite and since iterating the RG procedure diminish it (in units of the lattice spacing), then it must be an unstable surface (this is, the RG flow moves away from the surface). This picture is schematized in Fig. 2.2. Let us call $\mathcal{R}$ the RG transformation which maps a set of couplings $\mathbf{J}_l$ into $\mathbf{J}_{l+1}$ (alternatively, it can be viewed as transforming the Hamiltonians), this is

$$\mathcal{R}(\mathbf{J}_l) = \mathbf{J}_{l+1}.$$

The fixed points $\mathbf{J}^*$ correspond to the case

$$\mathcal{R}(\mathbf{J}^*) = \mathbf{J}^*.$$

Linearising the flow around the fixed and computing the eigenvalues of the stability matrix at the fixed point allows to calculate the critical exponents as we show now.

---

[1]Of course, a smooth dependence of the coupling on T is assumed, at least for $T > 0$.

[2]Consider for example the liquid-gas phase transition discussed in Chapter 1, in practice one needs to fine-tune two parameters, the temperature and the pressure or, in the magnetic case, the external magnetic field (to zero). However, since the critical point exhibits $\mathbb{Z}_2$ symmetry, it is conventional to restrict to the subspace of theories which exhibit this symmetry and, therefore, only one parameter needs to be fine-tuned.
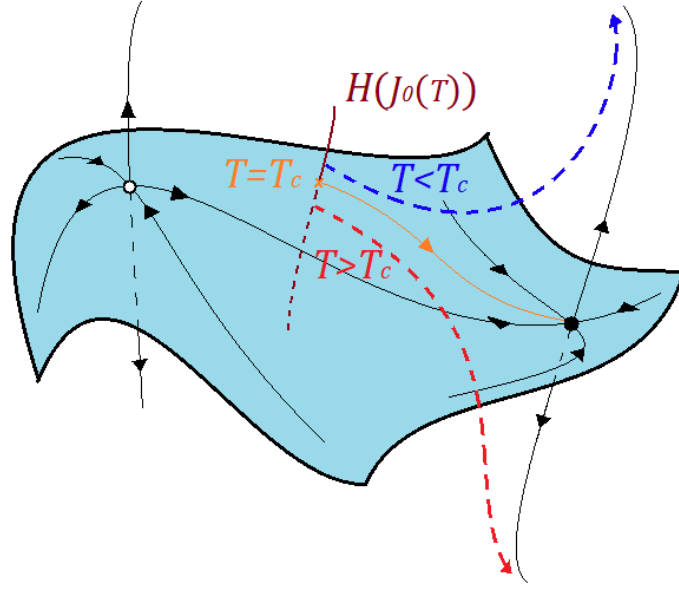
Figure 2.2: Representation of the unstable critical surface. The brown line represents the family of microscopic Hamiltonian indexed by temperature, the blue (red) line represents a RG flow at $T < T_c$ $(T > T_c)$ and the orange line is a RG flow at the critical temperature $T = T_c$.

Indeed, consider a point in parameter space $\mathbf{J}$ which is close to a fixed point

$$J_\alpha = J_\alpha^* + \delta J_\alpha. \tag{2.10}$$

After applying the RG procedure one arrives at a new parameter, $\mathbf{J}'$, which is also close to the fixed point and whose difference with the fixed point is given by $\delta\mathbf{J}'$. Linearizing the procedure one can write

$$\delta J_\alpha' = \sum_\beta T_{\alpha\beta}\delta J_\beta. \tag{2.11}$$

where the matrix $T_{\alpha\beta}$ defined by

$$T_{\alpha\beta} \equiv \left.\frac{\partial\mathcal{R}_\alpha(J)}{\partial J_\beta}\right|_{J^*},$$

depends, of course, on the RG procedure parameter n (the block size of the coarse-graining). The eigenvectors and corresponding eigenvalues of the matrix

$T_{\alpha\beta}$ are called $\mathbf{v}^{(i)}$ and λ_i, respectively. This is,

$$\sum_{\beta} T_{\alpha\beta} v_{\beta}^{(i)} = \lambda_i v_{\alpha}^{(i)}. \tag{2.12}$$

We assume now that the matrix $T_{\alpha\beta}$ is diagonalizable. This assumption allows us to express any point of parameter space as a linear combination of the eigenvectors, in particular:

$$\delta J_{\alpha} = \sum_{i} t_i v_{\alpha}^{(i)}, \tag{2.13}$$

where the t_i are called the *scaling parameters*. Then, the new parameter $\delta \mathbf{J}'$ after one iteration is just

$$\delta J_{\alpha}' = \sum_{\beta} T_{\alpha\beta} \sum_{i} t_i v_{\beta}^{(i)} = \sum_{i} t_i \lambda_i v_{\alpha}^{(i)} = \sum_{i} t_i' v_{\alpha}^{(i)}, \tag{2.14}$$

where in the last equality we defined $t_i' \equiv t_i \lambda_i$. Then, after the sth iteration the last expression becomes

$$\delta J_{\beta}^{(s)} = \sum_{i} t_i^{(s)} v_{\alpha}^{(i)}, \tag{2.15}$$

with $t_i^{(s)} \equiv t_i \lambda_i^s$. It is clear from this why the t_i are called "scaling parameters". Three cases arise at this point depending on the value of λ:

- If $\lambda_i > 1$ the scaling parameter grows under the RG procedure, and t_i is called a *relevant parameter or field*.
- If $\lambda_i < 1$ the scaling fields decreases under the RG procedure, and t_i is called an *irrelevant parameter or field*.
- If $\lambda_i = 1$ then t_i is called a *marginal parameter or field* and one must go beyond the linear aproximation to determine the flow's behaviour.

If there are no marginal parameters, and there are K relevant parameters, then in order to be on the critical surface one must fine-tune these K relevant parameters. The standard situation is to have to fine-tune only one parameter to be on the critical surface. [1] The fixed points that are reached by fine-tunning one parameter (or relevant field, say the *temperature*) are associated with a critical point, those which are reached by fine-tunning two parameters

---

[1]At least, from the viewpoint of accesibility, these are the ones with the most practical relevance.

are associated with a tricritical and so forth.[1] Let us focus from now on, on the case with a single relevant parameter. Then, it is useful to sort, and label, the eigenvalues in descending order (i.e. $\lambda_1 > 1 > \lambda_2 > \lambda_3, \ldots > 0$[2], since there is only one relevant field in this case). Consider now that we are close to a fixed point and consider the correlation function $G(\mathbf{r}, t_1, t_2, \ldots)$ which is a function of the distance between spins (see Eq.(1.28)) and the actual values of parameters (i.e. a function of the scaling parameters $t_1, t_2, \ldots$). Notice that the relevant field vanishes linearly (barring coincidences) with the temperature in the critical surface and we can choose

$$t_1 \sim t = \frac{T - T_c}{T_c}.$$

When applying the RG procedure s times, the distances and the system parameters (scaling parameters) evolve and then Eq.(2.9) can be re-written

$$G(\mathbf{r}, t_1, t_2, \ldots) = n^{-2d_\phi s} G(\frac{\mathbf{r}}{n^s}, t_1', t_2', \ldots), \tag{2.16}$$

with $t_i' = \lambda_i^s t_i$. By standing on the critical surface (this is $t_1 = 0$), one can put $n^s = r/a$ in Eq.(2.16) and this yields

$$G(\mathbf{r}, 0, t_2, \ldots) = \left(\frac{r}{a}\right)^{-2d_\phi s} G(a, 0, \lambda_2^s t_2, \ldots). \tag{2.17}$$

Which means that, for distances $r \gg a$, if the RG procedure have washed out enough short-distance fluctuations (in terms of the scaling parameters and the RG parameter this means that $\lambda_2^s |t_2| \ll 1$) the system becomes scale-invariant. It is mandatory in order to reach a fixed point of the RG equations, to pick properly the field scaling dimension d_ϕ. Afterwards, we can relate, by matching Eq.(2.17) and Eq.(1.35), the parameter d_ϕ with the anomalous dimension η as:

$$d_\phi = \frac{d - 2 + \eta}{2}. \tag{2.18}$$

Instead of starting on the critical surface, consider now $t_1 \neq 0$. Since the RG procedure modifies distances with a factor of n, the eigenvalue λ_1 takes

---

[1]Whenever the fixed point at criticality of the Ising model, or similar systems, is refered as "critical point" it is assumed that the magnetic field is set to zero from scratch. This is in direct connection with the discussion about the codimension of the critical surface, see above. If this field is taken into account we would have two relevant directions.

[2]The values of λ_i must be strictly positive because we are assuming a smooth evolution of parameters.

the form:

$$\lambda_1 = n^{y_1} \tag{2.19}$$

with y_1 the *scaling dimension* of v_1. One can apply the RG procedure until $\lambda_1^s t_1 = (n^s)^{y_1} t_1 \sim \pm 1$, where the sign $\pm$ depends on whether $T > T_c$ (+) or $T < T_c$ (−). One can then show that the correlation length, ξ, is identified with the quantity $\hat{\xi} \equiv a|t_1|^{-\frac{1}{y_1}}$. Indeed, this identification leads $n^s = \hat{\xi}/a$ (which is equivalent to integrate all fluctuations up to the correlation length), and the correlation function is:

$$G(\mathbf{r}, t_1, t_2, \dots) = \left(\frac{\hat{\xi}}{a}\right)^{-2d_\phi} G(\frac{ra}{\hat{\xi}}, \pm 1, \lambda_2^s t_2, \dots). \tag{2.20}$$

If $|t_1|$ is small enough (this is, if the correlation length is sufficiently large or equivalently $|t| \ll 1$) then $\lambda_2^s \ll 1, \dots$; and therefore under this assumption

$$G(\mathbf{r}, t_1, t_2, \dots) \approx \left(\frac{\hat{\xi}}{a}\right)^{-2d_\phi} G(\frac{ra}{\hat{\xi}}, \pm 1, 0, 0, \dots) = r^{-2d_\phi} f_\pm\left(\frac{r}{\hat{\xi}}\right). \tag{2.21}$$

Comparing Eq.(2.21) with Eq.(1.32), one confirms that $\hat{\xi}$ can be identified with ξ. Moreover, we can readily identify the critical exponent ν with the inverse of the largest eigenvalue of the RG flow equations around the fixed point[1],

$$\nu = \frac{1}{y_1}. \tag{2.22}$$

Considering how the correlation functions of the system change under the RG procedure (in some cases in presence of an external magnetic field[2]) one can

---

[1]This deduction manifestly shows that $\nu = \nu'$. This is, the critical exponent ν defined from above or below T_c is the same even though f_+ may be different from f_-. One word of caution must be said about this: for this to be true we must require that the correlation length away from T_c not to be divergent (which is indeed the case of the present example). However, it happens that when the correlation length diverges, below or above the critical temperature, critical exponents could be different when measured in the broken or symmetric phase, see for example [58].

[2]Notice, however, that adding an external magnetic field leads to another relevant direction.

deduce all the scaling laws between the critical exponents defined in Eq.(1.39):

$$\alpha = 2 - \nu D \tag{2.23}$$

$$\beta = \frac{\nu}{2}\big(D - 2 + \eta\big) \tag{2.24}$$

$$\delta = \frac{D + 2 - \eta}{D - 2 + \eta} \tag{2.25}$$

$$\gamma = \nu\big(2 - \eta\big) \tag{2.26}$$

What must be understood of this picture is that Wilson's RG procedure washes out the rapid or microscopic fluctuations without altering the long distance physics. Since this regime is not altered by the RG procedure, any fixed point it reach exhibit the same long distance behaviour as the systems as its starting point on the curve $\mathcal{C}_\Lambda$. But more generally, it explains manifestly how the concept of universality arises. For instance, suppose there is another curve, say $\mathcal{C}'_\Lambda$, corresponding to another microscopic theory but with the same symmetries (so its RG flow lives in the same parameter space). If there are points in $\mathcal{C}'_\Lambda$ and in $\mathcal{C}_\Lambda$ which are in the same basin of attraction of certain fixed point[1] then, since this fixed point is the one controlling the long range physics of *both* theories, they are in the same universality class regarding its phase transition. This is depicted in Fig. 2.3. Moreover, it seems appropriate to discuss, at this point, the relevance of the first irrelevant operator. Typically the eigenvalues of the RG transformation take discrete values and the systems approach the fixed point along the least irrelevant direction. This allows for the computation of corrections to the scaling behaviour close to criticality, which can be obtained by computing the first irrelevant eigenvalue $\omega \equiv y_2$.

By studying the characteristics of the critical point of the RG flow, one can in principle compute all the long range physics quantities of the system under study.

2.2   Non-Perturbative Renormalization Group

Let us adopt now a continuous formulation, with continuous variables $\phi(x)$ instead of discrete spins values S_i. In the Ising model close to criticality, this is equivalent to having coarse-grained the system up to a volume L^D such as

---

[1]This is, both trajectories end up in this fixed point.
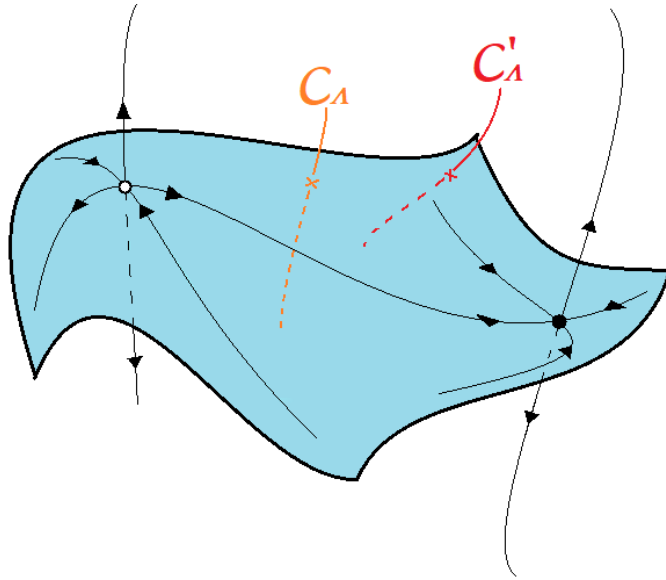
Figure 2.3: Representation of the origin of universality in the RG framework. The curves $\mathcal{C}_\Lambda$ and $\mathcal{C}'_\Lambda$ represent the points in parameter space for two microscopic theories with the same symmetries when varying a control parameter, say the temperature. The white dot on the surface represent a tricrital point and the black dot is the critical point (features highlighted by depicting the stables and unstables directions in each case).

$L \ll \xi$. The partition function is written as:

$$\mathcal{Z} = \int \mathcal{D}\phi \, e^{-\hat{H}[\mathbf{J}_0, \phi]} \tag{2.27}$$

where the integration can be done over Fourier variables $\phi(q)$.[1] One of the issues to solve is the non-analyticities appearing in the ultraviolet. For this, one must introduce an ultraviolet cut-off Λ in such a way that the momentum to be considered satisfy $p \lesssim \Lambda$. One way of implementing the ultraviolet regulator is to consider a model on a lattice, with lattice spacing a. In this case, only modes with each component of the momenta verifying $p < 2\pi/a$ are present. In what follows the effects of momentum higher than the ultraviolet cut-off are considered as being already taken into account in the Hamiltonian by some renormalization procedure (this is what's typically done in the continuum case).

Computing the integral Eq.(2.27) presents the same infrared divergences as

---

[1]Due to Parseval's theorem this is the same as integrating over direct space. We use the same notation for functions in direct space and in Fourier space. It will be clear what variable is meant by context or, when necessary, by explicitly telling.

for the discrete case on the lattice described previously. Wilson's RG can be viewed as performing an integration over a thin shell of momenta between $\frac{\Lambda}{n}$ and Λ, see Fig. 2.4. This is, integrating out fast (or short range) fluctuations and then rescale and resize the system.
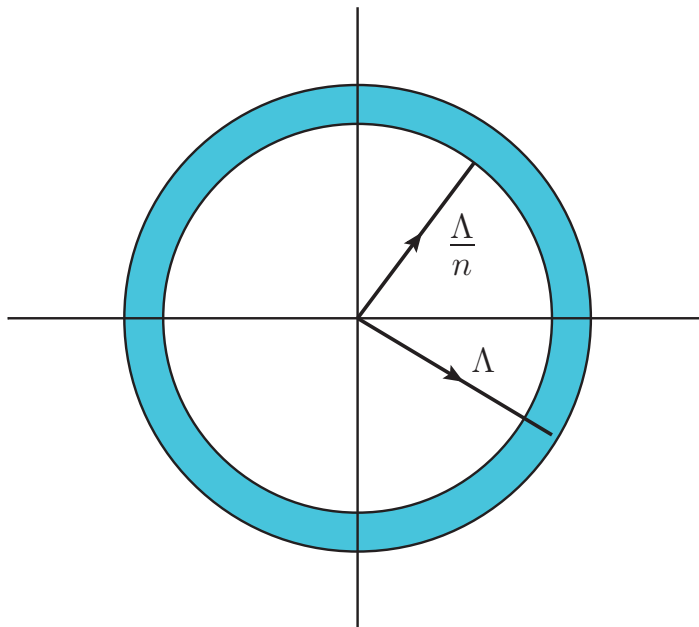
Figure 2.4: Representation of the momentum shell integration of Wilson's RG.

An alternative approach to implementing Kadanoff-Wilson's ideas, was proposed by Polchinski in the early 80's [59]. It consists in modifying the Hamiltonian with a regulating term, in the form of a mass-like term (quadratic in the fields), which effectively freezes the fast (ultraviolet) fluctuations. The present form of Kadanoff-Wilson's ideas, although similar to the Polchinski approach in some respect, consist in modifying the Hamiltonian with an *infrared* mass-like term. This new approach is known as the Non-Perturbative Renormalization Group (NPRG)[1] and it was implemented, among others, by C. Wetterich in the 90's [5, 6, 7, 8, 9] (see [10] for an introduction to the Wilson's RG and the NPRG).

The idea is to freeze slow modes fluctuations up to some scale k by introducing a big mass to these modes. This is achieved by adding to the original Hamiltonian a *regulating term* of the form

$$\Delta H_k[\phi] = \frac{1}{2} \int_q \tilde{R}_k(q)\phi(q)\phi(-q), \qquad (2.28)$$

---

[1]The NPRG is sometimes called Functional Renormalization Group (FRG) or Exact Renormalization Group (ERG)

29

that leaves the fast modes (small distances) unaltered while the fluctuations of the slow modes is reduced.

The regulator function $\tilde{R}_k$ is chosen to be translation and rotational invariant, i.e. it is a function of the modulus of q. In direct space, Eq.(2.28) can be written as:

$$\Delta H_k[\phi] = \frac{1}{2} \int_{x,y} \phi(x) R_k(|x-y|) \phi(y), \tag{2.29}$$

where the isometric properties of it become evident.

The function $\tilde{R}_k$ is the Fourier transform of $R_k(|x-y|)$ but from this point forward the "$\sim$" will be dropped and it will be clear from context what function is being considered. Because of translation and rotation invariance, the regulator function must be a function of $|q|$. Moreover, it should go sufficiently rapidly to zero for $q \gg k$ and must behave as a mass of order k for the slow modes, i.e. $R_k(q) \sim Z_k k^2$ for $q \ll k$ (and for $k = \Lambda$ all modes should be frozen), where Z_k is a renormalization factor to be discussed in detail below.

The function $R_k(q)$ is schematically depicted in Fig. 2.5. Typical examples of this function are:

$$E_k(q^2) = \alpha Z_k k^2 e^{-q^2/k^2}, \tag{2.30}$$

$$W_k(q^2) = \alpha Z_k k^2 \frac{q^2/k^2}{e^{q^2/k^2} - 1}, \tag{2.31}$$

$$\Theta_k^n(q^2) = \alpha Z_k k^2 \left(1 - \frac{q^2}{k^2}\right)^n \theta\left(1 - \frac{q^2}{k^2}\right). \tag{2.32}$$
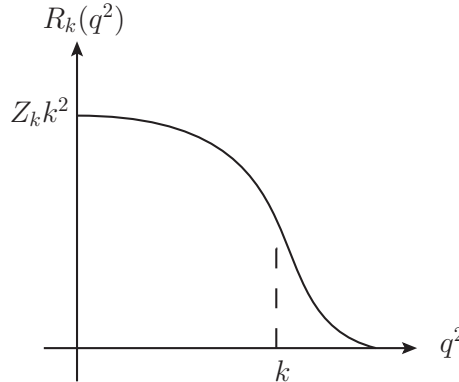
Figure 2.5: Schematic form of the regulator function.

We now discuss the structure and properties of the renormalization group equation in the NPRG. To do this, start with the Helmholtz free energy $W \equiv \log(Z)$, up to a $-k_B T$ factor, in the presence of the regulator and a source B for the field ϕ:

$$e^{W_k[B]} = \int \mathcal{D}\phi\, e^{-\hat{H}[\mathbf{J},\phi] - \Delta H_k[\phi] + \int_x B(x)\phi(x)} \tag{2.33}$$

It is usual to work with the *RG time* $t \equiv \log(k/\Lambda)$ instead of k, or just *time* for short. By applying a time derivative, $\partial_t = k\partial_k$, at fixed source B on Eq.(2.33) one can deduce an exact evolution equation for the Helmholtz free energy, see Appendix A.

$$\partial_t W_k[B] = -\frac{1}{2}\int_{x,y} \partial_t R_k(|x - y|)\left(\frac{\delta^2 W_k[B]}{\delta B(x)\delta B(y)} + \frac{\delta W_k[B]}{\delta B(x)}\frac{\delta W_k[B]}{\delta B(y)}\right). \tag{2.34}$$

This approach is similar to the one of Polchinki [59] and it is actually possible to make a direct connection between the two equations [7, 8]. It is however more convenient to work with the Gibbs free energy, or running effective action, of the system instead of the Helmholtz free energy. As we will show, the evolution equation of the effective action has a one loop structure that only involves 1PI diagrams and this makes it better suited for approximations [7, 8] (this will be further discussed in the context of the Derivative Expansion, see Sec.2.3). Taking the Legendre transform of the free energy $W_k[B]$ with respect of B allows to define the effective action $\Gamma_k[\varphi]$ as:

$$\Gamma_k[\varphi] + \Delta H_k[\varphi] = -W_k[B] + \int_x B(x)\varphi(x), \tag{2.35}$$

where $\varphi(x) = \langle \phi(x) \rangle_B = \frac{\delta W_k}{\delta B(x)}$.

It is shown in Appendix A that after some algebra one arrives at Wetterich's equation for the flow of this running effective action:

$$\partial_t \Gamma_k[\varphi] = \frac{1}{2}\int_{x,y} \partial_t R_k(|x - y|) G_k[x, y; \varphi] \tag{2.36}$$

where $G_k[x, y; \varphi]$ is the full propagator which satisfies

$$\int_z G_k[x, z; \varphi]\left(\frac{\delta^2\Gamma_k}{\delta\varphi(z)\delta\varphi(y)} + R_k(z, y)\right) = \delta(x - y).$$

As explained before, in order to obtain a fixed point, it is necessary to introduce dimensionless, renormalized, variables which corresponds to the rescaling

discussed in Section 2.1.3:

$$\tilde{x} \equiv kx \tag{2.37}$$

$$\tilde{\varphi}_a(\tilde{x}) \equiv k^{-(d-2)/2} Z_k^{1/2} \varphi_a(x) \tag{2.38}$$

where Z_k is the *field-renormalization* factor introduced in R_k and which is related to the factor n^{d_ϕ} in Eq.(2.7) for k small enough as

$$n^{d_\phi} \sim \frac{Z_k}{(k/\Lambda)^{(d-2)/2}}.$$

Of course, Γ_k is already dimensionless because of the choice of absorbing the factor $k_B T$ in the partition function definition Eq.(2.27). From this, it is straighforward to deduce a scale independent expression for the flow of the effective action:

$$
\partial_t \Gamma_k[\tilde{\varphi}] = \int_{\tilde{x}} \frac{\delta \Gamma_k}{\delta \tilde{\varphi}(\tilde{x})} \big(\tilde{x}_\mu \tilde{\partial}_\mu + D_\varphi^k \big) \tilde{\varphi}(\tilde{x})
$$
$$
+ \frac{1}{2} \int_{\tilde{x},\tilde{y}} (2d - 2D_\varphi^k + \tilde{x}_\mu \tilde{\partial}_\mu^{\tilde{x}} + \tilde{y}_\mu \tilde{\partial}_\mu^{\tilde{y}}) \tilde{R}(|\tilde{x} - \tilde{y}|) \tilde{G}_k[\tilde{x}, \tilde{y}; \tilde{\varphi}], \tag{2.39}
$$

where $D_\varphi^k = (d - 2 + \eta_k)/2$, $R_k(x) = Z_k k^{d+2} \tilde{R}(\tilde{x})$ and $\eta_k = -\partial_t \log(Z_k)$ which is called the *running anomalous dimension* of the field. At the fixed point, η_k coincides with the critical exponent η, see Eq.(1.35). The factor Z_k can be fixed in various ways. Moreover, in order to compute, for example, the running anomalous dimension, its relation to Γ_k must be made explicit (see below). At the end of the day the way in which it is fixed, must not make any difference. However, since usually approximation schemes are employed to solve Eq.(2.39), this will introduce a dependence on the normalization procedure. More precisely, the fixed point of Eq.(2.39) is reached when $\partial_t \Gamma_k = 0$. After that, returning to dimension-full variables yields the fixed point equation:

$$
0 = \int_x \frac{\delta \Gamma_k}{\delta \varphi(x)} \big(x_\mu \partial_\mu + D_\varphi^k \big) \varphi(x)
$$
$$
+ \frac{1}{2} \int_{x,y} (2d - 2D_\varphi^k + x_\mu \partial_\mu^x + y_\mu \partial_\mu^y) R(|x - y|) G_k[x, y; \varphi]. \tag{2.40}
$$

In many cases it is useful to work in Fourier space. In Fourier variables, Eq.(2.36) reads:

$$\partial_t \Gamma_k[\varphi] = \frac{1}{2} \int_q \partial_t R_k(q) G_k[q, -q; \varphi]. \tag{2.41}$$

It is convenient to represent Eq.(2.41) by the diagram shown in Fig. 2.6.

$$\partial_t \Gamma_k = \frac{1}{2} \bigcirc\!\!\!\!\!\times$$

Figure 2.6: Diagramatic representation of Wetterich's equation.

For many purposes it is useful to work in a uniform field. This is because vertex and propagators, when considering an uniform field, conserve momenta. In general, the vertex $\Gamma_k^{(n)}$ is defined as

$$\Gamma_k^{(n)}[x_1, \ldots, x_n; \varphi] \equiv \frac{\delta^n \Gamma_k}{\delta\varphi(x_1)\ldots\delta\varphi(x_n)}. \tag{2.42}$$

It proves useful to define this quantity in a homogeneous field configuration as $\Gamma_k^{(n)}(x_1, \ldots, x_n; \phi) \equiv \Gamma_k^{(n)}[x_1, \ldots, x_n; \varphi(x) \equiv \phi]$. In a uniform field the system is translational invariant implying conservation of momenta (the same applies for the propagators). Because of this, it is useful to factorize a Dirac's delta function from the definition of the Fourier transform of $\Gamma_k^{(n)}$ and to consider vertex as a function of $n-1$ momenta and propagators as a function of just one momenta. This is:

$$(2\pi)^d \delta(\sum_{i=1}^{n} p_i)\Gamma_k^{(n)}(p_1, \ldots, p_{n-1}; \phi) \equiv \int_{x_1,\ldots,x_n} e^{-i\sum_{i=1}^{n} x_i \cdot p_i}\Gamma_k^{(n)}(x_1, \ldots, x_n; \phi), \tag{2.43}$$

and

$$(2\pi)^d \delta(q+q')G_k(q; \phi) \equiv \int_{x_1,x_2} e^{-i(q\cdot x_1 + q'\cdot x_2)}G_k(x_1, x_2; \phi). \tag{2.44}$$

where it is clear that $G_k(q; \phi) \equiv G_k(q, -q; \phi)$.

With these definitions, differentiating Eq.(2.36) twice with respect to the field at points x_1 and x_2, evaluating in a uniform field and Fourier transforming, yields

$$\partial_t \Gamma_k^{(2)}(p; \phi) = -\frac{1}{2}\int_q \partial_t R_k(q)G_k(q; \phi)\Gamma_k^{(4)}(q, p, -q; \phi)G_k(q; \phi)$$

$$+ \int_q \partial_t R_k(q)G_k(q; \phi)\Gamma_k^{(3)}(q, p; \phi)G_k(p+q; \phi)\Gamma_k^{(3)}(p+q, -q; \phi)G_k(q; \phi), \tag{2.45}$$

whose diagramatic representation is shown in Fig. 2.7 (although these diagrams

can also represent the non-uniform case, the fact that we don't have momenta conservation make the calculations more clumsy).

$$\partial_t \Gamma_k^{(2)} = -\tfrac{1}{2}$$

Figure 2.7: Diagramatic representation of the NPRG flow equation for $\Gamma_k^{(2)}$.

This diagramatic representation helps to visualize and to compactify expressions. Lines represent propagators with a definite momenta, the cross represents the time derivative of the regulating function, $\partial_t R_k$, and the black dots with n lines attached to it represent the n point proper vertex, $\Gamma_k^{(n)}$ which impose momentum conservation.

Now, we return to the point of fixing the Z_k factor which appears in Eq.(2.39). To fix its value, it is customary to impose, for example:

$$\left. \frac{\mathrm{d}\Gamma_k^{(2)}(p; \phi_0)}{\mathrm{d}p^2} \right|_{p=0} = 1, \tag{2.46}$$

where ϕ_0 is the value at which the potential exhibits a minima, this is $\Gamma_k^{(1)}(\phi_0) = 0$. However, this is just a convention and other fixation could be used.

Before continuing, notice that there are some subtleties or precisions to be made when doing these computations. For example, is not the same to consider R_k as a function of two variables and Fourier transform it, and to consider it as a function of one variable before transforming it, say $x - y$. The difference of these two definitions is proportional to a Dirac's delta. Up to this point R_k was never considered as a function of two variables. Nevertheless, it can be found in the literature in both ways. The same point can be addressed for the $\Gamma_k^{(n)}$, since the effective action is translational invariant (or x-independent), one can choose a reference point to be zero and consider $\Gamma_k^{(n)}$ as a function of $n-1$ space points. The difference of the Fourier transform of these two interpretations is, again, a Dirac's delta times a $(2\pi)^d$ factor. One last precision to be made is that one can work with momentum dependent or space dependent fields, and when doing this there is an ambiguity when refering to $\Gamma_k^{(n)}(q_1, \ldots, q_n)$ which

can be interpreted as the Fourier transform of $\Gamma_k^{(n)}(x_1, \ldots, x_n)$ or as

$$\frac{\delta^n \Gamma_k}{\delta\varphi(q_1) \ldots \delta\varphi(q_n)}.$$

In any case, these two definitions are equivalent up to a factor $(2\pi)^d$ to some power, and one just needs to keep track of this factors. To avoid any ambiguity, in this work the convention used is to consider the regulator as a function of just one space variable, $\Gamma_k^{(n)}$ in uniform field as a function of $n-1$ variables in Fourier space as defined in Eq.(2.43).

Wetterich's equation for Γ_k involves $\Gamma_k^{(2)}$ and equation for $\Gamma_k^{(2)}$ involves $\Gamma_k^{(3)}$ and $\Gamma_k^{(4)}$. This is a general property: when computing the flow of $\Gamma_k^{(n)}$ by differentiating n times with respect to the field, one obtains an equation which involves all vertices up to $\Gamma_k^{(n+2)}$. This leads to an infinite tower of equation which cannot be closed without extra information. Even though Eq.(2.41) is an exact evolution equation, in general, there are no known solutions and it is necesary to employ approximation schemes to tackle it.

In the next section some of these approximation schemes are presented, but before doing so let us remark some features of the NPRG equation, Eq.(2.41).

First of all, what should be noticed is that the role of the regulating term is to interpolate between the Hamiltonian and the Gibbs free energy. This is done by considering more and more fluctuations as the scale k of the regulator is lowered, starting from $k = \Lambda$, where all modes are frozen by saying that $R_\Lambda(q) = \infty$ for all q, and going to $k = 0$, where all fluctuations have been taken into account. Indeed, it is clear that at $k = 0$, $R_k(q) = 0$ for any q, and all function become the standard thermodynamic functions ($\Gamma_k \to$ Gibbs free energy, $W_k \to$ Helmholtz free energy, etc.). On the other hand, Eq.(2.36) is an exact functional integro-differential evolution equation whose initial condition at scale $k = \Lambda$ is $\Gamma_{k=\Lambda}[\varphi] = H[\mathbf{J}_0, \varphi]$, see App.A. Otherwise said, the initial condition for the effective action is just the microscopic Hamiltonian.

The effective action, as its name well states, describes an effective system for which all dependence in scales above k have been washed out. This is because of the factor $\partial_t R_k$ in the flow equation, which only allows fluctuations with momenta $q \lesssim k$ to contribute to the flow at scale k. This is, at scale k fluctuations above this scale have already been integrated into the effective action. As a consequence of this, if there is some physical mass scale m (not the mass scales that are in the microscopic action/Hamiltoninan) in the theory but we are already at scales $k^2 \ll m^2 < \Lambda^2$, then we are not able to *see* or *know*

of the existence of a *microscopic* mass. To understand this better, consider Ocatvio Ocampo's painting *Visiones del Quijote* in Fig. 2.8. At first glance it is a painting of Don Quixote, however, taking a closer look one can see that there are smaller structures. The big Quixote image has a length scale that can be associated with a small physical mass m. However, the size of the smaller structure (this is Don Quixote himself, Sancho Panza, Rocinante, some windmills, etc.) are associated with a bigger mass scale M which, when looked from far cannot be recognized and the only scale surviving is the one of Don Quixote's portrait, this is to say m. However, these smaller scales (bigger mass M) contribute each in its own way, to build up the portrait (for example, Rocinante's legs give rise to an old and marked neck, Don Quixote's spear forms a long and thin moustache, the windmills and wind conform Quixote's hair, etc.). From far or squinting the eyes, which amounts to perform the renormalization group procedure to scales larger than the scales of the bigger structures ($k < m$), one can barely tell whether these smaller scales (M) are really there and, if so, how are they.

Figure 2.8: *Visiones del Quijote* painted by Octavio Ocampo in 1989.

On top of this ultraviolet regularization, the regulator at $k \neq 0$ plays the role of a mass for fluctuations with momenta $q \lesssim k$ and therefore removes infrared divergences. Since everything is regular, the consequences of this property altogether with the previous features is that at finite k it allows for

a power expansions in, for example, $\nabla\varphi$. This is important when looking at the long-range physics, where the field varies slowly, and is at the heart of the Derivative Expansion (DE) approximation scheme to be described in the next section.

One last consideration is that it may happen that the microscopic Hamiltonian and the measure are invariant under a certain symmetry. If on top of that we consider a regulating term invariant under this symmetry (this may depend on the regulator, R_k, chosen), then the effective action Γ_k will enjoy the same symmetry property for any k. This is the case of isometries for the regulators mentioned. When the regulating term is not invariant under the considered symmetry, then the symmetry will be broken by this regulating term at any finite k. In Chapter 4 this situation will be worked out for the case of scale and conformal symmetries.

2.3 Approximations and General Results

As stated previously, in general it is not possible to solve Eq.(2.41) exactly. One is then forced to use approximations in order to say something about the physics of the system. One could expand the effective action in powers of the fields up to some power, this is known as *Field Expansion* (FE). Another possibility, named after the authors, is the *Blaizot-Méndez-Wschebor approximation* (BMW) that consists in power expanding the vertex functions, in the exact flow equation, in the internal momentum. The *Derivative Expansion* (DE), which is the main approximation used in this thesis, consists in truncating the momentum-dependence of the vertices (otherwise stated, it consists in ansatz for the effective action which involves all terms, compatible with the symmetries of the system, with up to a given number of derivatives over the field). Let us mention two other approximations are the famous ϵ-expansion and the $\frac{1}{N}$-expansion (or large N approximation). In this subsection a description of the general procedure of these approximations is presented.

2.3.1 Derivative Expansion

When one is interested in the long-range physics, it seems natural to think that Taylor expanding and truncating in momenta will be a good approximation. This is the main idea behind the DE. This approximation is well-suited for studying the long-distance properties of the system since higher momentum dependence are neglected, which is to say. In fact, it proved to be a good

approximation scheme for $\mathbb{Z}_2$ and $O(N)$ models(see for example, [9, 60, 13, 12]). Moreover, this approximation scheme has been shown to give the exact critical exponents at leading orders in the limit $N \to \infty$ (see below), $\epsilon = 4 - d$ (see below) and $\epsilon = d - 2$ (for $N \geq 2$), see for example [9, 61, 10].

We discuss this approximation in the context of the $\mathbb{Z}_2$ and $O(N)$ models. The approximation consists in taking the most general ansatz for the effective action Γ_k, with a general dependence on the field $\rho = \frac{\varphi^2}{2}$ ($\mathbb{Z}_2$ model) or $\rho = \sum_a \frac{\varphi_a \varphi_a}{2}$ ($O(N)$ model), but up to a certain number of derivatives.

The first level of approximation is called *Local Potential Approximation* (LPA) and it is the $\mathcal{O}(\partial^0)$. For the $\mathbb{Z}_2$ model, this consists in taking as ansatz for the effective action the potential plus an unrenormalized kinetic term (this is the most basic):

$$\Gamma_k[\varphi] = \int_x \left\{ \frac{1}{2} (\nabla \varphi)^2 + U_k(\rho) \right\}, \tag{2.47}$$

and similarly for the $O(N)$ model:

$$\Gamma_k[\varphi] = \int_x \left\{ \frac{1}{2} \sum_a \nabla \varphi_a \cdot \nabla \varphi_a + U_k(\rho) \right\}. \tag{2.48}$$

The $\mathcal{O}(\partial^2)$ of the DE, consists in considering the φ dependence of all terms with two gradients. In the Ising case it leads to the ansatz:

$$\Gamma_k[\varphi] = \int_x \left\{ \frac{Z_k(\rho)}{2} (\nabla \varphi)^2 + U_k(\rho) \right\}. \tag{2.49}$$

At this point a remark must be made, $Z_k(\rho)$ is the customary name given to the function in front of the kinetic term, but it is important to keep in mind that it is a different entity than the renormalization factor whose standard nomenclature is the same Z_k. In the $O(N)$ model, the ansatz for the effective action takes the form:

$$\Gamma_k[\varphi] = \int_x \left\{ \frac{Z_k(\rho)}{2} \sum_a \nabla \varphi_a \nabla \varphi_a + \frac{Y_k(\rho)}{4} (\nabla \rho)^2 + U_k(\rho) \right\}. \tag{2.50}$$

We recall that $\rho = \sum_a \frac{\varphi_a \varphi_a}{2}$ which is the invariant quantity under the $O(N)$ symmetry. At odds with the $N = 1$ case, which is the same as $\mathbb{Z}_2$, there are two independent tensorial structures of indices with two gradients, δ_{ab} and $\varphi_a \varphi_b$. The expressions at order $\mathcal{O}(\partial^4)$ are given in Chapter 3.

The derivative expansion was known to produce results that were in good agreement with the common knowledge, and in many cases it seemed much more powerful and suited than other techniques. However, until recently there

was no compelling argument to explain this apparent good convergence properties. It was argued that the NPRG equations have a dressed one-loop structure where all propagators are regularized in the infrared, ensuring the smoothness of the vertices as a function of momenta and allowing such an expansion. Moreover, the loop diagrams include the derivative of the regulating function $\partial_t R_k(q)$ in the numerator. This implies that all internal momenta are dominated by the momentum range $q \lesssim k$ and as a consequence an expansion in all momenta (internal and external) gives equations that couple only weakly to the regime of momenta $p \gg k$. The validity of this approximation has been discussed in [62, 63].

In each model the radius of convergence of the expansion in momenta, which is related to the nearest pole on the complex plane of p^2, is different. For the $O(N)$ models it has been shown to be of the order $q^2/k^2 \simeq 4 - 9$ (depending if we are in the symmetric or broken phase) [12]. This is consistent with the fact that DE shows a rapid apparent convergence at low orders for $O(N)$ models. In fact, the DE has been pushed with success to the order $\mathcal{O}(\partial^4)$ [60] and $\mathcal{O}(\partial^6)$ [12] for the Ising universality class, giving excellent results that improve significantly with the order of the DE. This allowed to understand why this approximation scheme, in the context of the NPRG and for $O(N)$ models, has rather good convergence properties with a small parameter of order $\sim \frac{1}{4}$ or smaller.

It is worth to mention that the DE is an expansion around zero momenta. In presence of the regulator, the physics of the system at criticality is recovered once $k \ll p \ll \Lambda$. However, we can extract the properties defined at zero momentum like critical exponents, among other universal and non-universal quantities (see for example [9]) from the regime $p \ll k$. The BMW is another method which does not rely on an expansion around zero momenta and, consequently, enables the recovery of non-vanishing momentum properties. For details on this method see [62].

2.3.2 ϵ-Expansion

The ϵ-Expansion is an expansion around the upper critical dimension. This approximation was first introduced by Kenneth Wilson and Michael Fisher in 1972 [3]. They managed to find a family of fixed points for the RG equations which controlled the physics of a wide variety of phase transitions. They were able to do it by extending the dimension d to the complex plane. In particular, they could solve the equations when expanding and truncating

them in a parameter

$$\varepsilon = D_{up} - d,$$

with D_{up} the upper critical dimension (which is 4 for the Ising and $O(N)$ models).

The first order approximation can be obtained by fixing vertices and propagators, in the *right hand side* of Eq.(2.41), as their *tree-level*[1] expressions. This means that using as microscopic Hamiltonian[2],

$$H = \int_x \left\{ \frac{1}{2} (\nabla \phi)^2 + \frac{r}{2} \phi^2 + \frac{u}{4!} \phi^4 \right\} \tag{2.51}$$

and evaluating the vertex functions at zero field, these later become:

$$\Gamma_k^{(2,tree)}(p) = r + p^2, \tag{2.52}$$

$$\Gamma_k^{(3,tree)}(p_1, p_2) = 0, \tag{2.53}$$

$$\Gamma_k^{(4,tree)}(p_1, p_2, p_3) = u, \tag{2.54}$$

$$\Gamma_k^{(n,tree)}(p_1, \ldots, p_{n-1}) = 0 \qquad n \geq 5. \tag{2.55}$$

Finally, it is worth to mention that the first order correction of the ϵ-expansion is scheme-independent or independent of the choice of regulator for universal quantities. In relation with the tree-level diagrams mentioned above there is a way of organizing the perturbative diagrams known as the *loop expansion*. In fact the linear behaviour in ϵ is obtained in the NPRG using *tree-level* expressions for the vertex and propagators because of the, already, *one-loop* structure of Eq.(2.41) has. Indeed, the first correction in ϵ is obtained from perturbation theory with *one-loop* diagrams.

For corrections higher than linear in ϵ, it is required more than *one-loop* diagrams. For the Ising model universality class, the first corrections in ϵ for

---

[1]In the perturbation theory sense.
[2]This is justified because of universality.

the critical exponents η and ν are[1] [64]:

$$\eta = \frac{\epsilon^2}{54} + \mathcal{O}(\epsilon^3), \tag{2.56}$$

$$\nu = \frac{1}{2} + \frac{\epsilon}{12} + \frac{7\epsilon^2}{162} + \mathcal{O}(\epsilon^3). \tag{2.57}$$

The expressions for the $O(N)$ models are [64]:

$$\eta = \frac{N+2}{2(N+8)^2}\epsilon^2 + \mathcal{O}(\epsilon^3), \tag{2.58}$$

$$\nu = \frac{1}{2} + \frac{N+2}{4(N+8)}\epsilon + \frac{(N+2)(N^2+23N+60)}{8(N+8)^3}\epsilon + \mathcal{O}(\epsilon^3), \tag{2.59}$$

and they reduce to the Ising model ones, Eq.(2.56), for $N = 1$. In [64] more quantities, such as the critical exponent ω, as well as other approximation schemes are reviewed.

2.3.3 $\frac{1}{N}$-Expansion

When considering the $O(N)$ model, there are some loops that involve also a sum over internal indices and therefore imply for each of them a factor of N. Since at the fixed point the size of couplings scales with different powers of N, it is necessary to make explicit a N-dependence in the couplings in order to take the limit $N \to \infty$. To be explicit, for a microscopic Hamiltonian of the form
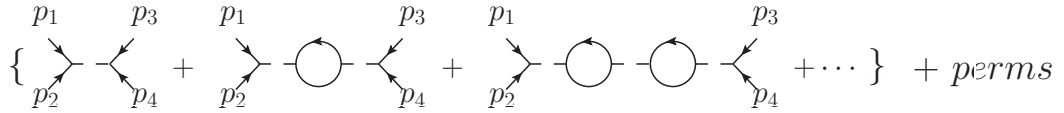
$$H = \int_x \left\{ \frac{1}{2}\sum_a \nabla\phi_a \nabla\phi_a + \frac{r}{2}\sum_a \phi_a^2 + \frac{u}{4!}\left(\sum_a \phi_a^2\right)^2 \right\}, \tag{2.60}$$

one takes the limit of $N \to \infty$ at constant $\hat{u} \equiv uN$. The leading diagrams contributing to $\Gamma^{(2)}$ and $\Gamma^{(4)}$, at zero field, are shown in Figs.2.9-2.10.
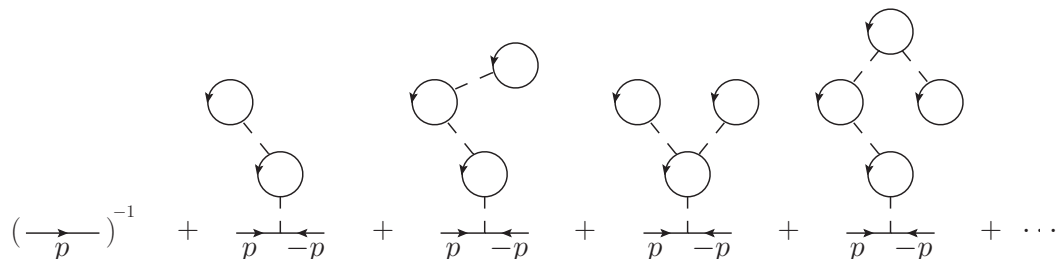
Figure 2.9: Leading contribution to $\Gamma^{(2)}$ in a N^{-1} expansion.

---

[1]The computation of the critical exponents η and ν up to ϵ^2 involves *two-loops* diagrams.

$$\{ \rangle\!-\!\langle + \rangle\!-\!\bigcirc\!-\!\langle + \rangle\!-\!\bigcirc\!-\!\bigcirc\!-\!\langle + \cdots \} + perms$$
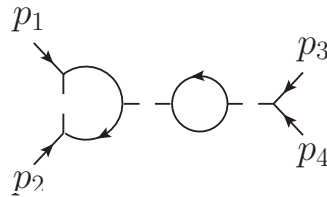
Figure 2.10: Leading contribution to $\Gamma^{(4)}$ in a N^{-1} expansion. The fourth momentum is fixed by momentum conservation $p_4 \equiv -(p_1 + p_2 + p_3)$. The propagators are to be understood as already including all contributions depicted in Fig.2.9.

where the 4 point interaction is:

$$\rangle\!-\!\langle = \frac{\hat{u}}{3N}\delta_{i_1,i_2}\delta_{i_3,i_4}.$$

The $\frac{1}{N}$-Expansion is a way of organizing the diagrams to compute just a given number of them, and to consider this as a good approximation. It consists in adding all perturbative diagrams up to a given power in $\frac{1}{N}$.

Since each interaction comes with a factor $\frac{1}{N}$, at leading order one needs to construct diagram with the type of loops that do contribute with a factor of N. Otherwise stated, diagrams with loops not contributing with a factor of N, like the one in Fig. 2.11, are subleading compared to diagrams which do contribute with this factor. In Chapter 5 this approximation is used to compute the

Figure 2.11: Subleading contribution to $\Gamma^{(4)}$ in a N^{-1} expansion with respect to contributions of Fig. 2.10.

scaling dimensions of some operators in relation to the presence of conformal invariance. We can use this approximation scheme in the NPRG framework by introducing an infrared regulator in propagators in order to deduce the flow and the scaling dimensions of the couplings (or of the operators associated with the couplings):

$$\frac{1}{q^2 + r} \rightarrow \frac{1}{q^2 + r + R_k(q)} \tag{2.61}$$

and study the running of the various renormalized couplings when varying the regulator (for example, the running of r^k defined as $\Gamma^{(2)}_{k,i_1 i_2}(p=0) \equiv r^k \delta_{i_1 i_2}$).

The critical exponents η, ν and ω (first correction to the leading scaling behaviour ν^{-1}) in dimension $d=3$, have been computed up to order $\mathcal{O}(N^{-3})$ for η and to order $\mathcal{O}(N^{-2})$ for ν and ω, see [64]. Their estimates are given by:

$$\eta = \kappa\left(1 - \frac{8}{3}\kappa\left[1 + \frac{3}{512}\Upsilon\kappa\right]\right) + \mathcal{O}(N^{-4}), \tag{2.62}$$

$$\nu = 1 - \kappa\left(4 - \left[\frac{56}{3} - \frac{9\pi^2}{2}\right]\kappa\right) + \mathcal{O}(N^{-3}), \tag{2.63}$$

$$\omega = 1 - \kappa\left(8 - 2\left[\frac{104}{3} - \frac{9\pi^2}{2}\right]\kappa\right) + \mathcal{O}(N^{-3}), \tag{2.64}$$

where $\kappa = \frac{8}{3\pi^2 N}$ and $\Upsilon = \frac{797}{18} - \zeta(2)\left(27\log(2) - \frac{61}{4}\right) + \zeta(3)\frac{189}{4}$. In Chapter 3 we compare the estimates of these exponents for the values of $N=5$, $N=10$, $N=20$ and $N=100$ to our implementation of the DE at order $\mathcal{O}(\partial^4)$. For a review on this approximation scheme see [65].

Chapter 3

Derivative Expansion for the $O(N)$ Model at order $\mathcal{O}(\partial^4)$

> Les grandes personnes aiment les chiffres. Quand vous leur parlez d'un nouvel ami, elles ne vous questionnent jamais sur l'essentiel. Elles ne vous disent jamais : « Quel est le son de sa voix ? Quels sont les jeux qu'il préfère ? Est-ce qu'il collectionne les papillons ? »
>
> — Antoine de Saint-Exupéry, *Le Petit Prince*

In this chapter we study the $O(N)$ model by means of the derivative expansion. We compute, for the first time, the critical exponents η, ν and ω for several values of N at order $\mathcal{O}(\partial^4)$ of the DE. The results obtained are in very good agreement with reported results obtained by other methods and, in fact, compete with the most precise of the literature. Most of this chapter is based on an article already submitted for publication, see [18].

Part of the motivation for doing this computation is that for $N = 2$ a controversy exists, from a long time now, about the actual value of the heat capacity critical exponent α, or ν according to the scaling relation in Eq.(2.23). Experiments [15] and predictions of Monte Carlo simulations [16], which is the most accurate estimation of ν, are in disagreement beyond error bars. During the course of this work, a precise conformal bootstrap computation appeared [19]. Up to that work, the conformal bootstrap was not able to refute one of the positions in the dispute. Our findings, as well as the conformal bootstrap ones, align with those of Monte Carlo simulation and refute the experiments.

In the first section of this chapter, we present for some values of N the different universality classes to which the $O(N)$ models belong. Afterwards, the order $\mathcal{O}(\partial^4)$ of the derivative expansion for the $O(N)$ models is discussed

and the algorithmic procedure of the DE is depicted. A proposal for the estimation of central values and error bars within the DE is presented in a third section altogether with the analysis of the available data for the $N = 1$ case from [12]. The results obtained for the critical exponents η, ν and ω for general N values are presented in a fourth section.

3.1   Physics of $O(N)$ Models

As explained in Chapter 2, very different physical systems exhibit an identical power law behaviour of their thermodynamic properties in the critical regime (i.e. close to their second order phase transition). This phenomenon, called universality, is what ultimately motivates the study of $O(N)$ models. When the long distance physics of two systems is governed by the same fixed point, they are said to belong to the same universality class.

The $O(N)$ models consists of models for which the order parameter is an N component field and the microscopic hamiltonian is invariant under orthogonal transformations of the N components. There are many physical systems, in particular for small values of N, which are in the universality class of an $O(N)$ model. We comment here briefly about the physics of a system in the universality classes of the $O(2)$ model, also called XY model; the $O(3)$ case or Heisenberg model and the $O(0)$ model, which must be understood as evaluating the RG flow equations at $N = 0$. We refer to [66] for a review on many physical properties of these models. The $O(1)$ model is nothing but the $\mathbb{Z}_2$ model whose universality class was discussed in Chapter 1.

3.1.1   Isotropic Ferromagnet or the $O(3)$ Model

The canonical example for systems exhibiting a critical behaviour in the universality class of the $O(3)$ model is that of an isotropic ferromagnet. A ferromagnet is a material which exhibit spontaneous magnetization below a certain critical temperature, denominated Curie temperature. Let us consider a material with a crystal structure where the different atoms or molecules have a magnetic moment. The different "units" in the crystal structure interact with each other via this magnetic moment through what is usually called *exchange interaction*. This interaction is in fact a product of a quantum mechanical effect, namely the *Pauli exclusion principle*, and can be ferromagnetic or antiferromagnetic [67, 68]. Pauli exclusion principle consists in that the wave functions describing the state of identical fermions (particles with half-integer

spin value) must be antisymmetric under the exchange of two of them and, therefore, particles can not be in the same quantum mechanical state [this is at odds with bosons (particles with integer spin value)].

In a nutshell, if the space part of the wave function describing two such fermion is symmetric the spin part must be antisymmetric and vice versa. If fermions are not interacting with each other, the energy of these two states is the same. However, for electrons interacting via a Coulomb interaction, the energy levels of the space-symmetric and the space-antisymmetric states are modified due to a factor called *exchange integral* which can be either positive or negative. The net effect of this interaction, when the exchange integral leads to a ferromagnetic behaviour (energy level of the spin-symmetric wave function is lower than the spin-antisymmetric one), is that of aligning the spins in the same direction, while it anti-aligns the spins when the exchange integral leads to an antiferromagnetic behaviour (energy level of the spin-symmetric wave function is higher than the spin-antisymmetric one). Moreover, this exchange integral depends on the overlap between the space parts of the wave function for each fermion and, consequently, it is short ranged. This is at odds with the magnetic dipole interaction which is a long-range interaction but it is much less intense than the exchange interaction, in ferromagnetic or antiferromagnetic materials.

The fermions in the case of ferromagnetic materials may be, for example, unpaired electrons in the valence band. This is the case of iron or cobalt. However, the underlying physics can not be reduced to valence band since, for instance, copper is not ferromagnetic although it has one unpaired electron and depending on the crystal structure iron may not be ferromagnetic.

To fix ideas, suppose the material is ferromagnetic. If the temperature is high enough, the thermal noise in the material ends up spoiling this tendency to order and the system does not show a macroscopic magnetization. We say that, in this case, the system isin the disordered or high temperature phase, dominated by entropy. However, when the temperature is low enough, the tendency to align due to the exchange interaction prevails over the thermic noise and the system exhibits a macroscopic effect of magnetization. In that case we say that the system is in the ordered or low temperature phase.

The simplest model of the previous system is to consider the magnetic moments as being quantum mechanical operators spins s located on the sites

of a lattice. The isotropic Hamiltonian for such a simple system will be

$$H_{qHm} = -\frac{1}{2} \sum_{r,r'} J(r,r') s(r) \cdot s(r'), \tag{3.1}$$

where $J(r,r')$ is the exchange interaction that falls with the separation of r and r' and the subscript qHm stands for *quantum Heisenberg model*, because this model is the quantum mechanical Heisenberg model in absence of an external magnetic field. When the interaction is $J > 0$ it is said to be a ferromagnetic interaction, while is antiferromagnetic when it is $J < 0$. In reality it can happen that it is ferromagnetic for some pairs of spins and antiferromagnetic for others, but let us just consider the case $J > 0$. When there are no favoured directions, as is the case of Eq.(3.1) we have an isotropic magnet. However, sometimes there may be a favoured direction due to the underlying crystal structure and the interaction is not isotropic. If the interactions tend to align spins in some direction, we are in the case of a uniaxial ferromagnet. When the interaction favours a certain plane, we are in an easy plane ferromagnet. Here we consider the case were there are no preferred direction and we may simplify the model to being with fully rotational symmetry (i.e. it depends on the products $s(r) \cdot s(r')$). Moreover, at finite temperature, thermal fluctuations dominate with respect to quantum mechanical ones and we may consider the spins to be a 3 component vector with fixed length. In this case the Hamiltonian takes the form:

$$H_{cHm} = -\frac{1}{2} \sum_{r,r'} J(r,r') \vec{S}(r) \cdot \vec{S}(r'), \tag{3.2}$$

where now the $\vec{S}$ are classical vectors with 3 components and where cHm stands for *classical Heisenberg model*. This simplified model is, of course, in the universality class of the $O(3)$, since at criticality its microscopic features, as for example the structure of the underlying lattice, can be neglected. Moreover, there may be anisotropic interactions that are subdominant at large distances and the model is still in the same universality class as the $O(3)$ model. Of course, these features will affect non-universal quantities such as the critical temperature or, more generally, the equation of state.

3.1.2 ^4He Fluid-Superfluid or the $O(2)$ Model

The $O(2)$ universality class governs the critical physics of an easy plane ferro-magnet, briefly described above, where the classical spins live on a plane and the Hamiltonian has the form of Eq.(3.2). However, let us discuss another physical system whose critical behaviour is also governed by the $O(2)$ fixed point. This is the case of superfluid Helium-4. Atoms of Helium-4 are bosons and it is important not to confuse it with Helium-3 atoms that also exhibit a transition to a superfluid phase but since they are fermions its phenomenology is more alike the Bardeen-Cooper-Schrieffer theory of superconductivity. Another interesting fact to highlight about Helium-4 is that its transition is along a line, see Fig.3.1, instead of being a point (as is the case of the liquid-vapour critical point, see Chapter 1). This one feature ease a little the experimental setup.
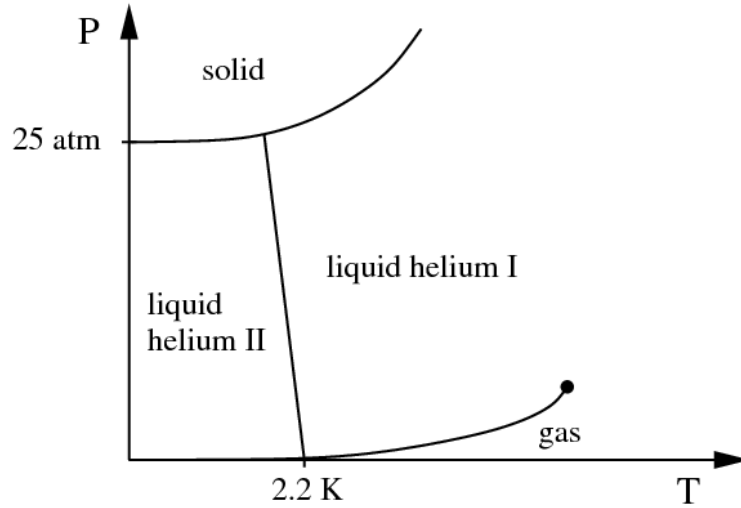
Figure 3.1: Schematic representation of the phase diagram of ^4He at low temperatures (figure from [69]).

Consider Helium-4 in a fluid state (disordered or high temperature phase). Its bosonic nature means that when lowering the temperature, a macroscopic part of the atoms composing the fluid can access the same quantum state, forming a condensate similar to what is called a Bose-Einstein condensate. The main difference with the Bose-Einstein condensate being the existence of interactions which, if no other ingredient is present, would prevent superfluidity due to collisions between excited and ground state atoms. An argument, due to Landau [70], shows that if the velocity of a fluid in such a state is less than a critical value given by

$$v_c = min_p \left\{ \frac{\varepsilon_p}{p} \right\},$$

where ε_p is the energy of an excited state with momentum p, the system can not dissipate since no other state can be excited. However, it happens that the condensate has a gapless mode with $\varepsilon_{p=0} = 0$, also called a Goldstone mode. Nevertheless, for Helium-4 the dispersion relation of the Goldstone mode is linear yielding a non-zero v_c and, consequently, Helium-4 exhibits no dissipation at its condensate state for velocities below this v_c, i.e. it is a superfluid state (ordered or low temperature phase).

Consider the wave function $\Psi(r)$ describing the condensate state or the superfluid phase. This wave function is a complex number, which for many purposes we can regard as it being a classical field. Given the fact that the Helium-4 atoms have a short-range repulsion, we can regard them as being localized in a lattice or being described with a Guínzburg-Landau type Hamiltonian, see Eq.(2.60). Now, it happens that the transition to the disordered phase is driven by fluctuation on the phase of $\Psi(r)$ rather than its modulus. Therefore, taking all this into account, we can regard $\Psi(r)$ as being a classical field describing the physics of a two-component fixed length vectors located on a lattice. This transition is in the same universality class as the one of the easy plane ferromagnet and in the same universality class as the $O(2)$ model.

3.1.3 Self Avoiding Linear Polymer Chains or the $O(0)$ Model

A linear polymer is a macromolecule which is composed of many repeated units, called monomers, in a long and flexible chain structure. Examples of linear polymers are teflon or nylons. When the polymer is inside a dilute solvent they can have many types of structures. In particular, when the interaction between different units in the chain is repulsive, the polymer does not form loops of monomers. However, when the interaction is attractive enough the chain tends to form a compact molecule. It so happens that the transition between these two phases is a continuous one and it is observed to have non-trivial critical exponents. The polymer in the linear or extended phase (the disordered or high entropy phase) can be represented by a random walk in a lattice for which intersections are forbidden. This constraint originates from the repulsion of monomers (called steric repulsion) and is an important interaction to take into account when modelling its dynamics. However, if the probability for intersections is small enough, we can neglect all interactions. Imagine that we are in that circumstance and consider a walk of length $\mathcal{N}$ in a lattice with lattice spacing a. Consider the walk being a set of vectors $\{\mathbf{r}_i\}$ with

$i = 1, \ldots, \mathcal{N}$ and $|\mathbf{r}_i| = a$. If we were to compute the mean square distance between end points of the chain it would be

$$\langle R^2 \rangle = \Big\langle \Big(\sum_{i=1}^{\mathcal{N}} \mathbf{r}_i \Big)^2 \Big\rangle.$$

Since the interactions can be neglected, any step of the walk r_i can be in any direction and, therefore, it is:

$$r_{rsm} \equiv \sqrt{\langle R^2 \rangle} = a\mathcal{N}^\nu, \tag{3.3}$$

with $\nu = 1/2$. It can be shown that for a model of the polymer at dimensions $d > 4$, the repulsive interaction is in fact irrelevant and that, in those dimensions, this critical exponent for a polymer chain is indeed $\nu = 1/2$. However, at dimensions $d < 4$ the interaction cannot be neglected and the critical exponents are no longer Gaussian.

Paul Flory derived an exact equation for the critical exponent ν [71] which, for $d < 4$, reads:

$$\nu = \frac{3}{d+2}. \tag{3.4}$$

This equation recover not only the $d = 4$ behaviour but also, the $d = 2$ exact behaviour and is therefore a good educated guess, at least. Flory's theory relies on the assumption that one can regard the polymer as composed of an ideal chain and a dilute gas of monomers. Although reasonable, this theory does not model properly the polymer physics. The reasons it fails to give the correct result is that the model overestimates the repulsion between monomers because it does not take into account correlation of monomers along the chain. Also, the theory overestimates the contribution from entropy by considering an ideal chain. These two contributions tend to compete and the resulting prediction is rather good due to error cancellation but, of course, the supposed exact result is not correct.

It was Pierre-Gilles de Gennes who made the correspondence between the self-avoiding random walks and the $O(N)$ model in the limit $N \to 0$ [72]. This matching can be done by choosing a particular Hamiltonian for $O(N)$ models which, at any order of a high temperature expansion, can be mapped to the self-avoiding random walks in the limit $N \to 0$. It happens that due to universality, if one is interested in studying the critical properties of this continuous phase transition, we can forget about the complicated microscopic theory of interactions of the monomers composing the polymers or the specific $O(N)$

Hamiltonian used for the de Gennes mapping, and study instead a standard $O(N)$ model which belongs to the same universality class.

3.2 Γ_k for $O(N)$ Models at Order $\mathcal{O}(\partial^4)$ of the Derivative Expansion and its Implementation

For $O(N)$ models the derivative expansion at *zeroth*-order (LPA) consists of just one unkown function, namely the potential $U(\rho)$. When considering the *first*-order (order $\mathcal{O}(\partial^2)$), two extra functions come into play, that are called $Z(\rho)$ and $Y(\rho)$ in the literature (see Eq.(2.50)). The *second*-order or order $\mathcal{O}(\partial^4)$, involves ten extra functions that we choose to name as $W_{ki}(\rho)$, with i ranging from 1 to 10. We recall that, in the $\mathbb{Z}_2$ case there are three independent functions associated with 4 derivatives, called $W_{ka}(\rho)$, $W_{kb}(\rho)$ and $W_{kc}(\rho)$ [60]. The ansatz considered[1] is then:

$$
\begin{aligned}
\Gamma_k[\varphi] \equiv \int_x \Bigg\{ & U_k(\rho) + \frac{Z_k(\rho)}{2}\big(\partial_\nu \varphi_a\big)^2 + \frac{Y_k(\rho)}{4}\big(\partial_\nu \rho\big)^2 + \frac{W_{k1}(\rho)}{2}\big(\partial_\mu \partial_\nu \varphi_a\big)^2 \\
& + \frac{W_{k2}(\rho)}{2}\big(\varphi_a \partial_\mu \partial_\nu \varphi_a\big)^2 + W_{k3}(\rho)\partial_\mu \rho \partial_\nu \varphi_b \partial_\mu \partial_\nu \varphi_b + \frac{W_{k4}(\rho)}{2}\varphi_b \partial_\mu \varphi_a \partial_\nu \varphi_a \partial_\mu \partial_\nu \varphi_b \\
& + \frac{W_{k5}(\rho)}{2}\varphi_c \partial_\mu \rho \partial_\nu \rho \partial_\mu \partial_\nu \varphi_c + \frac{W_{k6}(\rho)}{4}\big((\partial_\mu \varphi_a)^2\big)^2 + \frac{W_{k7}(\rho)}{4}\big(\partial_\mu \varphi_a \partial_\nu \varphi_a\big)^2 \\
& + \frac{W_{k8}(\rho)}{2}\big(\partial_\mu \varphi_a \partial_\mu \rho\big)^2 + \frac{W_{k9}(\rho)}{2}\big(\partial_\mu \varphi_a\big)^2\big(\partial_\nu \rho\big)^2 + \frac{W_{k10}(\rho)}{4}\big((\partial_\mu \rho)^2\big)^2 \Bigg\}.
\end{aligned}
$$
(3.5)

It is worth mentioning that the number of extra functions to be computed at order $\mathcal{O}(\partial^6)$ for $O(N)$ models is 48, see its ansatz at Appendix E. This is at odds with the $\mathbb{Z}_2$ case, where these are only 8, see [12]. Moreover, the total number of functions for the $O(N)$ at order $\mathcal{O}(\partial^4)$ is the same as the total number of functions for the $\mathbb{Z}_2$ case at order $\mathcal{O}(\partial^6)$, which is 13. The number of functions that needs to be computed, as well as the higher order vertex function from where they are derived, is an delicate issue since it is one of the major limitations at the time of implementing the approximation scheme at even higher orders, see below.

We describe here the algorithmic procedure to obtain the flow equation of

---

[1]Other equivalent ansatze, which are related to the one given by integration by parts, can be considered. The set of functions in the anstaz form a basis for the approximation at that order.

two functions, say $W_{k\,1}(\rho)$ and $W_{k\,2}(\rho)$. This will already include all the ingredients needed for the computation of any other quantity. Since these functions are related to operators with 2 fields being derived, both flow equations are obtained from the flow of $\Gamma_k^{(2)}$, where the gradients act on two fields only, in a homogeneous field configuration. So, we first deduce the exact flow equation for $\Gamma_k^{(2)}$ in a uniform field, this is

$$
\partial_t \Gamma^{(2)}(n_1, p, n_2) = -\frac{1}{2} \int_q \partial_t R_k(q) G_k(i, q, j) \left[\Gamma_k^{(4)}(j, q, n_1, p, n_2, -p, b) \right.
$$

$$
\left. -\Gamma_k^{(3)}(j, q, n_1, p, l) G_k(l, p+q, a) \Gamma_k^{(3)}(a, p+q, n_2, -p, b) \right] G_k(b, q, i). \quad (3.6)
$$

The left hand side, as well as the right hand side, of the expression can be split in two, a part proportional to $\delta_{n_1 n_2}$ and a part proportional $\varphi_{n_1}\varphi_{n_2}$, this amounts to recognize the colour structure (higher order vertex functions will have a richer colour structure). We now plug in the ansatz for Γ_k, Eq.(3.5), in this expression. Since $\Gamma_k^{(2)}$ is a function of p^2 and we are making an ansatz which involves at most 4 derivatives, we will see that within each colour structure, there is a further classification in different external momentum structure. For $\Gamma_k^{(2)}$ this is just a part independent of p, a part proportional to p^2 and a part proportional to p^4. Of course, for higher order vertices, the momentum structure will, also, be much richer.

The same can be said about the right hand side after performing angular integration (this is because there will be a priori terms proportional to $(p \cdot q)^m$). Moreover, the angular integral can always be performed analytically and it only remains the radial integral to be perform numerically, see Appendix F. The equations are found, after doing this classification, by noticing that each structure is independent and therefore, we can safely say that the part in the left hand side proportional to a particular structure of colour and momenta is equal to the corresponding one in the right hand side.

In the example considered so far, the left hand side can be written as:

$$
\delta_{n_1 n_2} \left(\partial_t U_k'(\rho) + p^2 \partial_t Z_k(\rho) + p^4 \partial_t W_{k\,1}(\rho) \right)
$$

$$
+\varphi_{n_1}\varphi_{n_2} \left(\partial_t U_k''(\rho) + \frac{p^2}{2} \partial_t Y_k(\rho) + p^4 \partial_t W_{k\,2}(\rho) \right). \quad (3.7)
$$

So, in this way we can obtain the β functions for the W_k's. It is to remark that before doing so, we need to introduce dimensionless variables as explained in Chapter 2. For more details on parameters specifications and the algorithm

involved in the numerical computations, see Appendix F.

Now, an important point must be mention. Typically, when implementing the derivative expansion, this procedure has been followed naively, plugging in the right hand side the expression for the vertex functions as they come from the ansatz Eq.(3.5). However, when we do this we are including, in the product of vertices, terms which add up to a power of momenta higher than the order of the derivative expansion being implemented. For instance, for the flow of $W_{k\,2}$ we could obtain contribution proportional to the product of two $W_{k\,8}$ which, in fact, is a contribution of order $\mathcal{O}(p^8)$. In the work presented in this chapter, as is done also in [12], we dropped all such terms since their correction is of higher order than the one under consideration. We will call the previous version of implementing the DE as *full*, and we call *truncated* version to the strict polynomial expansion case which only keep terms, coming from the product of vertices, up to the considered order of the DE.

If we are implementing the DE at order $\mathcal{O}(\partial^s)$, then the difference of the two forms is, at least, of order $\mathcal{O}(\partial^{s+2})$. So, choosing one method or the other is, in principle, just a matter of choice (see however, Chapter 6 for a short discussion regarding this). Nevertheless, we emphasize that although for small orders of the DE this may very well be a matter of choice, when going to higher orders of the DE, such as order $\mathcal{O}(\partial^6)$ for the Ising model or order $\mathcal{O}(\partial^4)$ for the $O(N)$ models, using the *full* version of the DE makes flow equations much bigger and hard to handle and, is not worth the trouble. We checked that the difference in the predictions at $\mathcal{O}(\partial^2)$ from one method and the other is, indeed, below the precision at that order. We also verified this at order $\mathcal{O}(\partial^4)$ of the $N = 1$ case, see Chapter 6.

One last observation: There are two reasons why the number of independent functions at a given order of the derivative expansion is important. First, the time requirements for computing quantities grows quadratically with the number of functions (the growth is quadratic at the very least, since in fact the size of equations also grow, see the next point). This is because to obtain some critical properties we need to compute the stability matrix, at the fixed point, which goes with the square of the number of fields. Second, and maybe most importantly, the procedure to obtain and simplify the flow equations to arrive at *friendly*[1] expressions requires manual manipulations on the deduction of intermediate expressions which may induce errors and which in the worst case scenario, are nearly impossible to detect. Therefore, the growth on the number

---

[1]Which are not so friendly anyway.

of functions of the derivative expansion is the biggest setback for computing higher orders within this approximation scheme. Nevertheless, in this respect one must emphasize that the time spent for computing a fixed point solution and critical exponents is of about a couple of hours in an average personal computer. This is to be compared with the most precise Monte Carlo simulation performed in the XY model [20] which took the order of 10^2 years of CPU time. Additionally, a recent result from the conformal bootstrap program [19], also for the $O(2)$ model, and with a precision similar (but smaller) than the one of [20] also took the order of 10^2 years of CPU time.

3.3 Estimating Central Values and Error Bars Within the Derivative Expansion: An Analysis of the Ising Model at Order $\mathcal{O}(\partial^6)$

We now review the Ising model universality class which is the only case where the order $\mathcal{O}(\partial^6)$ of the derivative expansion has been implemented. This was done in [12] altogether with a discussion of the convergence properties of the DE, in relation with the critical exponents ν and η. In that work, the family of regulators used are the ones in Eqs.(2.30-2.32). In Fig.3.2 we show the curves presented in [12] for critical exponents η and ν in terms of the regulator parameter α for the exponential regulator E_k. The fact that there exists results at such a high order of the DE is fundamental for the present analysis and, as we shall see, for predictions within $O(N)$ models. This analysis of the previous results for the Ising model case [12], will enable us to justify a new criterion for estimating DE predictions of physical quantities as well as their associated error bars.

As is evident from looking at Fig.3.2, it is necessary to fix the overall scale of regulator in order to obtain good convergence properties in the DE. Of course, this can be concluded because we know the nearly exact result from the conformal bootstrap [73]. The observed behaviour is that when increasing the order of the DE, the critical exponents alternate in concavity and around the *exact* result of the CB converging rather fast to those values, except at order $\mathcal{O}(\partial^6)$ where there is an overlap for predictions coming from $\mathcal{O}(\partial^4)$ and $\mathcal{O}(\partial^6)$, see below. Another observed behaviour is that the steepness of the curves increases with the order of the DE making of the utmost importance to properly choose the parameter α via some criterion, the practical implementa-
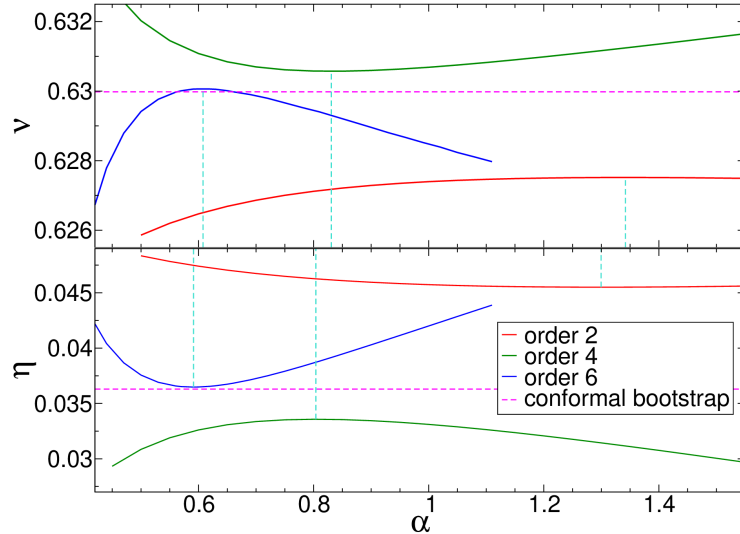
Figure 3.2: Dependence of the critical exponents $\nu(\alpha)$ and $\eta(\alpha)$ with the coefficient α for different orders of the DE (figure from [12]). LPA results do not appear within the narrow ranges of values chosen here.

tion is a rather natural one: we consider as central value the value that present less dependence in the regulator, this is known as the *principle of minimal sensitivity* (PMS). Indeed, this is a reasonable criterion based in the fact that we want to compute quantities which, of course, should not depend on the regulator. The dependence on the regulator shape and scale is just an artefact of the approximation scheme implemented on top of the exact evolution equation for the effective action Eq.(2.36).

Let us discuss the convergence properties of the derivative expansion. Consider for the moment a massive theory described by a Ginzburg-Landau Hamiltonian (see Chapter 1) away but near criticality. These types of theories are unitary when considering its Minkowskian continuation. In particular, the theory presents for $\Gamma^{(2)}$ the closest singularities to the origin in the complex plane p^2 at $9m^2$ and $4m^2$ for the symmetric and broken phase, respectively. A momentum expansion around zero momentum is therefore convergent with a finite radius of convergence. In particular, the coefficients c_n in the expansion

$$\frac{\Gamma^{(2)}(p,m)}{\Gamma^{(2)}(0,m)} = 1 + \frac{p^2}{m^2} + \sum_{n=2}^{\infty} c_n \left(\frac{p^2}{m^2}\right)^n, \qquad (3.8)$$

are universal and, for n large enough, they behave as $c_{n+1} \sim -r_c c_n$ with r_c equal to $1/9$ or $1/4$ for the symmetric and broken phase, respectively. Now, for the critical theory the regulator in the NPRG plays the role of a momentum dependent mass, and therefore we should expect a similar behaviour if all

55

	Regulator	ν	η	ω
LPA	W_k	0.65059(2062)	0	0.6541(1756)
	Θ_k^3	0.65003(2006)	0	0.6551(1746)
	Θ_k^4	0.65020(2023)	0	-
	Θ_k^8	0.65056(2059)	0	-
	E_k	0.65103(2106)	0	0.6533(1764)
$\mathcal{O}(\partial^2)$	W_k	0.62779(218)	0.04500(870)	0.8702(405)
	Θ_k^2	0.62814(183)	0.04428(798)	-
	Θ_k^3	0.62802(195)	0.04454(824)	0.8698(401)
	Θ_k^4	0.62793(204)	0.04474(844)	-
	Θ_k^8	0.62775(222)	0.04509(879)	-
	E_k	0.62752(245)	0.04551(921)	0.8707(410)
$\mathcal{O}(\partial^4)$	W_k	0.63027(30)	0.03454(176)	0.8313(16)
	Θ_k^3	0.63014(17)	0.03507(123)	0.8310(13)
	Θ_k^4	0.63021(24)	0.03480(150)	-
	Θ_k^8	0.63036(39)	0.03426(204)	-
	E_k	0.63057(60)	0.03357(272)	0.8321(24)
$\mathcal{O}(\partial^6)$	W_k	0.63017(20)	0.03581(49)	-
	Θ_k^4	0.63013(16)	0.03591(39)	-
	Θ_k^8	0.63012(15)	0.03610(20)	-
	E_k	0.63007(10)	0.03648(18)	-
CB [73][74]		0.629971(4)	0.0362978(20)	0.82968(23)

Table 3.1: Raw results of the DE for the Ising critical exponents ν and η in $d = 3$ from [12] and for ω from present work obtained with various families of regulators. The numbers in parentheses for DE results give the distance of the results to the CB values (taken from [73] for critical exponents η and ν and from [74] for ω) given here as the almost exact reference, while the numbers in parentheses for the CB results are strict bounds.

correlation functions behave as in the massive theory for squared momenta $\lesssim k^2/r_c$. However, although the scale k acts as if there was a mass of order m, the specific relation between m and k depends on the profile of the regulator as well as the specific value of α. So, in order to enhance convergence properties, we need to *fine-tune* the parameter α, which in practice is done by implemented the PMS criterion. We remark that despite its undeniable phenomenological success, a formal justification of PMS is still missing. See however Chapter 6 on this point. We further emphasize that given the alternating nature of predictions of these critical exponents, except at order $\mathcal{O}(\partial^6)$ where we observe an overlap with the preceding order, the PMS also yields the fastest apparent convergence to the exact results.

In Table 3.1 we present the results for critical exponents η and ν from [12] for all the regulators considered in this work. Based on these data, the authors

of [12] conjectured the existence of an absolute extreme value (maximum or minimum depending on the considered order of the DE) in terms of regulators families and PMS for each critical property, which could not be crossed. This information, if true, can be exploited in order to give more precise and accurate predictions, as we describe below. Although this could indeed be true, as data in Table 3.1 and Fig.3.2 show regarding order $\mathcal{O}(\partial^6)$ for the ν exponent, taking the extrema in any situation is not reasonable. This is easy to recognize by noting that the dispersion data for estimates of the ν critical exponents at order $\mathcal{O}(\partial^4)$ overlap with the dispersion data at order $\mathcal{O}(\partial^6)$. It is then not reasonable to consider the order $\mathcal{O}(\partial^6)$ estimates as bounds for the exact value. So, whenever there are strong indications that make us believe in the alternation and bounds of successive orders of the DE, an improved estimation of central values and error bars can be implemented as explained below. Nevertheless, whenever this is not the case, a safer or conservative criterion should be used.

Unimproved Estimation of Central Values and Error Bars

We start by stating how we compute our estimation whenever we are not confident enough about the alternating nature of results (or for that matter, also when we are certain that it does not alternate). This can happen because dispersion, in regulator families, of the estimation of certain quantity intersect or because we do not observe a concavity alternation, as is the case of the ω critical exponent for $N = 1$, see Table 3.1. In those cases, we need to use a conservative estimate of the quantity to be computed, say Q.

When considering different families of regulators, we always choose as the predicted value of a certain family, its value at the PMS. However, let us note that sometimes it might happen that there is no PMS, in the sense that the curve has no extrema. In that situation we continue the spirit of the PMS and consider as the predicted value the one that depends less on the regulator. In the cases we observed, this always corresponded to an inflexion point. In any case, these values are the ones reported in the tables of *raw* data for different N in Appendix C. We name this PMS values as $Q_f^{(s)}$, where the s refers to the order of the DE and the f refers to the regulator family being considered (for example, in Table 3.1 $\nu_W^{(2)}$ is the value 0.62779 obtained with Wetterich regulator at order $\mathcal{O}(\partial^2)$).

We will take our estimate Q at order $\mathcal{O}(\partial^s)$ for the quantity Q to be in the

middle of the dispersion range of regulator families:

$$\bar{Q}^{(s)} \equiv \frac{max_f\{Q_f^{(s)}\} + min_f\{Q_f^{(s)}\}}{2}. \tag{3.9}$$

Now, the error associated will be a result of two contributions. One of these contributions comes, of course, from the dispersion of values in regulator families, we consider this error $\Delta_{reg}Q$, as being equal to the diameter of the dispersion values, this is

$$\Delta_{reg}Q^{(s)} \equiv max_f\{Q_f^{(s)}\} - min_f\{Q_f^{(s)}\}. \tag{3.10}$$

The reason to do this is that we choose the center of the dispersion, but we did not have any reason to opt for any particular value. Moreover, we do not know for a fact that there are no other families which yield lower o higher values for the quantity Q.

The second contribution to the error estimate can only be employed when, at least, two consecutive orders have been considered. Since the DE convergence parameter is of order 1/4 to 1/9, we consider that the result at order $\mathcal{O}(\partial^s)$ has also an error $\hat{\Delta}Q^{(s)}$ of about a 1/4 of the distance between the s and $s-2$ estimate, specifically:

$$\hat{\Delta}Q^{(s)} \equiv \frac{|\bar{Q}^{(s)} - \bar{Q}^{(s-2)}|}{4}. \tag{3.11}$$

We must take into account one final correction to this error bar estimate since, although they may seem reasonable in principle, it can happen that they become abnormally small in some cases. For instance, it can happens that when varying a parameter, say the dimension d or the number of components N of the model,[1] estimates from consecutive orders cross for spurious reasons. This will give an error estimate suspiciously small. In order to amend this peculiar situation, we use two different criteria. First, if the error estimate of the previous order divided by four is bigger than the resulting error, we consider the error to be the one corresponding to the previous order divided by four. This situation arose for the critical exponent ω at order $\mathcal{O}(\partial^4)$ for $N = 2$. Secondly, if no error estimate is available at the previous order (as is the case of order LPA), we rely on the fact that the DE is exact in the $N \to \infty$ limit, and consider the error bars to be monotonously decreasing functions of

---

[1]Both the dimension d and the number of components N of the model enter the flow equation as free parameters.

N. We implement it by considering as error the immediately smaller studied value of N. We comment that this situation arose at order $\mathcal{O}(\partial^2)$ for the critical exponent ω for values $N = 3$, $N = 4$ and $N = 5$ and at order $\mathcal{O}(\partial^4)$ also for the critical exponent ω but for $N = 2$. However, in this last case we used the first criterion.

Let us emphasize the fact that at order LPA this procedure does not yield a reliable estimate (because we do not have a precedent order) and, consequently, we do not give an associated error to order LPA. Leaving aside order LPA, this method can be applied to any quantity which can be computed at consecutive orders of the DE and in particular is applied for the estimate of central value and error in Table 3.2. Moreover, we computed also the critical exponent ω whose reported value in Table 3.2 is obtained in this fashion. This exponent was computed in this way for all considered values of N, since its behaviour does not seem to respond to an alternating behaviour with alternating bounds. In particular and complementing the reported results in [12], we present in Fig.3.3 its behaviour at successive orders (up to order $\mathcal{O}(\partial^4)$) for the exponential regulator E_k and compare it against the CB estimate.
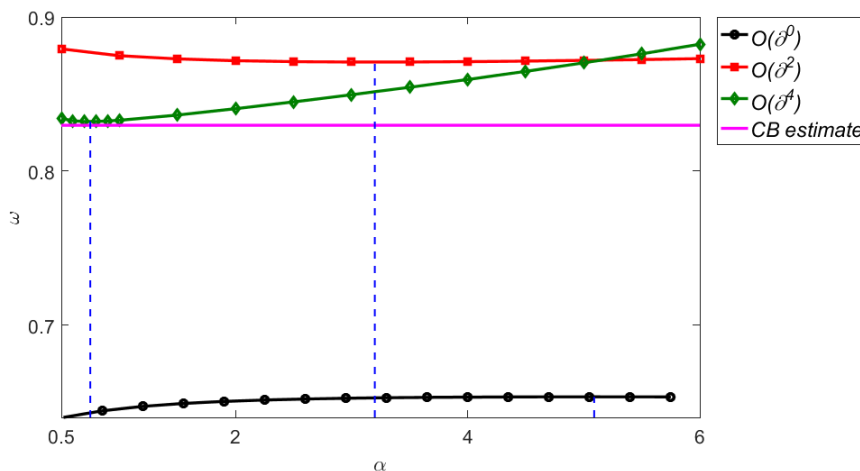
Figure 3.3: Critical exponent ω of the Ising model up to order $\mathcal{O}(\partial^4)$ for the regulator E_k as a function of the regulator parameter α. Conformal bootstrap estimate from [74] are given for comparison.

Improved Criterion For Central Values and Error Bars

As previously discussed, we can take advantage of the alternating structure of the successive orders of the DE in conjunction with the small expansion parameter r_c. This is only applicable whenever we have strong indications that the results are indeed alternating, so that PMS also yields the fastest apparent

convergence. When this is the case, we know that the PMS prediction for any regulator at order $\mathcal{O}(\partial^s)$ of the DE is an upper bound if the PMS value is a minimum and it constitutes a lower bound if the PMS value is a maximum.

Suppose that at order $\mathcal{O}(\partial^s)$, the PMS for the quantity Q to be computed, with the improved estimate, corresponds to a maximum (minimum). In this case, to compute the improved estimate at order $\mathcal{O}(\partial^s)$, we first define $Q_{ext}^{(s)} \equiv max_f\{Q_f^{(s)}\}$ ($Q_{ext}^{(s)} \equiv min_f\{Q_f^{(s)}\}$) which we already now is a lower (upper) bound for the quantity of interest. Moreover, we also know that $Q_{ext}^{(s-2)}$ corresponds to an upper (lower) bound for this same quantity. This information tells us that the actual value for the quantity Q is, in fact, in between these two values, $Q_{ext}^{(s-2)}$ and $Q_{ext}^{(s)}$. We can now use the knowledge that the error committed from one order to the next is reduced by a factor of about $1/4$ to $1/9$ and that the actual value is closer to $Q_{ext}^{(s)}$ than to $Q_{ext}^{(s-2)}$. Therefore, we consider an improved estimate $\hat{Q}^{(s)}$ of the quantity Q by moving the value $Q_{ext}^{(s)}$ towards $Q_{ext}^{(s-2)}$ half the estimate of error committed, this is

$$\frac{|Q_{ext}^{(s)} - Q_{ext}^{(s-2)}|}{8},$$

which yields the improved central value estimate $\tilde{Q}^{(s)}$ for the quantity Q:

$$\tilde{Q}^{(s)} \equiv \frac{7Q_{ext}^{(s)} + Q_{ext}^{(s-2)}}{8}. \tag{3.12}$$

We also take the improved error estimate $\hat{\Delta}Q^{(s)}$ at order $\mathcal{O}(\partial^s)$ to be:

$$\hat{\Delta}Q^{(s)} \equiv \frac{|Q_{ext}^{(s)} - Q_{ext}^{(s-2)}|}{8}. \tag{3.13}$$

We can not emphasize enough the fact that we need to have firm reasons to believe that this alternating behaviour is taking place in order to implement this improved estimates of central values and errors. An undoubtedly requirement is that the dispersion of values with regulator families, do not intersect at successive orders. As previously stated, this is not fulfilled in the case of the critical exponent ν for orders $\mathcal{O}(\partial^4)$ and $\mathcal{O}(\partial^6)$. However, as we shall see, we can apply this method for the η critical exponent in all cases and to the critical exponent ν for $O(N)$ models with $1 \leq N \leq 5$. The critical exponent ω does not seem to alternate and we are not confident to apply this improved criterion in any considered case.

We finish this section by presenting the final predictions from the DE with

	ν	η	ω
LPA	0.64956	0	0.654
$O(\partial^2)$	0.6308(27)	0.0387(55)	0.870(55)
$O(\partial^4)$	0.62989(25)	0.0362(12)	0.832(14)
$O(\partial^6)$	0.63012(16)	0.0361(11)	
CB	0.629971(4)	0.0362978(20)	0.82968(23)
6-loop, $d = 3$	0.6304(13)	0.0335(25)	0.799(11)
ϵ-expansion, $\mathcal{O}(\epsilon^5)$	0.6290(25)	0.0360(50)	0.814(18)
ϵ-expansion, $\mathcal{O}(\epsilon^6)$	0.6292(5)	0.0362(6)	0.820(7)
High-T.	0.63012(16)	0.03639(15)	0.83(5)
MC	0.63002(10)	0.03627(10)	0.832(6)

Table 3.2: Final estimates of central values and error bars for $N = 1$ in $d = 3$, from the derivative expansion up to order $\mathcal{O}(\partial^6)$ for critical exponents η and ν and up to order $\mathcal{O}(\partial^4)$ for ω. The raw data used for η and ν are taken from [12] while the one for ω correspond to the present work. All this data is presented in Table 3.1. These are compared against reported results in the literature: Results of the CB are taken from [73] for η and ν, and from [74] for ω; Monte Carlo estimates are extracted from [75]; High-temperature expansion taken from [76]; 6-loops at $d = 3$ perturbative RG values reported in [77] and finally, ϵ−expansion at order $\mathcal{O}(\epsilon^5)$ were reported in [77] and at order $\mathcal{O}(\epsilon^6)$ in [78].

these two criteria by using the available raw data from [12] for critical exponents η and ν and the produced in the present work for the critical exponent ω. In Table 3.1 we condensate all the raw data used. The final results for $N = 1$ are shown in Table 3.2.

We comment that the estimates at all orders of the DE expansion are consistent. Moreover, there is a clear improvement of precision with consecutive orders of the DE. It may not look his way for the estimates at order $\mathcal{O}(\partial^6)$, however, the main reason for this is that order $\mathcal{O}(\partial^4)$ is computed, for η and ν, with the improved estimate but for order $\mathcal{O}(\partial^6)$ we could not do that. As a consequence, the improvement in precision is marginal. Since the conformal bootstrap method yields rigorous bounds for the critical exponents, we consider them as exact. We see that all estimates are compatible with the CB estimates which allows us to conclude that both our criteria for estimating central values and error bar are reasonable. Furthermore, leaving CB aside (which reached an astonishing precision), the attained precision for the critical exponent ν within the DE is just slightly worst than the one of MC and equal or better than any other. This is not the case of the critical exponent η for which the convergence is a bit slower. Critical exponent ω is obtained with a precision similar, but smaller, than perturbation theory and the MC estimates. Overall, the results are encouraging and motivate the extension of this analysis

to the $O(N)$ models.

## 3.4 The Critical Exponents of $O(N)$ Models

In this section we present the critical exponents for $O(N)$ models. We do so by also comparing with reported results and by using the improved estimates whenever possible. In Appendix C we present all the raw data for the considered values of N which we list: $\{-2, 0, 2, 3, 4, 5, 10, 20, 100\}$. The behaviour of critical exponents within the DE up to order $\mathcal{O}(\partial^4)$ as a function of N from $N = 0$ up to $N = 100$, altogether with their error estimates, are shown in Fig.3.4 for η, in Fig.3.5 for ν and in Fig.3.6 for ω.
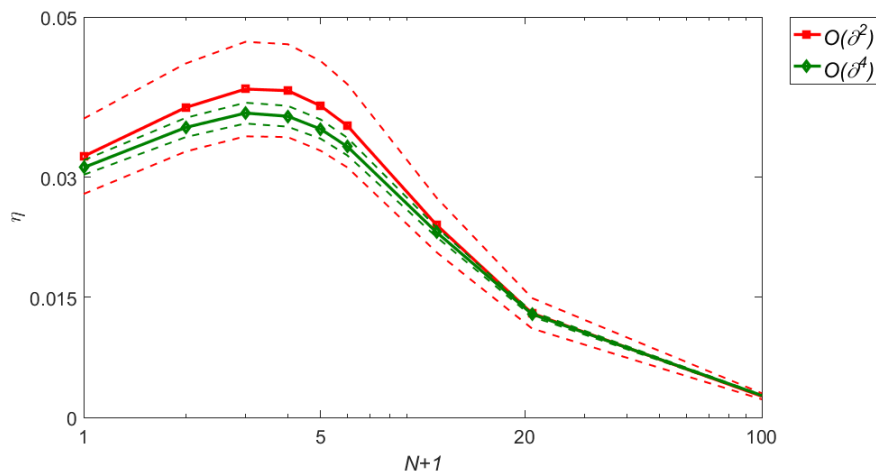
Figure 3.4: Final estimates of critical exponent η as a function of N at $d = 3$ at order $\mathcal{O}(\partial^2)$ (red) and order $\mathcal{O}(\partial^4)$ (green) of the DE. Error bars are given with dashed lines.

As we see in Figs.3.4-3.6, our proposed method for estimating central values and error bars is self-consistent, as estimates from order $\mathcal{O}(\partial^4)$ lay, generally, inside error bars of order $\mathcal{O}(\partial^2)$ and for the cases it does not lay inside, a finite (non vanishing) overlap exists. We further want to bring the attention to the peculiar behaviour of critical exponent ω at order LPA in relation to higher orders. As seen for critical exponent ν, although LPA is a bit off, the qualitative shape with N is the same at order LPA, $\mathcal{O}(\partial^2)$ or $\mathcal{O}(\partial^4)$. However, this is not the case for ω (except for $N \gtrsim 5$).

We split the presentation of results in three parts. One corresponding to unitary models with small values of N. Specifically the $O(3)$, $O(4)$, $O(5)$ models and, in particular, the $O(2)$ model and the controversy regarding Helium-4. A second part which correspond to large values of N, specifically $N = 10$,
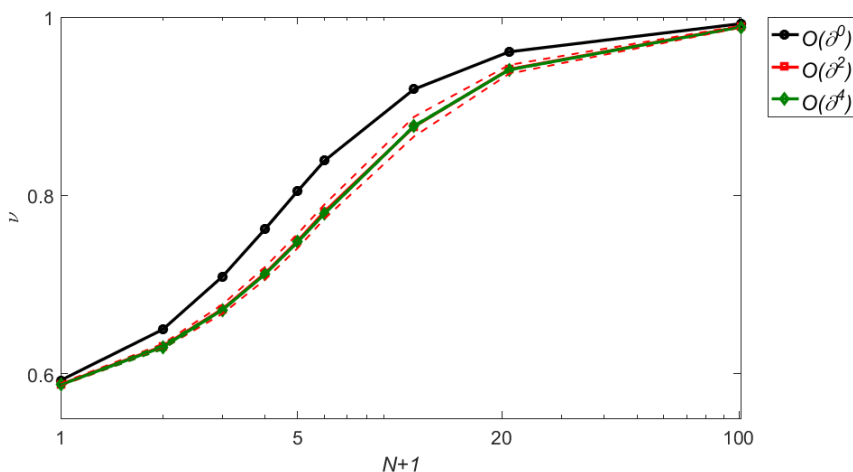
Figure 3.5: Final estimates of critical exponent ν as a function of N at $d = 3$ at order LPA (black), order $\mathcal{O}(\partial^2)$ (red) and order $\mathcal{O}(\partial^4)$ (green) of the DE. Error bars are given with dashed lines. The precision at order $\mathcal{O}(\partial^4)$ is so good that dashed lines can not be recognized.
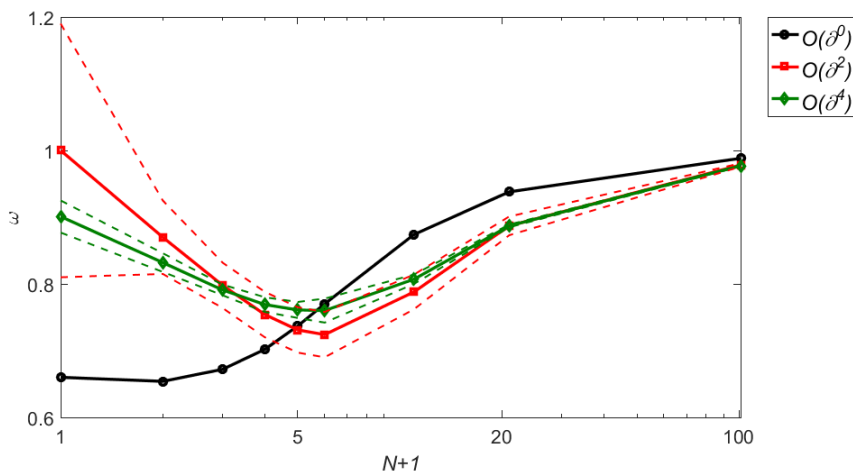
Figure 3.6: Final estimates of critical exponent ω as a function of N at $d = 3$ at order LPA (black), order $\mathcal{O}(\partial^2)$ (red) and order $\mathcal{O}(\partial^4)$ (green) of the DE. Error bars are given with dashed lines.

$N = 20$ and $N = 100$. A third and final part containing some analytical extension to cases where unitarity of the theory is doubtfully realized, this is the case of $N = 0$ and $N = -2$.

3.4.1 Critical Exponents η, ν and ω for $O(2)$, $O(3)$, $O(4)$ and $O(5)$ Models.

For these values the improved estimate is used for critical exponents η and ν. Critical exponent ω is computed using the unimproved estimate. We show in

Fig. 3.7 the typical curves for critical exponents, from top to bottom, η, ν and ω for the $O(2)$ model. We present the curves only for $N = 2$ with the exponential regulator E_k, but all the curves for this case are similar than the ones for the other values of N and other regulators (for the values $N = 2$, $N = 3$, $N = 4$ and $N = 5$).

The final predictions for the $O(2)$ model are presented in Table 3.3. While the raw data leading to it can be found in Appendix C. The results are compared to the prediction from multiple methods and experiments.

	ν	η	ω
LPA	0.7090	0	0.672
$O(\partial^2)$	0.6725(52)	0.0410(59)	0.798(34)
$O(\partial^4)$	0.6716(6)	0.0380(13)	0.791(8)
CB (2016)	0.6719(12)	0.0385(7)	0.811(19)
CB (2019)	0.6718(1)	0.03818(4)	0.794(8)
6-loop $d = 3$	0.6703(15)	0.0354(25)	0.789(11)
$\epsilon-$expansion, $\mathcal{O}(\epsilon^5)$	0.6680(35)	0.0380(50)	0.802(18)
$\epsilon-$expansion, $\mathcal{O}(\epsilon^6)$	0.6690(10)	0.0380(6)	0.804(3)
MC+High-T. (2006)	0.6717(1)	0.0381(2)	0.785(20)
MC (2019)	0.67169(7)	0.03810(8)	0.789(4)
Helium-4 (2003)	0.6709(1)		
Helium-4 (1984)	0.6717(4)		
XY-AF ($CsMnF_3$)	0.6710(7)		
XY-AF ($SmMnO_3$)	0.6710(3)		
XY-F (Gd_2IFe_2)	0.671(24)	0.034(47)	
XY-F (Gd_2ICo_2)	0.668(24)	0.032(47)	

Table 3.3: Final estimates of central values and error bars for $N = 2$ in $d = 3$, from the derivative expansion up to order $\mathcal{O}(\partial^4)$ for critical exponents η, ν and ω. The raw data used for computing these estimates is presented in Appendix C. These are compared against reported results in the literature: Results to the CB in 2016 are taken from [79] for η and ν and from [80] for ω; the CB estimates from 2019 were extracted from [19]; combined MC and High-Temperature analysis was presented in [81]; a recent MC estimate from 2019 taken from [20]; 6-loops, at $d = 3$, perturbative RG values given in [77] and $\epsilon-$expansion at order $\mathcal{O}(\epsilon^5)$ from [77] and order $\mathcal{O}(\epsilon^6)$ from [78]. Experimental results are also presented for the most precise measurements: Helium-4 superfluid from [15] and [82] for ν; XY-antiferromagnets ($CsMnF_3$ from [83] and $SmMnO_3$ from [84]) and XY-ferromagnets (Gd_2IFe_2 and Gd_2ICo_2 from [85]). Whenever needed, scaling relations are used in order to express results in terms of η and ν.

Our results clearly align with those of Monte Carlo and conformal bootstrap, regarding the controversy for the heat capacity critical exponent α, and exclude the experimental result [15]. This may have two different interpretations, one of them (and the most likely one) is that the error bar of the
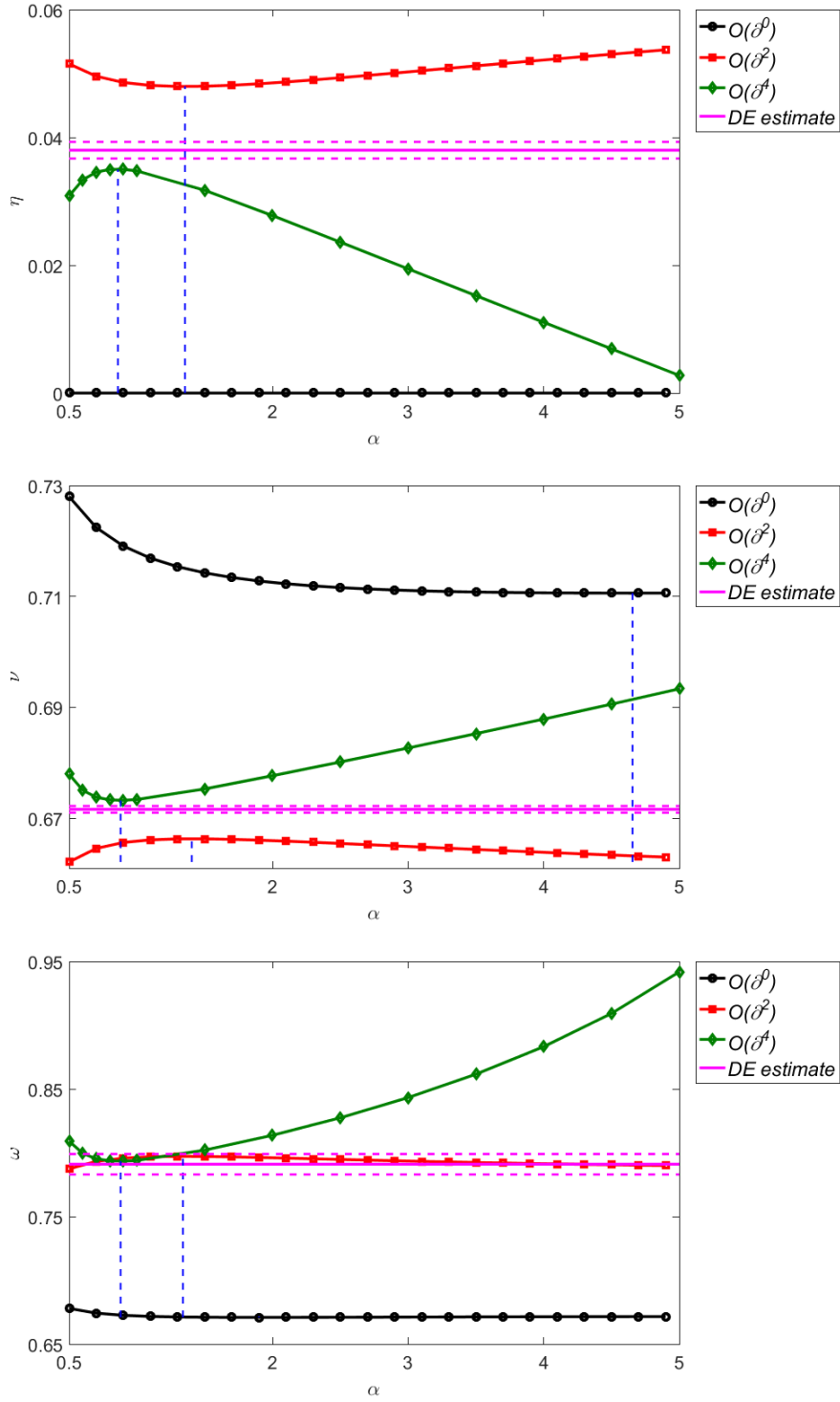
Figure 3.7: Critical exponents η, ν and ω with $N = 2$ and $d = 3$, up to order $\mathcal{O}(\partial^4)$ of the DE for the exponential regulator Eq.(2.30), as well as the final order $\mathcal{O}(\partial^4)$ DE estimate for these quantities. Error bars are given with dashed line.

experiment has been underestimated or that the experiment had some sort of systematic error and needs to be repeated. The other possible explanation is

that the $O(2)$ model does not control the long range physics of the Helium-4 λ-transition. This last explanation is not very likely because, in general, scale invariant theories (fixed points of the NPRG) are a discrete set and since the $O(2)$ model critical exponents coincide in the first three digits, this would mean that the fluid-superfluid critical point of Helium-4 is very close to the one corresponding to the $O(2)$ model.

The results for cases $N = 3$, $N = 4$ and $N = 5$ are given in Tables 3.4-3.6. We observe that this method has similar accuracy for $N = 3$ and $N = 4$ as MC estimates for exponent ν, but is more accurate than any other field theoretical method. At $N = 5$ the reached precision of the DE surpass even that of MC, although probably not the same numerical effort was put into computing exponents for the $O(5)$ as it was done for the $O(2)$ case. For the critical exponent ω our error bar predictions for $O(3)$, $O(4)$ and $O(5)$ models are only surpassed by the ϵ-expansion estimate at order $\mathcal{O}(\epsilon^6)$ (whenever available). However, a word of caution worth mentioning since for all the observed cases, ϵ-expansion predictions appears to be off with respect to all other methods. A plausible explanation is that, perhaps, in those cases the error bars of the order $\mathcal{O}(\epsilon^6)$ are being underestimated. Finally, we mention that the predictions for critical exponent η are more imprecise than those of Monte Carlo estimates or the ϵ-expansion at order $\mathcal{O}(\epsilon^6)$ (except for $N = 5$ where they are not available), but they match the precision of conformal bootstrap for $N = 3$ and are already more precise for $N = 4$. The 6-loop perturbative RG estimates at $d = 3$ are, in all 4 cases, more imprecise.

3.4.2   Critical Exponents η, ν and ω for $O(10)$, $O(20)$ and $O(100)$ Models.

In this section we present the critical exponents estimates for large values of N. When doing so, large-N expansion will become very accurate and we mainly compare to it. We highlight that we estimated the error for the large-N expansion to be equal to the distance with the previous order. This may be an overestimation of the error. However, it could also be an underestimation of the errors since, as can be seen in the expressions of Eq.(2.62), the coefficients of this expansion are not of order 1. This is clearly the case for critical exponent ω at $N = 5$ where the estimates of the large-N expansion are evidently off, see Fig.3.6.

For these values of N, all DE results for exponent ν and ω are taken using the unimproved estimates, while for the exponent η we use the improved

	ν	η	ω
LPA	0.7620	0	0.702
$O(\partial^2)$	0.7125(71)	0.0408(58)	0.754(34)
$O(\partial^4)$	0.7114(9)	0.0376(13)	0.769(11)
CB	0.7120(23)	0.0385(13)	0.791(22)
6-loop $d = 3$	0.7073(35)	0.0355(25)	0.782(13)
$\epsilon-$expansion, $\mathcal{O}(\epsilon^5)$	0.7045(55)	0.0375(45)	0.794(18)
$\epsilon-$expansion, $\mathcal{O}(\epsilon^6)$	0.7059(20)	0.0378(5)	0.795(7)
MC	0.7116(10)	0.0378(3)	0.773
MC+High-T.	0.7112(5)	0.0375(5)	
Ferromagnet Gd_2BrC	0.7073(43)	0.032(10)	
Ferromagnet Gd_2IC	0.7067(60)	0.061(15)	
Ferromagnet $CdCr_2Se_4$	0.656(56)	0.041(23)	

Table 3.4: Final estimates of central values and error bars for $N = 3$ in $d = 3$, from the derivative expansion up to order $\mathcal{O}(\partial^4)$ for critical exponents η, ν and ω. The raw data used for computing these estimates is presented in Appendix C. These are compared against reported results in the literature: Results from CB are ginve in [79] for η and ν, and in [80] for ω; MC estimates were presented in [86] for η and ν, and in [87] for ω; combined MC and High-Temperature analysis extracted from [88]; 6-loops, at $d = 3$, perturbative RG values were taken from [77] and ϵ-expansion at order $\mathcal{O}(\epsilon^5)$ is extracted from [77] and at order $\mathcal{O}(\epsilon^6)$ from [78]. Experimental results are also presented for the most precise measurements: Isotropic ferromagnets Gd_2BrC and Gd_2IC from [89] and $CdCr_2Se_4$ from [90]. Whenever needed, scaling relations are used in order to express results in terms of η and ν.

	ν	η	ω
LPA	0.805	0	0.737
$O(\partial^2)$	0.749(8)	0.0389(56)	0.731(34)
$O(\partial^4)$	0.7478(9)	0.0360(12)	0.761(12)
CB	0.7472(87)	0.0378(32)	0.817(30)
6-loop $d = 3$	0.741(6)	0.0350(45)	0.774(20)
$\epsilon-$expansion, ϵ^5	0.737(8)	0.036(4)	0.795(30)
$\epsilon-$expansion, ϵ^6	0.7397(35)	0.0366(4)	0.794(9)
MC	0.7477(8)	0.0360(4)	0.765

Table 3.5: Final estimates of central values and error bars for $N = 4$ in $d = 3$, from the derivative expansion up to order $\mathcal{O}(\partial^4)$ for critical exponents η, ν and ω. The raw data used for computing these estimates is presented in Appendix C. These are compared against reported results in the literature: results of CB for η and ν obtained from [17] and ω from [80]; Monte Carlo estimates for η and ν are given in [91] and for ω in [87]; 6-loops, at $d = 3$, perturbative RG values are taken from [77] and ϵ-expansion at order $\mathcal{O}(\epsilon^5)$ is extracted from [77] and at order $\mathcal{O}(\epsilon^6)$ from [78].

estimate. The results for $O(10)$, $O(20)$ and $O(100)$ are given in Tables 3.7-3.9. Typical curves for the exponents are shown in Fig.3.8 for the regulator E_k for the case of $N = 20$.

	ν	η	ω
LPA	0.839	0	0.770
$O(\partial^2)$	0.782(8)	0.0364(52)	0.724(34)
$O(\partial^4)$	0.7797(9)	0.0338(11)	0.760(18)
6-loop $d = 3$	0.766	0.034	
MC	0.728(18)		
Large-N	0.71(7)	0.031(15)	0.51(6)

Table 3.6: Final estimates of central values and error bars for $N = 5$ in $d = 3$, from the derivative expansion up to order $\mathcal{O}(\partial^4)$ for critical exponents η, ν and ω. The raw data used for computing these estimates is presented in Appendix C. These are compared against reported results in the literature: results of Monte Carlo are taken from [92]; Large-N expansion are computed using expressions given in Eq.(2.62), see [93, 94, 95], and 6-loops, at $d = 3$, perturbative RG values taken from [96].

	ν	η	ω
LPA	0.919	0	0.874
$O(\partial^2)$	0.877(11)	0.0240(34)	0.788(26)
$O(\partial^4)$	0.8776(10)	0.0231(6)	0.807(7)
6-loop $d = 3$	0.859	0.024	
Large-N	0.87(2)	0.023(2)	0.77(1)

Table 3.7: Final estimates of central values and error bars for $N = 10$ in $d = 3$, from the derivative expansion up to order $\mathcal{O}(\partial^4)$ for critical exponents η, ν and ω. The raw data used for computing these estimates is presented in Appendix C. These are compared against reported results in the literature: Large-N expansion estimates are taken with expressions given in Eq.(2.62), see [93, 94, 95], and 6-loops, at $d = 3$, perturbative RG values were taken from [96].

	ν	η	ω
LPA	0.9610	0	0.938
$O(\partial^2)$	0.9414(49)	0.0130(19)	0.887(14)
$O(\partial^4)$	0.9409(6)	0.0129(3)	0.887(2)
CB	0.9416(87)	0.0128(16)	
6-loop $d = 3$	0.930	0.014	
Large-N	0.941(5)	0.0128(2)	0.888(3)

Table 3.8: Final estimates of central values and error bars for $N = 20$ in $d = 3$, from the derivative expansion up to order $\mathcal{O}(\partial^4)$ for critical exponents η, ν and ω. The raw data used for computing these estimates is presented in Appendix C. These are compared against reported results in the literature: results of CB are given in [17]; Large-N expansion estimates are taken with expressions given in Eq.(2.62), see [93, 94, 95], and 6-loops, at $d = 3$, perturbative RG values were taken from [96].

We observe that our estimates for exponent ν is more precise than any other method up to $N = 100$ where the error made is equal to the estimated one of the large-N expansion. We also note, that the only agreement with the
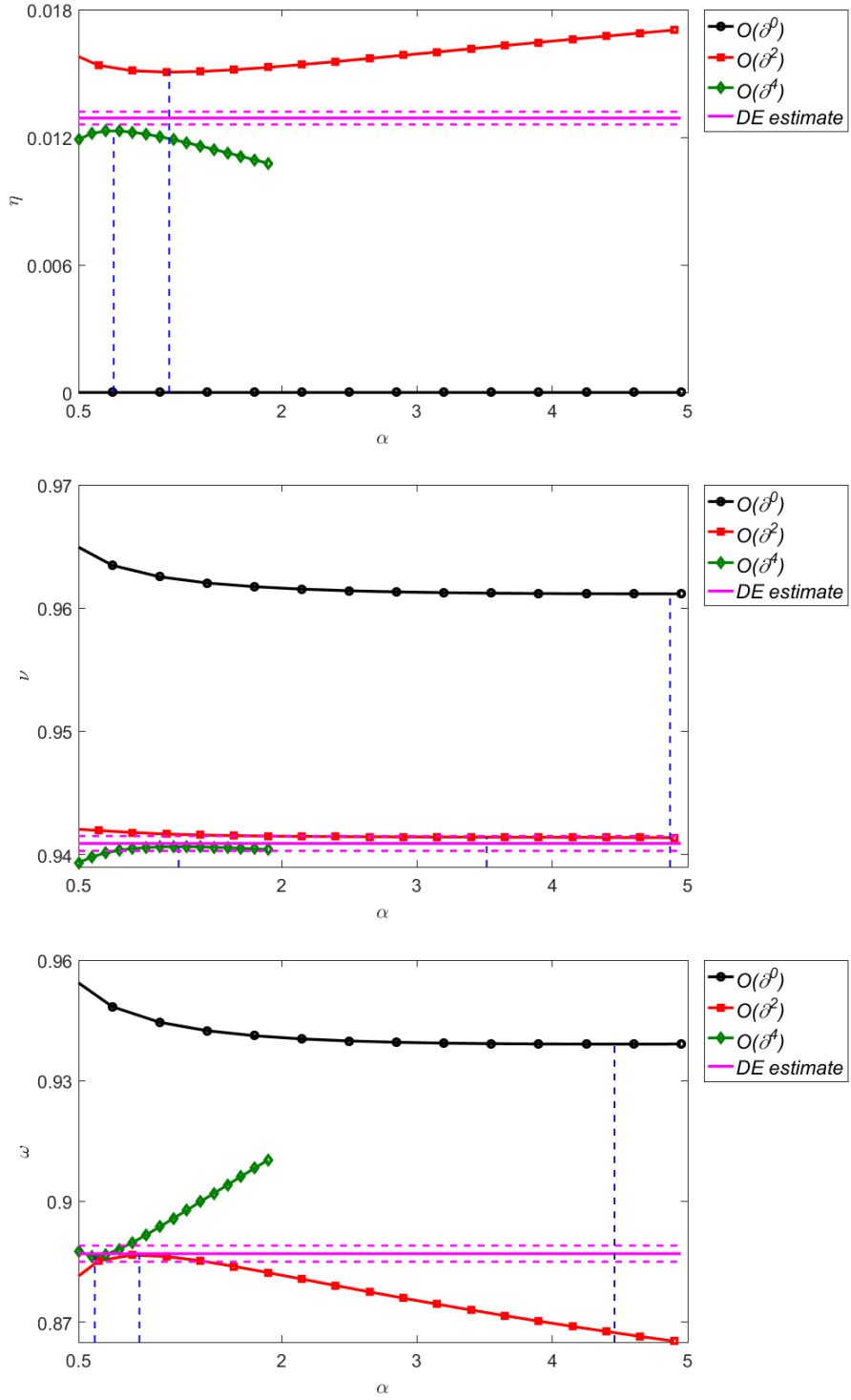
Figure 3.8: Critical exponents η, ν and ω with $N = 20$ and $d = 3$, up to order $\mathcal{O}(\partial^4)$ of the DE for the exponential regulator Eq.(2.30), as well as the final order $\mathcal{O}(\partial^4)$ DE estimate for these quantities. Error bars are given with dashed lines.

critical exponent ω for the large N expansion is the one at $N = 20$. For smaller values of N (i.e. $N = 5$ and $N = 10$) it seems that the large-N approximation

	ν	η	ω
LPA	0.9925	0	0.9882
$O(\partial^2)$	0.9892(11)	0.00257(37)	0.9782(26)
$O(\partial^4)$	0.9888(2)	0.00268(4)	0.9770(8)
Large-N	0.9890(2)	0.002681(1)	0.9782(2)

Table 3.9: Final estimates of central values and error bars for $N = 100$ in $d = 3$, from the derivative expansion up to order $\mathcal{O}(\partial^4)$ for critical exponents η, ν and ω. The raw data used for computing these estimates is presented in Appendix C. These are compared against results given by the Large-N expansion estimates taken with expressions given in Eq.(2.62), see [93, 94, 95].

underestimates the actual value while for higher values of N (the only studied case being the $N = 100$) it appears to be an overestimation. However, this discrepancy could be a product of an underestimation of error bars either from our method (although this does not seems to be the case for moderate values of N) or from the large N expansion. Note that even a small underestimation of any of the errors would lead to estimates marginally compatible for the case $N = 100$, however the cases $N = 5$ and $N = 10$ requires more than a small adjustment to become compatible.

3.4.3 Critical Exponents η, ν and ω for the Analytical Extension of $O(N)$ Models to $N = -2$ and $N = 0$.

This section deals with the estimates for cases where unitarity is most probably not realized. This is a good place to test the accuracy of the derivative expansion and its convergence properties. The case $N = 0$ corresponds to the system of self-avoiding walks [72] and is related to the critical regime of highly diluted linear polymers solutions [71]. The case $N = -2$, which can be matched to the *loop-erased random walks* (LERW) consisting of a simple random path in which loops are erased once they are formed [97, 98], works as a benchmark. This is because, for this analytical extension of the $O(N)$ models, the values of critical exponents η and ν are known to be exactly 0 and 1/2, respectively.

These cases are interesting because it allows us to study the convergence of the derivative expansion in non-unitary cases. We still assume the convergence of the DE given with a factor of 1/4 in order to estimate error bars, but we will not use the improved method for estimate the critical exponents. We start with the case of $N = 0$ for which we show the typical curves in Fig.3.9. We show in Table 3.10 our final estimates in conjunction with a comparison with

reported results of the literature. We remark that the results coming from CB for the case of $N = 0$ do not have the same level of rigour than the ones for unitary theories and in these cases their error bars can not be considered as rigorous bounds.

	ν	η	ω
LPA	0.5925	0	0.66
$O(\partial^2)$	0.5879(13)	0.0326(47)	1.00(19)
$O(\partial^4)$	0.5876(2)	0.0312(9)	0.901(24)
CB	0.5876(12)	0.0282(4)	
Series LDM	0.58785(40)	0.0327(22)	
MC	0.58759700(40)	0.0310434(30)	0.899(14)
6-loop $d = 3$	0.5882(11)	0.0284(25)	0.812(16)
$\epsilon-$expansion, ϵ^5	0.5875(25)	0.0300(50)	0.828(23)
$\epsilon-$expansion, ϵ^6	0.5874(3)	0.0310(7)	0.841(13)
Polymer solution	0.586(4)		

Table 3.10: Final estimates of central values and error bars for $N = 0$ in $d = 3$, from the derivative expansion up to order $\mathcal{O}(\partial^4)$ for critical exponents η, ν and ω. The raw data used for computing these estimates is presented in Appendix C. These are compared against reported results in the literature: results from the CB are taken from [99]; Monte Carlo estimates are given in [100, 101]; Length doubling method series predictions are reported in[102]; 6-loops, at $d = 3$, perturbative RG values given in [77] and $\epsilon-$expansion at order $\mathcal{O}(\epsilon^5)$ from [77] and order $\mathcal{O}(\epsilon^6)$ from [78]. Experimental results for the most precise experiment (polystyrene benzene dilute solutions) are given in [103].

The case $N = -2$ is peculiar within the DE. This is because, for fortuitous reasons η and ν critical exponents are obtained exactly at order LPA. Because of the approximation itself, the critical exponent η is set to 0 from scratch at LPA, this is true for all N values. This is why, it is just a coincidence that the exact result for $N = -2$ is recovered at LPA for this exponent. On top of this, the flow of the mass term at zero field in the LPA is proportional to

$$\delta_{ij}(N + 2),$$

and so, the mass parameter does not flow at $N = -2$. As a consequence, we recover the result $\nu = 1/2$. This analysis is no longer true at higher orders of the DE. However, as can be seen in the results for this case given in Table 3.11, the exact results are very well recovered within error bars. We remark that order $\mathcal{O}(\partial^2)$ seems more accurate for critical exponents η and ν than order $\mathcal{O}(\partial^4)$. However, the results are within error bars and a possible explanation for this phenomenon is that order $\mathcal{O}(\partial^2)$ being more similar to order LPA and
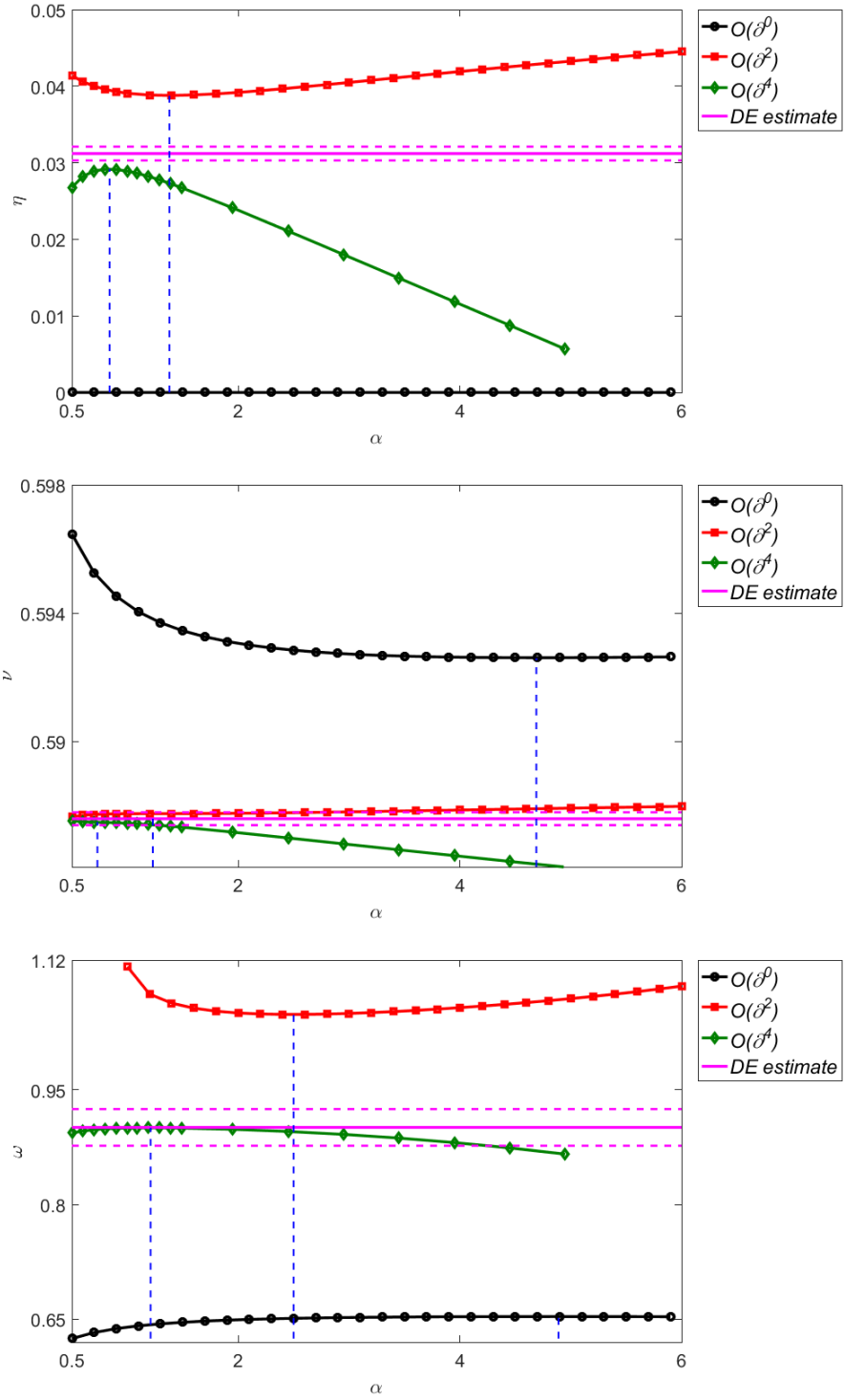
Figure 3.9: Critical exponents η, ν and ω with $N = 0$ and $d = 3$, up to order $\mathcal{O}(\partial^4)$ of the DE for the exponential regulator Eq.(2.30), as well as the final order $\mathcal{O}(\partial^4)$ DE estimate for these quantities. Error bars are given with dashed lines.

this, in turn, giving exact values for these exponents, translates into a better fulfilment of the exact results. Since the estimates for this critical exponents

	ν	η	ω
LPA	1/2	0	0.700
$O(\partial^2)$	0.5000(12)	0.0000(47)	0.84(19)
$O(\partial^4)$	0.5001(1)	0.0004(9)	0.838(24)
exact	1/2	0	
6-loop			0.83(1)

Table 3.11: Final estimates of central values and error bars for $N = -2$ in $d = 3$, from the derivative expansion up to order $\mathcal{O}(\partial^4)$ for critical exponents η, ν and ω. The raw data used for computing these estimates is presented in Appendix C. These are compared against reported results in the literature: Exact results for η and ν (see for example [104, 97, 98]) or perturbative results [97, 98].

are peculiar because of the crossing of consecutive orders, we used as error bar estimates those of the case $N = 0$ for critical exponents η and ν. However, for critical exponent ω we used our unimproved estimate directly at $N = -2$.

In summary, we pushed successively the derivative expansion of the NPRG for the $O(N)$ models to order $\mathcal{O}(\partial^4)$. We computed accurately the critical exponents η, ν and ω with a precision comparable to the best estimates in the literature and, in many cases, surpassing them. Regarding the long-standing controversy between MC and experiments for the critical exponent ν of the $O(2)$ model, we were able to contribute by showing that the DE estimates agrees with MC simulations, and the new CB estimates, but exclude the experiments. Additionally to pushing the DE to order $\mathcal{O}(\partial^4)$, we suggest a criterion for estimating quantities within this approximation scheme that can be implemented in many situations. In particular, it can be applied in conjunction with the DE at order $\mathcal{O}(\partial^4)$ (for which the algorithm is already operative) to compute many other physical properties, both universal and non-universal, of the $O(N)$ models with high precision.

Chapter 4

Scale and Conformal Symmetries

One of the most important ideas in physics is the concept of symmetry. This concept is at the heart of many fundamental theories in one way or another. This is obvious when looking at the paradigmatic example of relativity where one of the axioms establishes that the speed of light is the same in any reference frame. This implies that the speed of light is an invariant of the theory that is kept unchanged under Poincaré transformations.

In critical phenomena when a scale transformation is applied the long range quantities remain invariant. When discussing the existence of a fixed point of the RG transformation, the concept of scale invariance popped up. Indeed, this is a characteristic feature of critical phenomena in statistical systems and is due to the divergence of the correlation length. This is nothing but another way of saying that dilation is a symmetry of the fixed point Hamiltonian, or that the long range physics is invariant under scale transformations.

Sometimes systems at criticality are not only scale invariance but invariant under a wider symmetry group, called *conformal group*. A conformal transformation is a coordinate transformation that preserves angles. In the '70s there were many groups working on conformal invariant theories. In particular, there was an emergent idea named *Conformal Bootstrap* by Migdal [105] which consists in a non perturbative approach to solve[1] conformal field theories. After the works by Ferrara, Grillo and Gatto [106] in 1973, by Polyakov [107] in 1974 and for the two dimensional case by Belavin, Polyakov and Zamolodchikov [108] in 1984, among others, conformal symmetry regained a lot of attention recently when the ideas of the conformal bootstrapwere successfully

---

[1]By solve we mean computing physical quantities without approximations.

used to compute with great precision quantities in the 3 dimensional Ising model [14, 109].

In the present chapter the focus is on discussing isometries, scale and conformal transformations in the NPRG framework and, in particular, the relation between conformal and dilation symmetries. This is the preamble for the next two chapters, where we will use the present formalism. In Chapter 5, we study the possible presence of conformal invariance in the $O(N)$ models and, moreover, prove that it is indeed realized for some specific values of N. This is done by using a sufficient condition we give in Section 4.2. Later on, in Chapter 6, we use the formalism developed in Section 4.3 in order to use the restrictions that conformal invariance imposes to the Ising model universality class within the derivative expansion approximation scheme.

This chapter is organized as follows. In the first section we present, within the NPRG framework, Noether's theorem and Ward identities for conformal group transformations (specifically translations, rotations, dilatations and special conformal transformations). A consequence of the Ward identities for the conformal group transformation is shown in a second section, where a sufficient condition is given for the realization of conformal invariance when dilatation invariance, as well as rotation and translation invariance, is present. A final section is devoted to the development of a framework for using conformal invariance in order to study the critical physics of a ϕ^4 theory within the NPRG.

4.1 Conformal Group Transformations in the Non Perturbative Renormalization Group

In this section we consider Noether's theorem[1] for the different transformations of the conformal group, discussed in Appendix B, in the context of the NPRG. These are *translations*, *rotations*, *dilations* and *special conformal* transformations. In Appendix B it is shown that all these transformations, written in their infinitesimal version as

$$x_\mu \to x'_\mu = x_\mu + \varepsilon_\mu(x), \tag{4.1}$$

leave angles invariant (i.e. the metric is only rescaled locally). It is important to remark that in this section, the Hamiltonian (or euclidean action) is assumed

---

[1]Noether's Theorem is an important result in physics, which states that any continuous symmetry of a system implies the existence of a conservation law.

to be invariant under the whole conformal group. However, in real systems scale and, if realized, conformal invariance occurs only at long distance.

Applying these transformations on the system impose restrictions on the form of the energy-momentum tensor $T_{\mu\nu}$ and another quantity called the *virial current* J_μ. The general results are that translation invariance fixes $\partial_\nu T_{\mu\nu}$. This implies that any two energy-momentum tensors differing in a total derivative $\partial_\rho Y_{\mu\nu\rho}$, of a tensor $Y_{\mu\nu\rho}$ antisymmetric in ν and ρ, are equally valid. Rotation invariance restricts the possible forms of $T_{\mu\nu}$ in such a way that it is possible to choose $T_{\mu\nu}$ to be symmetric in μ and ν. Imposing scale invariance introduces a new quantity, namely the virial current J_μ. Finally, requiring a conformal invariant Hamiltonian restricts the virial current to be a total derivative $\partial_\nu L_{\mu\nu}$, which gives the freedom to choose a null virial current. In addition to these statements, we arrive at concrete relations between derivatives of the effective action Γ_k and the energy-momentum tensor $T_{\mu\nu}$. On top of these restrictions, modified Ward identities in presence of a regulator for all conformal transformation are deduced. Finally, we emphasize that these Ward identities can be interpreted as the generators of conformal transformations acting on the effective action and that these satisfy the conformal algebra. Then, these generators are used to reconstruct the sufficient condition for scale invariance to imply conformal invariance given in [27]. Polchinski in [110] established a similar sufficient condition for scale invariance to imply conformal invariance. His approach was similar to what is done in this section.

4.1.1 Translations

In translations and rotations the Jacobian determinant in front of the transformed field, $\left|\frac{\partial x'}{\partial x}\right|$, is just 1. However, for a dilatations and special conformal transformations, see below, it genuinely contribute because, under such transformations, the field is deformed.

A translation consists in a transformation where $\varepsilon_\mu(x)$ takes the constant form Eq.(B.12) in Appendix B, this is

$$\varepsilon_\mu^{(T)} = a_\mu.$$

This implies that the field transform as:

$$\varphi(x_\sigma) \rightarrow \varphi'(x'_\sigma) = \left|\frac{\partial x'}{\partial x}\right|^{-D_\varphi/d} \varphi(x_\sigma) = \varphi(x_\sigma), \qquad (4.2)$$

and therefore is

$$\varphi(x_\sigma) = \varphi'(x'_\sigma) = \varphi'(x_\sigma + a_\sigma) = \varphi'(x_\sigma) + a_\mu \partial_\mu \varphi(x_\sigma) + \mathcal{O}(a_\mu a_\nu), \qquad (4.3)$$

which simplifies to:

$$\delta\varphi(x) = -a_\mu \partial_\mu \varphi(x) = -a_\mu P_\mu \varphi(x), \qquad (4.4)$$

where P_μ is the generator of translations defined in Appendix B.

Noether's theorem is obtained by considering temporarily a variation dependent on the position $a_\mu(x)$. This implies in particular that if the Hamiltonian is translational invariant, the invariance is lost when $a_\mu(x)$ varies with position. For such a general transformation the variation of the Hamiltonian is:

$$\delta H = -\int_x a_\mu(x) \partial_\mu \varphi(x) \frac{\delta H}{\delta \varphi(x)} = -\int_x a_\mu(x) \partial_\nu \big(T_{\mu\nu}(x)\big)$$

$$\underset{a_\mu(x) \to a_\mu}{=} -a_\mu \int d^d x \, \partial_\nu \big(T_{\mu\nu}(x)\big) = 0 \qquad (4.5)$$

In this way, when a_μ is constant the Hamiltonian becomes explicitly invariant. Therefore, Eq.(4.5) defines the divergence of the *stress-energy* tensor $T_{\mu\nu}$ as:

$$\partial_\nu \big(T_{\mu\nu}(x)\big) \equiv \frac{\delta H}{\delta \varphi(x)} \partial_\mu \varphi(x), \qquad (4.6)$$

which tells us that the energy-momentum tensor $T_{\mu\nu}$ is conserved on shell (this is, imposing the equation of motion $\frac{\delta H}{\delta \varphi(x)} = 0$). Note that this does not fix completely the energy-momentum tensor because it can be redefined by adding a total derivative of a rank three tensor $\partial_\rho Y_{\mu\nu\rho}(x)$ but requiring $Y_{\mu\nu\rho}$ to be antisymmetric in $\nu \leftrightarrow \rho$. To be explicit, if $T_{\mu\nu}(x)$ is the energy-momentum tensor, then $T'_{\mu\nu}(x)$ defined as

$$T'_{\mu\nu}(x) = T_{\mu\nu}(x) + \partial_\rho Y_{\mu\nu\rho}(x), \qquad (4.7)$$

is another valid definition of the energy-momentum tensor, which satisfies $\partial_\nu T'_{\mu\nu} = \partial_\nu T_{\mu\nu} = \frac{\delta H}{\delta \varphi(x)} \partial_\mu \varphi(x)$.

As for the regulating term, since it is translational invariant by construction

its variation under this transformation reads:

$$\delta\Delta H_k = -\frac{1}{2}\int_{x,y} R_k(|x-y|)\big(a_\mu(x)\partial_\mu^x\varphi(x)\varphi(y)+a_\mu(y)\partial_\mu^y\varphi(y)\varphi(x)\big)$$

$$\underset{a_\mu(x)\to a_\mu}{=} -a_\mu\int_{x,y} R_k(|x-y|)\partial_\mu^x\varphi(x)\varphi(y)=0. \tag{4.8}$$

Applying the variation of the fields Eq.(4.4) to the extended functional integral Eq.(2.33) we get:

$$\left\langle \delta H + \delta\Delta H_k + \int_x J(x)a_\mu(x)\partial_\mu\varphi(x)\right\rangle_J = 0 \tag{4.9}$$

where $\langle\cdot\rangle_J$ is the mean value in presence of the source $J(x)$.

Pluggin in the variations for H and ΔH_k and since this equality must be true for any infinitesimal a_μ we conclude that:

$$J(x)\partial_\mu\frac{\delta W_k}{\delta J(x)}=\partial_\nu\langle T_{\mu\nu}(x)\rangle_J+\int_x R_k(|x-y|)\left\{\partial_\mu^x\frac{\delta W_k}{\delta J(x)}\frac{\delta W_k}{\delta J(y)}+\partial_\mu^x\frac{\delta^2 W_k}{\delta J(x)\delta J(y)}\right\} \tag{4.10}$$

Doing a generalized Legendre transformation of the field we arrive at the expression for Noether's theorem for translations in presence of a regulator:

$$\partial_\mu\varphi(x)\frac{\delta\Gamma_k}{\delta\varphi(x)}=\partial_\nu\langle T_{\mu\nu}(x)\rangle_{J_\varphi}+\int_y R_k(|x-y|)\partial_\mu^x\left(\Gamma_k^{(2)}+R_k\right)^{-1}_{x,y} \tag{4.11}$$

where $\langle\cdot\rangle_{J_\varphi}$ is the mean value in presence of the source $J(x)$, defined implicitly as the value $J_\varphi(x)$ such that $\left.\frac{\delta W_k}{\delta J(x)}\right|_{J_\varphi}=\varphi(x)$.

Integrating Eq.(4.11) in x yields the Ward identity for translations, which can be interpreted as a translation operator $\mathcal{P}_\mu$ acting on the effective action:

$$\mathcal{P}_\mu\Gamma_k \equiv \int_x \partial_\mu\varphi(x)\frac{\delta\Gamma_k}{\delta\varphi(x)}=0 \tag{4.12}$$

Leaving translations aside, for non-zero spin fields the remaining transformations take slightly different forms than the ones we present here. This must be kept in mind.

4.1.2 Rotations

Rotations are generated by a transformation where ε_μ in Eq.(4.1) is of the form given by Eq.(B.14) in Appendix B, this is

$$\varepsilon_\mu^{(R)} = -2m_{\mu\nu}x_\nu,$$

with $m_{\mu\nu}$ antisymmetric. When applied to the scalar field, it transforms as:

$$\varphi(x_\sigma) \to \varphi'(x'_\sigma) = \left|\frac{\partial x'}{\partial x}\right|^{-D_\varphi/d} \varphi(x_\sigma) = \varphi(x_\sigma), \tag{4.13}$$

which can be further worked to yield

$$\varphi(x_\sigma) = \varphi'(x'_\sigma) = \varphi'(x_\sigma - 2m_{\sigma\beta}x_\beta) = \varphi'(x_\sigma) - 2m_{\mu\nu}x_\nu\partial_\mu\varphi'(x_\sigma) + \mathcal{O}(m_{\alpha\gamma}m_{\rho\delta}), \tag{4.14}$$

to finally yield:

$$\delta\varphi(x) = -m_{\mu\nu}(x_\mu\partial_\nu - x_\nu\partial_\mu)\varphi(x) = -m_{\mu\nu}J_{\mu\nu}\varphi(x), \tag{4.15}$$

where $J_{\mu\nu}$ is the generator of rotations defined in Appendix B.

As before, upgrading $m_{\mu\nu} \to m_{\mu\nu}(x)$, at the expense of a non-zero variation of the Hamiltonian and the regulating term (which are invariant under rotations), yields:

$$
\begin{aligned}
\delta H &= -\int_x \frac{\delta H}{\delta\varphi(x)} m_{\mu\nu}(x)\big(x_\mu\partial_\nu\varphi(x) - x_\nu\partial_\mu\varphi(x)\big) \\
&= -\int_x m_{\mu\nu}(x)\big(x_\mu\partial_\rho T_{\nu\rho}(x) - x_\nu\partial_\rho T_{\mu\rho}(x)\big) \\
&= -\int_x m_{\mu\nu}(x)\Big\{\partial_\rho\big(x_\mu T_{\nu\rho}(x) - x_\nu T_{\mu\rho}(x)\big) + T_{\mu\nu}(x) - T_{\nu\mu}(x)\Big\} \\
&\underset{m_{\mu\nu}(x)\to m_{\mu\nu}}{=} -m_{\mu\nu}\int_x \partial_\nu\Big\{\partial_\rho\big(x_\mu T_{\nu\rho}(x) - x_\nu T_{\mu\rho}(x)\big)\Big\} \\
&\qquad\qquad -m_{\mu\nu}\int_x \Big\{T_{\mu\nu}(x) - T_{\nu\mu}(x)\Big\} = 0
\end{aligned}
\tag{4.16}
$$

Which shows that when $m_{\mu\nu}(x) \to m_{\mu\nu}$, rotation invariance implies that the antisymmetric part of the energy-momentum tensor must be the divergence of another local tensor, $\partial_\rho M_{\mu\nu\rho}(x)$ antisymmetric in $\mu \leftrightarrow \nu$ by construction. It turns out that, in fact, this does not define a new quantity since $M_{\mu\nu\rho}$ can be related to the arbitrariness in the definition of the energy-momentum tensor,

namely $Y_{\mu\nu\rho}$ in Eq.(4.7). Indeed, defining

$$T_{\mu\nu}(x) - T_{\nu\mu}(x) = 2\partial_\rho M_{\mu\nu\rho}(x) \tag{4.17}$$

and making use of the freedom to redefine the energy momentum tensor (i.e. Eq.(4.7)) we obtain:

$$
\begin{aligned}
T'_{\mu\nu}(x) - T'_{\nu\mu}(x) &= 2\partial_\rho M_{\mu\nu\rho}(x) + \big(\partial_\rho Y_{\mu\nu\rho}(x) - \partial_\rho Y_{\nu\mu\rho}(x)\big) \\
&= 2\partial_\rho\Big(M_{\mu\nu\rho}(x) + \frac{Y_{\mu\nu\rho}(x) - Y_{\nu\mu\rho}(x)}{2}\Big).
\end{aligned} \tag{4.18}
$$

So, choosing an $Y_{\mu\nu\rho}$ in Eq.(4.7) with antisymmetric part in $\mu \leftrightarrow \nu$ equal to $\partial_\sigma \tilde{Y}_{\mu\nu\rho\sigma} - M_{\mu\nu\rho}$, where $\tilde{Y}_{\mu\nu\rho\sigma}$ is antisymmetric separately in $\mu \leftrightarrow \nu$ and $\rho \leftrightarrow \sigma$, yields

$$T'_{\mu\nu} = T_{\mu\nu} + \partial_\rho\left(\frac{Y_{\mu\nu\rho} + Y_{\nu\mu\rho}}{2} - M_{\mu\nu\rho} + \partial_\sigma \tilde{Y}_{\mu\nu\rho\sigma}\right).$$

Inserting this expression in Eq.(4.18) gives

$$T'_{\mu\nu} - T'_{\nu\mu} = 2\partial_\rho\partial_\sigma \tilde{Y}_{\mu\nu\rho\sigma} = 0.$$

To conclude, rotation invariance does not bring anything else into play beyond allowing to work with a symmetric energy-momentum tensor. It is rather simple to check that Noether's theorem for this transformation is already implied by Noether's theorem for translations Eq.(4.11). Indeed, applying this transformation to the functional integral Eq.(2.33) yields:

$$
\begin{aligned}
J(x)(x_\mu\partial_\nu - x_\nu\partial_\mu)\frac{\delta W_k}{\delta J(x)} =& x_\mu\partial_\rho\langle T_{\nu\rho}(x)\rangle_J - x_\nu\partial_\rho\langle T_{\mu\rho}(x)\rangle_J \\
&+ \int_x R_k(|x-y|)(x_\mu\partial_\nu^x - x_\nu\partial_\mu^x)\Big\{\frac{\delta W_k}{\delta J(x)}\frac{\delta W_k}{\delta J(y)} + \frac{\delta^2 W_k}{\delta J(x)\delta J(y)}\Big\}. \tag{4.19}
\end{aligned}
$$

After doing a generalized Legendre transform gives Noether's theorem for rotation which is just a combination of translation times x:

$$
\begin{aligned}
\frac{\delta\Gamma_k}{\delta\varphi(x)}(x_\mu\partial_\nu - x_\nu\partial_\mu)\varphi(x) =& x_\mu\partial_\rho\langle T_{\nu\rho}(x)\rangle_{J_\varphi} - x_\nu\partial_\rho\langle T_{\mu\rho}(x)\rangle_{J_\varphi} \\
&+ \int_y R_k(|x-y|)(x_\mu\partial_\nu^x - x_\nu\partial_\mu^x)\Big(\Gamma_k^{(2)} + R_k\Big)_{x,y}^{-1}. \tag{4.20}
\end{aligned}
$$

From this follows the Ward identity for rotations with a symmetric choice of the stress-energy tensor, which can be identified with a rotation operator $\mathcal{J}_{\mu\nu}$

acting on Γ_k, takes the standard form:

$$\mathcal{J}_{\mu\nu}\Gamma_k \equiv \int_x \frac{\delta\Gamma_k}{\delta\varphi(x)}(x_\mu\partial_\nu - x_\nu\partial_\mu)\varphi(x) = 0. \tag{4.21}$$

4.1.3 Dilations

Next consider the transformation with ε_μ fixed by Eq.(B.15) from Appendix B, this is

$$\varepsilon_\mu^{(T)} = \lambda x_\mu.$$

This leads to what is known as dilations. Under dilatations, the field does not only transform because of the change of coordinate $x \to x'$, but also because of a genuine modification of the field, which is accounted by the Jacobian determinant in front of the transformed field. For dilatations we have:

$$\varphi(x_\sigma) \to \varphi'(x'_\sigma) = \left|\frac{\partial x'}{\partial x}\right|^{-D_\varphi/d} \varphi(x_\sigma) = (1+\lambda)^{-D_\varphi}\varphi(x_\sigma), \tag{4.22}$$

which can be further worked to yield

$$\varphi(x_\sigma) = \varphi'(x'_\sigma)(1+\lambda)^{D_\varphi} = \varphi'(x_\sigma) + \lambda(D_\varphi + x_\nu\partial_\nu)\varphi'(x_\sigma) + \mathcal{O}(\lambda^2), \tag{4.23}$$

which in summary yields:

$$\delta\varphi(x) = -\lambda(D_\varphi + x_\mu\partial_\mu)\varphi(x) = -\lambda D\varphi(x), \tag{4.24}$$

where D is the generator of dilatations defined in Appendix B and we recall that D_φ is the scaling dimension of the field. Unlike the case for translations and rotations, the regulating term is not invariant under dilatations transformations. For the Hamiltonian, relaxing for a moment the infinitesimal parameter λ to be x-dependent, its variation takes the form:

$$\begin{aligned}
\delta H &= -\int_x \frac{\delta H}{\delta\varphi(x)}\lambda(x)(D_\varphi + x_\mu\partial_\mu)\varphi(x) \\
&= -\int_x \lambda(x)\Big(x_\mu\partial_\nu T_{\mu\nu}(x) + D_\varphi\varphi(x)\frac{\delta H}{\delta\varphi(x)}\Big) \\
&= -\int_x \lambda(x)\Big\{\partial_\nu\big[x_\mu T_{\mu\nu}(x)\big] - T_{\nu\nu}(x) + D_\varphi\varphi(x)\frac{\delta H}{\delta\varphi(x)}\Big\} \tag{4.25}
\end{aligned}$$

Since we are imposing the Hamiltonian to be scale invariant, this implies

that there is a vector $J_\mu(x)$, named *virial current*, that satisfies:

$$\partial_\mu J_\mu(x) = -T_{\mu\mu}(x) + D_\varphi \varphi(x) \frac{\delta H}{\delta \varphi(x)}. \tag{4.26}$$

With this in mind, the invariance of the Hamiltonian when $\lambda(x) \to \lambda$ is made explicit:

$$\delta H = - \int_x \lambda(x) \Big\{ \partial_\nu \big[x_\mu T_{\mu\nu}(x) \big] + \partial_\nu J_\nu(x) \Big\}$$
$$\underset{\lambda(x) \to \lambda}{=} -\lambda \int_x \partial_\nu \Big\{ x_\mu T_{\mu\nu}(x) + J_\nu(x) \Big\} = 0. \tag{4.27}$$

Notice that in this case, the current associated to dilatations transformations can be written in terms of the energy-momentum tensor and the term $D_\varphi \varphi(x) \frac{\delta H}{\delta \varphi(x)}$. Note also that:

$$\delta \Delta H_k = - \int_{x,y} \lambda R_k(|x-y|) \varphi(y) \big(D_\varphi + x_\nu \partial_\nu \big) \varphi(x) \tag{4.28}$$

Applying the x-dependent transformation to the functional integral Eq.(2.33) yields:

$$\Big\langle \int_x \big\{ \lambda(x) J(x) \big(D_\varphi + x_\mu \partial_\mu \big) \varphi(x) \big\} + \delta H + \delta \Delta H_k \Big\rangle_J = 0, \tag{4.29}$$

and since this equation is valid for any $\lambda(x)$ it is then found that:

$$J(x)\big(D_\varphi + x_\mu \partial_\mu\big) \frac{\delta W_k}{\delta J(x)} = \partial_\nu \big(x_\mu \langle T_{\mu\nu}(x) \rangle_J + \langle J_\nu(x) \rangle_J \big)$$
$$+ \int_y R_k(|x-y|) \big(D_\varphi + x_\mu \partial_\mu \big) \Big(\frac{\delta W_k}{\delta J(y)} \frac{\delta W_k}{\delta J(x)} + \frac{\delta^2 W_k}{\delta J(x) \delta J(y)} \Big) \tag{4.30}$$

Again, doing a generalized Legendre transformation on the $J(x)$ variable, one arrives at Noether's theorem for dilations:

$$\frac{\delta \Gamma_k}{\delta \varphi(x)} \big(D_\varphi + x_\mu \partial_\mu \big) \varphi(x) = \partial_\nu \Big(x_\mu \langle T_{\mu\nu}(x) \rangle_{J_\varphi} + \langle J_\nu(x) \rangle_{J_\varphi} \Big)$$
$$+ \int_y R_k(|x-y|) \big(D_\varphi + x_\mu \partial_\mu \big) \Big(\Gamma_k^{(2)} + R_k \Big)_{x,y}^{-1}. \tag{4.31}$$

This expression in conjunction with Noether's theorem for translation sim-

plifies to the following expression:

$$D_\varphi\varphi(x)\frac{\delta\Gamma_k}{\delta\varphi(x)} =$$

$$\langle T_{\mu\mu}(x)\rangle_{J_\varphi} + \langle\partial_\mu J_\mu(x)\rangle_{J_\varphi} + D_\varphi\int_y R_k(|x-y|)\big(\Gamma_k^{(2)} + R_k\big)^{-1}_{x,y}. \quad (4.32)$$

Consider again Eq.(4.31), integrating in x and performing integration by parts on the term with the regulator yields the Ward identity for dilations in presence of the infrared regulator:

$$\mathcal{D}\Gamma_k \equiv \int_x \frac{\delta\Gamma_k}{\delta\varphi(x)}\big(D_\varphi + x_\mu\partial_\mu\big)\varphi(x)$$

$$+ \frac{1}{2}\int_{x,y}\big(2d - 2D_\varphi + x_\nu\partial_\nu^x + y_\nu\partial_\nu^y\big)R_k(|x-y|)\big(\Gamma_k^{(2)} + R_k\big)^{-1}_{x,y} = 0. \quad (4.33)$$

One important remark at this point is that Eq.(4.33) is nothing but the fixed point equation Eq.(2.40) once that $D_\varphi = \frac{d-2+\eta}{2}$ with $\eta = \eta_*$.

4.1.4 Special Conformal Transformations

Finally we consider the special conformal transformations. These correspond to taking ε_μ given by Eq.(B.17) in Appendix B, which is

$$\varepsilon_\mu^{(SC)} = (x_\nu x_\nu)c_\mu - 2(x_\nu c_\nu)x_\mu.$$

As for dilations, the field must be also rescaled when applying a special conformal transformation, this is:

$$\varphi(x_\sigma) \to \varphi'(x_\sigma') = \left|\frac{\partial x'}{\partial x}\right|^{-D_\varphi/d}\varphi(x_\sigma) = (1 + 2D_\varphi c_\nu x_\nu)\varphi(x_\sigma) + \mathcal{O}(c_\rho c_\beta). \quad (4.34)$$

This expression can be worked out further to get

$$\varphi(x_\sigma) = \varphi'(x_\sigma')(1 - 2D_\varphi c_\nu x_\nu) + \mathcal{O}(c_\rho c_\beta)$$

$$= \varphi'(x_\sigma) + c_\nu(x^2\partial_\nu - 2x_\nu x_\mu\partial_\mu - 2D_\varphi x_\nu)\varphi'(x_\sigma) + \mathcal{O}(\lambda^2), \quad (4.35)$$

or in short:

$$\delta\varphi(x) = -c_\nu\big(x^2\partial_\nu - 2x_\nu x_\mu\partial_\mu - 2x_\nu D_\varphi\big)\varphi(x) = -c_\nu K_\nu\varphi(x) \quad (4.36)$$

83

where K_ν is the generator of special conformal transformations defined in Appendix B.

Considering the variation of the action and relaxing c_μ to depend on x (i.e. $c_\mu \to c_\mu(x)$) we end up with a Noether's theorem for conformal transformations that is not independent of the ones for translations and dilatations combined. The variation of the Hamiltonian is:

$$
\begin{aligned}
\delta H &= \int_x \frac{\delta H}{\delta \varphi(x)} c_\mu(x) \Big\{ 2D_{\varphi^2} x_\mu + 2x_\mu x_\nu \partial_\nu - x^2 \partial_\mu \Big\} \varphi(x) \\
&= \int_x c_\mu(x) \Big\{ 2x_\mu \big(T_{\nu\nu}(x) + \partial_\nu J_\nu(x) \big) + 2x_\mu x_\nu \partial_\rho T_{\nu\rho}(x) - x^2 \partial_\nu T_{\mu\nu}(x) \Big\} \\
&= \int_x c_\mu(x) \Big\{ \partial_\rho \Big(2x_\mu J_\rho(x) + 2x_\mu x_\nu T_{\nu\rho}(x) - x^2 T_{\mu\rho}(x) \Big) - 2J_\mu(x) \Big\}. \quad (4.37)
\end{aligned}
$$

Since we are imposing the Hamiltonian to be invariant when $c_\mu(x) \to c_\mu$ (this is, invariant under a special conformal transformation), this imposes the restriction that the virial current must be a total derivative, i.e. $J_\mu(x) = \partial_\nu L_{\mu\nu}(x)$. This makes the Hamiltonian explicitly invariant under special conformal transformations:

$$
\begin{aligned}
\delta H &= \int_x c_\mu(x) \partial_\rho \Big\{ 2x_\mu J_\rho(x) + 2x_\mu x_\nu T_{\nu\rho}(x) - x^2 T_{\mu\rho}(x) - 2L_{\mu\rho}(x) \Big\} \\
&\underset{c_\mu(x) \to c_\mu}{=} c_\mu \int_x \Big\{ \partial_\rho \Big(2x_\mu J_\rho(x) + 2x_\mu x_\nu T_{\nu\rho}(x) - x^2 T_{\mu\rho}(x) \Big) - 2J_\mu(x) \Big\} = 0.
\end{aligned}
$$
$$(4.38)$$

Then, the only extra information coming from this analysis is that the requirement for the Hamiltonian to be conformal invariant is equivalent to ask that the virial current J_μ is a total derivative. Considering the functional integral (2.33) we conclude that:

$$
\Big\langle \int_x \big\{ c_\nu(x) \big(J(x) \big(2x_\nu D_\varphi + 2x_\nu x_\mu \partial_\mu - x^2 \partial_\nu \big) \varphi(x) \big\} - \delta H - \delta \Delta H_k \Big\rangle_J = 0. \quad (4.39)
$$

Finally, note that:

$$
\delta \Delta H_k = \int_{x,y} c_\nu(x) R_k(x-y) \varphi(y) \big(2x_\nu D_\varphi + 2x_\nu x_\mu \partial_\mu - x^2 \partial_\nu \big) \varphi(x). \quad (4.40)
$$

Differentiating Eq.(4.39) respect to $c_\nu(x)$ we arrive at:

$$
\begin{aligned}
&\Big\langle \big(J(x)\big(2x_\nu D_\varphi + 2x_\nu x_\mu \partial_\mu - x^2 \partial_\nu\big)\varphi(x)\big) \\
&\quad -\partial_\rho\Big(2x_\mu J_\rho(x) + 2x_\mu x_\nu T_{\nu\rho}(x) - x^2 T_{\mu\rho}(x) - 2L_{\mu\rho}\Big) \\
&\quad -\int_y R_k(x-y)\varphi(y)\big(2x_\nu D_\varphi + 2x_\nu x_\mu \partial_\mu - x^2 \partial_\nu\big)\varphi(x)\Big\rangle_J = 0. \qquad (4.41)
\end{aligned}
$$

It turns out that the arbitrariness in the fixing of $T_{\mu\nu}$ allows to work with a energy-momentum tensor that absorbs the virial current and is equivalent to work with $J_\mu = 0$ [110]. This is achieved by the following redefinition:

$$
\begin{aligned}
T'_{\mu\nu}(x) = T_{\mu\nu}(x) &- \frac{1}{d-2}\Big(\partial_\mu\partial_\alpha L_{\alpha\nu} + \partial_\nu\partial_\alpha L_{\alpha\mu} - \partial^2 L_{\mu\nu} - \delta_{\mu\nu}\partial_\alpha\partial_\beta L_{\alpha\beta}\Big) \\
&- \frac{1}{(d-2)(d-1)}\Big(\delta_{\mu\nu}\partial^2 L_{\alpha\alpha} - \partial_\mu\partial_\nu L_{\alpha\alpha}\Big), \qquad (4.42)
\end{aligned}
$$

which explicitly requires $d > 2$[1]. So, we drop the $L_{\mu\nu}$ term in Eq.(4.41).

One can do a Legendre transformation on the $J(x)$ variable of Eq.(4.41) (keeping in mind that we set $J_\mu(x)$ to zero), to arrive at Noether's theorem for special conformal transformations:

$$
\begin{aligned}
\frac{\delta\Gamma_k}{\delta\varphi(x)}\big(x^2\partial_\mu &- 2x_\mu x_\nu \partial_\nu - 2D_\varphi x_\mu\big)\varphi(x) \\
&= -\partial_\nu\big\langle 2x_\mu J_\nu(x) + 2x_\mu x_\rho T_{\rho\nu}(x) - x^2 T_{\mu\nu}(x)\big\rangle_{J_\varphi} \\
&\quad - \int_y R_k(|x-y|)\big(2x_\nu D_\varphi + 2x_\nu x_\mu \partial_\mu - x^2 \partial_\nu\big)\Big(\Gamma_k^{(2)} + R_k\Big)^{-1}_{x,y}. \qquad (4.43)
\end{aligned}
$$

We point out that this expression does not have any extra information with respect to Noether's theorem for dilatations, Eq.(4.32), once that $J_\mu = 0$. Integrating Eq.(4.43) over x and integrating by parts the regulating term we arrive at the conformal Ward identy, which can be interpreted as the action of a conformal operator $\mathcal{K}_\mu$ on the effective action:

$$
\begin{aligned}
\mathcal{K}_\mu\Gamma_k \equiv \int_x \frac{\delta\Gamma_k}{\delta\varphi(x)}\big(x^2\partial_\mu &- 2x_\mu x_\nu \partial_\nu - 2D_\varphi x_\mu\big)\varphi(x) \\
-\frac{1}{2}\int_{x,y}\bigg(&(x_\mu + y_\mu)\big(2d - 2D_\varphi\big) - 2x_\nu x_\mu \partial_\mu^x + x^2 \partial_\nu^x \\
&- 2y_\nu y_\mu \partial_\mu^y + y^2 \partial_\nu^y \bigg) R_k(|x-y|)\Big(\Gamma_k^{(2)} + R_k\Big)^{-1}_{x,y}. \qquad (4.44)
\end{aligned}
$$

---

[1]The case $d = 2$ can be treated similarly, see [110].

4.2 Scale and Conformal Transformations in Critical Phenomena

Regarding conformal invariance and critical phenomena there are two main lines of work. On one hand one could inquire on what are the necessary and sufficient conditions to have conformal invariance when scale invariance is already present and also whether a particular system is conformal invariant or not. On the other hand, there is the question of what extra information can be used when conformal invariance is stated. This line of thought was followed with great successes by CB and we want to follow the same line in the NPRG approach.

The presence of scale invariance in the critical regime of many physical systems is already enough, in principle, to characterize entirely the fixed point and, together with some regularity requirements [8, 111, 112] it fixes all quantities related to the long distance regime. However, solving exactly the NPRG flow equation for the effective action Eq.(2.41) is in general a challenging task. Because of the inherent complexity of the NPRG flow equation and the fact that conformal invariance is considerably more restrictive than mere scale invariance (see, for example, [113]), understanding why the presence of conformal invariance is generally realized has an interest beyond the academic. Indeed, taking it into explicit consideration may bring valuable information to compute critical quantities. In fact, for bidimensional systems conformal invariance is even more restrictive than in higher dimensions [108, 114] and it was proven in 1986 by Zamolodchikov [54] that, in unitary theories, conformal invariance is realized whenever scale invariance is. In higher dimension this result is no longer true and moreover, although not many, there are known counterexamples [115, 56]. Recently there was some progress studying the 4 dimensional case [116, 117, 118, 119].

4.2.1 Sufficient Condition for Scale to Imply Conformal Invariance

Although there are no known result about necessary and sufficient conditions for conformal invariance to be realized, there exists sufficient conditions. In 1988 Polchinski found such a condition [110] suited for systems where the interactions are sufficiently short-ranged. This is because it is based on well defined local quantities such as the stress energy tensor $T_{\mu\nu}(x)$ and the virial

current $J_\mu(x)$. It turns out that the term breaking conformal symmetry is related to the virial current (see Eq.(4.38)), which if it exists must have certain properties as we discuss below (we already discussed some of its properties in Section 4.1). The sufficient condition is then immediately deduced: if in a given system there is no way of constructing such a quantity with the correct properties, then it can not exist and therefore conformal invariance is ensured. More recently, a similar sufficient condition, equivalent in the physical interpretation but with slightly different hypothesis, was proved in the framework of the NPRG [27]. At odds with the sufficient condition given in [110], the sufficient condition in [27] is based on the regularity of the RG flow around the fixed point. It is worth to mention that this difference is important when one is interested in systems such as the *long range Ising model* where the interactions are not restricted to nearest neighbours but decay as a power law of the spins separation. For sufficiently slow decay of the interactions with distance, the system is still extensive but belongs to a different universality class than the standard Ising model [120]. Here I discuss the sufficient condition given in [27], the other sufficient condition given in [110] can be retrieved rather easily from the discussion in Section 4.1. For the sufficient condition, it proves useful to reformulate the previous Ward identities Eq.(4.12), Eq.(4.21), Eq.(4.33) and Eq.(4.44) in the following way:

- *Ward identity for translations*

$$\mathcal{P}_\mu \Gamma_k \equiv \int_x \partial_\mu \varphi(x) \frac{\delta \Gamma_k}{\delta \varphi(x)} = 0 \qquad (4.45)$$

- *Ward identity for rotations*

$$\mathcal{J}_{\mu\nu} \Gamma_k \equiv \int_x \big(x_\mu \partial_\nu - x_\nu \partial_\mu \big) \varphi(x) \frac{\delta \Gamma_k}{\delta \varphi(x)} = 0 \qquad (4.46)$$

- *Ward identity for dilation*

$$
\begin{aligned}
\mathcal{D} \Gamma_k \equiv \int_x \big(x_\nu \partial_\nu + D_\phi \big) \varphi(x) \frac{\delta \Gamma_k}{\delta \varphi(x)} \\
+ \int_{x,y} \big(x_\nu \partial_\nu^x + y_\nu \partial_\nu^y + D_R \big) R_k(x,y) \frac{\delta \Gamma_k}{\delta R_k(x,y)} = 0
\end{aligned}
\qquad (4.47)
$$

- *Ward identity for special conformal*

$$\mathcal{K}_\mu \Gamma_k \equiv \int_x \left(K_\mu^x - 2x_\mu D_\varphi \right) \varphi(x) \frac{\delta \Gamma_k}{\delta \varphi(x)}$$
$$+ \int_{x,y} \left(K_\mu^x + K_\mu^y - D_R(x_\mu + y_\mu) \right) R_k(x,y) \frac{\delta \Gamma_k}{\delta R_k(x,y)} = 0 \quad (4.48)$$

where $D_R \equiv (2d - 2D_\varphi)$ and $K_\mu^x \equiv x^2 \partial_\mu^x - 2x_\mu x_\nu \partial_\nu^x$ and

$$\frac{\delta \Gamma_k}{\delta R(x,y)} = \frac{1}{2} \left(\Gamma_k^{(2)}(x,y) + R(x,y) \right)^{-1}.$$

Notice that we have rewritten Eq.(4.33) and Eq.(4.44) in Eq.(4.47) and Eq.(4.48), respectively, as simultaneous variations of the field $\varphi(x)$ and $R_k(x,y)$ where we are interpreting $R_k(x,y)$ as a bilocal source. When presented in this form, the Ward identities become linear identities.

Now, consider a perturbation around the fixed point

$$\Gamma_k[\tilde{\varphi}] = \Gamma^*[\tilde{\varphi}] + \varepsilon e^{\lambda t} \gamma[\tilde{\varphi}]. \quad (4.49)$$

Inserting it into the dimensionless flow equation, Eq.(2.39), and expanding at first order in ε yields

$$\lambda \gamma[\tilde{\varphi}] = \int_{\tilde{x}} (\tilde{x}_\nu \tilde{\partial}_\nu + D_\varphi^*) \tilde{\varphi}_i(\tilde{x}) \frac{\delta \gamma}{\delta \tilde{\varphi}_i(\tilde{x})}$$
$$- \frac{1}{2} \int_{\tilde{x},\tilde{y},\tilde{z},\tilde{w}} (\tilde{x}_\nu \tilde{\partial}_\nu^{\tilde{x}} + \tilde{y}_\nu \tilde{\partial}_\nu^{\tilde{y}} + 2d - 2D_\varphi^*) \tilde{R}(|\tilde{x} - \tilde{y}|) \tilde{G}^*(\tilde{x},\tilde{z}) \tilde{\gamma}^{(2)}(\tilde{z},\tilde{w}) \tilde{G}^*(\tilde{w},\tilde{y}).$$
$$(4.50)$$

This is an eigenvalue equation which can also be interpreted as

$$\lambda \gamma[\tilde{\varphi}] = \mathcal{D} \gamma[\tilde{\varphi}].$$

Considering for a moment that the system is translational, rotational and scale invariant but not conformal invariant, it would happen that the r.h.s. of Eq.(4.48) is no longer zero. Now, it is straightforward to check that the transformations $\mathcal{P}_\mu$, $\mathcal{J}_{\mu\nu}$, $\mathcal{D}$ and $\mathcal{K}_\mu$ defined in Eq.(4.45)-(4.48) satisfy the commutation relations of the conformal algebra given in Appendix B up to a global sign (this is because the generators $\mathcal{P}_\mu, \mathcal{J}_{\mu\nu}, \mathcal{D}$ and $\mathcal{K}_\mu$ are not the ones defined in Appendix B, but rather they apply to functionals). It proves useful to define the action of the special conformal operator $\mathcal{K}_\mu$ onto the effective

action Γ_k as:

$$\Sigma_\mu \equiv \mathcal{K}_\mu \Gamma_k, \tag{4.51}$$

which, for a non conformal invariant system, it would be $\Sigma_\mu \neq 0$.

Using that $[\mathcal{P}_\mu, \mathcal{K}_\nu] = 2(\delta_{\mu\nu}\mathcal{D} - \mathcal{J}_{\mu\nu})$ (see Appendix B), one immediately concludes that for an effective action Γ_k, which is translational, rotational and scale invariant, Σ_ν satisfies $\mathcal{P}_\mu \Sigma_\nu = 0$. This means that the quantity Σ_ν is translational invariant, which implies that Σ_ν can be written as the integral over the x coordinate of a function of the field and derivatives of the field but without explicit appearance of the x variable.

Now, the commutation relation $[\mathcal{D}, \mathcal{K}_\mu] = -\mathcal{K}_\mu$ can be rewritten (again, for a translational, rotational and scale invariant Γ_k) in terms of Σ_μ as

$$\mathcal{D}\Sigma_\mu = -\Sigma_\mu. \tag{4.52}$$

Comparing with Eq.(4.50), this implies that Σ_μ at the fixed point is an integrated vector operator with scaling dimension -1. The sufficient condition then follows naturally: If there is no integrated vector operator with scaling dimension -1, then the only solution to Eq.(4.52) is $\Sigma_\mu = 0$ which implies that the conformal Ward identity is fulfilled.

To end this section let us make some remarks about the plausibility of having, indeed, conformal invariance at $d = 3$ in view of the sufficient condition. In principle, it appears very likely that conformal invariance is indeed realized since its breaking implies the existence of a quantity with very precise features. This is, it must be an operator which only depends on the field and its derivatives. Furthermore, it must be an eigen operator of the generator of dilatations with eigenvalue -1. This is still not enough, but we must further demand that it is not a total derivative.

Let us assume for a moment that, indeed, exists such an operator with scaling dimension -1 at $d = 3$. If this happens it may be that the scaling dimension exactly cross the value -1 at $d = 3$. So, for dimensions slightly above or below (we refer here to the analytical continuation notion of dimension) the theory is conformal invariant. But based on continuity argument of the correlations functions with the dimension d, this implies that at $d = 3$ the theory must be also conformal invariant and consequently, it restricts even more the scaling dimension of the breaking term of conformal invariance. This term must retain a scaling dimension of -1 for a segment around $d = 3$. We observe such a situation where the scaling dimension of an operator is indepen-

dent of dimension in Appendix G. However, these type of operators, which are called *redundant* operators, are not possible candidates for breaking conformal symmetry, see Appendix G. As far as we know, this situation is not realized for *non-redundant* operators. One last possibility is that around $d = 3$ there is a continuum of eigenvalues of the generator of dilatations. However, there is no indication that this can happen. In any case, a general proof is still lacking since these arguments are far from rigorous. In Chapter 5 we present a study of the realization of conformal invariance in $O(N)$ models and give a proof for specific values of N.

4.3 Scale and Special Conformal Ward Identities Within the Non Perturbative Renormalization Group

In the last years there has been some effort in studying the impact that conformal invariance has within the NPRG. In particular, we mention the studies of the presence of conformal invariance in the critical regime of a variety of models using the NPRG framework [27, 28], as well as some derivation of the formalism of Ward identities or constraints over the energy-momentum tensor [27, 121, 122, 123, 124, 125]. Many of these developments are already derived in the previous sections. In particular Ward identitites for scale and special conformal transformations. In this section we present an equation which isolates the extra information that special conformal Ward identity has with respect to dilatation Ward identity, as well as preparing the ground for Chapter 6 where we use conformal invariance information to produce concrete results within the derivative expansion of the non-perturbative renormalization group.

We assume from now on that the system under consideration is invariant under the full conformal group. Let us start by recalling, and rewriting, the Ward identities for dilatations transformations Eq.(4.53)

$$\int_x \left(x_\nu \partial_\nu + D_\phi \right) \varphi(x) \frac{\delta \Gamma_k}{\delta \varphi(x)} = - \int_{x,y} \partial_t R_k(x-y) \frac{\delta \Gamma_k}{\delta R_k(x-y)} \qquad (4.53)$$

and for special conformal transformations Eq.(4.54)

$$\int_x \left(K_\mu^x - 2 x_\mu D_\varphi \right) \varphi(x) \frac{\delta \Gamma_k}{\delta \varphi(x)} = \int_{x,y} (x_\mu + y_\mu) \partial_t R_k(x-y) \frac{\delta \Gamma_k}{\delta R_k(x-y)}, \quad (4.54)$$

In the previous expressions we used (as it was already implied in Eq.(2.39)) that $(2d - 2D_\varphi + 2x_\mu \partial_\mu^x)R_k(x) = \partial_t R_k(x)$ and we recall is $K_\mu^x = x^2 \partial_\mu^x - 2x_\mu x_\nu \partial_\nu^x$.

We deduce, now, dilatation and special conformal Ward identity for $\Gamma^{(n)}$ (see Eq.(2.42)) in momentum space. This is done by differentiating n times with respect to the field $\varphi(x_i)$, imposing one of the coordinate to zero, say x_n, and finally performing Fourier transformation on the remaining variables.

4.3.1 Dilatation Equation for $\Gamma_k^{(n)}$

Consider Eq.(4.53) and differentiate it with respect to $\varphi(x_1)$ to get

$$
\int_x \Gamma_k^{(2)}[x, x_1; \varphi]\big(D_\varphi + x_\mu \partial_\mu\big)\varphi(x) + \big(D_\varphi - d - x_{1\mu}\partial_\mu^{x_1}\big)\Gamma_k^{(1)}[x_1; \varphi] =
$$
$$
\frac{1}{2}\int_{x,y,z_1,z_2} \partial_t R_k(x-y)G[y, z_1; \varphi]\Gamma_k^{(3)}[z_1, x_1, z_2; \varphi]G[z_2, x; \varphi].
$$
$$(4.55)$$

When taking more and more (functional) derivatives, the right hand side becomes bigger and so, for short, when differentiating n times we write it as

$$
\frac{1}{2}Tr\left[\partial_t R_k G \tilde{H}^{(n)}[x_1, x_2, \ldots, x_n; \varphi]G\right],
$$

where the trace implies many integrations over implicit space variables and in particular $\tilde{H}^{(n)}$ is, in fact, a function of $n+2$ space variables. Now, continuing differentiating Eq.(4.55) with respect to $\varphi(x_2), \ldots, \varphi(x_n)$ and evaluating it on a uniform field $\varphi(x) = \phi$ yield:

$$
\phi D_\varphi \int_x \Gamma_k^{(n+1)}(x, x_1, \ldots, x_n; \phi) + \Big(2D_\varphi - 2d - \sum_{i=1}^n x_{i\mu}\partial_\mu^{x_i}\Big)\Gamma_k^{(n)}(x_1, \ldots, x_n; \phi) =
$$
$$
\frac{1}{2}Tr\left[\partial_t R_k G \tilde{H}^{(n)}(x_1, x_2, \ldots, x_n; \phi)G\right], \quad (4.56)
$$

where we defined $\tilde{H}^{(n)}(x_1, x_2, \ldots, x_n; \phi) \equiv \tilde{H}^{(n)}[x_1, x_2, \ldots, x_n; \varphi(x) \equiv \phi]$. If we set $x_n = 0$ and then carry out a Fourier transform over the remaining variables, after noting that $\Gamma_k^{(n+1)}(x_1, \ldots, x_n, q = 0) = \int_x \Gamma_k^{(n+1)}(x_1, \ldots, x_n, x)$, we arrive

at the following expression for the Dilatation Ward Identity for $\Gamma^{(n)}$:

$$\left[\left(\sum_{i=1}^{n-1} p_{i\nu}\frac{\partial}{\partial p_i^\nu}\right) - d + nD_\varphi + \phi D_\varphi \frac{\partial}{\partial\phi}\right]\Gamma^{(n)}(p_1,\ldots,p_{n-1};\phi) =$$

$$\frac{1}{2}\int_q \dot{R}(q)G^2(q;\phi)H^{(n)}(p_1,\ldots,p_{n-1},q,-q;\phi), \qquad (4.57)$$

Where it was used that $\Gamma_k^{(n+1)}(p_1,\cdots,p_n,0) = \partial_\phi\Gamma_k^{(n)}(p_1,\cdots,p_n)$ and where $H^{(n)}(p_1,\ldots,p_{n-1},q,q')$ is just short for the Fourier transform of $\tilde{H}^{(n)}(x_1,\ldots,x_{n-1},0,z_1,z_2)$ over the variables $x_1,\ldots,x_{n-1}$ and two extra space variables z_1 and z_2 on which $\tilde{H}$ really depends and are made implicit, in its definitions, through out the $Tr[\cdot]$.

We remark that Eq.(4.57) is just the standard Ward identity for dilatations but, instead of having a vanishing right hand side, there is a non-standard term consequence of the presence of the regulator.

4.3.2 Special Conformal Equation for $\Gamma_k^{(n)}$

We can do the same manipulation over the special conformal Ward identity Eq.(4.54). We differentiate it n times with respect to $\varphi(x_1),\ldots,\varphi(x_n)$ which leads to

$$-\sum_{i=1}^n\left(x_i^2\partial_\mu^{x_i} - 2x_{i\mu}x_{i\nu}\partial_\nu^{x_i} - 2(d-D_\varphi)x_{i\mu}\right)\Gamma_k^{(n)}(x_1,\ldots,x_n)$$

$$- 2D_\varphi\int_x x_\mu\varphi(x)\Gamma_k^{(n+1)}(x,x_1,\ldots,x_n) =$$

$$\frac{1}{2}\int_{x,y,z_1,z_2}(x_\mu+y_\mu)\partial_t R_k(x-y)G(y,z_1)\tilde{H}^{(n)}(x_1,\ldots,x_n,z_1,z_2)G(z_2,x).$$

$$(4.58)$$

Following the same steps as before, evaluating in a uniform field $\varphi(x) = \phi$ setting $x_n = 0$ and then carry out a Fourier transform over the remaining

variables, we arrive at the special conformal Ward identity for $\Gamma_k^{(n)}$:

$$
\left[\sum_{i=1}^{n-1} p_{i\mu} \frac{\partial^2}{\partial p_i^\nu \partial p_i^\nu} - 2 p_{i\nu} \frac{\partial^2}{\partial p_i^\nu \partial p_i^\mu} - 2 D_\varphi \frac{\partial}{\partial p_i{}^\mu} \right] \Gamma^{(n)}(p_1, \ldots, p_{n-1})
$$
$$
- 2\phi D_\varphi \frac{\partial}{\partial r^\mu} \left(\Gamma^{(n+1)}(p_1, \ldots, p_{n-1}, r) \right) \Big|_{r=0} =
$$
$$
- \frac{1}{2} \int_q \dot{R}(q) G^2(q) \left(\frac{\partial}{\partial q^\mu} + \frac{\partial}{\partial q'^\mu} \right) H^{(n)}(p_1, \ldots, p_{n-1}, q, q') \Big|_{q'=-q} \qquad (4.59)
$$

Once again, we point out that Eq.(4.59) is just the standard Ward identity for special conformal transformations but, instead of having a vanishing right hand side, there is a non-standard term consequence of the presence of the regulator.

One can notice the resemblance between both equations and in fact, in many situations, they encode the same information. For example, we show that both equations are the same for the vertex $\Gamma_k^{(2)}$. Moreover and without going in details, for any $\Gamma_k^{(n)}$ there exists certain exceptional momentum configurations for which both equations hold the same information.

4.3.3 Compatibility for $\Gamma_k^{(2)}$

We prove that the special conformal Ward identity Eq.(4.59) is just a consequence of the dilatation Ward identity Eq.(4.57) (and rotation invariance) in the case of $\Gamma_k^{(2)}$. We do not show the equivalence for $\Gamma_k^{(1)}$ but we stress that it cannot be recovered from the expression in Fourier space. This is because when deriving those expressions, we set the space coordinates x_n to zero and, since conformal Ward identity is proportional to the space coordinates, setting $x_1 = 0$ yields a trivial equation "$0 = 0$". To do this, first notice that

$$
\frac{\partial}{\partial r^\mu} \Gamma_k^{(3)}(p, r) \Big|_{r=0} = \frac{\partial}{\partial r^\mu} \Gamma_k^{(3)}(-p-r, r) \Big|_{r=0}
$$
$$
= \frac{\partial}{\partial r^\mu} \Gamma_k^{(3)}(p+r, -r) \Big|_{r=0}
$$
$$
= \frac{\partial}{\partial p^\mu} \Gamma_k^{(3)}(p, 0) - \frac{\partial}{\partial r^\mu} \Gamma_k^{(3)}(p, r) \Big|_{r=0}
$$
$$
= \frac{\partial}{\partial p^\mu} \frac{1}{2} \Gamma_k^{(3)}(p, 0)
$$
$$
= \frac{\partial}{\partial p^\mu} \frac{1}{2} \partial_\phi \Gamma_k^{(2)}(p), \qquad (4.60)
$$

where in the last equality it was used that

$$\Gamma_k^{(n+1)}(p_1, \ldots, p_{n-1}, r; \phi) = \partial_\phi \Gamma_k^{(n)}(p_1, \ldots, p_{n-1}; \phi).$$

This transforms the term $2\phi D_\varphi \frac{\partial}{\partial r^\mu} \Gamma^{(3)}(p, r)\Big|_{r=0}$ into $\frac{\partial}{\partial p^\mu} \phi D_\varphi \partial_\phi \Gamma^{(2)}(p)$.

Secondly, the term on the right hand side can be worked out similarly using the symmetries that the $H^{(n)}$ functions has. These are:

- $H^{(n)}(p_i, \cdots, p_{n-1}, q, q') = H^{(n)}(P(p_i, \cdots, p_{n-1}), q, q')$ where $P(p_i)$ is any permutation of the p's.
- $H^{(n)}(p_1, \cdots, p_{n-1}, q, q') = H^{(n)}(-(p_1+\cdots+p_{n-1}+q+q'), \cdots, p_{n-1}, q, q')$
- $H^{(n)}(p_1, \cdots, p_{n-1}, q, q') = H^{(n)}(p_1, \cdots, p_{n-1}, q', q)$

With these properties in mind, we can manipulate the right hand side of the special conformal Ward identity for the vertex function $\Gamma_k^{(2)}$ in the following manner:

$$\begin{aligned}
(\frac{\partial}{\partial q_\mu} + \frac{\partial}{\partial q'_\mu}) H^{(2)}(p, q, q')|_{q'=-q} &= (\frac{\partial}{\partial q_\mu} + \frac{\partial}{\partial q'_\mu}) H^{(2)}(-p-q-q', q, q')|_{q'=-q} \\
&= (\frac{\partial}{\partial q_\mu} + \frac{\partial}{\partial q'_\mu}) H^{(2)}(p+q+q', -q, -q')|_{q'=-q} \\
&= 2\frac{\partial}{\partial p_\mu} H^{(2)}(p, q, -q) - (\frac{\partial}{\partial q_\mu} + \frac{\partial}{\partial q'_\mu}) H^{(2)}(p, q, q')|_{q'=-q} \\
&= \frac{\partial}{\partial p_\mu} H^{(2)}(p, q, -q). \quad (4.61)
\end{aligned}$$

The last piece of the puzzle is quite obvious now, we just apply a p^μ derivative on Eq.(4.57) for the $\Gamma_k^{(2)}$, this reads:

$$\begin{aligned}
\frac{\partial}{\partial p^\mu} \left(p_\nu \frac{\partial}{\partial p^\nu} - d + 2D_\varphi + \varphi D_\varphi \frac{\partial}{\partial \varphi} \right) \Gamma^{(2)}(p) &= \\
&= \left(p_\nu \frac{\partial^2}{\partial p^\nu \partial p^\mu} + (2D_\varphi - d + 1)\frac{\partial}{\partial p^\mu} + \frac{\partial}{\partial p^\mu} \varphi D_\varphi \frac{\partial}{\partial \varphi} \right) \Gamma^{(2)}(p) \\
&= \left(-p_\mu \frac{\partial^2}{\partial p^\nu \partial p^\nu} + 2p_\nu \frac{\partial^2}{\partial p^\nu \partial p^\mu} + 2D_\varphi \frac{\partial}{\partial p^\mu} + \frac{\partial}{\partial p^\mu} \varphi D_\varphi \frac{\partial}{\partial \varphi} \right) \Gamma^{(2)}(p) \\
&\quad + \textcolor{red}{\left(p_\mu \frac{\partial^2}{\partial p^\nu \partial p^\nu} - p_\nu \frac{\partial^2}{\partial p^\nu \partial p^\mu} + (-d+1)\frac{\partial}{\partial p^\mu} \right) \Gamma^{(2)}(p)} \\
&= \frac{\partial}{\partial p_\mu} \int_q \dot{R}(q) G^2(q) H^{(4)}(p, q, -q). \quad (4.62)
\end{aligned}$$

the term in red is just zero because of rotation Ward identity (as can be easily checked). Recognizing the terms already worked out in Eq.(4.60) and

Eq.(4.61), we check that we arrive at not other equation than Eq.(4.59).

In summary, this means that conformal Ward identity applied to $\Gamma_k^{(2)}(p; \phi)$ does not have more information than dilatation Ward identity. Notice that this result is trivially satisfied at $\phi = 0$ and $k = 0$, but it is not so for $k \neq 0$ and $\phi \neq 0$. It is worth mentioning that this result is also true for higher order vertices in exceptional momentum configurations. Although we do not give the proof here, we make use of this result in Chapter 6.

4.3.4 Extra Restrictions From Conformal Invariance: An Exact Relation

When considering n-point vertex functions with $n \geq 3$, dilatation Ward identity and special conformal Ward identity are no longer equivalent in a general momentum configuration. However, all the information of dilatation Ward identity is contained in the special conformal Ward identity. It is then important to be able to disentangle the extra information that conformal invariance gives with respect to the information that dilatation invariance.

In this section we take one step in this direction by obtaining an exact equation which only contains the extra information coming from conformal invariance. To avoid overloading the notation, we drop the k subscript on the vertex function $\Gamma_k^{(n)}$. Start by considering Eq.(4.57) for a generic vertex $\Gamma^{(n)}$ and consider the right hand side of this equation as a function of the external momenta and the field $A^{(n)}(p_1, \ldots, p_{n-1}, \phi)$. This is:

$$\left(nD_\varphi - d + \phi D_\varphi \frac{\partial}{\partial \phi} + \sum_{i=1}^{n-1} p_i^\nu \frac{\partial}{\partial p_i^\nu} \right) \Gamma^{(n)}(p_1, \ldots, p_{n-1}, \phi) =$$
$$A^{(n)}(p_1, \ldots, p_{n-1}, \phi). \qquad (4.63)$$

The reasoning goes as follows. We first assume $A^{(n)}(p_1, \ldots, p_{n-1}, \phi)$ as given. This makes dilatation Ward identity for $\Gamma_k^{(n)}$ a linear equation and, in fact, solvable in terms of $A^{(n)}$. However, we do not really know $A^{(n)}$. After this, we repeat this process for $\Gamma_k^{(n+1)}$. These two functions, $\Gamma_k^{(n)}$ and $\Gamma_k^{(n+1)}$, are the ones appearing in the special conformal Ward identity for $\Gamma_k^{(n)}$. This allows us to write down a constraint which combines, both special conformal and dilatation Ward identity, into a single equation (which, in fact, becomes trivially satisfied in the cases $n = 1$ and $n = 2$, where the two Ward identities coincide). In

order to do this program, we make the change of variables:

$$u_i^\mu \equiv p_i^\mu \rho^\beta, \tag{4.64}$$

$$\Gamma_k^{(n)}(p_1, \ldots, p_{n-1}, \phi) \equiv \phi^\delta \rho^\alpha f^{(n)}(u_1, \ldots, u_{n-1}, \rho), \tag{4.65}$$

$$A^{(n)}(p_1, \ldots, p_{n-1}, \phi) \equiv \phi^\delta \rho^\alpha \hat{A}^{(n)}(u_1, \ldots, u_{n-1}, \rho), \tag{4.66}$$

where α and β are some numbers to be specified and δ equals 1 if n is odd and 0 if n is even. These changes lead to:

$$\phi^\delta \rho^\alpha \left((\delta + 2\alpha) D_\varphi + 2 D_\varphi \rho \frac{\partial}{\partial \rho} + (1 + 2\beta D_\varphi) \sum_{i=1}^{n-1} u_i^\nu \frac{\partial}{\partial u_i^\nu} \right.$$
$$\left. + n D_\varphi - d \right) f^{(n)}(u_1, \ldots, u_{n-1}, \rho) = \phi^\delta \rho^\alpha \hat{A}^{(n)}(u_1, \ldots, u_{n-1}, \rho). \tag{4.67}$$

This equation may be simplified by setting the values $\alpha \equiv \frac{d}{2D_\varphi} - \frac{n+\delta}{2}$ and $\beta \equiv -\frac{1}{2D_\varphi}$, yielding:

$$2 D_\varphi \rho \frac{\delta}{\delta \rho} f^{(n)}(u_1, \ldots, u_{n-1}, \rho) = \hat{A}^{(n)}(u_1, \ldots, u_{n-1}, \rho). \tag{4.68}$$

We now consider dilatation Ward identity for $\Gamma^{(n+1)}$, apply a p_n^μ derivative and afterwards we evaluate it at $p_n = 0$ yielding:

$$\left((n+1) D_\varphi - d + 1 + \phi D_\varphi \frac{\partial}{\partial \phi} + \sum_{i=1}^{n-1} p_i^\nu \frac{\partial}{\partial p_i^\nu} \right) \Gamma_\mu^{(n)}(p_1, \ldots, p_{n-1}, \phi) =$$
$$A_\mu^{(n)}(p_1, \ldots, p_{n-1}, \phi), \tag{4.69}$$

where we introduced the definitions:

$$\Gamma_\mu^{(n)}(p_1, \ldots, p_{n-1}, \phi) \equiv \frac{\partial}{\partial p_n^\mu} \Gamma^{(n+1)}(p_1, \ldots, p_n, \phi) \Big|_{p_n=0}, \tag{4.70}$$

$$A_\mu^{(n)}(p_1, \ldots, p_{n-1}, \phi) \equiv \frac{\partial}{\partial p_n^\mu} A^{(n+1)}(p_1, \ldots, p_n, \phi) \Big|_{p_n=0}. \tag{4.71}$$

We perform again similar changes of variables, as in Eqs.(4.64-4.66):

$$u_i^\mu \equiv p_i^\mu \rho^\beta, \tag{4.72}$$

$$\Gamma_k^{(n)}(p_1, \ldots, p_{n-1}, \phi) \equiv \phi^{1-\delta} \rho^\gamma g_\mu^{(n)}(u_1, \ldots, u_{n-1}, \rho), \tag{4.73}$$

$$A_\mu^{(n)}(p_1, \ldots, p_{n-1}, \phi) \equiv \phi^{1-\delta} \rho^\gamma \hat{A}_\mu^{(n)}(u_1, \ldots, u_{n-1}, \rho), \qquad (4.74)$$

and in the same way, setting $\gamma \equiv \frac{d - 2D_\varphi - 1}{2D_\varphi} - \frac{n - \delta}{2}$ and $\beta \equiv -\frac{1}{2D_\varphi}$ yields:

$$2D_\varphi \rho \frac{\partial}{\partial \rho} g_\mu^{(n)}(u_1, \ldots, u_{n-1}, \rho) = \hat{A}_\mu^{(n)}(u_1, \ldots, u_{n-1}, \rho) \qquad (4.75)$$

At this point we consider special conformal Ward identity for $\Gamma^{(n)}$ Eq.(4.59) in terms of the previously considered changes of variables:

$$\phi^\delta \rho^{\alpha+\beta} \left(\left[\sum_{i=1}^{n-1} u_{i\mu} \frac{\partial^2}{\partial u_i^\nu \partial u_i^\nu} - 2u_{i\nu} \frac{\partial^2}{\partial u_i^\nu \partial u_i^\mu} - 2D_\varphi \frac{\partial}{\partial u_i^\mu} \right] f^{(n)}(u_1, \ldots, u_{n-1}, \rho) \right.$$
$$\left. - 2^{2-\delta} D_\varphi g_\mu^{(n)}(u_1, \ldots, u_{n-1}, \rho) \right) = \phi^\delta \rho^{\alpha+\beta} \hat{B}_\mu^{(n)}(u_1, \ldots, u_{n-1}, \rho), \quad (4.76)$$

where the right hand side of Eq.(4.59) is defined as $\phi^\delta \rho^{\alpha+\beta} \hat{B}_\mu^{(n)}(u_1, \ldots, u_{n-1}, \rho)$. One can work out this expression in order to make use of Eq.(4.68) and Eq.(4.75). This is accomplished by applying $2D_\varphi \rho \partial_\rho$ on Eq.(4.76) (without the prefactor $\phi^\delta \rho^{\alpha+\beta}$). This leads to:

$$\left[\sum_{i=1}^{n-1} u_{i\mu} \frac{\partial^2}{\partial u_i^\nu \partial u_i^\nu} - 2u_{i\nu} \frac{\partial^2}{\partial u_i^\nu \partial u_i^\mu} - 2D_\varphi \frac{\partial}{\partial u_i^\mu} \right] \hat{A}^{(n)}(u_1, \ldots, u_{n-1}, \rho)$$
$$- 2^{2-\delta} D_\varphi \hat{A}_\mu^{(n)}(u_1, \ldots, u_{n-1}, \rho) = 2D_\varphi \frac{\partial}{\partial \rho} \hat{B}_\mu^{(n)}(u_1, \ldots, u_{n-1}, \rho), \qquad (4.77)$$

Finally, going back to the original form of the right hand sides of Eq.(4.57) and Eq.(4.59), rewriting everything in terms of the original momentum variables and dropping a global factor of $\phi^{-\delta} \rho^{-\alpha-\beta}$ we arrive at an exact equation that combines dilatation Ward identity and special conformal Ward identity:

$$0 = \int_q \partial_t R_k(q) G^2(q) \times$$
$$\left\{ \left(\sum_{i=1}^{n-1} p_i^\mu \frac{\partial^2}{\partial p_i^\nu \partial p_i^\nu} - 2p_i^\nu \frac{\partial^2}{\partial p_i^\nu \partial p_i^\mu} - 2D_\varphi \frac{\partial}{\partial p_i^\mu} \right) H^{(n)}(p_1, \ldots, p_{n-1}, q, -q) + \right.$$
$$\left(\frac{\partial}{\partial q^\mu} + \frac{\partial}{\partial q'^\mu} \right) \left[nD_\varphi + 1 - d + \sum_{i=1}^{n-1} p_i^\nu \frac{\partial}{\partial p_i^\nu} \right] H^{(n)}(p_1, \ldots, p_{n-1}, q, q') \Big|_{q'=-q}$$
$$\left. + \phi D_\varphi \left(\frac{\partial}{\partial q^\mu} + \frac{\partial}{\partial q'^\mu} - 2\frac{\partial}{\partial p_n^\mu} \right) H^{(n+1)}(p_1, \ldots, p_n, q, q') \Big|_{q'=-q\,;\,p_n=0} \right\}. \quad (4.78)$$

As we showed, special conformal Ward identity does not have any new information with respect to dilatation Ward identity for the $\Gamma_k^{(2)}$ and, in that

case, the equation becomes $0 = 0$. This is because there are no angles involved when there is just one external momentum. The same is true if we put all but one external momenta to zero in the equation for $\Gamma_k^{(n)}$. One last detail to mention about Eq.(4.78) is that the prefactor $G^2(q)$ can be moved through out the operators in front of the H's functions as $\tilde{H}^{(n)} = G(q)H^{(n)}G(q')$ and we obtain an equivalent equation with operators acting on $\tilde{H}$'s with only a prefactor of $\partial_t R_k(q)$.

4.3.5 Extra Restrictions From Conformal Invariance: Approximate Relation at a Given Order of the DE

When one considers any approximation scheme it can happen, and usually does, that it is not possible to satisfy simultaneously both dilatation and special conformal Ward identities Eq.(4.57) and Eq.(4.59), respectively. This is because, dilatation Ward identity already establishes a compatible and complete system of equations that fully determine the fixed point. So, adding extra equations seem to over-constraints the problem and, in general grounds, there are no solutions. However, this can be exploited in the following manner. Instead of considering the exact relation Eq.(4.78), we can go a different way and analyse what happens within an *approximation scheme of choice* (ASC) to Eq.(4.59). In this thesis we mainly focused on the derivative expansion approximation scheme and so, we consider it to be our ASC. We already discussed in Chapter 3 how to satisfy Eq.(4.57) within this approximation scheme. We remark that special conformal Ward identity does not have any new information at order LPA and order $\mathcal{O}(\partial^2)$ with respect to dilatation Ward identity. This is because all information at these orders of the DE can be extracted from the vertex functions $\Gamma_k^{(1)}$ and $\Gamma_k^{(2)}$ and, in turn, we can extract all the information relative to these ansatz of from the vertex function $\Gamma_k^{(1)}$ and $\Gamma_k^{(2)}$. It happens that when one plugs in the ansatz of the DE at order $\mathcal{O}(\partial^4)$ or higher in Eq.(4.59), one can construct more independent equations[1] that when plugging in the ansatz in Eq.(4.57). In particular, when considering the order $\mathcal{O}(\partial^4)$ of the DE, we can construct from conformal Ward identity, the same equations than with dilatations plus one more extra restriction.

There are more than one way of exploiting the fact that there are extra

---

[1]The equivalence of conformal and dilatation Ward identities at order LPA is not evident from the Fourier transformed expressions Eq.(4.57) and Eq.(4.59).

restrictions that arise from special conformal invariance at $\mathcal{O}(\partial^4)$ or higher of the DE.

One way to go, and that we exploit in detail in Chapter 6, is to study the breaking of conformal invariance of the Wilson-Fisher fixed point found using only dilatation Ward identity as a function of a free parameter. For example, study the breaking of conformal invariance as a function of the parameter α of the regulator function of choice (see for example Eq.(2.30)-Eq.(2.32)) and instead of using the PMS criterion, consider as the optimal value of α the one that breaks the least conformal invariance that we call *maximal conformality criterion* (MCC) and consequently call this value α_{MCC}. Of course, this criterion is still ambiguous and a concrete implementation will depend on the ASC. For example, for the Ising model at order $\mathcal{O}(\partial^4)$ there is just one extra equation coming from special conformal Ward identity, whereas at order $\mathcal{O}(\partial^6)$ there are four extra restrictions and one stills needs to specify a criterion to say what is to *better* satisfy conformal invariance.

Another possible approach, not studied in this thesis but that we could study in the future, is to add as many possible functions from higher orders of the DE in order to have as many equations as independent functions.

To finish this chapter, I would like to highlight that while studying the constraints that dilatation and special conformal Ward identities imposes on the vertex functions, many other approaches were considered, with partial success, with the aim of isolating the extra restrictions of conformal invariance or writing down a simple constraint. Moreover, there are many other approaches that still remain to be tried. It is clear that we are far from exhausting the information that comes from conformal invariance. Moreover, the use of conformal invariance within the NPRG as we presented here can give rise to new or improved approximation schemes. Furthermore, the possibility of exact results (probably exploiting the identity in Eq.(4.59)) is not inconceivable.

Chapter 5

Studies on the Realization of Conformal Invariance in the $O(N)$ Model

The presence of conformal invariance in the Ising model was explored via Monte Carlo simulations in [126, 127]. In 2016 it was proved by Delamotte, Tissier and Wschebor [27] that, under rather general hypothesis, the Ising model is indeed conformal invariant at criticality. This was done by making use of the sufficient condition discussed in Chapter 4. On top of this, a Monte Carlo simulation which aimed at testing the sufficient condition was performed [128]. The conclusions, of course, go in the same line: *the Ising model is conformal invariant.* Studies for the realization of conformal invariance in the long range Ising model were also performed [129] with the same conclusion. It is believed that the $O(N)$ model is conformal invariant too, although there was no proof of it so far. This chapter is based on our published paper [28]. We present the results given there as well as extending the discussion in some cases. We also give in Appendix D a one loop calculation of the scaling dimension of possible breaking terms for the cubic anisotropy model. While doing so, we consider possible breaking which are not $O(N)$ invariant but are invariant under the symmetries of an hyper-cubic lattice. The conclusions are that the leading candidates for breaking conformal invariance have scaling dimension much larger than -1 and, according to the sufficient conditions, conformal symmetry is realized in these models also.

The conformal bootstrap program has been applied to this models for several values of N [79] (see Chapter 3). The overall results are that the predictions coming from the conformal bootstrap are in good agreement with Monte

Carlo simulations and other methods [16, 88], see also Chapter 3. Although one could be satisfied with the agreement of results as a strong indication, there is still no formal studies about if indeed the $O(N)$ model is conformal invariant. This chapter aims at filling this gap by presenting the study of the plausibility for the presence of conformal invariance in the $O(N)$ model by making use of the sufficient condition of Chapter 4. The approach considered here is to compute the scaling dimension of integrated vector operators, candidates for the symmetry breaking term Σ_μ in Eq.(4.51). The operators considered are supposed to mix with the most relevant one (this is, they have non-zero overlap with the most relevant eigenoperator of the dilation transformation) and, therefore, exhibit the smallest possible scaling dimension of an integrated vector operator. By showing that this *smallest possible* scaling dimension is always much higher than the -1 value that Σ_μ should have in order to yield a possible breaking of conformal invariance, we give strong evidence that the $O(N)$ model is conformal invariant for all $N \geq 0$.

I present calculations of scaling dimension of the most relevant integrated vector operators within three approximation schemes: the ϵ-expansion, the large N limit and the derivative expansion at order $\mathcal{O}(\partial^3)$. The ϵ-expansion and the large N limit describe accurately the behaviour near four dimensions and very large N values, respectively. The results from these two approximation schemes are shown to coincide in their common domain of validity. Moreover, the DE approximation scheme recovers the results from the other two schemes in the corresponding limits and therefore is, at the very least, an educated interpolation scheme (we recall, however, that in Chapter 3 it has been shown that the derivative expansion seems to converge properly to the exact value with a reduction of error bars of around 1/9 to 1/4 at each successive order). The results obtained support the fact that the $O(N)$ models are conformal invariant at criticality. Finally, I present a proof for the invariance under conformal transformation in the critical regime of the $O(2)$, $O(3)$ and $O(4)$ models, based on well established correlation inequalities [130, 131, 132, 133, 134, 135] for these models and on the already existing proof for the Ising model [27].

5.1 $O(N)$ Studies on Conformal Symmetry

In this section we present evidence that the $O(N)$ model is conformal invariant for all values of N. To do this, first we find the Wilson-Fisher fixed point of

the model and then we introduce a small vectorial perturbations of the general form $v_\mu \mathcal{V}_\mu$, where $\mathcal{V}_\mu$ is some integrated vector operator and v_μ is a coupling to this operator. We then compute the flow of v_μ at linear order in v. Note that, by isometries, the Wilson-Fisher fixed point has $v_\mu^* = 0$. As a consequence it is sufficient to compute the flow at linear order in v_μ. Explicitly, we introduce a combination of vectorial perturbations $\delta H = v_\mu^i \mathcal{V}_\mu^i$ within each approximation scheme (which are consistent with each other in compatible limits). By doing this procedure we obtain the evolution equations for these operators at linear level at the fixed point:

$$\partial_t v_\mu^i = \sum_j M_{ij}^* v_\mu^j, \tag{5.1}$$

where M^* is the stability matrix of this vector sector evaluated at the fixed point. Computing the (smallest) eigenvalues of M^* yield the scaling dimension of the most relevant vector operators.

Without loss of generality, because of universality, we consider for the first two approximation schemes, the microscopic Hamiltonian given by Eq.(2.60) that we recall here

$$H = \int_x \left\{ \frac{1}{2} \partial_\mu \phi_i \partial_\mu \phi_i + \frac{r}{2} \phi_i \phi_i + \frac{u}{4!} \phi_i \phi_i \phi_j \phi_j \right\}.$$

As described in Chapter 2, for the derivative expansion we will consider, instead, an ansatz for Γ_k to be specified later.

5.1.1 ϵ-Expansion

In $d = 4$ the fixed point controlling the phase transition is Gaussian. As a consequence, the scaling dimension of vector operators is obtained simply by dimensional analysis, with the dimension of the field being 1. It is simple to show that the lowest scaling dimension of a vector operator with the properties described above is 3 and that there are two independent $O(N)$-invariant vector operators with this dimension. This conclusion can be obtained by noticing that local operators with 1 derivative are always total derivatives and therefore are discarded based on the fact that the breaking of conformal invariance is an integrated vector operator, which would yield $\int_x f(\phi) \partial_\mu \phi(x) = 0$. Therefore, the first candidate has at least 3 derivatives and 4 fields. We find by inspection that there are two such terms for $O(N)$ models. When considering $2n + 1$ derivatives acting on two fields we obtain again a total derivative since $\int_x \partial_{\alpha_1} \dots \partial_{\alpha_m} \varphi(x) \partial_\mu (\partial_{\alpha_{m+1}} \dots \partial_{\alpha_n} \varphi(x))$, where

there are n contracted derivatives, can always be transformed by integration by parts into $\int_x \partial_{\nu_1} \ldots \partial_{\nu_n} \varphi(x) \partial_\mu (\partial_{\nu_1} \ldots \partial_{\nu_n} \varphi(x)) = 0$. In the following I will introduce the perturbation with not only the leading order vector operators (this is, with canonical dimension 3 at $d = 4$), but also operators with 3 derivatives and scaling dimension 5 in $d = 4$. Before doing so, note that there are more operators with scaling dimension 5 at $d = 4$. However, these involve at least five derivatives and, since its behaviour will not be captured in the DE study at order $\mathcal{O}(\partial^3)$, I will not consider them in order to be able to compare both approximation schemes (however, in Appendix H these are included just for the $N = 1$ case).

We therefore add the perturbation

$$
\delta H = \int_x \left\{ \frac{a_\mu^\Lambda}{4} \phi_i \partial^\mu \phi_i \partial_\nu \phi_j \partial_\nu \phi_j + \frac{b_\mu^\Lambda}{2} \phi_i \partial_\nu \phi_i \partial_\nu \phi_j \partial^\mu \phi_j + \frac{c_\mu^\Lambda}{4} \phi_i \phi_j \phi_k \partial^\mu \phi_i \partial^\mu \phi_j \partial^\mu \phi_k \right.
$$
$$
\left. + \frac{\tilde{a}_\mu^\Lambda}{4} \phi_k \phi_k \phi_i \partial^\mu \phi_i \partial_\nu \phi_j \partial_\nu \phi_j + \frac{\tilde{b}_\mu^\Lambda}{2} \phi_k \phi_k \phi_i \partial_\nu \phi_i \partial_\nu \phi_j \partial^\mu \phi_j \right\} \tag{5.2}
$$

to the microscopic Hamiltonian Eq.(2.60). We highlight that the 2 most relevant vector operators at $d = 4$ are the ones proportional to a_μ^Λ and b_μ^Λ.

In order to compute the scaling dimension at leading order in $\epsilon = 4 - d$ we need to compute only the one-loop diagrams. The calculation is performed within the NPRG framework. Of course, since the first correction in the ϵ-expansion is scheme-independent, the calculation could be performed within other approaches, such as the Minimal Substraction scheme.

Start by observing that at tree-level (zero loop) the effective action takes its bare form:

$$
\Gamma_k^{(tree)}[\varphi] = \int_x \left\{ r\rho + \frac{u}{3!} \rho^2 + \frac{a_\mu}{4} \partial_\mu \rho \partial_\nu \varphi_i \partial_\nu \varphi_i + \frac{b_\mu}{2} \partial_\mu \varphi_i \partial_\nu \varphi_i \partial_\nu \rho \right.
$$
$$
\left. + \frac{\tilde{a}_\mu}{2} \rho \partial_\mu \rho \partial_\nu \varphi_i \partial_\nu \varphi_i + \tilde{b}_\mu \rho \partial_\mu \varphi_i \partial_\nu \varphi_i \partial_\nu \rho + \frac{c_\mu}{4} \partial_\mu \rho \partial_\nu \rho \partial_\nu \rho \right\}. \tag{5.3}
$$

Differentiating successively with respect to $\varphi_{n_i}(x_i)$ and Fourier transforming, we obtain the form of the non-zero vertices at zero external field:

$$
\Gamma_{i_1 i_2}^{(2,tree)}(p_1) = \delta_{i_1 i_2}(r + p_1^2) \tag{5.4}
$$

$$\Gamma^{(4,tree)}_{i_1 i_2 i_3 i_4}(p_1, p_2, p_3) = \frac{u}{3}\left[\delta_{i_1 i_2}\delta_{i_3 i_4} + \delta_{i_1 i_3}\delta_{i_2 i_4} + \delta_{i_1 i_4}\delta_{i_2 i_3}\right] +$$

$$\left\{ (p_1 + p_2)^\mu \left(p_1 \cdot p_2 - p_3 \cdot p_4\right)\delta_{i_1 i_2}\delta_{i_3 i_4} + (p_1 + p_3)^\mu \left(p_1 \cdot p_3 - p_2 \cdot p_4\right)\delta_{i_1 i_3}\delta_{i_2 i_4}\right.$$

$$\left. + (p_1 + p_4)^\mu \left(p_1 \cdot p_4 - p_2 \cdot p_3\right)\delta_{i_1 i_4}\delta_{i_2 i_3}\right\} i\frac{a_\mu - b_\mu}{2}$$

$$- i\frac{b_\mu}{2}\left(p_1^\mu p_1^2 + p_2^\mu p_2^2 + p_3^\mu p_3^2 + p_4^\mu p_4^2\right)\left(\delta_{i_1 i_2}\delta_{i_3 i_4} + \delta_{i_1 i_3}\delta_{i_2 i_4} + \delta_{i_1 n_i}\delta_{i_2 i_3}\right)$$

$$(5.5)$$

$$\Gamma^{(6,tree)}_{i_1 i_2 i_3 i_4 i_5 i_6}(p_1, p_2, p_3, p_4, p_5) = \delta_{i_1 i_2}\delta_{i_3 i_4}\delta_{i_5 i_6}\left\{ i(\tilde{a}_\mu + \tilde{b}_\mu)\left[(p_1 + p_2)^\mu p_1 \cdot p_2\right.\right.$$

$$+ (p_3 + p_4)^\mu p_3 \cdot p_4 + (p_5 + p_6)^\mu p_5 \cdot p_6\Big] + i\tilde{b}_\mu\big[p_1^\mu p_1^2 + p_2^\mu p_2^2 + p_3^\mu p_3^2 + p_4^\mu p_4^2$$

$$+ p_5^\mu p_5^2 + p_6^\mu p_6^2\big] - i\frac{c_\mu}{2}\big[(p_1 + p_2)^\mu (p_3 + p_4) \cdot (p_5 + p_6)$$

$$\left.\left. + (p_3 + p_4)^\mu(p_1 + p_2) \cdot (p_5 + p_6) + (p_5 + p_6)^\mu(p_1 + p_2) \cdot (p_3 + p_4)\right]\right\} + \text{perms.}$$

$$(5.6)$$

In the previous equations, the index k on the coupling constants has been omitted to simplify notation. The momenta p_4 in $\Gamma^{(4)}$ and p_6 in $\Gamma^{(6)}$ are fixed by momentum conservation: $\sum_{i=1}^{n} p_i = 0$, with $n = 4$ and $n = 6$ respectively. The flow of a_μ and b_μ are deduced from the flow equation of $\Gamma^{(4)}$ at zero external field, which is obtained by differentiating four times the RG equation [Eq.(2.41)] and evaluating it at $\phi = 0$. We obtain:

$$\partial_t \Gamma^{(4)}_{i_1 i_2 i_3 i_4}(p_1, p_2, p_3) = \int_q \partial_t R_k\left(q^2\right) G_k^2\left(q^2\right)\left(-\frac{1}{2}\Gamma^{(6)}_{k,k,i_1,i_2,i_3,i_4}(q, -q, p_1, p_2, p_3)\right.$$

$$\left. + G_k\left((q + p_1 + p_2)^2\right) \Gamma^{(4)}_{k i_1 i_2 l}(q, p_1, p_2)\Gamma^{(4)}_{l i_3 i_4 k}(q + p_1 + p_2, p_3, p_4) + 2 \text{ perms.}\right).$$

$$(5.7)$$

The flow of $\tilde{a}_\mu$, $\tilde{b}_\mu$ and c_μ are deduced from the flow equation of $\Gamma^{(6)}$ at zero external field, which is obtained by differentiating six times the RG equation

[Eq.(2.41)] and evaluating it at $\phi = 0$. This is:

$$\partial_t \Gamma^{(6)}_{i_1 i_2 i_3 i_4 i_5 i_6}(p_1, p_2, p_3, p_4, p_5) = \int_q \partial_t R_k \left(q^2\right) G_k^2 \left(q^2\right) \times$$

$$\left(-\frac{1}{2} \Gamma^{(8)}_{k,k,i_1,i_2,i_3,i_4,i_5,i_6}(q, -q, p_1, p_2, p_3, p_4, p_5) + \left[G_k \left((q + p_1 + p_2)^2\right) \times \right.\right.$$

$$\Gamma^{(4)}_{k i_1 i_2 l}(q, p_1, p_2) \Gamma^{(6)}_{l i_3 i_4 i_5 i_6 k}(q + p_1 + p_2, p_3, p_4, p_5, p_6) + 14 \text{ perms.} \Big]$$

$$+ \left[G_k \left((q + p_1 + p_2)^2\right) G_k \left((q + p_1 + p_2 + p_3 + p_4)^2\right) \Gamma^{(4)}_{k i_1 i_2 l}(q, p_1, p_2) \times \right.$$

$$\Gamma^{(4)}_{l i_3 i_4 m}(q + p_1 + p_2, p_3, p_4) \Gamma^{(4)}_{m i_5 i_6 k}(q + p_1 + p_2 + p_3 + p_4, p_5, p_6) + 44 \text{ perms.} \Big] \bigg).$$

$$(5.8)$$

At one loop, we replace the vertices in the right hand side of the flow equation by its tree-level form given in Eq.(5.4)-(5.6) and perform the sum over indices in the product of $\Gamma_k^{(n,tree)}$'s. The computation is significantly simplified because we keep only terms which are at most linear in a_μ, b_μ, $\tilde{a}_\mu$, $\tilde{b}_\mu$ and c_μ (we recall that at the fixed point all these couplings are zero, see discussion before Eq.(5.1)).

The next step consists in identifying the prefactors of a given structure which involves both vector indices and momenta [see Eq.(5.4)-(5.6)] in the left hand side and right hand side of the flow equations, Eq.(5.7) and Eq.(5.8). This implies that we must expand the right hand side in powers of the external momenta and extract terms of order zero and order three in momenta.

Two extra simplifications takes place. On one hand, it happens that for the flow $\Gamma_k^{(4)}$ the product of the two $\Gamma_k^{(4,tree)}$, including summing over indices, has contributions only with 0 and 3 powers of the external momenta as the desired structures. As a consequence, we can put in the propagator $G(q + p_x)$ (with p_x a sum of two external momentum) the external momenta to zero. On the other hand, although this does not happen for the flow of $\Gamma_k^{(6)}$, where propagators must be expanded in order to obtain the momentum structures, the integrals appearing are either

$$I \equiv \int_q \partial_t R_k(q^2) G_k^3(q^2), \tag{5.9}$$

or the specific combination:

$$\int_q \partial_t R_k(q^2) G_k^2(q^2)(3q^2 G_k'(q^2) + q^4 G_k''(q^2)), \tag{5.10}$$

105

which can be shown to be $-I$ (see Appendix H).

From this observations we can now extract the flows at one loop of u, a_μ, b_μ, $\tilde{a}_\mu$, $\tilde{b}_\mu$ and c_μ, which read:

$$\partial_t u = \frac{(N+8)}{3} u^2 I,$$

$$\partial_t a_\mu = \frac{u}{3} \left[(N+4)\, a_\mu + 4b_\mu \right] I - 3\left[(N+2)\tilde{a}_\mu + c_\mu \right] \int_q \partial_t R_k(q^2) G_k^2(q^2),$$

$$\partial_t b_\mu = \frac{u}{3} \left[2a_\mu + (N+6)\, b_\mu \right] I - 3\left[(N+2)\tilde{b}_\mu + c_\mu \right] \int_q \partial_t R_k(q^2) G_k^2(q^2),$$

$$\partial_t c_\mu = \frac{u}{3} \left[(3N+22)c_\mu - (N-4)\tilde{a}_\mu - (N-8)\tilde{b}_\mu \right] I, \qquad (5.11)$$

$$\partial_t \tilde{a}_\mu = \frac{u}{9} \left[(6N+65)\tilde{a}_\mu + 17\tilde{b}_\mu + c_\mu \right] I,$$

$$\partial_t \tilde{b}_\mu = \frac{u}{9} \left[5\tilde{a}_\mu + (6N+65)\tilde{b}_\mu + 7c_\mu \right] I,$$

where only linear contributions in the vector couplings have been kept.

We now consider the dimensionless variables:

$$\begin{aligned}
\hat{u} &= k^{d-4}u, & \hat{a}_\mu &= k^{d-1}a_\mu, \\
\hat{b}_\mu &= k^{d-1}b_\mu, & \hat{c}_\mu &= k^{2d-3}c_\mu, \\
\hat{\tilde{b}}_\mu &= k^{2d-3}\tilde{b}_\mu, & \hat{\tilde{a}}_\mu &= k^{2d-3}\tilde{a}_\mu, & .
\end{aligned} \qquad (5.12)$$

To ease notation we drop the "$\wedge$" over variables and we arrive at the flow equations for the dimensionless variables:

$$\partial_t u = -\epsilon u + \frac{(N+8)\,u^2 J}{3}$$

$$\partial_t a_\mu = (3-\epsilon)\, a_\mu + \frac{uJ}{3} \left[(N+4)\, a_\mu + 4b_\mu \right] - 3K\left[(N+2)\tilde{a}_\mu + c_\mu \right]$$

$$\partial_t b_\mu = (3-\epsilon)\, b_\mu + \frac{uJ}{3} \left[2a_\mu + (N+6)\, b_\mu \right] - 3K\left[(N+2)\tilde{b}_\mu + c_\mu \right]$$

$$\partial_t c_\mu = (5-2\epsilon)\, c_\mu + \frac{uJ}{3} \left[(3N+22)c_\mu - (N-4)\tilde{a}_\mu - (N-8)\tilde{b}_\mu \right] \qquad (5.13)$$

$$\partial_t \tilde{a}_\mu = (5-2\epsilon)\, \tilde{a}_\mu + \frac{uJ}{9} \left[(6N+65)\tilde{a}_\mu + 17\tilde{b}_\mu + c_\mu \right]$$

$$\partial_t \tilde{b}_\mu = (5-2\epsilon)\, \tilde{b}_\mu + \frac{uJ}{9} \left[5\tilde{a}_\mu + (6N+65)\tilde{b}_\mu + 7c_\mu \right]$$

where K is the dimensionless version of $\int_q \partial_t R_k(q^2) G_k^2(q^2)$ and J is the dimen-

sionless version of I.[1] The Wilson-Fisher fixed point solution reads:

$$u^* = 3\frac{\epsilon}{(N+8)J}, \quad a^*_\mu = 0, \quad b^*_\mu = 0, \quad \tilde{a}^*_\mu = 0, \quad \tilde{b}^*_\mu = 0, \quad c^*_\mu = 0. \quad (5.14)$$

Substituting the fixed point solution in Eq.(5.13) we can obtain the linearised flow for the vector couplings around the fixed point (or basically, the stability matrix):

$$\begin{aligned}
\partial_t a_\mu &= 3a_\mu + \frac{4\epsilon}{(N+8)}\left[-a_\mu + b_\mu\right] - 3K\left[(N+2)\tilde{a}_\mu + c_\mu\right], \\
\partial_t b_\mu &= 3b_\mu + \frac{2\epsilon}{(N+8)}\left[a_\mu - b_\mu\right] - 3K\left[(N+2)\tilde{b}_\mu + c_\mu\right], \\
\partial_t \tilde{a}_\mu &= 5\tilde{a}_\mu + \frac{\epsilon}{3(N+8)}\left[17\tilde{a}_\mu + 17\tilde{b}_\mu + c_\mu\right], \\
\partial_t \tilde{b}_\mu &= 5\tilde{b}_\mu + \frac{\epsilon}{3(N+8)}\left[5\tilde{a}_\mu + 17\tilde{b}_\mu + 7c_\mu\right], \\
\partial_t c_\mu &= 5c_\mu - \frac{\epsilon}{(N+8)}\left[(N-4)\tilde{a}_\mu + (N-8)\tilde{b}_\mu - (N+6)c_\mu\right].
\end{aligned} \quad (5.15)$$

Diagonalization of the stability matrix in the vectorial sector then leads to the following results for the scaling dimensions:

$$\begin{aligned}
&\lambda_1 = 3 - \frac{6\epsilon}{N+8} + \mathcal{O}(\epsilon^2), &&\lambda_2 = 3 + \mathcal{O}(\epsilon^2), \\
&\lambda_3 = 5 + \frac{2\epsilon}{N+8} + \mathcal{O}(\epsilon^2), &&\lambda_4 = 5 + \frac{12\epsilon}{N+8} + \mathcal{O}(\epsilon^2), \\
&\lambda_5 = 5 + \frac{(10+3N)\epsilon}{3N+24} + \mathcal{O}(\epsilon^2).
\end{aligned} \quad (5.16)$$

In the following analysis we keep only the most relevant couplings and, as such, put $\tilde{a}_\mu$, $\tilde{b}_\mu$ and c_μ to zero in order to interpret the eigenvectors asociated with the eigenvalues λ's. The surviving scaling dimensions are λ_1 and λ_2. The eigenvectors of the stability matrix are also interesting because they characterize the vector operators associated with each of these scaling dimensions. This leads us to introduce the combinations in the reduced stability matrix (this is, without $\tilde{a}_\mu$, $\tilde{b}_\mu$ and c_μ):

$$\begin{aligned}
a'_\mu &= a_\mu - b_\mu \\
b'_\mu &= a_\mu + 2b_\mu
\end{aligned} \quad (5.17)$$

---

[1]As is well known [9], the integral $J = 1/(16\pi^2) + \mathcal{O}(\epsilon)$, independently of the particular choice of the regulator R_k. This ensures the universality of the β functions given here.

which diagonalize the flows:

$$\partial_t a'_\mu = \left(3 - \frac{6\epsilon}{N+8}\right) a'_\mu$$

$$\partial_t b'_\mu = 3 b'_\mu. \tag{5.18}$$

Rewriting the perturbation Hamiltonian (without $\tilde{a}_\mu$, $\tilde{b}_\mu$ and c_μ), Eq.(5.2), in terms of these combinations, we obtain (up to an integration by parts which simplifies the b'_μ term):

$$\int d^d x \left\{ \frac{a'_\mu}{6} \phi_i \partial_\nu \phi_j \left[\partial_\mu \phi_i \partial_\nu \phi_j - \partial_\nu \phi_i \partial_\mu \phi_j\right] + \frac{b'_\mu}{24} \phi_i \phi_i \phi_j \partial^2 \partial_\mu \phi_j \right\}. \tag{5.19}$$

In the $N = 1$ case, there exists only one integrated vector operator with scaling dimension 3 at $d = 4$. Indeed, in that case, the coefficients of a_μ and b_μ in the integrand of Eq.(5.2) are equal, which may seem in conflict with the fact that we found two scaling dimensions which are perfectly regular in the limit $N \to 1$. However, the term proportional to a'_μ in Eq.(5.19) vanishes for $N = 1$. The scaling dimension associated with a'_μ must therefore be rejected and we are left with λ_2 only, which resolves this apparent paradox.[1] We remark that the other scaling dimension that holds for $N = 1$ corresponds to λ_4.

We also showed in [28] (see Appendix G for the proof) that the second scaling dimension of Eq.(5.16) is 3 at all orders of perturbation theory, as a consequence of a non-renormalization theorem. This results from the fact that the associated operator, proportional to b'_μ in Eq.(5.19) is redundant [136].

5.1.2 $\frac{1}{N}$-Espansion

For the large-N limit, we consider the same Hamiltonian of Eq.(2.60) perturbed with Eq.(5.20) (this is the same as the one in Eq.(5.2) but putting $\tilde{a}$ and $\tilde{b}$ to zero). This simplifies the computation but it retains most of the important results. This is:

$$\delta H = \int d^d x \left\{ \frac{a_\mu}{4} \phi_i \partial^\mu \phi_i \partial_\nu \phi_j \partial_\nu \phi_j + \frac{b_\mu}{2} \phi_i \partial_\nu \phi_i \partial_\nu \phi_j \partial^\mu \phi_j \right.$$
$$\left. + \frac{c_\mu}{4} \phi_i \phi_j \phi_k \partial^\mu \phi_i \partial^\mu \phi_j \partial^\mu \phi_k \right\}. \tag{5.20}$$

---

[1]The eigenvector analysis is still true when including the couplings $\tilde{a}_\mu$, $\tilde{b}_\mu$ and c_μ. However, since this analysis is more cumbersome and gives the same conclusions, we don't present it.

The scaling dimensions of the vector operators considered in Eq.(5.2) can be deduced from the calculation of $\Gamma^{(2)}$, $\Gamma^{(4)}$ and $\Gamma^{(6)}$ at vanishing external field in the large N limit. We recall that, as usual, the large N limit is performed at fixed $\hat{u} = uN$, $\hat{a}_\mu = a_\mu N$, $\hat{b}_\mu = b_\mu N$ and $\hat{c}_\mu = c_\mu N^2$. In fact, since the rescaling of a_μ, b_μ and c_μ plays no role when considering the flows linearised in a_μ, b_μ and c_μ we ignore it below [see Eq.(5.42)]. However, we do rescale u.

The diagrams contributing at leading order in the large N expansion of correlation functions are well-known (see for example, [65]).[1] Since some simplifications (see below) take place, the diagrams that finally contribute are schematically depicted for the two, four and six-point vertices in Fig.5.1, Fig.5.2 and Fig.5.3 respectively. In the last two, it is understood that the propagators are effective propagators where all cactus diagrams contributing at leading order to $\Gamma^{(2)}$ have already been re-summed (i.e. they are understood as re-summed according to Fig.5.1). The 4-point (resp. 6-point) interaction
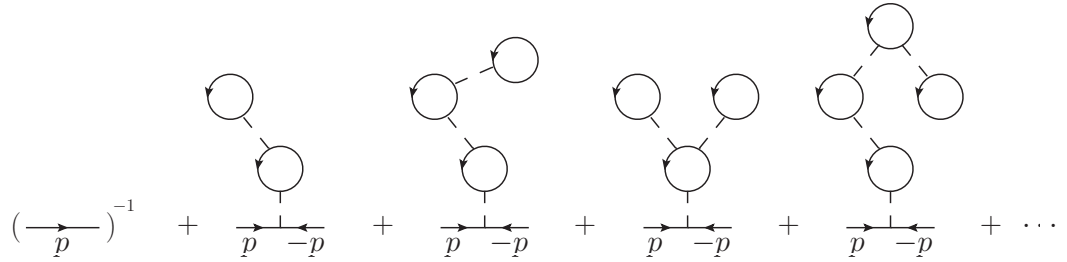
Figure 5.1: Leading contribution to $\Gamma^{(2)}$ in a N^{-1} expansion.
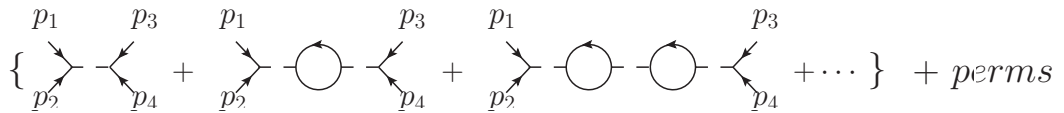
Figure 5.2: Leading contribution to $\Gamma^{(4)}$ in a N^{-1} expansion. Propagators must be understood as re-summed according to Fig.5.1.

is represented here by two (resp. three) full lines connected with dotted lines (the full lines representing the Kronecker δ in vector indices). Note also that we only need to work at vanishing external field for determining the scaling dimension of the vector operators, which considerably simplifies the calculation.

As before, the bare propagators, the 4-point vertex and the 6-point vertex are already the same as those given in Eq.(5.4), Eq.(5.5) and Eq.(5.6) (recall that for this $\tilde{a}_\mu$ and $\tilde{b}_\mu$ are set to zero), respectively.

---

[1] In the case of multicritical fixed points, the large N limit can be more subtle, see [137].
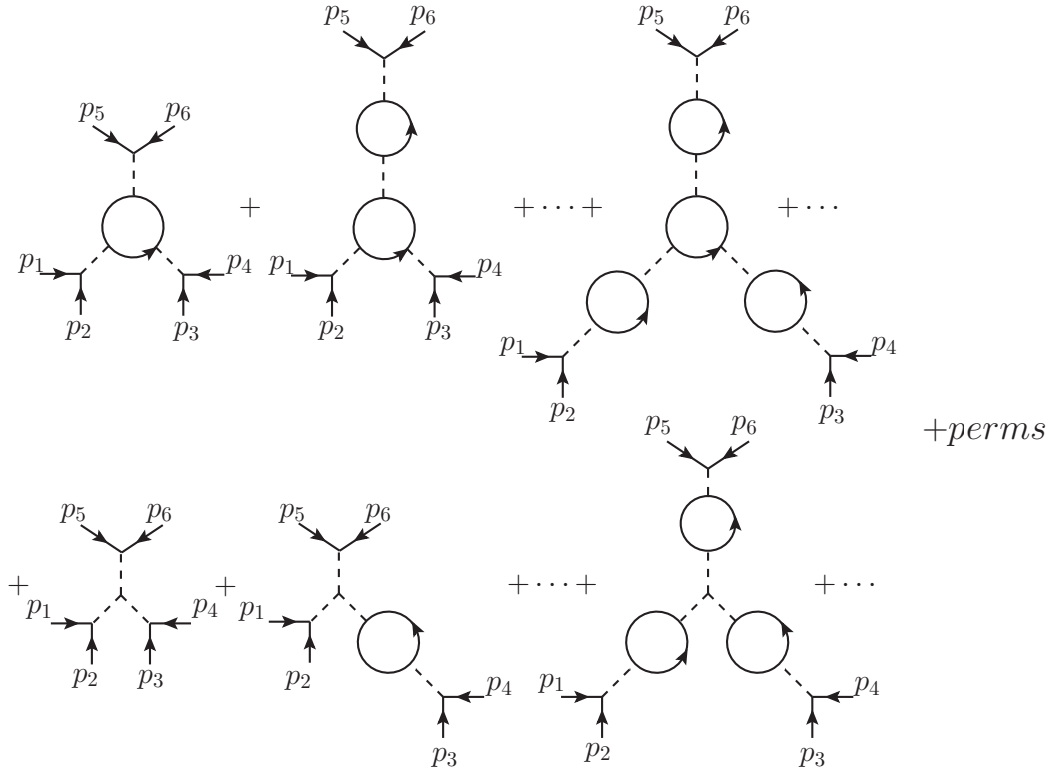
Figure 5.3: Leading contribution to $\Gamma^{(6)}$ in a N^{-1} expansion. Propagators must be understood as re-summed according to Fig.5.1.

To proceed, we have to compute the inverse propagator, the 4-point vertex and the 6-point vertex and extract the part linear in a_μ, b_μ and c_μ. Before doing so, let us discuss some major simplifications which take place:

First, for the 4-point vertex all diagrams where the a_μ and b_μ couplings appear in a vertex in the middle of a diagram (that is if they connect two closed loops) turn out to be zero. Stated otherwise, the perturbation can only occur when it is connected to an external leg. This phenomenon is a consequence of the following property: the contribution linear in a_μ or b_μ in the 4-point vertex which is proportional to $\delta_{i_1 i_2}\delta_{i_3 i_4}$ vanishes in the exceptional configurations where the momenta are opposite by pairs in different delta's (that is, if $p_1 + p_3 = p_2 + p_4 = 0$ or if $p_1 + p_4 = p_2 + p_3 = 0$). As a consequence, for a diagram made of a chain of bubbles (see Fig.5.2), if a $\Gamma^{(4)}$ connecting two bubbles is replaced by a perturbation a_μ or b_μ, the diagram vanishes.

Second, the 6-point vertex associated with c_μ gives no contribution to the 4-point vertex and only diagrams with 4-point vertices contribute, as depicted in Fig.5.2. This closely resembles the property mentioned previously that a_μ and b_μ do not appear in an inner vertex of the chains. Moreover, the specific

momentum structure appearing in the c_μ vertex [see Eq.(5.6)], implies that it cannot appear attached to an external leg. We conclude that c_μ does not contribute to the flow of a_μ and b_μ at leading order in $1/N$. This implies that although we need to compute the part of the 6-point vertex that is just linear in c_μ, the contributions proportional to a_μ and b_μ are unimportant for the scaling dimensions. This is because, as mentioned above, there is no contribution linear in c_μ to the flows of a_μ and b_μ, which makes the stability matrix triangular. We denote X_a and X_b the contributions linear in a_μ and b_μ to the flow of c_μ.

Third, the situation is even simpler in the calculation of $\Gamma^{(2)}$ because, by conservation of momenta, the external legs have opposite momenta. In this case, the 4-point vertex coming from the perturbation does not even contribute when attached to the external legs. As a consequence, the cactus diagrams for $\Gamma^{(2)}$ are independent of a_μ and b_μ. This result is important because it implies that the inverse full propagator (which re-sums all cactus diagrams for $\Gamma^{(2)}$) is independent of a_μ, b_μ and c_μ.

In the following, we consider, as usual, dimensionless couplings but keep the same symbols as for the dimensionful quantities in order to simplify notation. Moreover, we add an index Λ on the coupling to denote microscopic or bare value.

Computation of $\Gamma^{(2)}$

We first discuss the (standard) calculation of $\Gamma^{(2)}$ at leading order. As emphasized above, we can remove a_μ, b_μ and c_μ from this calculation. The sum of the cactus diagrams shown in Fig.5.1 leads to

$$\Gamma^{(2)}_{ij}(p) = \delta_{ij}\left\{p^2 + r^\Lambda + \frac{\hat{u}^\Lambda}{6}\int_q \frac{1}{q^2 + r^\Lambda + \overline{\Sigma}\left(r^\Lambda\right)}\right\} = \delta_{ij}\left\{p^2 + r\right\} \qquad (5.21)$$

where $r = r^\Lambda + \overline{\Sigma}\left(r^\Lambda\right)$ and $\overline{\Sigma}\left(r^\Lambda\right)$ satisfies the gap equation:

$$\overline{\Sigma}\left(r^\Lambda\right) = \frac{\hat{u}^\Lambda}{6}\int_q \frac{1}{q^2 + r^\Lambda + \overline{\Sigma}\left(r^\Lambda\right)}. \qquad (5.22)$$

As is well known, the only effect of the cactus diagrams is to modify the mass.

Computation of $\Gamma^{(4)}$

In contrast to $\Gamma^{(2)}$, the $\Gamma^{(4)}$ vertex has corrections linear in a_μ^Λ and b_μ^Λ to leading order in the $\frac{1}{N}$ expansion (i.e. to order $\frac{1}{N}$). It is convenient to decompose the 4-point vertex function as $\Gamma^{(4)} = \Gamma_u^{(4)} + \Gamma_{a_\mu}^{(4)} + \Gamma_{b_\mu}^{(4)}$, where the first term is independent of a_μ and b_μ, the second term is linear in a_μ and the third is linear in b_μ. We omit all other terms which do not enter into the calculation of the scaling dimensions we are interested in.

The term $\Gamma_u^{(4)}$ is the simplest one since it corresponds to the usual theory with $a_\mu^\Lambda = b_\mu^\Lambda = 0$. This gives the standard large-N result:

$$\Gamma_{u,i_1,i_2,i_3,i_4}^{(4)}(p_1,p_2,p_3) = \frac{\hat{u}^\Lambda}{3N}\left[\frac{\delta_{i_1 i_2}\delta_{i_3 i_4}}{1+\frac{\hat{u}^\Lambda}{6}\Pi\left(p_1+p_2\right)} + \frac{\delta_{i_1 i_3}\delta_{i_2 i_4}}{1+\frac{\hat{u}^\Lambda}{6}\Pi\left(p_1+p_3\right)} \right.$$
$$\left. + \frac{\delta_{i_1 i_4}\delta_{i_2 i_3}}{1+\frac{\hat{u}^\Lambda}{6}\Pi\left(p_1+p_4\right)}\right] \quad (5.23)$$

where the function $\Pi\left(p\right)$ is defined as:

$$\Pi\left(p\right) = \int_q \frac{1}{q^2+r}\frac{1}{\left(q+p\right)^2+r} \quad (5.24)$$

We now consider $\Gamma_{a_\mu}^{(4)}$. For simplicity, we focus on the contribution proportional to $\delta_{i_1 i_2}\delta_{i_3 i_4}$. The other contribution are obtained by permutations of the external legs. The set of diagrams which contribute is easy to characterize because, as previously discussed, the perturbation (a_μ in this case) must be attached to the external legs. The chain of bubbles diagrams for $\Gamma_{a_\mu}^{(4)}$ are depicted in Fig.5.4.
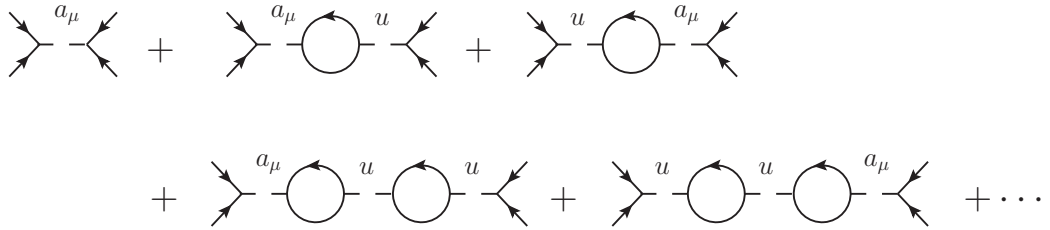
Figure 5.4: Diagrams contributing to $\Gamma_{a_\mu}^{(4)}$.

The diagram with n couplings $\hat{u}^\Lambda$ and one $\hat{a}_\mu^\Lambda$ connected to p_1 and p_2 is

equal to:

$$\frac{i\hat{a}_\mu^\Lambda}{2N} \int_q \frac{(p_1 + p_2)^\mu \left[p_1 \cdot p_2 + q \cdot (q + p_1 + p_2)\right]}{\left[q^2 + r\right]\left[(q + p_1 + p_2)^2 + r\right]} \left(\frac{-\hat{u}^\Lambda}{4!}\right)^n \frac{4^n n! C_n^{n+1}}{(n+1)!} \left(\Pi \left(p_1 + p_2\right)\right)^{(n-1)},$$

$$(5.25)$$

If $\hat{a}_\mu^\Lambda$ is connected to p_3 and p_4, we get:

$$\frac{i\hat{a}_\mu^\Lambda}{2N} \int_q \frac{(p_1 + p_2)^\mu \left[-q \cdot (q + p_1 + p_2) - p_3 \cdot p_4\right]}{\left[q^2 + r\right]\left[(q + p_1 + p_2)^2 + r\right]} \left(\frac{-\hat{u}^\Lambda}{4!}\right)^n \frac{4^n n! C_n^{n+1}}{(n+1)!} \left(\Pi \left(p_1 + p_2\right)\right)^{(n-1)}.$$

$$(5.26)$$

When adding both diagrams we get the result for n couplings $\hat{u}^\Lambda$ and one $\hat{a}_\mu^\Lambda$:

$$\frac{i\hat{a}_\mu^\Lambda}{2N} \left(-\frac{\hat{u}^\Lambda}{6}\Pi \left(p_1 + p_2\right)\right)^n (p_1 + p_2)^\mu \left[p_1 \cdot p_2 - p_3 \cdot p_4\right]. \qquad (5.27)$$

Note that the previous construction does not make sense for $n = 0$. However, it happens that Eq.(5.27) evaluated at $n = 0$ indeed represents the contribution of the first diagram of Fig.5.4 with one a_μ and no $\hat{u}$. It is straightforward to sum this general expression for all n to get:

$$\Gamma_{a_\mu}^{(4)} = \frac{i\hat{a}_\mu^\Lambda}{2N \left(1 + \frac{\hat{u}^\Lambda}{6}\Pi \left(p_1 + p_2\right)\right)} (p_1 + p_2)^\mu \left[p_1 \cdot p_2 - p_3 \cdot p_4\right] \delta_{i_1 i_2}\delta_{i_3 i_4} + 2 \text{ perms.}$$

$$(5.28)$$

The calculation for $\Gamma_{b_\mu}^{(4)}$ proceeds in the same way. The contribution of diagrams with one b_μ and n couplings $\hat{u}$ (again focusing on the contribution proportional to $\delta_{i_1 i_2}\delta_{i_3 i_4}$) is:

$$\frac{-i\hat{b}_\mu^\Lambda}{2N} \left(-\frac{\hat{u}^\Lambda}{6}\Pi \left(p_1 + p_2\right)\right)^n \left[p_1^\mu p_1^2 + p_2^\mu p_2^2 + p_3^\mu p_3^2 + p_4^\mu p_4^2 + (p_1 + p_2)^\mu \left(p_1 \cdot p_2 - p_3 \cdot p_4\right)\right].$$

$$(5.29)$$

To sum up, the four-point vertex with at most one a_μ or one b_μ is

$$\Gamma_{i_1 i_2 i_3 i_4}^{(4)}(p_1, p_2, p_3) = \frac{\delta_{i_1 i_2}\delta_{i_3 i_4}}{N\left(1 + \frac{\hat{u}^\Lambda}{6}\Pi \left(p_1 + p_2\right)\right)} \left\{\frac{\hat{u}^\Lambda}{3} + i\frac{\hat{a}_\mu^\Lambda - \hat{b}_\mu^\Lambda}{2}(p_1 + p_2)^\mu \left[p_1 \cdot p_2 - p_3 \cdot p_4\right]\right.$$
$$\left. - i\frac{\hat{b}_\mu^\Lambda}{2} \left(p_1^\mu p_1^2 + p_2^\mu p_2^2 + p_3^\mu p_3^2 + p_4^\mu p_4^2\right)\right\} + 2 \text{ perms.}$$

$$(5.30)$$

where, again, the permutations are obtained by a cyclic permutation of the external indices 2, 3 and 4.

Computation of $\Gamma^{(6)}$

The $\Gamma^{(6)}$ vertex has corrections linear in c_μ^Λ to leading order in the $\frac{1}{N}$ expansion (i.e. to order $\frac{1}{N^2}$), but it may also have contributions coming from the types of diagrams shown in Fig.5.5 where a_μ^Λ or b_μ^Λ is inserted at the core (i.e. the inner loop with three propagator) or, as before, attached to an external leg. As explained above, the contribution to $\Gamma_k^{(6)}$ proportional to a_μ and b_μ is of no interest for us since the stability matrix is upper diagonal and, therefore, we do not compute these quantities.
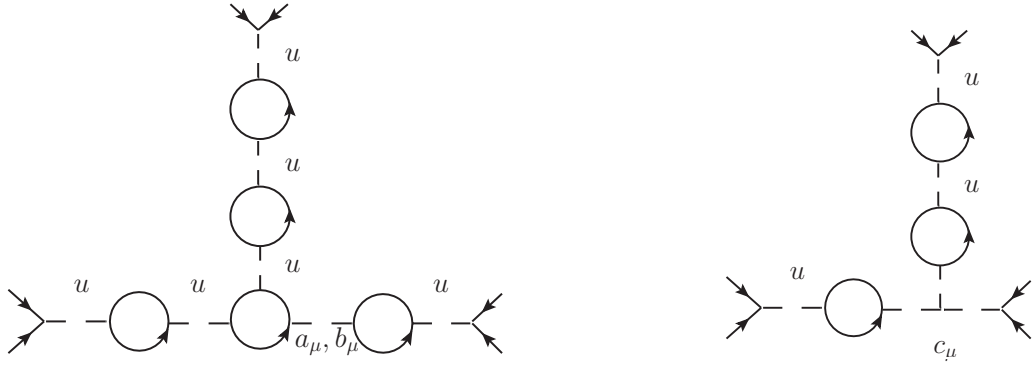
Figure 5.5: Left: a diagram contributing to $\Gamma^{(6)}$, linear in a_μ or b_μ. Right: a diagram contributing to $\Gamma^{(6)}$ proportional to c_μ.

The diagrams to be computed are exceptionally simple since they have a c_μ at the core with no loop (diagram on the right in Fig.5.5) and then just chain of bubbles with coupling u, these are schematically shown in Fig.5.5.

The diagram (proportional to $\delta_{i_1 i_2} \delta_{i_3 i_4} \delta_{i_5 i_6}$) with a chain composed of n_1 couplings $\hat{u}^\Lambda$ attached to the external momentums p_1 and p_2, a chain with n_2 couplings $\hat{u}^\Lambda$ attached to the external momentums p_3 and p_4, a chain with n_3 couplings $\hat{u}^\Lambda$ attached to the external momentums p_5 and p_6 and one $\hat{c}_\mu^\Lambda$ at the core is equal to:

$$
\frac{-i\hat{c}_\mu^\Lambda}{2N^2} \left(\frac{-\hat{u}^\Lambda}{4!} \right)^{n_1} \left(\frac{-\hat{u}^\Lambda}{4!} \right)^{n_2} \left(\frac{-\hat{u}^\Lambda}{4!} \right)^{n_3} \frac{4^{n_1+n_2+n_3}(n_1+n_2+n_3)! C_1^{n_1+n_2+n_3+1}}{(n_1+n_2+n_3+1)!}
$$
$$
\times \left(\Pi\, (p_1+p_2) \right)^{n_1} \left(\Pi\, (p_3+p_4) \right)^{n_2} \left(\Pi\, (p_5+p_6) \right)^{n_3}
$$
$$
\times \left[(p_1+p_2)^\mu (p_1+p_2)^2 + (p_3+p_3)^\mu (p_3+p_4)^2 + (p_5+p_6)^\mu (p_5+p_6)^2 \right] + \text{perms.}
$$
$$
\tag{5.31}
$$

Performing the sum for all possible values of n_1, n_2 and n_3 yields for the

$\Gamma^{(6)}$:

$$\Gamma^{(6)}_{i_1 i_2 i_3 i_4 i_5 i_6}(p_1, p_2, p_3, p_4, p_5) = \frac{1}{N^2}\left[\delta_{i_1 i_2}\delta_{i_3 i_4}\delta_{i_5 i_6}\left(-\frac{ic_\mu^\Lambda}{2}\frac{1}{1 + \frac{\hat{u}^\Lambda}{6}\Pi(p_1 + p_2)} \times \right.\right.$$

$$\frac{1}{1 + \frac{\hat{u}^\Lambda}{6}\Pi(p_3 + p_4)}\frac{1}{1 + \frac{\hat{u}^\Lambda}{6}\Pi(p_5 + p_6)} + Y_a(p_1, p_2, p_3, p_4, p_5)a_\mu^\Lambda$$

$$+ Y_b(p_1, p_2, p_3, p_4, p_5)b_\mu^\Lambda \Big)\Big\{ (p_1 + p_2)^\mu (p_1 + p_2)^2 +$$

$$\left.\left. (p_3 + p_4)^\mu (p_3 + p_4)^2 + (p_5 + p_6)^\mu (p_5 + p_6)^2 \right\} + 14 \text{ perms.}\right] \quad (5.32)$$

We need to mention that other structures in indices and momenta arise at $\mathcal{O}(N^{-2})$ and $\mathcal{O}(\partial^3)$ of the $\Gamma^{(6)}$. These are related to the, not considered, $\tilde{a}_\mu$ and $\tilde{b}_\mu$ in the ansatz. Dropping these structures may affect the obtained scaling dimensions and consequently we could find eigenvalues which differ from the common limit with the ϵ-expansion or the DE. It turns out, however, that they are not modified at all, as we check by comparing with the $\mathcal{O}(\partial^3)$ of the derivative expansion. This is because at the considered orders, the c_μ^Λ does not contribute to any of the structures belonging to a_μ, b_μ, $\tilde{a}_\mu$ and $\tilde{b}_\mu$.

Running Couplings

At this point we are in place to compute the scaling dimensions of the considered operators. This is done again in the NPRG framework by introducing an infrared regulator in the propagators:

$$\frac{1}{q^2 + r^\Lambda} \to \frac{1}{q^2 + r^\Lambda + R_k(q)} \quad (5.33)$$

and study the running of the various couplings when varying the regulator.

In this way, we define the renormalized couplings as:

$$\Gamma^{(2)}_{i_1 i_2}(0) = r^k \delta_{i_1 i_2}, \quad (5.34)$$

$$\Gamma^{(4)}_{i_1 i_2 i_3 i_4}(0, 0, 0) = \frac{\hat{u}^k}{3N}\left(\delta_{i_1 i_2}\delta_{i_3 i_4} + \delta_{i_1 i_3}\delta_{i_2 i_4} + \delta_{i_1 i_3}\delta_{i_2 i_4} \right), \quad (5.35)$$

$$\Gamma^{(4),\mathcal{O}(p^3)}_{i_1i_2i_3i_4}(p_1,p_2,p_3) = i\frac{\delta_{i_1i_2}\delta_{i_3i_4}}{2N}\left\{ (a^k_\mu - b^k_\mu)(p_1+p_2)^\mu \left[p_1\cdot p_2 - p_3\cdot p_4 \right] \right.$$
$$\left. - b^k_\mu \left(p_1^\mu p_1^2 + p_2^\mu p_2^2 + p_3^\mu p_3^2 + p_4^\mu p_4^2 \right) \right\} + 2 \text{ perms} \tag{5.36}$$

and

$$\Gamma^{(6),\mathcal{O}(p^3)}_{i_1i_2i_3i_4i_5i_6}(p_1,p_2,p_3,p_4,p_5) = -i\frac{\delta_{i_1i_2}\delta_{i_3i_4}\delta_{i_5i_6}c^k_\mu}{2N^2}\left\{ (p_1+p_2)^\mu (p_1+p_2)^2 \right.$$
$$\left. + (p_3+p_4)^\mu (p_3+p_4)^2 + (p_5+p_6)^\mu (p_5+p_6)^2 \right\} + 14 \text{ perms.}, \tag{5.37}$$

where now, the superscript k on the couplings means that this are defined at scale k.

One can then conclude that the running couplings are:

$$\hat{u}^k = \frac{\hat{u}}{1 + \frac{\hat{u}_\Lambda}{6}\Pi_k(0)}, \qquad a^k_\mu = \frac{a^\mu_\Lambda}{1 + \frac{\hat{u}_\Lambda}{6}\Pi_k(0)}, \qquad b^k_\mu = \frac{b^\mu_\Lambda}{1 + \frac{\hat{u}_\Lambda}{6}\Pi_k(0)}$$
$$c^k_\mu = \frac{c^\mu_\Lambda}{\left(1 + \frac{\hat{u}_\Lambda}{6}\Pi_k(0)\right)^3} + \hat{Y}_a a^\mu_\Lambda + \hat{Y}_b b^\mu_\Lambda, \qquad r_k = r^\Lambda + \overline{\Sigma}_k \tag{5.38}$$

where $\hat{Y}_a$ and $\hat{Y}_b$ are some contributions, which bare some unimportant relation with the functions Y_a and Y_b, and the functions $\overline{\Sigma}_k$ and Π_k are upgrades of their previous definition, but being calculated in presence of the infrared regulator:

$$\overline{\Sigma}_k(r_\Lambda) = \frac{\hat{u}_\Lambda}{6}\int_q \frac{1}{q^2 + r_k + R_k(q^2)} \tag{5.39}$$
$$\Pi_k(0) = \int_q \frac{1}{(q^2 + r_k + R_k(q^2))^2}. \tag{5.40}$$

Taking this into account, we obtain the flow of the running couplings:

$$\partial_t r^k = -\frac{\hat{u}^k}{6} \int_q \partial_t R_k(q) G_k^2(q)$$

$$\partial_t \hat{u}^k = -\frac{(\hat{u}^k)^3}{18} \int_q G_k^3(q) \int_{q'} \partial_t R_k(q') G_k^2(q') + \frac{(\hat{u}^k)^2}{3} \int_q \partial_t R_k(q) G_k^3(q)$$

$$\partial_t a_\mu^k = -\frac{a_\mu^k (\hat{u}^k)^2}{18} \int_q G_k^3(q) \int_{q'} \partial_t R_k(q') G_k^2(q') + \frac{a_\mu^k \hat{u}^k}{3} \int_q \partial_t R_k(q) G_k^3(q)$$

$$\partial_t b_\mu^k = -\frac{b_\mu^k (\hat{u}^k)^2}{18} \int_q G_k^3(q) \int_{q'} \partial_t R_k(q') G_k^2(q') + \frac{b_\mu^k \hat{u}^k}{3} \int_q \partial_t R_k(q) G_k^3(q) \qquad (5.41)$$

$$\partial_t c_\mu^k = -\frac{c_\mu^k (\hat{u}^k)^2}{6} \int_q G_k^3(q) \int_{q'} \partial_t R_k(q') G_k^2(q') + c_\mu^k \hat{u}^k \int_q \partial_t R_k(q) G_k^3(q)$$

$$+ X_a a_\mu^k + X_b b_\mu^k$$

where, in the previous equations, $G_k(q) = (q^2 + r_k + R_k(q^2))^{-1}$ and, again, X_a and X_b are some inconsequential factors related to $\hat{Y}_a$ and $\hat{Y}_b$. Introducing dimensionless and renormalized variables we arrive at the flow equations for the coupling (where we removed the superscript k):

$$\partial_t \hat{u} = (d-4)\hat{u} + \frac{\hat{u}^2 J}{3} + \frac{\hat{u}^3}{18} L$$

$$\partial_t a_\mu = (d-1) a_\mu + \frac{\hat{u} J}{3} a_\mu + \frac{\hat{u}^2}{18} L a_\mu$$

$$\partial_t b_\mu = (d-1) b_\mu + \frac{\hat{u} J}{3} b_\mu + \frac{\hat{u}^2}{18} L b_\mu \qquad (5.42)$$

$$\partial_t c_\mu = (2d-3) c_\mu + \hat{X}_a a_\mu + \hat{X}_b b_\mu + \hat{u} J c_\mu + \frac{\hat{u}^2}{6} L c_\mu$$

where $\hat{X}_a$ and $\hat{X}_b$ are the dimensionless versions of X_a and X_b, respectively, the dimensionless version of $\int_q \dot{R}_k(q) G_k^3(q)$ is J and L is the dimensionless version of the combination of integrals

$$-\int_q \dot{R}_k(q) G_k^2(q) \times \int_{q'} G_k^3(q').$$

As in the previous section, one can find the fixed-point solution $\hat{u}^*$ and substitute it in the flow for a_μ, b_μ and c_μ, obtaining

$$\partial_t a_\mu = 3 a_\mu,$$

$$\partial_t b_\mu = 3 b_\mu, \qquad (5.43)$$

$$\partial_t c_\mu = \hat{X}_a^* a_\mu + \hat{X}_b^* b_\mu + (9-d) c_\mu,$$

which implies that there are two operators with scaling dimension $3 + \mathcal{O}(1/N)$ and one with scaling dimension $9 - d$. In Eq.(5.43) $\hat{X}_a^*$ and $\hat{X}_b^*$ are the fixed point values. Note that when $d = 4 - \epsilon$, this limit coincides with the large-N limit of the ϵ-expansion given in Eq(5.16). Eq.(5.43) also implies that higher corrections in the ϵ-expansion are all suppressed by at least one power of N^{-1} in comparison to the tree-level expression. Note that one of these eigenvalues is 3 in all dimensions and for all N, due to the non-renormaization theorem shown in the Appendix G, whereas the independence of the other eigenvalue with respect to dimension is specific to the large-N limit.

It is immediately found that taking the limit $N \to \infty$ in Eq.(5.16) we recover the three scaling dimensions. This puts on evidence the agreement between the two approximation schemes, the ϵ-expansion and the $\frac{1}{N}$-expansion, in compatible limits.

5.1.3 Derivative Expansion at Order $\mathcal{O}(\partial^3)$ for the $O(N)$ Models

We now implement an approximation scheme which is exact in the limits $4 - d \ll 1$ and, separately, in the limit $N \to \infty$, and it is proven to be reasonably accurate for intermediate values of N and d. The scalar sector is known to be also exact at $d = 2 + \epsilon$, however this is not evident for vector operators and, therefore, we do not focus in this case. This approximation is the DE approximation of the NPRG at order $\mathcal{O}(\partial^3)$ (see Chapter 2). As previously described the DE procedure consists in taking an ansatz for the effective action $\Gamma_k[\phi]$ in which only terms with a finite number of derivatives of the fields appear, see Section 2.3. Equivalently, in Fourier space, it corresponds to expanding all proper vertices in power series of the momenta and truncating to a finite order.

Fixed Point and Flow Equations

We take the most general terms with the symmetries of the universality class of the $O(N)$ models. In a rotational invariant scalar model, only even powers of the derivatives appear. However, at odds with the work done on Chapter 3 we introduce now terms which break this symmetry (they behave as vectors) while preserving the $O(N)$ and translation symmetry. Indeed, if a virial current were to exist it would be of this form. We consider here the $\mathcal{O}(\partial^3)$ order of the DE that includes all possible independent terms with, at most, three derivatives

(which in fact, is the smallest number of derivatives we could have in order to introduce integrated vector operators). Our ansatz then reads

$$\Gamma_k = \int_x \left\{ U_k\left(\rho\right) + \frac{1}{2} Z_k\left(\rho\right) \partial_\mu \varphi_i \partial_\mu \varphi_i + \frac{1}{4} Y_k\left(\rho\right) \partial_\mu \rho \partial_\mu \rho \right.$$
$$\left. + \frac{1}{4} a_\mu\left(\rho\right) \partial_\mu \rho \partial_\nu \varphi_i \partial_\nu \varphi_i + \frac{1}{2} b_\mu\left(\rho\right) \partial_\mu \varphi_i \partial_\nu \varphi_i \partial_\nu \rho + \frac{1}{4} c_\mu\left(\rho\right) \partial_\mu \rho \partial_\nu \rho \partial_\nu \rho \right\}. \tag{5.44}$$

This ansatz is valid for $N \neq 1$. The $N = 1$ case is in the same universality class as the Ising model and, as discussed in Section 2.3, the structures $Z_k(\rho)$ and $Y_k(\rho)$ are not independent of each other. The same happens to the structures $a_\mu(\rho)$, $b_\mu(\rho)$ and $c_\mu(\rho)$. We therefore consider for $N = 1$ the following ansatz:

$$\Gamma_k = \int_x \left\{ U_k\left(\rho\right) + \frac{1}{2} Z_k\left(\rho\right) \partial_\mu \varphi \partial_\mu \varphi + \frac{1}{4} a_\mu\left(\rho\right) \varphi \partial_\mu \varphi \partial_\nu \varphi \partial_\nu \varphi \right\}, \tag{5.45}$$

where we dropped the index from the field for obvious reasons.

The terms present in Γ_k are of two types: the ones including the functions $U_k(\rho)$, $Z_k(\rho)$ and $Y_k(\rho)$ (or just $U_k(\rho)$ and $Z_k(\rho)$ for $N = 1$) which are present at order $\mathcal{O}(\partial^2)$ and are invariant under space rotations and the terms including the functions $a_\mu(\rho)$, $b_\mu(\rho)$ and $c_\mu(\rho)$ which break the rotational invariance.[1]

The calculation proceeds as follows. We compute the Wilson-Fisher fixed point setting $a_\mu(\rho)$, $b_\mu(\rho)$ and $c_\mu(\rho)$ to zero from scratch. This is due to the fact that the fixed point is rotational invariant. To do this, we derive the flow equations similar as we explained in Chapter 3, with the difference that we considered the full form of the flow equations, see Chapter 3 and Appendix F.

To extract the flow of the perturbations a_μ, b_μ and c_μ we need to compute the flow of $\Gamma_k^{(3)}(p_1, p_2; \varphi)$ in an uniform field at order $\mathcal{O}(p^3)$. At this order, of course, there are three independent tensorial structures in $\Gamma_k^{(3)}(p_1, p_2; \varphi)$. These are:

$$\Gamma_{p^3, i_1, i_2, i_3}^{(3)}(p_1, p_2; \varphi) = \left\{ \delta_{i_1 i_2} \varphi_{i_3} \left[-i \frac{a_\mu - b_\mu}{2} p_3^\mu \left(p_1 \cdot p_2\right) \right. \right.$$
$$\left. + i \frac{b_\mu}{2} \left[-p_1^\mu p_1^2 - p_2^\mu p_2^2 - p_3^\mu p_3^2 \right] \right] + 2 \text{ perms} \right\}$$
$$- i \frac{c_\mu}{2} \varphi_{i_1} \varphi_{i_2} \varphi_{i_3} \left[p_1^\mu p_1^2 + p_2^\mu p_2^2 + p_3^\mu p_3^2 \right] \tag{5.46}$$

---

[1]Note that we meant rotations of space coordinates and not in the internal space of the field.

where the two permutations are circular permutations of the external indices 1, 2 and 3 and where $p_3 = -p_1 - p_2$ due to momentum conservation. We recall that the scaling dimensions of vector operators is extracted from a linear stability analysis of the fixed point and since $a_\mu(\rho)$, $b_\mu(\rho)$ and $c_\mu(\rho)$ are zero at the fixed point, we are only interested in the flow at linear level. Despite this huge simplification, the resulting flow equations for these perturbations are too large to write them down here. The flow equations for the six functions were obtained through symbolic programming and are treated numerically, see Appendix F for numerical details.

Results From the Derivative Expansion at Order $\mathcal{O}(\partial^3)$

Before presenting the results, a word must be said regarding the character of the study. In contrast with the study of Chapter 3, where we were interest in giving the most precise estimation of critical exponents, here we aim at discard the value -1 as a possibility for the scaling dimension of integrated vector operators. As will be shown shortly, this value is undoubtedly excluded without the need of a precise calculation and therefore only one regulator was used, namely W_k given in Eq.(2.31). On top of this, we used extremely conservative error bar and not anything similar to the study of Chapter 3. On one hand, we did not need a huge precision and, on the other hand, the work presented in this chapter was done before the one presented in Chapter 3. We estimated our central values of the scaling via the PMS criterion (see Chapter 3 for a description and Chapter 6 for the study of its interpretation) at order $\mathcal{O}(\partial^3)$ of the DE. For error bars we also analysed the poorer approximation where the rotational invariant part of the NPRG flow is computed at order LPA, which corresponds to setting everywhere $Y_k = 0$, $Z_k = 1$, and considered the error as twice the difference between these two sets of results. In view of the analysis of Chapter 3 this is extremely pessimistic. However, it could happen that the two approximation cross for some value of N and d yielding a vanishing error bar (for a similar situation, see Chapter 3). This is unsatisfactory and so, to overcome this issue, we recalled that the DE is exact when $d \to 4$ limit and therefore imposed the error bars to be monotonously decreasing functions of dimension d for all N values considered.

We discuss separately the cases $N = 1$ and $N \neq 1$, because for the case $N = 1$ the number of independent structures appearing at orders $\mathcal{O}(\partial^2)$ and $\mathcal{O}(\partial^3)$ is smaller than for the case $N \neq 1$. For the purpose of this study, at order $\mathcal{O}(\partial^3)$ there are just one structure which scales as $3 + \mathcal{O}(\epsilon^2)$ and one
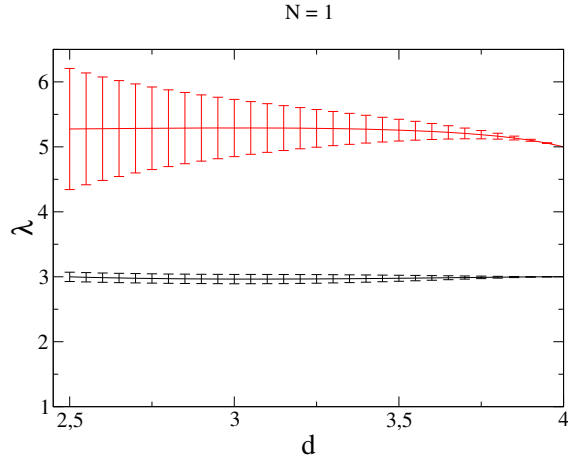
Figure 5.6: Scaling dimensions λ_2 and λ_3 for $N = 1$ as a function of the space dimension $d \in [2.5, 4]$. The error bar estimates are explained in the text.

which behaves as $5 + \mathcal{O}(\epsilon)$ (which is related to the perturbation $\varphi^3 \partial_\mu \varphi \partial_\nu \varphi \partial_\nu \varphi$). However, since there are vector operators with five derivatives which already have scaling dimension 5 at $d = 4$, we only expect a qualitative description of this later eigenvalue. In Fig.5.6 we show the two lowest eigenvalues, where the value -1 can be unambiguously rejected.

If we included terms with five derivatives we would obtain three extra eigenvalues $\sim 5 + \mathcal{O}(\epsilon)$. In Appendix H a one loop computation is performed in order to obtain the leading ϵ correction to the scaling dimensions of all operators with scaling dimension $5 + \mathcal{O}(\epsilon)$ including terms with five derivatives. We must emphasize that all these operators turn out to be redundant, see Appendix G, and are not possible candidates for breaking of conformal invariance. Anyway, this prove that the vector operator having lowest scaling dimension is, at least, of order 7 when $d \to 4$, making the breaking of conformal invariance even more unlikely. In any case, the presence of conformal invariance in the Ising model was already proven in [27]. We resume here the obtained results: the operator with 6 powers of the field and 3 derivatives has scaling dimension $5 + 4\epsilon/3 + \mathcal{O}(\epsilon^2)$ and the operators with 4 powers of the field and 5 derivatives yield the scaling dimensions $5 + \mathcal{O}(\epsilon^2)$, $5 - 4\epsilon/9 + \mathcal{O}(\epsilon^2)$ and $5 - 2\epsilon/3 + \mathcal{O}(\epsilon^2)$.

Now, we turn to the general $N \neq 1$ case. We present first the DE estimate, with error bars included, for the five most relevant scaling dimension in Fig.5.7 for several values of N, including the case $N = 0$ which describes self-avoiding polymers (see Chapter 3). We consider only these five, most relevant, scaling dimension for the same reasons we only consider two in the $N = 1$ case. The behaviour of operators with canonical scaling dimension 5 are not accurately described at order $\mathcal{O}(\partial^3)$ of the DE and to do this one should go to order

$\mathcal{O}(\partial^5)$. the five most relevant scaling dimensions of vector operators for various N. Indeed, this can be seen from the discussion in the ϵ-expansion, to have control over the operators of scaling dimension $5 + \mathcal{O}(\epsilon)$, we need, as for $N = 1$, to include perturbations with 4 fields and 5 derivatives, which are absent of the truncation considered in this whole study. If we were to include such $\mathcal{O}(\partial^5)$ terms, we would obtain 5 extra eigenvalues $\sim 5 + \mathcal{O}(\epsilon)$ instead of the 3 shown in Fig.5.7. For this reason, we expect that the two low-lying scaling dimensions are correctly described while the next 3 are only qualitatively reproduced. We can not consider seriously higher corrections because they are probably not under control in this truncation.

The first thing that pops up analysing Fig.5.7 is related to our goal. We are clearly excluding -1 as a possible value for the scaling dimension of vector operators (even employing extremely pessimistic error bars). Therefore, by invoking the sufficient condition discussed in Chapter 4, we conclude that conformal invariance is indeed realized at the critical point of $O(N)$ models, for all considered values of N and d. In fact, looking at the behaviour of these scaling dimensions in terms of N we can assert that conformal invariance is certainly realized in the critical regime of $O(N)$ models, for *any* N.

Now, we show the level of agreement between the DE estimates and the two previous approximation schemes. But before doing that, we start by re-marking, as we did in ϵ-expansion and in the large N previous sections, that one of the eigenvalues, λ_2, is equal to 3, within error bars, in agreement with the exact result given in the appendix G. In Fig.5.8, the scaling dimension λ_2 is shown for some values of N. One may wonder, however, about the origin of the small mismatch with the exact result. This happens because the fixed point is computed at next to leading order $\mathcal{O}(\partial^2)$, while the flows for the couplings of the vector perturbation are computed at leading order $\mathcal{O}(\partial^3)$. As a consequence there is a close, but not exact, matching between the flows of the potential and the function a_μ. In fact, we checked that we recover the exact result $\lambda_2 = 3$ if we compute the flow and the fixed point, before imposing the vector perturbation, at order LPA because in this case, everything is computed with the same accuracy.

We show in Fig.5.9 the leading scaling dimension λ_1 for some values of N in comparison with the estimation from the ϵ-expansion. Analysing Fig.5.9 makes evident the compatibility of both approximation schemes when $4 - d \ll 1$. On top of this, we see that the predictions of the $\mathcal{O}(\partial^3)$ approximation are very close to those of the ϵ-expansion [see Eq.(5.18)] for this eigenvalue, the
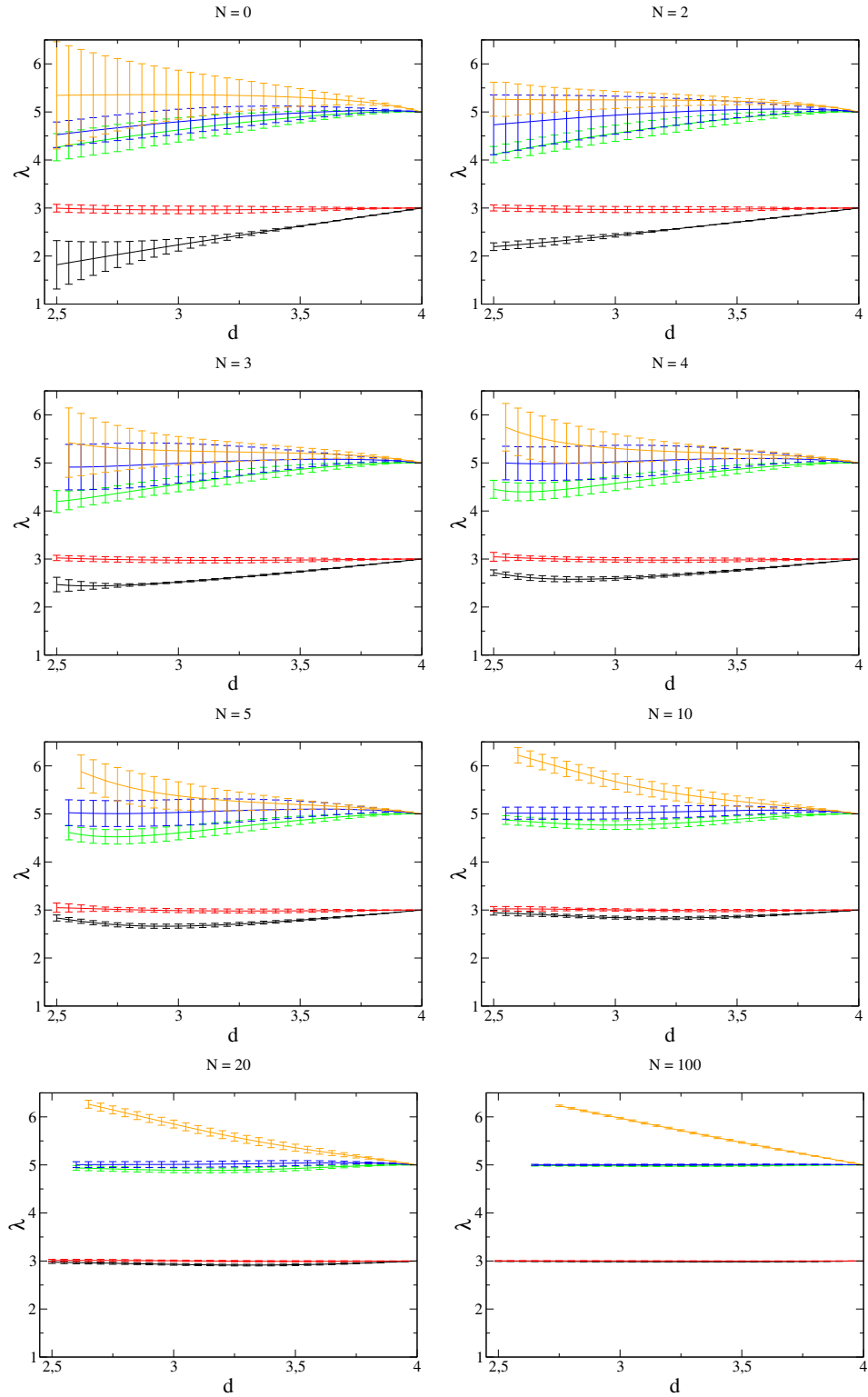
Figure 5.7: The five smallest scaling dimensions λ obtained in $\mathcal{O}(\partial^3)$ approximation of the NPRG equations are plotted as a function of dimension for various values of N. The strategy for evaluating error bar is explained in the text.
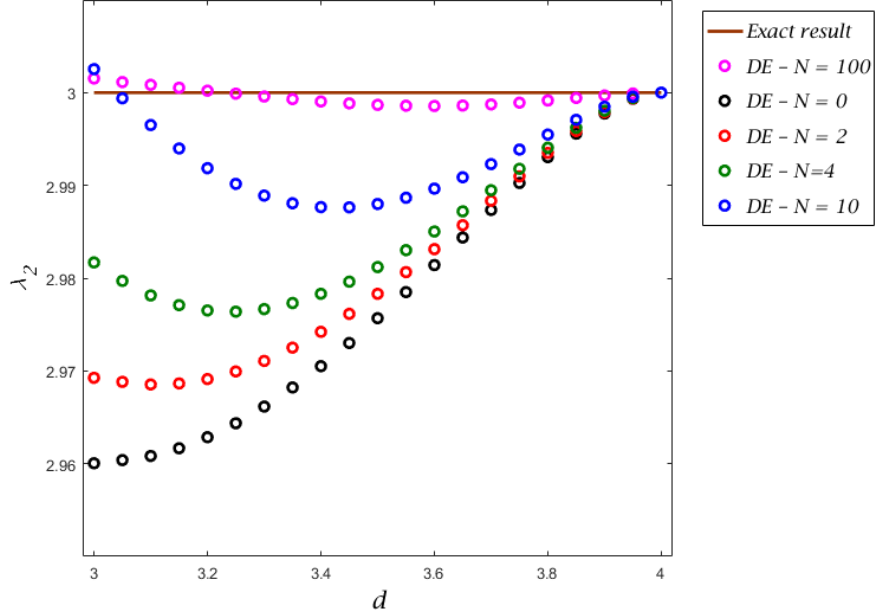
Figure 5.8: Scaling dimension estimate of the DE λ_2 as a function of dimension d for some values of N, along with the exact result. Error bars are avoided for clarity.

difference between them being at most of 5% for all values of N for $d \geq 3$.

The next scaling dimension λ_3 is also compared to the ϵ-expansion in Fig.5.10. However, the behaviour of λ_3 quickly depart from the linear behaviour, which indicates that the corrections of order $\mathcal{O}(\epsilon^2)$ must be large. Nonetheless, it is also evident that this correction must be further suppressed by powers of $1/N$.

Before continuing the comparison, we must stress that the estimates coming from the ϵ-expansion to λ_4 and λ_5 alternate relevance between them. This is, $\lambda_4 < \lambda_5$ for $N > 26/3$ and $\lambda_4 > \lambda_5$ for $N < 26/3$, see Eq.5.16. So, when comparing the linear behaviour this is taken into account. In Fig.5.11 we compare the prediction from the DE for λ_4 and the corresponding linear behaviour coming from the ϵ-expansion (either λ_4 or λ_5 as appropriate according to the previous discussion). The same conclusion is obtained, because the fast departure of the linear prediction of the ϵ-expansion, there must be an appreciable correction of order $\mathcal{O}(\epsilon^2)$ which is also further suppressed by some power of $1/N$.

Finally, let us compare the estimates of λ_5 from the DE with the ϵ-expansion estimates (again, keeping in mind the interchange of relevance with λ_4 at $N = 26/3$) as well as with the large N estimate. This comparison is presented in Fig.5.12 where it can be seen how the curves approach the expected large
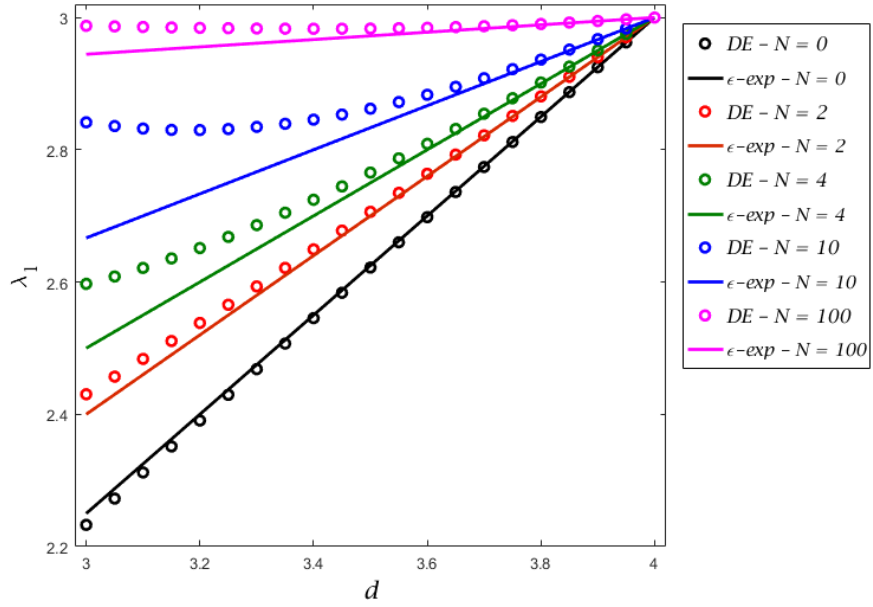
Figure 5.9: Scaling dimension estimate of the DE λ_1 as a function of dimension d for some values of N, along with their ϵ-expansion estimates. Error bars are avoided for clarity.
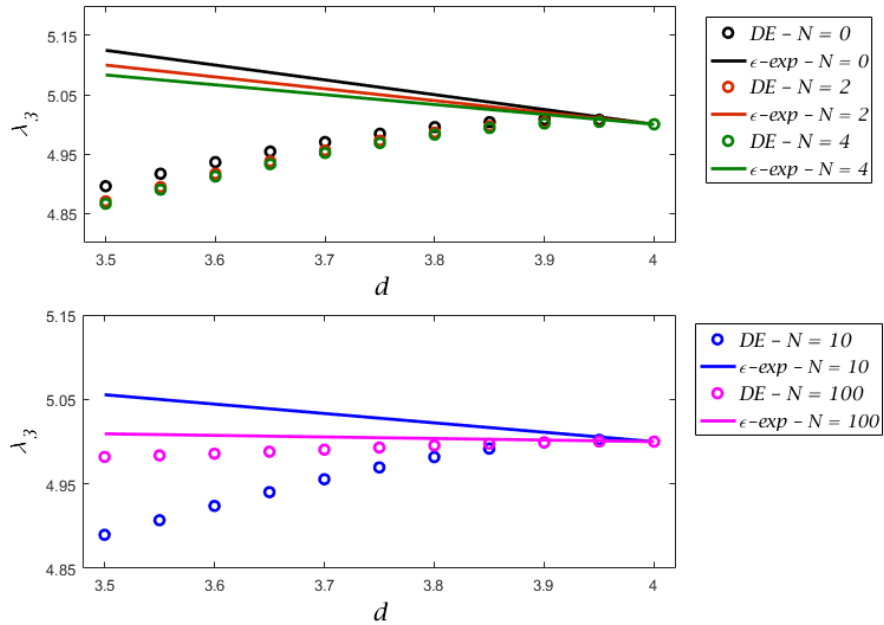
Figure 5.10: Scaling dimension estimate of the DE λ_3 as a function of dimension d for some values of N, along with their ϵ-expansion estimates. Error bars are avoided for clarity.
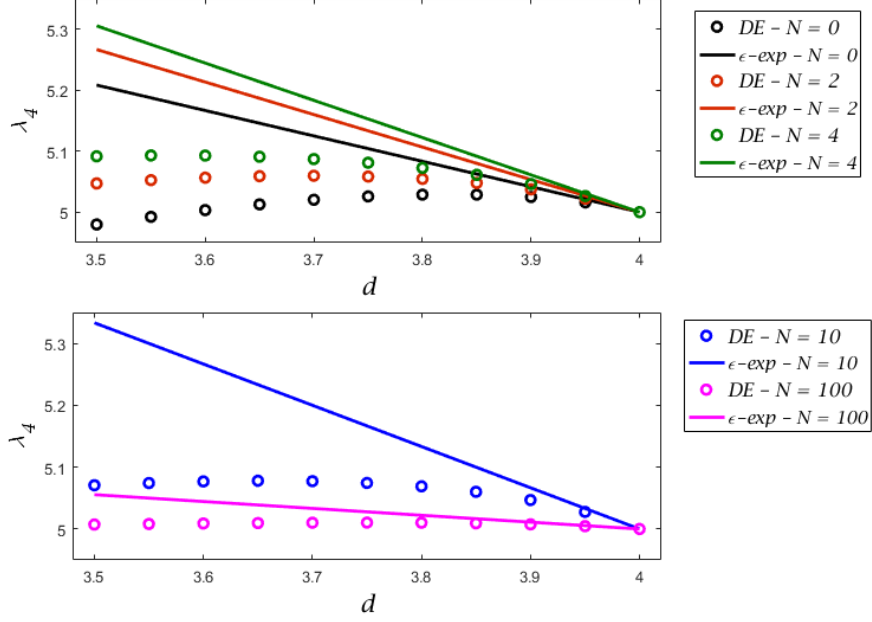
Figure 5.11: Scaling dimension estimate of the DE λ_4 as a function of dimension d for some values of N, along with their ϵ-expansion estimates. For $N = 0$, $N = 2$ and $N = 4$ the comparison is done with λ_5 of Eq.(5.16) whether for $N = 10$ and $N = 100$ it is compared to λ_4 from Eq.(5.16). Error bars are avoided for clarity.

N behaviour. Once again, regarding the ϵ-expansion it is clear that there is a relevant correction of order $\mathcal{O}(\epsilon^2)$ suppressed by some power of $1/N$.

From the previous discussion, it is clear that the scaling dimensions coming from the $\mathcal{O}(\partial^3)$ of the Derivative Expansion are nicely compatible with the results for the large N limit and with the ϵ-expansion, in their domain of validity, for λ_1, λ_2 at all values of N and for λ_3, λ_4 and λ_5 for big enough N. However, there is an appreciable mismatch with the ϵ-expansion at small values of N for λ_3, λ_4 and λ_5. In any case, it is important to remark that even that there exist a mismatch between ϵ-expansion and DE for operators with scaling dimension $5 + \mathcal{O}(\epsilon)$, the corrections are still very small compared to the value -1, which is still undoubtedly excluded.

5.2 Scale Invariance Implies Conformal Invariance in O(N) Models for $N \in \{2, 3, 4\}$

The results of the previous sections strongly indicate the realization of conformal invariance of $O(N)$ models for any N by showing that the scaling dimension of vector operators is unambiguously far from -1. However, they
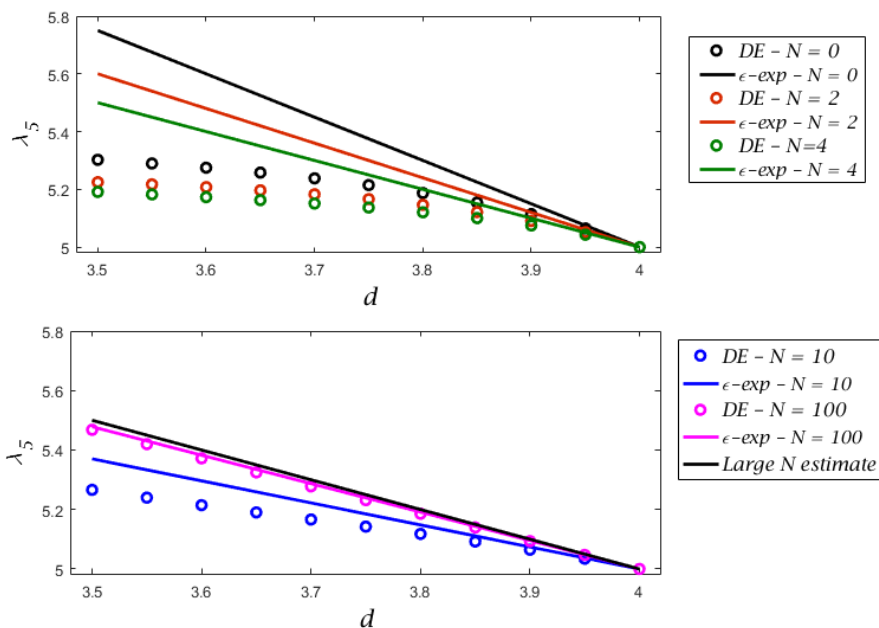
Figure 5.12: Scaling dimension estimate of the DE λ_5 as a function of dimension d for some values of N, along with their ϵ-expansion estimates. For $N = 0$, $N = 2$ and $N = 4$ the comparison is done with λ_4 of Eq.(5.16) whether for $N = 10$ and $N = 100$ it is compared to λ_5 from Eq.(5.16). Error bars are avoided for clarity.

do not constitute a proof and one can doubt about the quality of the considered approximation schemes (see however Chapter 3 for a discussion on the convergence of the DE).

In this section, we give a proof that conformal invariance is realized at the critical point of the $O(2)$, $O(3)$ and $O(4)$ models (see Chapter 3 for the physical realization of these models). The proof is done by extending the existing proof for the Ising model [27], by using known inequalities [130, 131, 132, 133, 134, 135] on correlation functions for the $O(N)$ model, which were shown to be valid for $N \in \{2, 3, 4\}$. It must be observed that if these inequalities happen to be proven for any other value of N of the $O(N)$ model, the proof is then automatically extended to that case. We start with a brief recall of the existing proof for the Ising model and afterwards we present the extension to the $O(N)$ models.

5.2.1 Brief Review of the Proof for the Ising Model

For the Ising model in dimension $d = 4$, the fixed point is Gaussian and the eigenvalues of the operators are given by their canonical dimensions. In this case the integrated vector operator with lowest dimension is $\int_x \phi \partial_\mu \phi (\partial \phi)^2$ and

its scaling dimension in the ϵ-expansion at first order is $3 + \mathcal{O}(\epsilon^2)$. However, it is not known, in principle, how the scaling of a generic vector operator varies as $d \to 3$. It turns out that this particular operator has scaling dimension exactly 3 at any dimension in spite of the no renormalization theorem shown in Appendix G. For a one loop computation of the next to leading (in relevance) integrated vector operators see Appendix H. To overcome the problem of computing the scaling dimension of vector operators at dimension 3, a lower bound was found for the scaling dimension of any vectorial operator [27].

We consider local operators $\mathcal{V}_\mu$ and instead of studying the RG flow around a fixed point, we extract the scaling dimension $D_\mathcal{V}$ of the vector operator by considering the power-law decay of correlation functions between two such vector operators. In general the two-point connected correlation function behaves at criticality like:

$$\langle \mathcal{V}_\mu(x)\mathcal{V}_\mu(y)\rangle_c \sim \frac{1}{|x-y|^{2D_\mathcal{V}}} \tag{5.47}$$

for large enough $|x - y|$. However, we may run into trouble because some operators may have correlation function which do not behave as a power-law as in Eq.(5.47), but rather as contact operators (that is, they are δ correlated; see for example [138]). We avoid this problem by rewriting the integrated operator in terms of another density (differing by total derivatives) to ensure that the correlation has a power-law decay. In what follows, we assume that an integrated vector operator can always be rewritten as the integral of a density whose correlation functions have a power-law behavior at long distances.

The idea of the proof is the following: (i) Bound the two-point connected correlation function of even and odd powers of the fields in the symmetric phase. (ii) Recognize that any local vector operator $\mathcal{V}_\mu$ on the lattice is a linear combination of vector operators of the form:

$$\mathcal{W}_\mu = \frac{1}{2}\partial_\mu\phi \sum_{s=\pm 1} \prod_{i=1}^{m-1} \phi(x + se_i^{(1)}). \tag{5.48}$$

(iii) Extend the bound to the two-point connected correlation function of $|\langle \mathcal{V}_\mu \mathcal{V}_\nu \rangle_c|$ and therefore bounding the scaling dimension, $D_\mathcal{V} \geq d - 1 + \eta$ or $D_V \geq -1 + \eta$, in its integrated version $V_\mu = \int_x \mathcal{V}_\mu(x)$, and since η is known to be strictly positive for the Ising model when $d < 4$ [1], this concludes the proof. We stress we are also bounding total derivates which, anyway, are not

---

[1]more generally, it is found to be strictly positive in an interacting theory whose Minkowskian extension is unitary [104, 139]

candidates for virial currents.

There is an extended bibliography on correlation inequalities which were used in many cases to prove some properties of statistical systems [140, 141, 142, 143, 144, 145]. In particular, we mention three inequalities which can be used to prove the realization of conformal invariance in Ising-like systems with ferromagnetic interactions. If A is a set of lattice points, we define $\varphi^A \equiv \prod_{i \in A} \varphi(i)$. With this definition, Griffiths's inequalities I and II [140, 141] (see also [146] for a different presentation) read:

$$\langle \varphi^A \rangle \geq 0 \tag{5.49}$$

and

$$\langle \varphi^A \varphi^B \rangle - \langle \varphi^A \rangle \langle \varphi^B \rangle \geq 0, \tag{5.50}$$

respectively. The third inequality that is used in the proof is due to Lebowitz [147]. It requires to use an extra copy of the system which we label with primed variables φ'. Lebowitz's inequality states

$$\langle (\varphi + \varphi')^A (\varphi - \varphi')^B \rangle - \langle \varphi + \varphi' \rangle^A \langle (\varphi - \varphi')^B \rangle \leq 0. \tag{5.51}$$

In order to prove the inequality $D_{\mathcal{V}} \geq d - 1 + \eta$, we start with the Ginzburg-Landau model (see Chapter 1) on a cubic lattice with lattice spacing a and a φ^4 interaction. For this model, which is in the Ising universality class, there is an inequality first proven in [143] and independently in [27], based on Eqs.(5.49-5.51), which states that at zero external magnetic field and for any temperature $T \geq T_c$:

$$0 \leq \langle \varphi^n(x) \varphi^m(y) \rangle - \langle \varphi^n(x) \rangle \langle \varphi^m(y) \rangle \leq \begin{cases} C(n,m) G(x-y) & \text{if n and m odd} \\ \hat{C}(n,m) G^2(x-y) & \text{if n and m even} \end{cases} \tag{5.52}$$

where $G(x-y) = \langle \varphi(x) \varphi(y) \rangle$, n and m are integers and $C(n,m)$ and $\hat{C}(n,m)$ are constants. Because at the critical point,

$$\langle \varphi^n(x); \varphi^m(y) \rangle \equiv \langle \varphi^n(x) \varphi^m(y) \rangle - \langle \varphi^n(x) \rangle \langle \varphi^m(y) \rangle$$

is a power law and $G(x-y) \propto |x-y|^{-(d-2+\eta)}$ we conclude that for m and n even and at the critical point:

$$\left| \langle \partial_\mu [\varphi^n(x)] \partial_\nu [\varphi^m(y)] \rangle \right| \leq \frac{\tilde{C}(n,m,\mu,\nu)}{|x-y|^{2(d-1+\eta)}} \tag{5.53}$$

where derivatives are a shortcut notation for appropriate finite difference expressions defined on the lattice. The term *appropriate* refers to the fact that, as will be explained, it is important to choose centred finite differences in order to ensure that the vector operators are odd under parity. As a consequence, for all operators $\mathcal{V}_\mu(x) = \partial_\mu(\varphi^n(x))$ with n even, one has $D_\mathcal{V} \geq d - 1 + \eta$.

Now, consider two different discretizations $\mathbf{O}_1^{(a)}(x)$ and $\mathbf{O}_1^{(b)}(x)$ of a given operator in the continuum and demand these discretized operators to have the same transformation rules as the operator in the continuum under the group of internal symmetries and under lattice isometries. Then, for arbitrary operators $\mathbf{O}_2(x), \mathbf{O}_3(x), \ldots$, we assume that

$$\left\langle \mathbf{O}_1^{(a)}(x_1)\mathbf{O}_2(x_2)\ldots\mathbf{O}_n(x_n) \right\rangle = Z_{a,b} \left\langle \mathbf{O}_1^{(b)}(x_1)\mathbf{O}_2(x_2)\ldots\mathbf{O}_n(x_n) \right\rangle \quad (5.54)$$

when the various points $x_1, x_2, \ldots, x_n$ are far apart (as compared to the lattice spacing a). This is, two different discretizations of a continuum operator have the same correlation functions at distances much larger than the lattice spacing a, up to a renormalization factor. For a discussion on this assumption, see [28].

We remark that, as a general rule, an operator mixes with *all* operators within the same sector. For example, the contribution to the left hand side of the correlation function in Eq.(5.54) from the operator $\mathbf{O}_1^{(a)}$ is dominated at long distances by the leading operator (i.e. the most relevant operator) of the decomposition of $\mathbf{O}_1^{(a)}$, say $\tilde{\mathbf{O}}_1$. Because operators $\mathbf{O}_1^{(a)}$ and $\mathbf{O}_1^{(b)}$ have the same symmetry properties, they mix with the same set of operators and, therefore, the contribution to the right hand side correlation function from operator $\mathbf{O}_1^{(b)}$ is also dominated at long distances by the leading operator $\tilde{\mathbf{O}}_1$ of the decomposition of $\mathbf{O}_1^{(b)}$. It could happen, however, that for accidental reasons, the leading contribution to the decomposition of an operator vanish and this *equivalence* in the long distance behaviour is no longer true. In any case, this will not affect the argument since it bounds the leading contribution and, consequently, any other.

Furthermore, when dealing with operators with derivatives, it is important to consider discretizations which preserve behave as the continuum limit under parity. This is important because at the lattice level, there is no notion of *vector* operator other than its properties under lattice symmetries. If this is not done properly, the scalar and vector sector would mix and the scaling behaviour of the continuum limit may not be the same as the discretized version. This is at the heart of any lattice simulation since, for instance, if two different discretization of an operator yielded different scaling behaviour of correlations

involving that operator, then, universality would be lost in consequence.

The discussion regarding the assumption, Eq.(5.54), is important because it was questioned in thefirst preprint version of [128]. In that preprint, the authors of [128] claimed the assumption to be wrong and allegedly shown a counterexample to the proof we give in this chapter, stating that if this assumption, first considered in [27], can not hold since there exists an operator which violates the bound $D_{\mathcal{V}} \geq d - 1 + \eta$. However, the counterexample is not valid because the operator considered is $SO(N)$ invariant instead of being $O(N)$ invariant.[1]

With this assumption we can complete the proof. Indeed, any vector operator even in φ can be discretized as a linear combination of operators of type of Eq.(5.48). And since these operators have the same large distance behaviour as the total derivative $\varphi^{n-1}(x)\partial_\mu\varphi(x)$, using the triangle inequality this implies that any vector operator even in φ has scaling dimension $D_{\mathcal{V}} \geq d - 1 + \eta$ which concludes the proof of conformal invariance in the critical regime of the Ising universality class.

5.2.2 Extension of the Proof to the $O(2)$, $O(3)$ and $O(4)$ Models

Any operator of the form

$$\mathcal{W}_\mu(x) = \frac{1}{2}(\partial_\mu\varphi_j)(x) \sum_{s=\pm 1} \varphi_j(x + se_0) \prod_{i=1}^{m-1} \varphi_{k_i}(x + se_i)\varphi_{k_i}(x + se_i'), \quad (5.55)$$

which is a generalization of the previous operators of Eq.(5.48), has the same naïve continuum limit as the total derivative $\partial_\mu(\varphi_i\varphi_i)^m$. As we did for the Ising model, we assume that operators which have the same continuum limit, have the same large distance behaviour. We can regularize any $O(N)$ invariant local vector operator $\mathcal{V}$ by a linear combination of operators of type given in Eq.(5.55). And since using triangle inequality we know that if we bound the scaling dimension of total derivatives, which by the assumption bound the scaling dimension of operators of type Eq.(5.55), we bound the scaling dimension of any local vector operator. We highlight that we consider only vector operators with correlation functions which are not delta short-range (i.e. they need to behave as power-laws in the critical point) .

---

[1]For details regarding the controversy see [148, 128]. The authors of [128] have withdrawn their claims from their published version, and subsequent preprint versions, but still claiming the assumption is wrong.

To generalize the proof to the $O(N)$ model we need to make use of some correlation inequalities which are only proved for the $O(2)$, $O(3)$ and $O(4)$ model. These are the Griffiths and Lebowitz inequalities [130, 131, 132, 133, 134, 135] and by its use we prove in Section 5.2.3 a generalization of the correlation inequality Eq.(5.52) which states that for $T \geq T_c$:

$$
\begin{aligned}
&|\langle \varphi_{i_1}(x) \cdots \varphi_{i_m}(x) \varphi_{j_1}(y) \cdots \varphi_{j_n}(y) \rangle \\
&- \langle \varphi_{i_1}(x) \cdots \varphi_{i_m}(x) \rangle \langle \varphi_{j_1}(y) \cdots \varphi_{j_n}(y) \rangle| \leq
\begin{cases}
CG(x-y) \; n,m \; odd \\
C'G^2(x-y) \; n,m \; even
\end{cases}
\end{aligned}
\tag{5.56}
$$

where $C(n,m)$, $\hat{C}(n,m)$ are constants and $G(x-y)$ is defined, in the disordered phase, through

$$
\langle \varphi_i(x) \varphi_j(y) \rangle = \delta_{ij} G(x-y).
\tag{5.57}
$$

With this result we conclude, as was done for the Ising model [27], that if at the critical point $|\langle \varphi_{i_1}(x) \cdots \varphi_{i_m}(x) \varphi_{j_1}(y) \cdots \varphi_{j_n}(y) \rangle - \langle \varphi_{i_1}(x) \cdots \varphi_{i_m}(x) \rangle \langle \varphi_{j_1}(y) \cdots \varphi_{j_n}(y) \rangle|$ behaves as a power of $|x-y|$ when $|x-y|$ is much larger than the lattice spacing, and since $G(x-y) \propto |x-y|^{-(d-2+\eta)}$ at the critical point, then this means that in this regime for any even n and m we obtain the bound:

$$
\left| \langle \partial_\mu (\varphi_{i_1}(x) \cdots \varphi_{i_m}(x)) \; \partial_\nu (\varphi_{j_1}(y) \cdots \varphi_{j_n}(y)) \rangle \right| \leq \frac{\tilde{C}(\mu,\nu)}{|x-y|^{2(d-1+\eta)}}.
\tag{5.58}
$$

This bounds the scaling dimension of local vector operator of the $O(2)$, $O(3)$ and $O(4)$ model as

$$
D_\mathcal{V} \geq d - 1 + \eta
$$

concluding the prove (recall that $\eta > 0$ for these models in $d < 4$).

5.2.3 A New Correlation Inequality for the $O(2)$, $O(3)$ and $O(4)$ Models

In this section we prove by induction the inequality Eq.(5.56) for $T \geq T_c$ for the $O(2)$, $O(3)$ and $O(4)$ models. Some of the inequalities obtained in [130, 131, 132, 133, 134, 135] for $N = 2, 3$, and 4, and which we will make use

of, are the following:

$$\langle \phi_1(x_1^{(1)}) \ldots \phi_1(x_{n_1}^{(1)}) \phi_2(x_1^{(2)}) \ldots \phi_2(x_{n_2}^{(2)}) \ldots \phi_N(x_1^{(N)}) \ldots \phi_N(x_{n_N}^{(N)}) \rangle \geq 0, \quad (5.59)$$

$$\langle \phi_\alpha(x_1) \ldots \phi_\alpha(x_n) \phi_\alpha(y_1) \ldots \phi_\alpha(y_m) \rangle \geq$$
$$\langle \phi_\alpha(x_1) \ldots \phi_\alpha(x_n) \rangle \langle \phi_\alpha(y_1) \ldots \phi_\alpha(y_m) \rangle, \quad (5.60)$$

$$\langle \phi_\alpha(x_1) \ldots \phi_\alpha(x_n) \phi_\beta(y_1) \ldots \phi_\beta(y_m) \rangle \leq$$
$$\langle \phi_\alpha(x_1) \ldots \phi_\alpha(x_n) \rangle \langle \phi_\beta(y_1) \ldots \phi_\beta(y_m) \rangle \quad \text{with } \alpha \neq \beta. \quad (5.61)$$

Inequality Eq.(5.59) and Eq.(5.60) are very similar to the Griffiths inequalities I and II for a scalar field and Eq.(5.61) is very similar to the Lebowitz inequality.

Since we approach the critical point from the disordered phase, $T \geq T_c$, to prove Eq.(5.56) we can restrict to n and m with the same parity. This is because, in the disordered phase, correlation functions with an odd number of fields vanish. We want to prove Eq.(5.56).

We stress that the inequality for the cases $n = 1$, $m = 1$ and $n = 0$, $m = 2$ are trivial. Consider first the case where n and m are odd. This case is simpler because the second term in the left hand side of Eq.(5.56) is zero due to $T \geq T_c$. Therefore, we consider the inequality to be valid for $n + m < \mathcal{N}$ and proceed by induction to prove its validity for $n + m = \mathcal{N}$. Because of $O(N)$ symmetry, the structure of the two point function must take the form:

$$G^o_{m,n}(x,y) \equiv \langle \varphi_{i_1}(x) \cdots \varphi_{i_m}(x) \varphi_{j_1}(y) \cdots \varphi_{j_n}(y) \rangle =$$
$$\sum_{l=0}^{\frac{n-1}{2}} f_l(x,y) \Big[\delta_{i_1 j_1} \cdots \delta_{i_{2l+1} j_{2l+1}} \delta_{i_{2l+2} i_{2l+3}} \delta_{j_{2l+2} j_{2l+3}} \cdots \delta_{i_{m-1} i_m} \delta_{j_{n-1} j_n} \quad (5.62)$$
$$+ \left(\frac{m!n!}{(2l+1)!\,(m-2l-1)!!\,(n-2l-1)!!} - 1 \right) \text{perms.} \Big],$$

where the o in $G^o_{m,n}(x,y)$ stands for *odd*. To understand this decomposition, consider any perturbative diagram contributing to the correlation function $G^o_{m,n}(x,y)$. Any field index of the correlation function in Eq.(5.62) must be contracted with some other index. This is a completely general property. Now, the index l in the sum labels the contributions where $2l + 1$ fields evaluated at position x are contracted with fields evaluated at position y. The functions f describe the dependence in space of each tensorial structure. Without loss of generality we can assume $m \geq n$, and the first step is to consider the general

configuration of indices:

$$i_k = \begin{cases} 1 & k = 1 \\ 2 & k = 2, \cdots, m \end{cases}$$

$$j_k = \begin{cases} 2 & k = 1, \cdots, 2s \\ 1 & k = 2s + 1, \cdots, n \end{cases}$$

with s ranging from 0 to $\frac{n-1}{2}$. The case $s = 0$ implies that all the j's are equal 1. We can apply the generalization of Lebowitz's inequality Eq.(5.61) to these index configurations on $G_{m,n}^o (x, y)$ to get:

$$
\begin{aligned}
0 \leq G_{m,n}^o (x, y) &= \sum_{t=0}^{t=s} \frac{(2s)! \, (n - 2s)!! \, (m - 1)!}{(2t)! \, (2s - 2t)!! \, (m - 1 - 2t)!!} f_t (x, y) \\
&\leq \langle \varphi_1 (x) (\varphi_1 (y))^{n-2s} \rangle \langle (\varphi_2 (x))^{m-1} (\varphi_2 (y))^{2s} \rangle \\
&\leq C G (x - y)
\end{aligned}
\tag{5.63}
$$

where we used in the first inequality one of the generalization of Griffiths's inequality, namely Eq.(5.59), and at the last inequality we made use of the validity of Eq.(5.56) for $\mathcal{N} - 1$ and at the fact that $\langle (\varphi_2 (x))^{m-1} (\varphi_2 (y))^{2s} \rangle$ is bounded by a constant. Now, using Eq.(5.62) in this index configuration we can bound the conical linear combination of f's functions up to s

$$
\sum_{t=0}^{t=s} \frac{(2s)! \, (n - 2s)!! \, (m - 1)!}{(2t)! \, (2s - 2t)!! \, (m - 1 - 2t)!!} f_t (x, y) \leq C G (x - y),
\tag{5.64}
$$

and taking s ranging from 0 to $\frac{n-1}{2}$ we subsequently bound each of the $f_s (x, y)$ and this in turn implies the fulfilment of Eq.5.56 for $n + m = \mathcal{N}$ when n and m are odd.

The even case is a bit different since the second term of the left hand side of Eq.(5.56) is nonzero. We again look (without loss of generality) at the structure of the two point function for $m \geq n$, but both of them even:

$$
G_{m,n}^e (x, y) \equiv \langle \varphi_{i_1} (x) \cdots \varphi_{i_m} (x) \; \varphi_{j_1} (y) \cdots \varphi_{j_n} (y) \rangle =
$$

$$
\sum_{l=0}^{\frac{n}{2}} g_l (x, y) \left(\delta_{i_1 j_1} \cdots \delta_{i_{2l} j_{2l}} \; \delta_{i_{2l+1} i_{2l+2}} \delta_{j_{2l+1} j_{2l+2}} \cdots \delta_{i_{m-1} i_m} \delta_{j_{n-1} j_n} + \right.
$$

$$
\left. \left(\frac{m! n!}{(2l)! \, (m - 2l)!! \, (n - 2l)!!} - 1 \right) \text{perms.} \right),
$$

$$
\tag{5.65}
$$

where now the e in $G^e_{m,n}(x,y)$ stands for *even*. We proceed in the same fashion as for the odd case. We take a configuration of indices to make use of Eq.(5.61) of the general form:

$$i_k = \begin{cases} 1 & k = 1 \\ 2 & k = 2, \cdots, m \end{cases}$$

$$j_k = \begin{cases} 2 & k = 1, \cdots, 2s-1 \\ 1 & k = 2s, \cdots, n \end{cases}$$

with s ranging from 1 to $\frac{n}{2}$. These configurations in combination with the Eq.(5.61) impose an upper bound on a strictly conical combination of the g_i functions *not* involving the g_0 function, to be specific:

$$\begin{aligned} 0 \leq G^e_{m,n}(x,y) &= \sum_{t=1}^{t=s} \frac{(2s-1)!\,(n-2s+1)!!\,(m-1)!}{(2t-1)!\,(2s-2t)!!\,(m-2t)!!} g_t(x,y) \\ &\leq \left\langle \varphi_1(x)(\varphi_1(y))^{n-2s+1} \right\rangle \left\langle (\varphi_2(x))^{m-1}(\varphi_2(y))^{2s-1} \right\rangle \\ &\leq C G^2(x-y) \end{aligned} \tag{5.66}$$

where, as for the odd case, we made use of Eq.(5.59) on the first inequality and of the validity of Eq.(5.56) for $n + m = \mathcal{N} - 1$. And in exactly the same way as before, we find a lower and an upper bound on a strict conical combination of g functions up until g_s. Varying s from 1 up to $\frac{n}{2}$ implies that the absolute value of each of these g_s function (with $s \neq 0$) is bounded by a constant times $G^2(x-y)$.

To complete the argument we need to involve the g_0 function. To do this we must proceed in another way since this term corresponds to the case where no index i is contracted to an index j. Therefore, let us consider the even simpler configuration where all indices i_t are equal to 1 and all indices j_t are equal to 2, this yields for the two-point function:

$$0 \leq G^e_{m,n}(x,y) = (m-1)!!\,(n-1)!!g_0(x,y) \leq \langle \varphi_1^m(0) \rangle \langle \varphi_1^n(0) \rangle, \tag{5.67}$$

where we used Eq.(5.59) in the first inequality and Eq.(5.61) in the last inequality (we used the same subscript afterwards because it makes no difference due to $O(N)$ symmetry). From this immediately follows that:

$$g_0(x,y) - \frac{\langle \varphi_1^m(0) \rangle \langle \varphi_1^n(0) \rangle}{(m-1)!!\,(n-1)!!} \leq 0. \tag{5.68}$$

Let us consider now that all indices i_t and j_t are equal to 1 which leads to a strict conical combination of *all* the g's functions. But this allows to use the other generalization of Griffiths's inequality Eq.(5.60) and gives a lower bound to the conical combination:

$$\sum_{s=0}^{\frac{n}{2}} \frac{m! n!}{(2s)! (m-2s)!! (n-2s)!!} g_s(x,y) \geq \langle \varphi_1^m(0) \rangle \langle \varphi_1^n(0) \rangle. \qquad (5.69)$$

We can combine now Eq.(5.68) with Eq.(5.69) to obtain the lower bound:

$$g_0(x,y) - \frac{\langle \varphi_1^m(0) \rangle \langle \varphi_1^n(0) \rangle}{(m-1)!! (n-1)!!}$$
$$\geq -\frac{1}{(m-1)!! (n-1)!!} \sum_{s=0}^{\frac{n}{2}} \frac{m! n!}{(2s)! (m-2s)!! (n-2s)!!} g_s(x,y)$$
$$\geq C G^2(x-y) \qquad (5.70)$$

where $C < 0$ is a constant. We have bounded all the g functions with the exception to the g_0 which is bounded minus a constant. Now, it turns out that the second term in the left hand side of Eq.(5.56) is exactly that constant:

$$\langle \varphi_{i_1}(x) \cdots \varphi_{i_m}(x) \rangle \langle \varphi_{j_1}(y) \cdots \varphi_{j_n}(y) \rangle = \qquad (5.71)$$
$$\left(\delta_{i_1 i_2} \delta_{j_1 j_2} \cdots \delta_{i_{m-1} i_m} \delta_{j_{n-1} j_n} + ((m-1)!! (n-1)!! - 1) \text{ perms} \right) \frac{\langle \varphi_1^m(0) \rangle \langle \varphi_1^n(0) \rangle}{(m-1)!! (n-1)!!}.$$

Therefore, inserting this and Eq.(5.65) into the left hand side of Eq.(5.56) we are left with the strictly conical combination of g's *not* including g_0, which was already shown to be bounded by $G^2(x-y)$. This concludes the proof of Eq.(5.56).

We conclude this chapter with a brief summary. This chapter focused on the plausibility for the realization of conformal invariance, in dimensions $2.5 \lesssim d < 4$, based on the sufficient condition described in Chapter 4. This sufficient condition states that if conformal invariance is not realized, it must exist an integrated vector operator dependent on the field and its derivatives, whose scaling dimension is exactly -1. We considered the most likely vector operator candidates for breaking conformal invariance and showed that their scaling dimension is much higher than the value -1 for all considered values of N. This gives strong indication that such a breaking term does not exists for the $O(N)$ models and, consequently, the critical regime of these models is conformal invariant. Additionally, we gave a proof for the realization of

136

conformal invariance, under mild assumptions, in the critical regime of the physically interesting cases $O(2)$, $O(3)$ and $O(4)$.

Chapter 6

Use of Conformal Invariance in the Non Perturbative Renormalization Group

As stated before, conformal invariance is believed to be realized in the critical regime of many systems. Moreover, it is conjectured that for a system whose Minkowkian extension is unitary and which presents translation and rotation invariance, the presence of scale invariance immediately implies invariance under the full conformal group.

The presence or not of conformal invariance is relevant because it strongly delimits the possible structure that a field theory could have [108, 113]. However, as discussed in Chapter 2, scale invariance is enough to determine the fixed point and critical properties of a given critical system. Indeed, within the NPRG framework we showed that the fixed point equation Eq.(2.40) from Chapter 2 is, in fact, no other than the Ward identity for dilatations Eq.(4.33). Because of this and the fact that the NPRG framework is a rather novel theoretical tool, whose properties and approximations are still being developed, up to now there has not been any use of conformal invariance to make quantitative predictions of physical quantities. In this chapter we give a first step at filling this gap by presenting the first use of conformal invariance within the NPRG. More precisely, we consider the consequences of conformal invariance at order $\mathcal{O}(\partial^4)$ of the derivative expansion in the Ising universality class ($N = 1$ of the $O(N)$ models).

In doing so, we also address an unanswered question about the principle of minimal sensitivity. As discussed in Chapter 3 (see also [12]), when using the DE of the NPRG it is crucial to fix the overall scale α of the regulator function

[see Eqs.(2.30-2.32)] in order to give precise predictions and, even more, for the DE to be convergent. This is enhanced by the fact that when going to high orders of the derivative expansion, predictions become more and more dependent on the regulator parameter α. This is clearly seen in Fig.3.2 where the curves for the critical exponents η, ν and ω become steeper with the order of the DE. Anticipating the results, at order $\mathcal{O}(\partial^4)$ of the DE, it happens that the value of α for which PMS is realized in the η exponent is, in fact, the value of α for which the single extra restriction coming from conformal Ward identity is best satisfied. Even more, critical exponent η is the only exponent which is, implicitly, varied in order to be *at* the fixed point. The other critical exponents studied arise from a linear stability analysis around this fixed point solution. If this is true at all orders of the DE, it means that considering the PMS on η is equivalent to consider the critical theory (i.e. fixed point solution) that is closer to being a conformal field theory. Moreover, it also justifies the fact that α_{PMS} for different critical exponents tend to approach each other at higher orders of the DE.

6.1 Compatibility Study for the Ising Model at $\mathcal{O}(\partial^4)$

As described in Chapter 4, when considering the DE of the NPRG at order $\mathcal{O}(\partial^s)$ for the scalar ϕ^4 theory with $s \geq 4$, special conformal Ward identity imposes more restrictions than solely dilatation Ward identity. What is more, conformal invariance imposes the same restrictions than scale invariance plus some extra constraints. Conformal invariance constraints have a Lorentz index and are extracted from *odd* powers of momentum (conformal Ward identity in Fourier variables has an extra momentum derivative with respect to dilatation Ward identity). Because of this, the independent dilatation constraints ($C_\mathcal{D}$) for a certain $\Gamma_k^{(n)}$ at order $\mathcal{O}(p^s)$ are extracted from dilatation Ward identity at order $\mathcal{O}(p^s)$. The independent extra constraints that special conformal Ward identity with respect to dilatation Ward identity ($C_{\mathcal{K}_\mu \backslash \mathcal{D}}$) imposes for a certain $\Gamma_k^{(n)}$ at order $\mathcal{O}(p^s)$ are extracted from conformal Ward identity at order $\mathcal{O}(p^s)$. from be extracted from they will be in order to ease notation we call conformal constraints at order $\mathcal{O}(\partial^s)$ to the ones arising from considering an ansatz for the effective action at order $\mathcal{O}(\partial^s)$ of the DE. We show in Table 6.1 the number of constraints that dilatation and special conformal Ward identities impose at order $\mathcal{O}(\partial^s)$ of the DE of the NPRG, with s up to 6, for the Ising and $O(N)$

models universality classes. Each constraint corresponds to a ρ-dependent identity (as is, for example, the fixed point equation for the potential). At any order of the derivative expansion dilatation Ward identity gives as many constraints as are independent functions (U_k, Z_k, etc.). However, imposing the ansatz of the derivative expansion at order $\mathcal{O}(\partial^s)$ yields, for $s \geq 4$, more independent constraints than there are independent functions.

$C_{\mathcal{D}}$ - Ising	$C_{\mathcal{K}_\mu \backslash \mathcal{D}}$ - Ising	$C_{\mathcal{D}}$ - $O(N)$	$C_{\mathcal{K}_\mu \backslash \mathcal{D}}$ - $O(N)$
$\mathcal{O}(p^2)$ - 1	$\mathcal{O}(p)$ - 0	$\mathcal{O}(p^2)$ - 2	$\mathcal{O}(p)$ - 0
$\mathcal{O}(p^4)$ - 3	$\mathcal{O}(p^3)$ - 1	$\mathcal{O}(p^4)$ - 10	$\mathcal{O}(p^3)$ - 3
$\mathcal{O}(p^6)$ - 8	$\mathcal{O}(p^5)$ - 4	$\mathcal{O}(p^6)$ - 48	$\mathcal{O}(p^5)$ - 22

Table 6.1: Total number of dilatation ($C_{\mathcal{D}}$) and extra conformal ($C_{\mathcal{K}_\mu \backslash \mathcal{D}}$) constraints for the Ising model and the $O(N)$ models.

At order $\mathcal{O}(\partial^4)$ the ansatz for the scalar ϕ^4 theory takes the form [60]:

$$\Gamma_k[\varphi] \equiv \int_x \left\{ U_k(\rho) + \frac{Z_k(\rho)}{2} (\partial_\nu \varphi)^2 + \frac{W_{k\,a}(\rho)}{2} (\partial_\mu \partial_\nu \varphi)^2 + \right.$$
$$\left. \frac{W_{k\,b}(\rho)}{2} \varphi \partial_\mu \partial_\mu \varphi (\partial_\nu \varphi)^2 + \frac{W_{k\,c}(\rho)}{2} \left((\partial_\mu \varphi)^2 \right)^2 \right\}. \qquad (6.1)$$

As usual, in order to obtain the flow equations, we differentiate Eq.(2.36) with respect to the field one, two, three or four times and after evaluating in a homogeneous field configuration and performing a Fourier transform we extract the flow equations for the functions $U_k, \ldots, W_{k\,c}$ from the different momentum structures. The fixed point equations for these functions are exactly the modified Ward identity for dilatations, in the presence of the infrared regulator, for different vertices $\Gamma_k^{(n)}$, see Eq.(4.57), projected in different structures. However, if we consider special conformal Ward identity Eq.(4.59) instead, we can extract one extra independent equation either from $\Gamma_k^{(3)}$ or $\Gamma_k^{(4)}$ at order $\mathcal{O}(p^3)$. Indeed, special conformal Ward identity for $\Gamma_k^{(3)}$ has three independent momentum structure at order $\mathcal{O}(p^3)$ (recall that Ward identity for special conformal transformations has the character of a vector, see Chapter 4) while dilatation has only two (already included in the three coming from conformal Ward identity). Now, it may be that this third equation was the equation for the third structure that arises from dilatation Ward identity for the vertex $\Gamma_k^{(4)}$. However, this is not the case and, in fact, conformal Ward identity for $\Gamma_k^{(4)}$ at order $\mathcal{O}(p^3)$ has four independent structure, where three of them yield equivalent equations than the ones coming from dilatation Ward identity while the fourth one is equivalent to the already existing for $\Gamma_k^{(3)}$.

Our approach consists then, in computing the extra constraint coming from the special conformal Ward identity for the vertex $\Gamma_k^{(3)}$ and evaluate it at the fixed point. Of course, there is no ambiguity in separating what is left hand side and what corresponds to the right hand side since one involves a momentum integral while the other corresponds to the dimensional part. However, since dilatation constraints are satisfied (indeed, we define the fixed point solution as the one satisfying dilatation Ward identity), we could add any combination of these and we could obtain an equivalent conformal constraint. This ambiguity can be avoided in the following way. Let us write schematically conformal and dilatation Ward identities for $\Gamma_k^{(n)}$ as:

$$C_{LHS}^{\mu\,(n)} = C_{RHS}^{\mu\,(n)} \tag{6.2}$$

and

$$D_{LHS}^{(n)} = D_{RHS}^{(n)}, \tag{6.3}$$

where subscript *LHS* and *RHS* stand for left hand side and right hand side, respectively. Now, it happens that for all the situations that we encountered where conformal and dilatation Ward identities are equivalent, the way of matching them is by applying the operator

$$-\left(\frac{2}{n} \sum_{i=1}^{n-1} \frac{\partial \cdot}{\partial p^\mu} \right)$$

onto Eq.(6.3). Therefore, we define:

$$
\begin{aligned}
\mathbb{C}_{LHS}^{\mu\,(n)} &= C_{LHS}^{\mu\,(n)} + \left(\frac{2}{n} \sum_{i=1}^{n-1} \frac{\partial D_{LHS}^{(n)}}{\partial p^\mu} \right) \\
\mathbb{C}_{RHS}^{\mu\,(n)} &= C_{RHS}^{\mu\,(n)} + \left(\frac{2}{n} \sum_{i=1}^{n-1} \frac{\partial D_{RHS}^{(n)}}{\partial p^\mu} \right).
\end{aligned}
\tag{6.4}
$$

This allows us to write down an unambiguous equation for the extra information which reads:

$$\mathbb{C}_{LHS}^{\mu\,(n)} = \mathbb{C}_{RHS}^{\mu\,(n)}, \tag{6.5}$$

or explicitly:

$$\left[\sum_{i=1}^{n-1}p_{i\mu}\frac{\partial^2}{\partial p_i^\nu \partial p_i^\nu}-2p_{i\nu}\frac{\partial^2}{\partial p_i^\nu \partial p_i^\mu}+2\frac{1-d}{n}\frac{\partial}{\partial p_i^\mu}+\frac{2}{n}\sum_{j=1}^{n-1}p_{i\nu}\frac{\partial^2}{\partial p_i^\nu \partial p_j^\mu}\right]\Gamma^{(n)}(p_1,\ldots,p_{n-1})$$

$$+2\phi D_\varphi\left(\frac{1}{n}\sum_{i=1}^{n-1}\frac{\partial}{\partial p_i^\mu}-\frac{\partial}{\partial r^\mu}\right)\Gamma^{(n+1)}(p_1,\ldots,p_{n-1},r)\bigg|_{r=0}=$$

$$\frac{1}{2}\int_q \dot{R}(q)G^2(q)\left(\frac{2}{n}\sum_{i=1}^{n-1}\frac{\partial}{\partial p_i^\mu}-\frac{\partial}{\partial q^\mu}-\frac{\partial}{\partial q'^\mu}\right)H^{(n)}(p_1,\ldots,p_{n-1},q,q')\bigg|_{q'=-q}$$
$$(6.6)$$

When dilatation and conformal Ward identities are equivalent it happens that the momentum configuration is not of a general form. We found that each side of Eq.(6.5) is equal to zero for the following exceptional momentum configurations:

- Even n with momentum configuration given by opposite pairs, this is $p_1=-p_2$, ..., $p_{n-1}=-p_n$ with p_n defined by momentum conservation.
- Odd n with momentum configuration given by opposite pairs and one of them set to zero, this is $p_1=-p_2$, ..., $p_{n-2}=p_{n-1}$, $p_n=0$ with p_n defined by momentum conservation.
- Same modulus momentum configuration for $n=3$, this is $p_1=p_2=p_3$, that we refer as *equimodular* momentum configuration.

It is possible that there exists other momentum configurations where both equations, namely Eq.(4.57) and Eq.(4.59), are equivalent (maybe a generalization of the *equimodular* momentum configuration or a mixture of the two types, or perhaps even some new structures) and understanding why this is so may bring valuable information. This deserves further study in the future.

Now, for a general momentum configuration of $\Gamma_k^{(3)}$, Eq.(6.5) at order $\mathcal{O}(p^3)$ only has one momentum structure yielding only one equation. This equation is therefore what we consider to be the unambiguous extra conformal constraint. We remark that there is one final source of arbitrariness which consists in an overall factor in Eq.(6.5) so our study will consists in subtracting the right hand side to the left hand side of this equation and divide by a characteristic constant, say the value of the left hand side of the equation at $\rho=0$. We define this as $\mathcal{A}(\rho)$ and it reads:

$$\mathcal{A}(\rho)=\frac{\mathbb{C}_{LHS}^{(n)}(\rho)-\mathbb{C}_{RHS}^{(n)}(\rho)}{\mathbb{C}_{LHS}^{(n)}(0)},\qquad(6.7)$$

142

where $\mathbb{C}_{LHS}^{(n)}(\rho)$ and $\mathbb{C}_{RHS}^{(n)}(\rho)$ are the part of $\mathbb{C}_{LHS}^{\mu\,(n)}$ and $\mathbb{C}_{RHS}^{\mu\,(n)}$, respectively, proportional to the momentum structure with the ρ dependence made explicit.

We mentioned in Chapter 3 that there is certain freedom when implementing the derivative expansion, this is the truncated and full forms of the flow equations. Usually, the derivative expansion is implemented in the full form. However, in Chapter 3, corresponding to [18], and in the study made in [12] the truncated form of the flow equations was used. It is important to emphasize that the difference between the full and truncated forms of the flow equation yield critical exponents, using PMS, whose difference is below the precision of the considered order. We show, just for the Θ_k^3 regulator, the estimated curve for the critical exponents in terms of α in Fig.6.1. The reason for considering this discussion in this Chapter is because, as we show below, the conformal constraint is less violated in the truncated form than in the full form of the flow equations for every considered regulator.
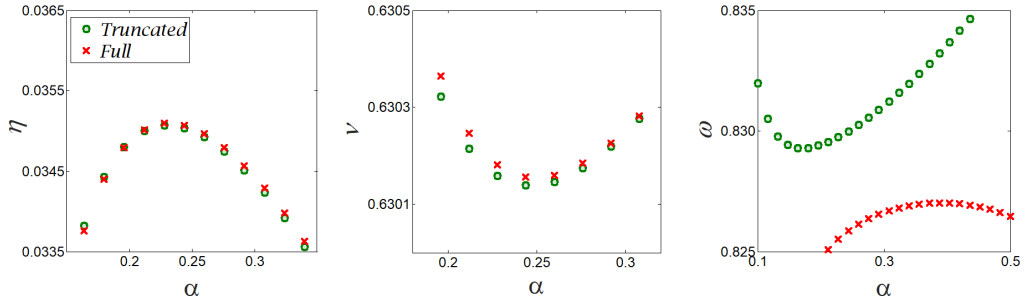
Figure 6.1: Critical exponents η, ν and ω for the Ising model at order $\mathcal{O}(\partial^4)$ of the DE with the Θ_k^3 regulator in the truncated and full form of the flow equations. We recall that the estimated central values and error bars at this order were: $\eta = 0.0362(12)$, $\nu = 0.62989(25)$ and $\omega = 0.832(14)$.

As can be seen in Fig.6.1, the prediction for the critical exponents η and ν are, indeed, very close. We recall that the error bars at order $\mathcal{O}(\partial^4)$ for the DE estimates of the critical exponents η and ν are 12×10^{-4} and 25×10^{-5}, respectively. However, the observed difference between truncated and full form for the critical exponent η is $\sim 2\%$ of its error bar, while it is $\sim 7\%$ of the error bar for the critical exponent ν. The situation for ω is very different. The curves for this critical exponent have different concavity and the mismatch is more profound. In order to reduce the difference between the estimates using the truncated and full form of the flow equations, it is important to implement the PMS (or some other criterion). When doing so, the difference in the predictions for the critical exponent ω, between the two forms of the flow equations is $\sim 16\%$ of the error bar at the considered order, being this

14×10^-3.

This brief analysis shows that both forms of the flow equations are consistent within error bars of the considered order of the derivative expansion. However, as anticipated, we show in the next section that the conformal constraint is not indifferent to the chosen form of the flow equations.

6.2 Analysis of the Extra Conformal Constraint

The derivative expansion, as we implement it, usually does break conformal invariance. Consequently we find

$$\mathcal{A}(\rho) \neq 0,$$

at the fixed point. The main Let us study how this breaking of conformal invariance depends on the regulator. Consequently we study for which value of α, $\mathcal{A}(\rho)$ is closer to zero. We vary α in a range which includes the PMS values $\alpha_{PMS}^{(\eta)}$, $\alpha_{PMS}^{(\nu)}$ and $\alpha_{PMS}^{(\omega)}$. The fulfilment of the conformal constraint $\mathcal{A}(\rho)$ with both the full (left) and truncated (right) form of the flow equations is shown in Fig.6.2 for the regulators E_k (up) and W_k (down) and in Fig.6.3 for regulators Θ_k^3 (up) and Θ_k^4 (down). Values of $\alpha_{PMS}^{(\eta)}$, $\alpha_{PMS}^{(\nu)}$ and $\alpha_{PMS}^{(\omega)}$ are also plotted for reference.

Let us remark a few features depicted in Figs.6.2-6.3. First, by looking at orders of magnitude of the breaking of conformal invariance, that is colour intensity, it is evident that, for each regulator, conformal constraint is much better satisfied in the *truncated* form of the flow equations. This is not trivial, and there are no reasons for this to be true at higher orders of the DE nor for other models. However, this is good news because, as stated in Chapter 3, the *truncated* form of flow equations are much simpler. An explanation for this, may be that the *full* form of the flow equations involve terms which, strictly speaking, corresponds to higher orders of the DE and are not well under control within the present order of the approximation. In particular, the extra constraint of conformal invariance becomes much bigger and much harder to balance the left hand side and right hand side of the constraint. This conclusion is also in agreement with the fact that $\alpha_{PMS}^{(\eta)}$, $\alpha_{PMS}^{(\nu)}$ and $\alpha_{PMS}^{(\omega)}$ are much more close to each other, this is particularly true for $\alpha_{PMS}^{(\omega)}$ which, for the *full* form of the flow equations, is very detached from $\alpha_{PMS}^{(\eta)}$ and $\alpha_{PMS}^{(\nu)}$. Second,
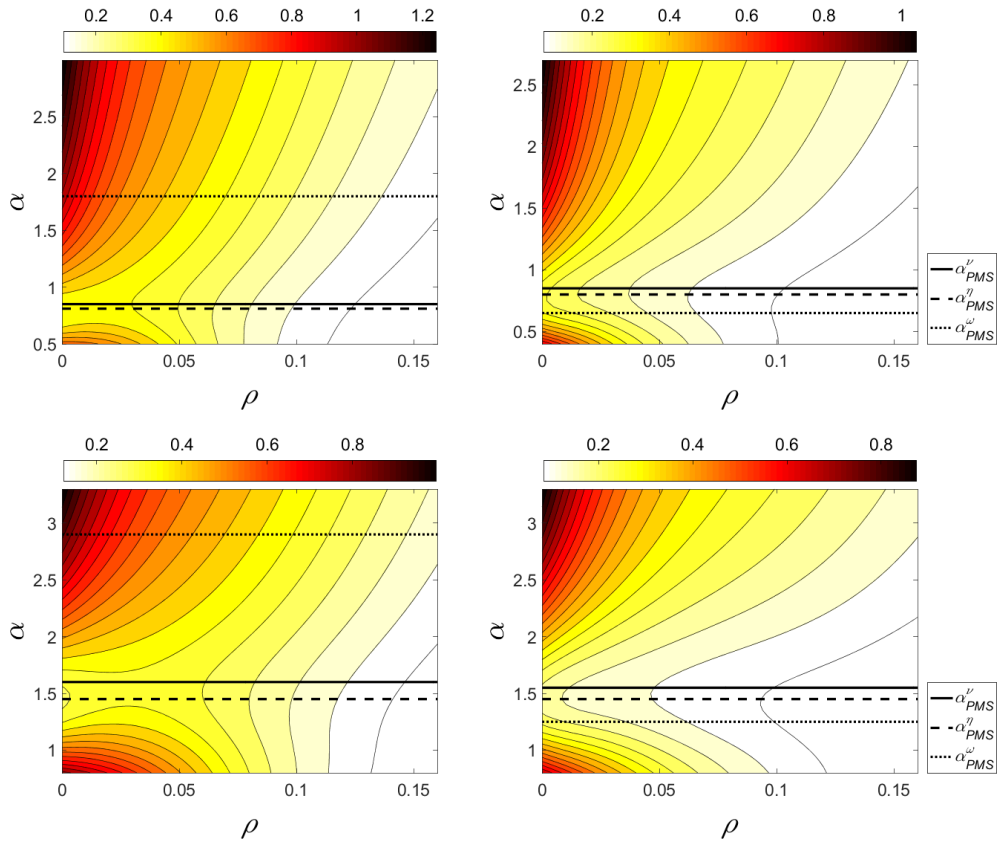
Figure 6.2: Conformal constraint at order $\mathcal{O}(\partial^4)$ of the DE in terms of α and ρ for a ϕ^4 scalar theory, for the *full* (left) and *truncated* (right) form of the flow equation for regulators E_k (up) and W_k (down) [see Eq.(2.30) and Eq.(2.31)]. PMS values for each situation are superimposed for reference.

independently of the regulator or if flow equations are taken in their *truncated* or *full* form, conformal invariance seems least broken around α^η_{PMS} and α^ν_{PMS}. This is a remarkable property of the PMS. It gives another justification for the use of the PMS which can now be interpreted not only as the overall scale of the regulator α for which physical results are less dependent on the regulator, but as the value of the overall scale for which the approximation scheme used best satisfies conformal invariance.

It proves useful for visualization of the breaking of conformal invariance to identify a single parameter to measure the breaking of conformal invariance for a given value of α, because the spread measure from Figs.6.2-6.3 is a bit hard to read, although it contains much more information than a single value for each α would. However, using a single indicator may help to read information regarding at precisely which value of α is conformal invariance best satisfied. In particular, because of the vicinity of α^η_{PMS} and α^ν_{PMS}, a legitimate question is then: for which of these values, if any, is conformal constraint best fulfilled.
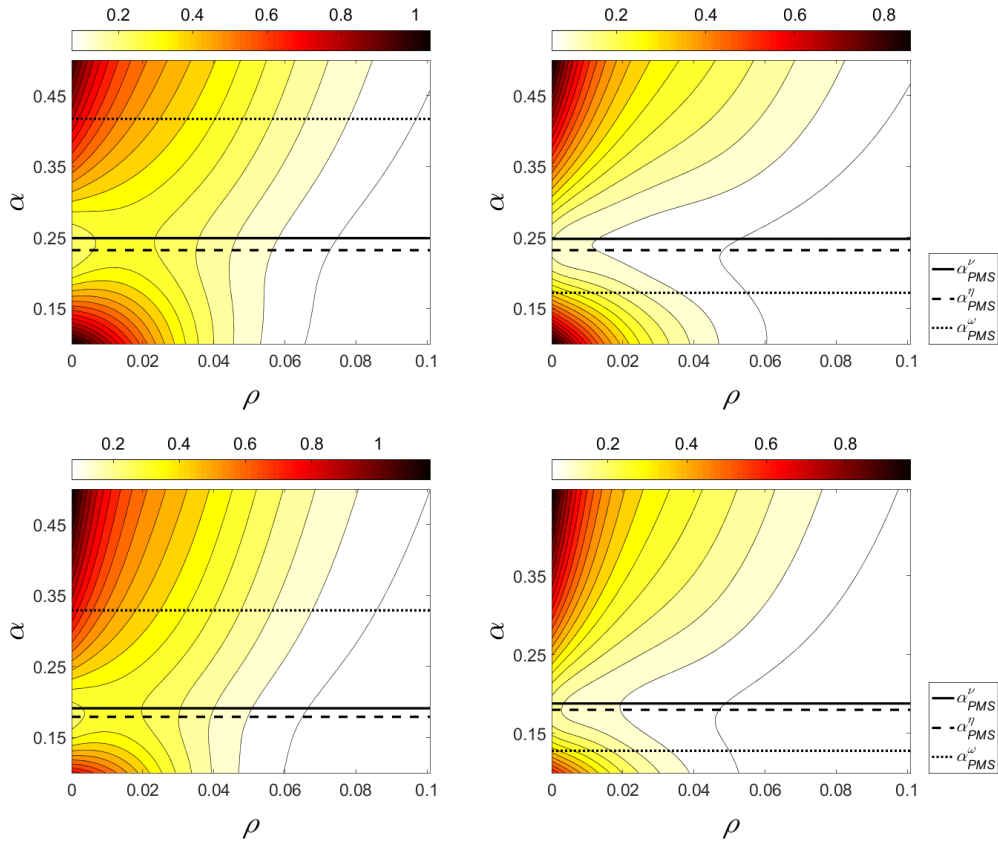
Figure 6.3: Conformal constraint at order $\mathcal{O}(\partial^4)$ of the DE in terms of α and ρ for a ϕ^4 scalar theory, for the *full* (left) and *truncated* (right) form of the flow equation for regulators Θ_k^3 (up) and Θ_k^4 (down) [see Eq.(2.32)]. PMS values for each situation are superimposed for reference.

Because we do not have, yet, a profound understanding of conformal invariance within the NPRG, we aim at answering this by choosing two simple measures, one of them is just to take as a measurement of *conformal error* the value of $\mathcal{A}$ at $\rho = 0$, we define then Δ_1 as

$$\Delta_1 \equiv \mathcal{A}(\rho = 0)/min_\alpha\big\{\mathcal{A}(\rho = 0)\big\}. \tag{6.8}$$

The second measure consists in adding up the breaking of the conformal constraint for all ρ, this is simply:

$$\Delta_2 \equiv \frac{\int \mathcal{A}(\rho)d\rho}{min_\alpha\big\{\int \mathcal{A}(\rho)d\rho\big\}}. \tag{6.9}$$

This makes sense because $\mathcal{A}(\rho) \underset{\rho\to\infty}{\to} 0$ rapidly enough. We considered the measures normalized, as presented in Eq.(6.8) and Eq.(6.9), because we are not interested in the specific value of $\mathcal{A}$, although in the future with a deeper

understanding of the subject it could be of interest. We show, both in the *truncated* and *full* form of the flow equations, these two measures for regulators E_k and W_k in Fig.6.4 and regulators Θ_k^3 and Θ_k^4 in Fig.6.5.
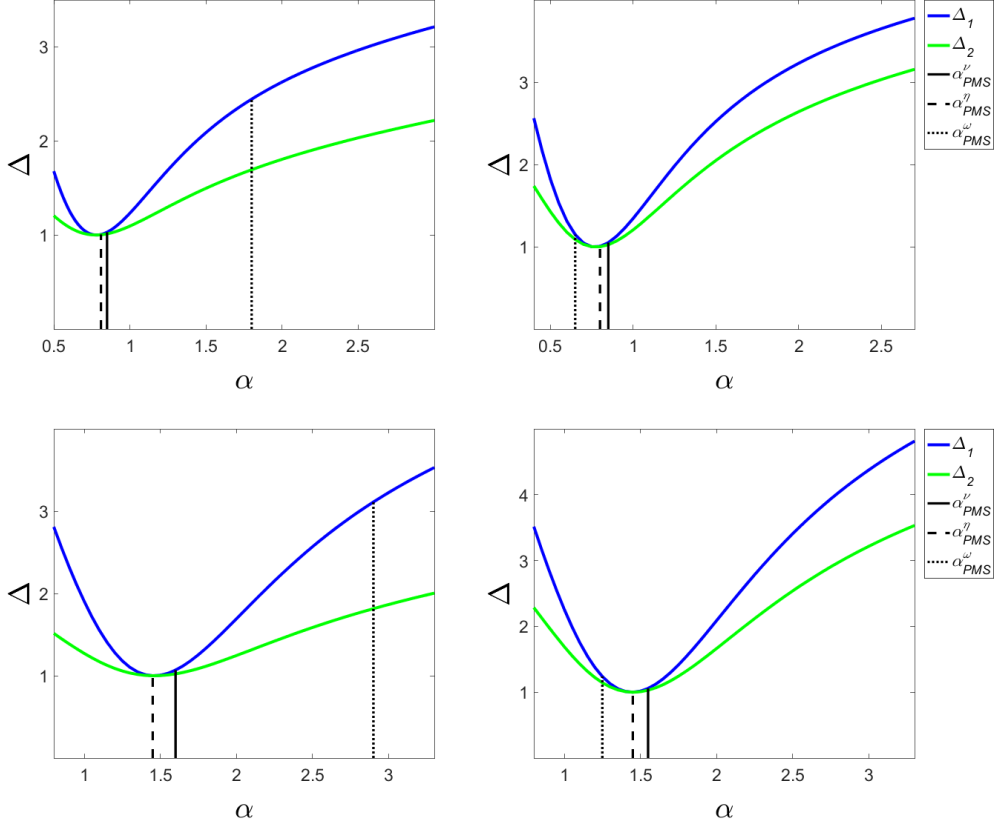
Figure 6.4: Measures of the breaking of conformal invariance Δ_1 and Δ_2 at order $\mathcal{O}(\partial^4)$ of the DE in terms of α for a ϕ^4 scalar theory, for the *full* (left) and *truncated* (right) form of the flow equation for regulators E_k (up) and W_k (down) [see Eq.(2.30) and Eq.(2.31)]. PMS values for each situation are superimposed for reference.

From Figs.6.4-6.5 it becomes clear that conformal invariance is best satisfied close to, or exactly at, α_{PMS}^η for all regulators and in both forms of the flow equations. This lead us to conjecture that the maximal conformality criterion (MCC) coincides with the PMS on η, at least for the ϕ^4, i.e.

$$\alpha_{MCC} = \alpha_{PMS}^\eta. \tag{6.10}$$

The principle of minimal sensitivity, up to now, was applied based on two arguments. First, since one is interested in computing physical quantities, which must be independent of the regulator of choice, it makes sense to consider a value of α where the results vary less. The second argument is an *a posteriori* one, it happens that the quality of the predictions when doing PMS increased
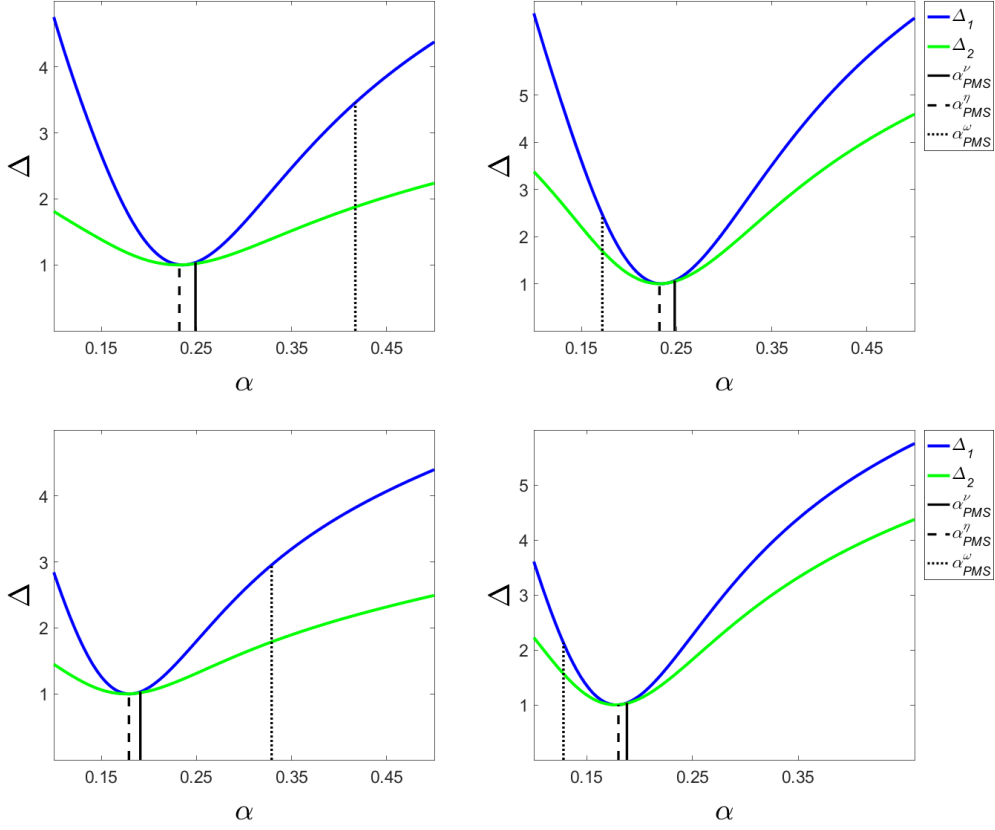
Figure 6.5: Measures of the breaking of conformal invariance Δ_1 and Δ_2 at order $\mathcal{O}(\partial^4)$ of the DE in terms of α for a ϕ^4 scalar theory, for the *full* (left) and *truncated* (right) form of the flow equation for regulators Θ_k^3 (up) and Θ_k^4 (down) [see Eq.(2.32)]. PMS values for each situation are superimposed for reference.

significantly with respect to a general fixed value for α, yielding in many cases the fastest apparent convergence. Moreover, as we go to higher orders of the DE, it is mandatory that we consider PMS because the curves for the physical quantities become steeper and steeper, see Chapter 3. These arguments, although reasonable, do not provide a full explanation and therefore can leave the PMS as suspicious. The findings presented in this chapter address this issue by showing that doing PMS, at least for η or ν, is more than just practical or reasonable because we are selecting the overall scale of the regulator α as one that respects the physics the most (at least for conformal invariant systems).

In an attempt to explain the conjecture Eq.(6.10), we remark that the critical exponent η is computed during the process of finding the fixed point solution unlike other critical exponents like ν or ω which are obtained via a linear stability analysis around the fixed point. What is important, and the main difference between these exponents for this reasoning, is that the

fixing of η is done prior to finding the fixed point as an indirect requirement for yielding the fixed point solution. However, this is not the case for other critical exponents. We could then say that the PMS on η is in fact a PMS on the most stable (regulator independent) fixed point.

Moreover, we could argue that the right thing to do, in fact, is to select the parameter α, for all the exponents and other physical quantities, as the one that makes the fixed point solution closer to being conformal invariant. Of course, doing this may spoil slightly the results from the DE of Chapter 3. However, a word of caution should be said before doing such an extrapolation from this analysis to the $O(N)$ case. This conclusion is preliminary, and one must keep in mind that it corresponds to a first study of the topic. Indeed, at order $\mathcal{O}(\partial^4)$, which is the first order within the DE where conformal invariance has something to add, the extra restrictions that it imposes are just one equation. However, as was stated in Chapter 4, if we consider order $\mathcal{O}(\partial^6)$ of the DE we are left with four extra equations and is far from evident what would be the outcome for a study with just one free parameter. Consequently, further study is required for a deeper comprehension and will be addressed in future works. Similar arguments to the ones just given, apply to the $O(N)$ case regarding the extrapolation of the present analysis. This is because at order $\mathcal{O}(\partial^4)$ there are already two extra constraints coming from conformal Ward identity (in addition to the ones of dilatation Ward identity), see Table 6.1.

Nevertheless and for the sake of the argument, if we are willing to believe that the conjecture given in Eq.(6.10) is, indeed, true we must emphasize that the *damage* over the results is not as bad as one may think. Although curves tend to be steeper for the critical exponents as we go higher in the order of approximation of the DE, it happens that α_{PMS}^ν and α_{PMS}^ω tend to approach each other and to $\alpha_{PMS}^\eta = \alpha_{MCC}$. This can be seen already from the displayed curves on Chapter 3, but for reference we give in Tables 6.2-6.10 a quantitative analysis of this new criterion. We show in these tables α_{PMS}^η, α_{PMS}^ν and α_{PMS}^ω as well as comparing the raw data (see Appendix C) used for the study of Chapter 3 with a raw data using only α_{MCC} for various $O(N)$ models at order $\mathcal{O}(\partial^4)$.

The presented data show that the variation, if any, between using PMS on exponents ν and ω or using the MCC is, in fact, very small. Therefore, the predictions given in Chapter 3 are barely, or not at all, affected by switching to the MCC. The difference in predictions is specially small for small values of N. What is more, it happens that in some cases the critical exponents ν and

	E_k	W_k	Θ_k^3
α_{MCC}	0.83(1)	1.48(1)	0.24(1)
$\eta(\alpha_{MCC})$	0.0292	0.0299	0.0303
α_{PMS}^ν	0.74(1)	1.25(1)	0.19(1)
$\nu(\alpha_{PMS}^\nu)$	0.5875	0.5875	0.5876
$\nu(\alpha_{MCC})$	0.5875	0.5875	0.5875
α_{PMS}^ω	1.20(1)	2.06(1)	0.33(1)
$\omega(\alpha_{PMS}^\omega)$	0.9005	0.9006	0.9007
$\omega(\alpha_{MCC})$	0.8994	0.8995	0.8995

Table 6.2: Comparison of raw data predictions for η, ν and ω at order $\mathcal{O}(\partial^4)$ of the DE using PMS and MCC for $N = 0$. PMS values of α for these quantities, with their error bars given in parenthesis, are also given for comparison.

	E_k	W_k	Θ_k^3
α_{MCC}	0.85(1)	1.51(1)	0.25(1)
$\eta(\alpha_{MCC})$	0.0336	0.0346	0.0351
α_{PMS}^ν	0.88(1)	1.61(1)	0.27(1)
$\nu(\alpha_{PMS}^\nu)$	0.6305	0.6302	0.6301
$\nu(\alpha_{MCC})$	0.6305	0.6303	0.6301
α_{PMS}^ω	0.74(1)	1.35(1)	0.22(1)
$\omega(\alpha_{PMS}^\omega)$	0.8321	0.8313	0.8310
$\omega(\alpha_{MCC})$	0.8323	0.8314	0.8311

Table 6.3: Comparison of raw data predictions for η, ν and ω at order $\mathcal{O}(\partial^4)$ of the DE using PMS and MCC for $N = 1$. PMS values of α for these quantities, with their error bars given in parenthesis, are also given for comparison.

	E_k	W_k	Θ_k^3
α_{MCC}	0.85(1)	1.52(1)	0.25(1)
$\eta(\alpha_{MCC})$	0.0350	0.0361	0.0367
α_{PMS}^ν	0.88(1)	1.59(1)	0.27(1)
$\nu(\alpha_{PMS}^\nu)$	0.6732	0.6725	0.6722
$\nu(\alpha_{MCC})$	0.6732	0.6725	0.6722
α_{PMS}^ω	0.87(1)	1.59(1)	0.27(1)
$\omega(\alpha_{PMS}^\omega)$	0.7934	0.7906	0.7893
$\omega(\alpha_{MCC})$	0.7934	0.7906	0.7894

Table 6.4: Comparison of raw data predictions for η, ν and ω at order $\mathcal{O}(\partial^4)$ of the DE using PMS and MCC for $N = 2$. PMS values of α for these quantities, with their error bars given in parenthesis, are also given for comparison.

ω present more than one PMS or, as is the case for example for the critical exponent ν at order $\mathcal{O}(\partial^4)$ of the $N = 0$ case, not PMS at all. Despite that, in all the studied cases, the behaviour of critical exponent η was never found to

	E_k	W_k	Θ^3_k
α_{MCC}	0.85(1)	1.52(1)	0.25(1)
$\eta(\alpha_{MCC})$	0.0347	0.0358	0.0363
α^ν_{PMS}	0.86(1)	1.57(1)	0.26(1)
$\nu(\alpha^\nu_{PMS})$	0.7136	0.7126	0.7122
$\nu(\alpha_{MCC})$	0.7136	0.7127	0.7123
α^ω_{PMS}	0.89(1)	1.61(1)	0.27(1)
$\omega(\alpha^\omega_{PMS})$	0.7729	0.7681	0.7659
$\omega(\alpha_{MCC})$	0.7730	0.7683	0.7663

Table 6.5: Comparison of raw data predictions for η, ν and ω at order $\mathcal{O}(\partial^4)$ of the DE using PMS and MCC for $N = 3$. PMS values of α for these quantities, with their error bars given in parenthesis, are also given for comparison.

	E_k	W_k	Θ^3_k
α_{MCC}	0.84(1)	1.51(1)	0.25(1)
$\eta(\alpha_{MCC})$	0.0332	0.0343	0.0348
α^ν_{PMS}	0.84(1)	1.54(1)	0.26(1)
$\nu(\alpha^\nu_{PMS})$	0.7500	0.7490	0.7487
$\nu(\alpha_{MCC})$	0.7500	0.7491	0.7487
α^ω_{PMS}	0.88(1)	1.60(1)	0.27(1)
$\omega(\alpha^\omega_{PMS})$	0.7649	0.7588	0.7561
$\omega(\alpha_{MCC})$	0.7651	0.7591	0.7566

Table 6.6: Comparison of raw data predictions for η, ν and ω at order $\mathcal{O}(\partial^4)$ of the DE using PMS and MCC for $N = 4$. PMS values of α for these quantities, with their error bars given in parenthesis, are also given for comparison.

	E_k	W_k	Θ^3_k
α_{MCC}	0.84(1)	1.50(1)	0.25(1)
$\eta(\alpha_{MCC})$	0.0313	0.0323	0.0327
α^ν_{PMS}	0.81(1)	1.49(1)	0.25(1)
$\nu(\alpha^\nu_{PMS})$	0.7815	0.7808	0.7806
$\nu(\alpha_{MCC})$	0.7815	0.7808	0.7806
α^ω_{PMS}	0.86(1)	1.58(1)	0.27(1)
$\omega(\alpha^\omega_{PMS})$	0.7648	0.7584	0.7558
$\omega(\alpha_{MCC})$	0.7649	0.7586	0.7562

Table 6.7: Comparison of raw data predictions for η, ν and ω at order $\mathcal{O}(\partial^4)$ of the DE using PMS and MCC for $N = 5$. PMS values of α for these quantities, with their error bars given in parenthesis, are also given for comparison.

give rise to any such ambiguity since it always alternates concavity and only presents one maximum or minimum depending on the order of the DE. This provide the MCC with a desirable feature: not only we are using just one fixed

	E_k	W_k	Θ_k^3
α_{MCC}	0.79(1)	1.42(1)	0.24(1)
$\eta(\alpha_{MCC})$	0.0218	0.0222	0.0225
α_{PMS}^{ν}	0.56(1)	1.03(1)	0.17(1)
$\nu(\alpha_{PMS}^{\nu})$	0.8771	0.8777	0.8780
$\nu(\alpha_{MCC})$	0.8777	0.8780	0.8784
α_{PMS}^{ω}	0.75(1)	1.41(1)	0.24(1)
$\omega(\alpha_{PMS}^{\omega})$	0.8081	0.8063	0.8062
$\omega(\alpha_{MCC})$	0.8082	0.8063	0.8062

Table 6.8: Comparison of raw data predictions for η, ν and ω at order $\mathcal{O}(\partial^4)$ of the DE using PMS and MCC for $N = 10$. PMS values of α for these quantities, with their error bars given in parenthesis, are also given for comparison.

	E_k	W_k	Θ_k^3
α_{MCC}	0.75(1)	1.36(1)	0.23(1)
$\eta(\alpha_{MCC})$	0.0123	0.0125	0.0126
α_{PMS}^{ν}	1.24(1)	1.99(1)	0.31(1)
$\nu(\alpha_{PMS}^{\nu})$	0.9406	0.9409	0.9411
$\nu(\alpha_{MCC})$	0.9403	0.9406	0.9409
α_{PMS}^{ω}	0.61(1)	1.17(1)	0.20(1)
$\omega(\alpha_{PMS}^{\omega})$	0.8863	0.8875	0.8884
$\omega(\alpha_{MCC})$	0.8874	0.8880	0.8888

Table 6.9: Comparison of raw data predictions for η, ν and ω at order $\mathcal{O}(\partial^4)$ of the DE using PMS and MCC for $N = 20$. PMS values of α for these quantities, with their error bars given in parenthesis, are also given for comparison.

	E_k	W_k	Θ_k^3
α_{MCC}	0.74(1)	1.32(1)	0.22(1)
$\eta(\alpha_{MCC})$	0.00260	0.00263	0.00264
α_{PMS}^{ν}	0.98(1)	1.63(1)	0.25(1)
$\nu(\alpha_{PMS}^{\nu})$	0.98877	0.98884	0.98888
$\nu(\alpha_{MCC})$	0.98875	0.98882	0.98888
α_{PMS}^{ω}	0.56(1)	1.02(1)	0.19(1)
$\omega(\alpha_{PMS}^{\omega})$	0.9767	0.9771	0.9772
$\omega(\alpha_{MCC})$	0.9771	0.9773	0.9774

Table 6.10: Comparison of raw data predictions for η, ν and ω at order $\mathcal{O}(\partial^4)$ of the DE using PMS and MCC for $N = 100$. PMS values of α for these quantities, with their error bars given in parenthesis, are also given for comparison.

point solution for all quantities, but we are selecting it unambiguously.

Although all the previous discussion seems favourable to the use the MCC, the reasons for not using this criterion (yet) is twofold: First, there is no

information coming from conformal constraints to the order LPA or order $\mathcal{O}(\partial^2)$. Second, we must proceed with caution because the study made here corresponds to the only constraint of the special conformal Ward identity to the Ising model universality class and the extension of the identification $\alpha_{MCC} \equiv \alpha^{\eta}_{PMS}$ to the $O(N)$ models is, for the moment, a conjecture. Because of these arguments, we do not present here new estimates of critical exponents for the $O(N)$ models. This shall be done after a deeper understanding of conformal constraints.

Chapter 7

Conclusions and Perspectives

The work done in this thesis can be roughly split in three parts. A first part concerns the convergence properties of the derivative expansion approximation scheme within the non perturbative renormalization group and its use for precise computation of critical exponents. A second part regarding the sufficient condition, exploiting various field theoretical approaches and statistical mechanics inequalities, for the presence of conformal invariance in the critical regime of $O(N)$ models. And a third part which attempts to exploit the information coming from conformal invariance in order to improve our knowledge of the non perturbative renormalization group as well as using it in our advantage to study systems. It is important to emphasize that this thesis opened many interesting perspectives. I will describe shortly some of them.

We pushed for the first time the derivative expansion approximation scheme to order $\mathcal{O}(\partial^4)$ for $O(N)$ models within the non perturbative renormalization group. This is not a purely academic task, but the $O(N)$ models are in the same universality classes than many physically interesting systems. For example, the limit $N \to 0$ describes the critical properties of polymers in dilute solutions which exhibit a continuous phase transition between a self-avoiding linear structure and a compact molecule structure. The $O(2)$ model characterize the critical behaviour of easy plane ferromagnets and the, so called, λ-transition between a fluid and a superfluid phase of the Helium-4. The critical properties of isotropic ferromagnets are descibed by the critical behaviour of the $O(3)$ model. There are more examples, the $O(4)$ model is believed to describe the finite temperature chiral transition of QCD with two light quarks, the $O(5)$ model may be related to high-T_c superconductors (although it is not clear if this is so). In doing so, we verified in these models the convergence properties of the method, finding that the successive orders improve their pre-

dictions by a factor of 4 to 9. On top of that, and by virtue of this result, of this result, we suggested a way of taking advantage of this information in order to make improved predictions of critical exponents. In particular, we manage to contribute to the long standing controversy between Monte Carlo simulations and experiments regarding the actual value of the specific heat critical exponent α (or equivalently, using scaling laws, ν), for which up to last year was considered unsettled. Our results, as well as the fairly new results from the conformal bootstrap program, align with Monte Carlo estimates and tend to point out a difficulty in these experiments. All our estimates, of critical exponents, are for all studied values of N, not only compatible with the best reported results in the literature, but in many cases surpass them. In other cases, the method proved to reach a similar level of precision, with the exception of particular cases, such as Monte Carlo estimates for $N = 0$ where an astonishing precision has been obtained. However, an extra advantage of the present method is the numerical time requirements. Take for example the case $N = 2$. Although Monte Carlo and conformal bootstrap estimates are somewhat more precise, they used for attaining such a precision, the order of 10^2 years of CPU time, while our whole computation (that is, generating the curve of exponents as a function of α) for that case take the order of a day in a personal laptop.

These results correspond to a first use of the method to compute a few quantities. So far, we have used the derivative expansion just to compute the 3 critical exponents η, ν and ω. Nevertheless, the method allows for the computation of other universal quantities (as well as non-universal), such as universal amplitude ratios or the coefficients c_i in the expansion Eq.(3.8), and we shall do so for several values of N in the near future. This first part of the thesis required the deduction of flow equations, which does not seem to be realizable manually and demands extensive codes of efficient symbolic programming.

The second part of the thesis focuses on the relation between conformal invariance and the non perturbative renormalization group. We tested the existent sufficient condition for the $O(N)$ models. The test consists in discarding the value -1 as the scaling dimension of possible candidates for the breaking of conformal invariance, which must be an integrated vector operator (invariant under translations and internal symmetries of the system). The results, although not surprising, give convincing evidence of the realization of conformal invariance in the critical regime of these models. This has been done within

three approximation schemes: the derivative expansion at order $\mathcal{O}(\partial^3)$; the large N limit and ϵ-expansion approximation schemes. Besides this testing regarding $O(N)$ we implemented a one loop computation of the scaling dimension of possible candidates for the breaking of conformal invariance for the cubic model. Parallel to this, we proved the existence of a family of operators whose scaling dimension can be computed exactly due to a no renormalization theorem. Unfortunately, this is of no importance for the sufficient condition since because these are redundant operators; a feature that prevents them of being candidates for the breaking of conformal invariance.

In addition to the testing of the sufficient condition, we proved (under general hypothesis) that the critical regime of the $O(2)$, $O(3)$ and $O(4)$ model is conformal invariant generalizing a previous result for $O(1)$ (or $\mathbb{Z}_2$). The proof holds only for these particular values of N because it is based on correlation inequalities which have been only proved for these values. Moreover, for the purpose of our proof, we developed a new correlation inequality which holds for these values. However, if the inequalities, on which the proof stands, happen to be extended for any other value of N, then our proof is automatically extended to that case.

For example, we intend to use correlation inequalities existing for the case $N = 0$ in order to extend even further our proof of conformal invariance to other models. Additionally, a brute force proof for the case "$N = \infty$" may be at reach and it will be explored. This second part of the thesis involved, also, symbolic programming code, as for the first part of the thesis. Complementary, standard field theoretical methods, as are the ϵ-expansion and large N limits, were employed in order to corroborate the symbolic deductions and to analytically study the regimes of validity of the methods. Additionally, we also explored the domain of exact correlation inequalities and contributed with a new one valid for some $O(N)$ models (which, in fact, was used for proving conformal invariance for the $O(N)$ models it holds true).

The third, and final, part of the thesis focus on the subject of what can be said, within the non perturbative renormalization group framework, once that conformal invariance is taken for granted. We managed to deduce an exact equation that holds the extra information that the special conformal Ward identity supply in addition to the dilatation Ward identity. This equation has not yet been exploited but it constitute a first step into understanding the role of conformal invariance in the NPRG framework. More precisely, we studied the only extra conformal constraint for $N = 1$ that appears at order $\mathcal{O}(\partial^4)$ of

the derivative expansion. This study provided a new physical interpretation for the principle of minimal sensitivity, but moreover it lead us to propose another criterion, namely the *maximal conformality criterion*, for fixing the overall scale of the regulator which, in principle, lacks of ambiguity issues present in the principle of minimal sensitivity. This does not mean that the principle of minimal sensitivity must be discarded since, in fact, they happen to yield essentially identical results (at least at the considered order).

To the best of my knowledge, this is the first time that conformal invariance has been employed for physical predictions within this framework. For this reason, there are numerous paths to explore and, in the forthcoming future, there is potentially a lot to be said about various aspects of theories which are conformal invariant. To name a few things at a close reach, we need to understand how are the extra constraints coming from conformal invariance for the $O(N)$ models at order $\mathcal{O}(\partial^4)$ and how they can be used in order to enhance our knowledge of the critical theory. The same can be inquired about the order $\mathcal{O}(\partial^6)$ of the Ising model. One possibility for using more conformal constraints is, for example, to employ them to fix higher order functions in the derivative expansion without actually going to this higher order.

Another possible path, but probably more challenging, is to exploit the exact equation which holds only the complementary information that conformal Ward identity has with respect to dilatation Ward identity. This path should, and will, be pursued with the hope of, maybe, finding some exacts analytical results.

Finally, I want to express that many other approaches to the topic of conformal invariance within the non perturbative renormalization group were considered. Some of these approaches will be revisited and further explored in the near future, but for reasons of compactness it was not suitable to present them in this thesis. One of these approaches concern the introduction of a source for the $\langle \phi^2 \rangle$ relevant operator. Another considered approach consists in working out correlation functions involving the stress-energy tensor. Conformal constraints at successive orders of the loop expansion were, also, considered and we glimpse on the possibility of generating linear constraints These were some headlines, but not all, of the considered approaches.

Bibliography

[1] Cmglee. https://commons.wikimedia.org/wiki/File:Phase_diagram_of_-water_simplified.svg, 2019.

[2] T. Shigeoka, N. Iwata, T. Kishino, M. Nishi, Y. Oohara, and H. Yoshizawa. Magnetic phase diagram of $NdRu_2Si_2$. *Physica B: Physics of Condensed Matter*, 186-188(C):652–654, may 1993.

[3] Kenneth G. Wilson and Michael E. Fisher. Critical exponents in 3.99 dimensions. *Physical Review Letters*, 28(4):240–243, jan 1972.

[4] Kenneth G. Wilson and J. Kogut. The renormalization group and the epsilon expansion. *Phys. Rep.*, 12(2):75–199, aug 1974.

[5] C. Wetterich. Average action and the renormalization group equations. *Nuclear Physics, Section B*, 352(3):529–584, apr 1991.

[6] Christof Wetterich. The average action for scalar fields near phase transitions. *Zeitschrift für Physik C Particles and Fields*, 57(3):451–469, sep 1993.

[7] Ulrich Ellwanger. Collective fields and flow equations. *Zeitschrift für Physik C Particles and Fields*, 58(4):619–627, 1993.

[8] Tim R. Morris. The exact renormalization group and approximate solutions. *International Journal of Modern Physics A*, 09(14):2411–2449, jun 1994.

[9] Jürgen Juergen Berges, Nikolaos Tetradis, and Christof Wetterich. Nonperturbative renormalization flow in quantum field theory and statistical physics. *Phys. Rept.*, 363(4-6):223–386, jun 2002.

[10] Bertrand Delamotte. An introduction to the nonperturbative renormalization group. *Lecture Notes in Physics*, 852:49–132, 2012.

[11] C. Bervillier. Wilson-Polchinski exact renormalization group equation for O(N) systems: Leading and next-to-leading orders in the derivative expansion. *J. Phys. Condens. Matter*, 17(20):S1929, may 2005.

[12] Ivan Balog, Hugues Chaté, Bertrand Delamotte, Maroje Marohnic, Nicolás Wschebor, Maroje Marohnić, and Nicolás Wschebor. Convergence of Nonperturbative Approximations to the Renormalization Group. *Phys. Rev. Lett.*, 123(24):240604, dec 2019.

[13] Léonie Canet, Bertrand Delamotte, Dominique Mouhanna, and Julien Vidal. Optimization of the derivative expansion in the nonperturbative renormalization group. *Physical Review D - Particles, Fields, Gravitation and Cosmology*, 67(6):065004, mar 2003.

[14] Sheer El-Showk, Miguel F. Paulos, David Poland, Slava Rychkov, David Simmons-Duffin, and Alessandro Vichi. Solving the 3D Ising model with the conformal bootstrap. *Physical Review D - Particles, Fields, Gravitation and Cosmology*, 86(2):025022, jul 2012.

[15] A. Lipa, A. Nissen, A. Stricker, R. Swanson, and P. Chui. Specific heat of liquid helium in zero gravity very near the lambda point. *Physical Review B - Condensed Matter and Materials Physics*, 68(17):174518, nov 2003.

[16] Massimo Campostrini, Martin Hasenbusch, Andrea Pelissetto, Paolo Rossi, and Ettore Vicari. Critical behavior of the three-dimensional XY universality class. *Physical Review B - Condensed Matter and Materials Physics*, 63(21):214503, may 2001.

[17] Filip Kos, David Poland, David Simmons-Duffin, and Alessandro Vichi. Bootstrapping the O(N) Archipelago. *JHEP*, 11(11):106, nov 2015.

[18] Gonzalo De Polsi, Ivan Balog, Matthieu Tissier, and Nicolás Wschebor. Precision calculation of critical exponents in the $O(N)$ universality classes with the nonperturbative renormalization group. jan 2020.

[19] Shai M. Chester, Walter Landry, Junyu Liu, David Poland, David Simmons-Duffin, Ning Su, and Alessandro Vichi. Carving out OPE space and precise $O(2)$ model critical exponents. dec 2019.

[20] Martin Hasenbusch. Monte Carlo study of an improved clock model in three dimensions. *Physical Review B*, 100(22):224517, dec 2019.

[21] T. Machado and N. Dupuis. From local to critical fluctuations in lattice models: A nonperturbative renormalization-group approach. *Physical Review E - Statistical, Nonlinear, and Soft Matter Physics*, E82(4):41128, oct 2010.

[22] Igor Boettcher, Jan M. Pawlowski, and Christof Wetterich. Critical temperature and superfluid gap of the unitary Fermi gas from functional renormalization. *Physical Review A*, 89(5):053630, may 2014.

[23] Léonie Leonie Canet, Hugues Chaté, Bertrand Delamotte, Hugues Chate, and Bertrand Delamotte. Quantitative phase diagrams of branching and annihilating random walks. *Physical Review Letters*, 92(25 I):255703, jun 2004.

[24] Léonie Leonie Canet, Bertrand Delamotte, Olivier Deloubriere, Nicolas Wschebor, Olivier Deloubrière, and Nicolas Wschebor. Nonperturbative renormalization-group study of reaction-diffusion processes. *Physical Review Letters*, 92(19):195703, may 2004.

[25] N. Dupuis and A. Rançon. Infrared behavior of interacting bosons at zero temperature. *Laser Physics*, 21(8):1470–1479, aug 2011.

[26] Wei-jie Fu, Jan M. Pawlowski, and Fabian Rennecke. The QCD phase structure at finite temperature and density. sep 2019.

[27] Bertrand Delamotte, Matthieu Tissier, and Nicolás Wschebor. Scale invariance implies conformal invariance for the three-dimensional Ising model. *Physical Review E*, 93(1):012144, jan 2016.

[28] Gonzalo De Polsi, Matthieu Tissier, and Nicolás Wschebor. Conformal Invariance and Vector Operators in the O(N) Model. *Journal of Statistical Physics*, 177(6):1089–1130, dec 2019.

[29] Gonzalo De Polsi, Ivan Balog, Nicolás Wschebor, and Matthieu Tissier. In preparation. 2020.

[30] Daniel Bernoulli. Hydrodynamica, sive de viribus et motibus fluidorum commentarii. *Opus academicum ab auctore, dum Petropoli ageret, congestum*, 1738.

[31] R. K. Pathria. *Statistical Mechanics*. Butterworth-Heinemann, 2nd edition, sep 1996.

[32] Ludwig Boltzmann. *Vorlesungen über Gastheorie: Th. Theorie van der Waals'; Gase mit zusammengesetzten Molekülen; Gasdissociation; Schlussbemerkungen*, volume 2. JA Barth, 1898.

[33] Lev Davidovich Landau and Evgenii Mikhailovich Lifshitz. *Statistical physics*, volume 5. Pergamon, 1958.

[34] Richard Chace Tolman. *The principles of statistical mechanics.* Courier Corporation, 1979.

[35] C. N. Yang and T. D. Lee. Statistical theory of equations of state and phase transitions. I. Theory of condensation. *Physical Review*, 87(3):404–409, aug 1952.

[36] T. D. Lee and C. N. Yang. Statistical theory of equations of state and phase transitions. II. Lattice gas and ising model. *Physical Review*, 87(3):410–419, aug 1952.

[37] J. D. van der Waals. *Over de continuiteit van den gas- en vloeistoftoest.* PhD thesis, 1873.

[38] J. Clerk-Maxwell. On the dynamical evidence of the molecular constitution of bodies. *Nature*, 11(279):357–359, 1875.

[39] W Lenz, Wilhelm Lenz, and W Lenz. Beitrag zum Verständnis der magnetischen Erscheinungen in festen Körpern. *Zeitschrift für Physik*, 21:613–615, 1920.

[40] Ernst Ising. Beitrag zur Theorie des Ferromagnetismus. *Zeitschrift für Physik*, 31(1):253–258, feb 1925.

[41] V L Ginzburg. Some Remarks on Phase Transitions of the Second Kind and the Microscopic theory of Ferroelectric Materials. *Soviet Phys. Solid State*, 2:1824–1834, 1961.

[42] A. K Krönig. *Grundzüge einer theorie der gase.* 1856.

[43] R. Clausius. XI. On the nature of the motion which we call heat . *The London, Edinburgh, and Dublin Philosophical Magazine and Journal of Science*, 14(91):108–127, aug 1857.

[44] J. Clerk Maxwell. XXII. On the dynamical theory of gases . *The London, Edinburgh, and Dublin Philosophical Magazine and Journal of Science*, 35(236):185–217, mar 1868.

[45] Pierre Weiss. L'hypothèse du champ moléculaire et la propriété ferro-magnétique. *Journal de Physique Théorique et Appliquée*, 6(1):661–690, 1907.

[46] L. Landau. The theory of phase transitions. *Nature*, 138(3498):840–841, nov 1936.

[47] Leo P. Kadanoff. More is the same; phase transitions and mean field theories. *Journal of Statistical Physics*, 137(5):777–797, dec 2009.

[48] Curtis G. Callan. Broken scale invariance in scalar field theory. *Physical Review D*, 2(8):1541–1547, oct 1970.

[49] K. Symanzik. Small distance behaviour in field theory and power counting. *Communications in Mathematical Physics*, 18(3):227–246, sep 1970.

[50] E. Stückelberg and A. Petermann. La normalisation des constantes dans la theorie des quanta. *Helv. Phys. Acta*, 26:499–520, may 1953.

[51] M. Gell-Mann and F. E. Low. Quantum electrodynamics at small distances. *Physical Review*, 95(5):1300–1312, sep 1954.

[52] Leo P. Kadanoff. Scaling laws for ising models near T_c. *Physics Physique Fizika*, 2(6):263–272, jun 1966.

[53] K. G. Wilson. Nobel Lecture: The Renormalization Group and Critical Phenomena. dec 1982.

[54] A B Zamolodchikov. "Irreversibility" of the flux of the renormalization group in a 2D field theory. *JETP Lett.*, 43(12):565–567, jun 1986.

[55] John L. Cardy. Is there a c-theorem in four dimensions? *Physics Letters B*, 215(4):749–752, dec 1988.

[56] Jean François Francois Fortin, Benjamín Grinstein, and Andreas Stergiou. Scale without conformal invariance: An example. *Physics Letters, Section B: Nuclear, Elementary Particle and High-Energy Physics*, 2012(7):1–19, jul 2011.

[57] I. Jack and H. Osborn. Analogs of the c-theorem for four-dimensional renormalisable field theories. *Nuclear Physics, Section B*, 343(3):647–688, oct 1990.

[58] F. Léonard and B. Delamotte. Critical Exponents Can Be Different on the Two Sides of a Transition: A Generic Mechanism. *Physical Review Letters*, 115(20):200601, nov 2015.

[59] Joseph Polchinski. Renormalization and effective lagrangians. *Nuclear Physics, Section B*, 231(2):269–295, jan 1984.

[60] Leonie Léonie Canet, Bertrand Delamotte, Dominique Mouhanna, and Julien Vidal. Nonperturbative renormalization group approach to the Ising model: A Derivative expansion at order partial**4. *Physical Review B - Condensed Matter and Materials Physics*, 68(6):64421, aug 2003.

[61] K.-I. Ken-Ichi Aoki, Keiichi Morikawa, Wataru Souma, Jun-Ichi J.-I. Sumi, and Haruhiko Terao. The Effectiveness of the Local Potential Approximation in the Wegner-Houghton Renormalization Group. *Progress of Theoretical Physics*, 95(2):409–420, feb 1996.

[62] Jean Paul Blaizot, Ramón Méndez-Galain, and Nicolás Wschebor. A new method to solve the non-perturbative renormalization group equations. *Physics Letters, Section B: Nuclear, Elementary Particle and High-Energy Physics*, 632(4):571–578, jan 2006.

[63] F. Benitez, J. P. Blaizot, H. Chaté, B. Delamotte, R. Méndez-Galain, and N. Wschebor. Nonperturbative renormalization group preserving full-momentum dependence: Implementation and quantitative evaluation. *Physical Review E - Statistical, Nonlinear, and Soft Matter Physics*, E85(2):26707, feb 2012.

[64] Hagen Kleinert and Verena Schulte-Frohlinde. *Critical Properties of ϕ^4-Theories*. World Scientific, dec 2001.

[65] Moshe Moshe and Jean Zinn-Justin. Quantum field theory in the large N limit: A review. 385(3-6):69–228, oct 2003.

[66] Andrea Pelissetto and Ettore Vicari. Critical phenomena and renormalization-group theory. 368(6):549–727, oct 2002.

[67] P. A. M. Dirac. On the Theory of Quantum Mechanics. *Proceedings of the Royal Society of London. Series A, Containing Papers of a Mathematical and Physical Character*, 112(762):661–677, oct 1926.

[68] W. Heisenberg. Mehrkörperproblem und Resonanz in der Quantenmechanik. *Zeitschrift für Physik*, 38(6-7):411–426, jun 1926.

[69] Andreas Schmitt. *Introduction to superfluidity: Field-theoretical approach and applications*, volume 888. Springer Verlag, jan 2015.

[70] L. Landau. Theory of the superfluidity of helium II. *Physical Review*, 60(4):356–358, aug 1941.

[71] P J Flory. *In Principles of polymer chemistry*. Cornell University Press, 1953.

[72] P. G. de Gennes. Exponents for the excluded volume problem as derived by the Wilson method. *Phys. Lett.*, A38(5):339–340, feb 1972.

[73] Filip Kos, David Poland, and David Simmons-Duffin. Bootstrapping Mixed Correlators in the 3D Ising Model. *JHEP*, 11(11):109, nov 2014.

[74] David Simmons-Duffin. The Lightcone Bootstrap and the Spectrum of the 3d Ising CFT. *JHEP*, 03(3):86, mar 2017.

[75] Martin Hasenbusch. Finite size scaling study of lattice models in the three-dimensional Ising universality class. *Phys. Rev. B*, 82(17):174433, nov 2010.

[76] Massimo Campostrini, Andrea Pelissetto, Paolo Rossi, and Ettore Vicari. 25th order high temperature expansion results for three-dimensional Ising like systems on the simple cubic lattice. *Phys. Rev.*, E65(6):66127, jun 2002.

[77] Riccardo Guida and Jean Zinn-Justin. Critical exponents of the N vector model. *J. Phys.*, A31(40):8103–8121, oct 1998.

[78] Mikhail V. Kompaniets and Erik Panzer. Minimally subtracted six loop renormalization of O(n)-symmetric ϕ^4 theory and critical exponents. *Phys. Rev.*, D96(3):36016, aug 2017.

[79] Filip Kos, David Poland, David Simmons-Duffin, and Alessandro Vichi. Precision islands in the Ising and O(N) models. *Journal of High Energy Physics*, 2016(8):1–16, aug 2016.

[80] Alejandro Castedo Echeverri, Benedict von Harling, and Marco Serone. The effective bootstrap. *Journal of High Energy Physics*, 2016(9):97, sep 2016.

[81] Massimo Campostrini, Martin Hasenbusch, Andrea Pelissetto, and Ettore Vicari. Theoretical estimates of the critical exponents of the superfluid transition in He4 by lattice methods. *Physical Review B*, 74(14), oct 2006.

[82] Alan Singasaas and Guenter Ahlers. Universality of static properties near the superfluid transition ^4He. *Phys. Rev. B*, 30(9):5103–5115, nov 1984.

[83] A. Oleaga, A. Salazar, and Yu M. Bunkov. 3D-XY critical behavior of $CsMnF_3$ from static and dynamic thermal properties. *Journal of Physics: Condensed Matter*, 26(9):96001, feb 2014.

[84] A Oleaga, A Salazar, D Prabhakaran, J.-G. Cheng, and J.-S. Zhou. Critical behavior of the paramagnetic to antiferromagnetic transition in orthorhombic and hexagonal phases of RMnO$_3$ ($R = Sm$, Tb, Dy, Ho, Er, Tm, Yb, Lu, Y). *Phys. Rev. B*, 85(18):184425, may 2012.

[85] R. Reisser, R. K. Kremer, and A. Simon. 3d-XY critical behavior of the layered metal-rich halides Gd_2IFe_2, Gd_2ICo_2 and Gd_2BrFe_2. *Physica B: Physics of Condensed Matter*, 204(1):265–273, jan 1995.

[86] Martin Hasenbusch and Ettore Vicari. Anisotropic perturbations in three-dimensional $O(N)$-symmetric vector models. *Phys. Rev. B*, 84(12):125136, sep 2011.

[87] Martin Hasenbusch. Eliminating leading corrections to scaling in the three-dimensional $O(N)$-symmetric φ^4 model: $N = 3$ and 4. *Journal of Physics A: Mathematical and General*, 34(40):8221–8236, oct 2001.

[88] Massimo Campostrini, Martin Hasenbusch, Andrea Pelissetto, Paolo Rossi, and Ettore Vicari. Critical exponents and equation of state of the three-dimensional Heisenberg universality class. *Physical Review B - Condensed Matter and Materials Physics*, 65(14):1–21, apr 2002.

[89] R. Reisser, R. K. Kremer, and A. Simon. Magnetic phase transition in the metal-rich rare-earth carbide halides Gd_2XC (X= Br,I). *Phys. Rev. B*, 52(5):3546–3554, aug 1995.

[90] Lei Zhang, Jiyu Fan, Li Li, Renwen Li, Langsheng Ling, Zhe Qu, Wei Tong, Shun Tan, and Yuheng Zhang. Critical properties of the 3D-Heisenberg ferromagnet $CdCr_2Se_4$. *EPL*, 91(5):57001, sep 2010.

[91] Youjin Deng. Bulk and surface phase transitions in the three-dimensional $O(4)$ spin model. *Phys. Rev. E*, 73(5):56116, may 2006.

[92] Xiao Hu. Bicritical and Tetracritical Phenomena and Scaling Properties of the SO(5) Theory. *Physical Review Letters*, 87(5), jul 2001.

[93] Yutaka Okabe and Michiyoshi Oku. $1/n$ Expansion up to Order $1/n^2$. III: Critical Exponents γ and ν for $d = 3$. *Progress of Theoretical Physics*, 60(5):1287–1297, nov 1978.

[94] Aleksandr Nikolaevich Vasil'ev, Yu M. Pis'mak, Yu R. Khonkonen, Yury Mikhailivich Pis' mak, and Yu R. Khonkonen. $1/n$ Expansion: Calculation of the exponents η and ν in the order $1/n^2$ for arbitrary number of dimensions. *Teoreticheskaya i Matematicheskaya Fizika*, 47(3):291–306, jun 1981.

[95] David J. Broadhurst, J. A. Gracey, and D. Kreimer. Beyond the triangle and uniqueness relations: Nonzeta counterterms at large N from positive knots. *Z. Phys.*, C75(3):559–574, mar 1997.

[96] S A Antonenko and A I Sokolov. Critical exponents for a three-dimensional O(n)-symmetric model withn>3. *Physical Review E*, 51(3):1894–1898, mar 1995.

[97] Kay Jörg Joerg Wiese and Andrei A. Fedorenko. Field Theories for Loop-Erased Random Walks. *Nucl. Phys.*, B946:114696, sep 2019.

[98] Kay Jörg Joerg Wiese and Andrei A. Fedorenko. Depinning transition of charge-density waves: mapping onto $O(n)$ symmetric ϕ^4 theory with $n \to -2$ and loop-erased random walks. *Phys. Rev. Lett.*, 123(19):197601, nov 2019.

[99] Hirohiko Shimada and Shinobu Hikami. Fractal dimensions of self-avoiding walks and Ising high-temperature graphs in 3D conformal bootstrap. *J. Statist. Phys.*, 165(6):1006, dec 2016.

[100] Nathan Clisby and Burkhard Dünweg. High-precision estimate of the hydrodynamic radius for self-avoiding walks. *Phys. Rev. E*, 94(5):52102, nov 2016.

[101] Nathan Clisby. Scale-free Monte Carlo method for calculating the critical exponent$\gamma$of self-avoiding walks. *Journal of Physics A: Mathematical and Theoretical*, 50(26):264003, jun 2017.

[102] Raoul D. Schram, Gerard T. Barkema, Rob H. Bisseling, and Nathan Clisby. Exact enumeration of self-avoiding walks on BCC and FCC lattices. *Journal of Statistical Mechanics: Theory and Experiment*, 2017(8):83208, aug 2017.

[103] J.P. Cotton. Polymer excluded volume exponent ν : An experimental verification of the n vector model for $n = 0$. *J. Physique Lett.*, 41(9):231–234, may 1980.

[104] Jean Zinn-Justin. *Quantum field theory and critical phenomena*, volume 113. Oxford University Press, 4th edition, jan 2002.

[105] A. A. Migdal. Conformal invariance and bootstrap. *Physics Letters B*, 37(4):386–388, dec 1971.

[106] S. Ferrara, A. F. Grillo, and R. Gatto. Tensor representations of conformal algebra and conformally covariant operator product expansion. *Annals of Physics*, 76(1):161–188, mar 1973.

[107] A. Polyakov. Non-Hamiltonian approach to conformal quantum field theory. *Soviet Journal of Experimental and Theoretical Physics*, jul 1974.

[108] A. A. Belavin, A. M. Polyakov, and A. B. Zamolodchikov. Infinite conformal symmetry in two-dimensional quantum field theory. *Nuclear Physics, Section B*, 241(2):333–380, jul 1984.

[109] Sheer El-Showk, Miguel F. Paulos, David Poland, Slava Rychkov, David Simmons-Duffin, and Alessandro Vichi. Solving the 3d ising model with the conformal bootstrap II. c-Minimization and precise critical exponents. *Journal of Statistical Physics*, 157(4-5):869–914, oct 2014.

[110] Joseph Polchinski. Scale and conformal invariance in quantum field theory. *Nuclear Physics, Section B*, 303(2):226–236, jun 1988.

[111] Tim R. Morris. The Renormalization group and two-dimensional multicritical effective scalar field theory. *Phys. Lett.*, B345(2):139–148, feb 1995.

[112] Tim R. Morris. On truncations of the exact renormalization group. *Physics Letters B*, 334(3-4):355–362, aug 1994.

[113] Philippe Di Francesco, Pierre Mathieu, David Sénéchal, and D Senechal. *Conformal Field Theory*. Graduate Texts in Contemporary Physics. Springer Science & Business Media, New York, 2012.

[114] Daniel Friedan, Zongan Qiu, and Stephen Shenker. Conformal invariance, unitarity, and critical exponents in two dimensions. *Physical Review Letters*, 52(18):1575–1578, apr 1984.

[115] V. Riva and J. Cardy. Scale and conformal invariance in field theory: A physical counterexample. *Physics Letters, Section B: Nuclear, Elementary Particle and High-Energy Physics*, 622(3-4):339–342, sep 2005.

[116] Markus A. Luty, Joseph Polchinski, and Riccardo Rattazzi. The a-theorem and the asymptotics of 4D quantum field theory. *Journal of High Energy Physics*, 2013(1):1–35, jan 2013.

[117] Anatoly Dymarsky, Zohar Komargodski, Adam Schwimmer, and Stefan Theisen. On scale and conformal invariance in four dimensions. *Journal of High Energy Physics*, 2015(10):1–24, oct 2015.

[118] Anatoly Dymarsky and Alexander Zhiboedov. Scale-invariant breaking of conformal symmetry. *Journal of Physics A: Mathematical and Theoretical*, 48(41):41FT01, sep 2015.

[119] Anatoly Dymarsky, Kara Farnsworth, Zohar Komargodski, Markus A. Luty, and Valentina Prilepina. Scale invariance, conformality, and generalized free fields. *Journal of High Energy Physics*, 2016(2):1–16, feb 2016.

[120] Abel Weinrib and B. I. Halperin. Critical phenomena in systems with long-range-correlated quenched disorder. *Physical Review B*, 27(1):413–427, jan 1983.

[121] Oliver J. Rosten. On functional representations of the conformal algebra. *European Physical Journal C*, 2017.

[122] Kevin Falls and Tim R. Morris. Conformal anomaly from gauge fields without gauge fixing. *Physical Review D*, 97(6):065013, mar 2018.

[123] Oliver J. Rosten. A Wilsonian energy-momentum tensor. *European Physical Journal C*, 78(4):1–18, apr 2018.

[124] Oliver J. Rosten. A conformal fixed-point equation for the effective average action. *International Journal of Modern Physics A*, 2019.

[125] Tim R. Morris and Roberto Percacci. Trace anomaly and infrared cutoffs. *Physical Review D*, 99(10):105007, may 2019.

[126] M. Billó, M. Caselle, D. Gaiotto, F. Gliozzi, M. Meineri, and R. Pellegrini. Line defects in the 3d Ising model. *Journal of High Energy Physics*, 2013(7):1–23, jul 2013.

[127] Catarina Cosme, J. M.Viana Parente Lopes, and João Penedones. Conformal symmetry of the critical 3D Ising model inside a sphere. *Journal of High Energy Physics*, 2015(8):1–15, aug 2015.

[128] Simão Meneses, João Penedones, Slava Rychkov, J. M. Viana Parente Lopes, and Pierre Yvernay. A structural test for the conformal invariance of the critical 3d Ising model. *Journal of High Energy Physics*, 2019(4):1–27, apr 2019.

[129] Miguel F. Paulos, Slava Rychkov, Balt C. van Rees, and Bernardo Zan. Conformal invariance in the long-range Ising model. *Nuclear Physics B*, 902:246–291, jan 2016.

[130] J. Bricmont. The Gaussian inequality for multicomponent rotators. *Journal of Statistical Physics*, 17(5):289–300, nov 1977.

[131] François Dunlop. Zeros of the partition function and Gaussian inequalities for the plane rotator model. *Journal of Statistical Physics*, 21(5):561–572, nov 1979.

[132] François Dunlop. Correlation inequalities for multicomponent rotators. *Communications in Mathematical Physics*, 49(3):247–256, oct 1976.

[133] James L. Monroe and Paul A. Pearce. Correlation inequalities for vector spin models. *Journal of Statistical Physics*, 21(6):615–633, dec 1979.

[134] H. Kunz, Ch Ed Pfister, and P. A. Vuillermot. Correlation inequalities for some classical spin vector models. *Physics Letters A*, 54(6):428–430, oct 1975.

[135] Alan D. Sokal. Mean-field bounds and correlation inequalities. *Journal of Statistical Physics*, 28(3):431–439, jul 1982.

[136] F. J. Wegner. Some invariance properties of the renormalization group. *Journal of Physics C: Solid State Physics*, 7(12):2098–2108, 1974.

[137] Shunsuke Yabunaka and Bertrand Delamotte. Why Might the Standard Large N Analysis Fail in the $O(N)$ Model: The Role of Cusps in Fixed Point Potentials. *Physical Review Letters*, 121(23):231601, dec 2018.

[138] Yu Nakayama. Conformal Contact Terms and Semi-Local Terms. jun 2019.

[139] K. Pohlmeyer. The Jost-Schroer theorem for zero-mass fields. *Communications in Mathematical Physics*, 12(3):204–211, sep 1969.

[140] Robert B. Griffiths. Correlations in Ising ferromagnets. I. *Journal of Mathematical Physics*, 8(3):478–483, mar 1967.

[141] Robert B. Griffiths. Correlations in Ising ferromagnets. II. External magnetic fields. *Journal of Mathematical Physics*, 8(3):484–489, mar 1967.

[142] Robert B. Griffiths. Correlations in Ising ferromagnets. III - A mean-field bound for binary correlations. *Communications in Mathematical Physics*, 6(2):121–127, jun 1967.

[143] Alan D. Sokal. More inequalities for critical exponents. *Journal of Statistical Physics*, 25(1):25–50, may 1981.

[144] S. Krinsky and V. J. Emery. Upper bound on correlation functions of Ising ferromagnet. *Physics Letters A*, 50(3):235–236, dec 1974.

[145] Robert B. Griffiths. Rigorous results for ising ferromagnets of arbitrary spin. *Journal of Mathematical Physics*, 10(9):1559–1565, sep 1969.

[146] J. Ginibre. General formulation of Griffiths' inequalities. *Communications in Mathematical Physics*, 16(4):310–328, dec 1970.

[147] Joel L. Lebowitz. GHS and other inequalities. *Communications in Mathematical Physics*, 35(2):87–92, jun 1974.

[148] Bertrand Delamotte, Matthieu Tissier, and Nicolás Wschebor. Comment on "A structural test for the conformal invariance of the critical 3d Ising model" by S. Meneses, S. Rychkov, J. M. Viana Parente Lopes and P. Yvernay. arXiv:1802.02319. feb 2018.

[149] H. Kleinert and V. Schulte-Frohlinde. Exact five-loop renormalization group functions of θ^4-theory with $O(N)$-symmetric and cubic interactions. Critical exponents up to ϵ^5. *Physics Letters B*, 342(1-4):284–296, jan 1995.

List of Tables

174

176

List of Figures

APPENDICES

Appendix A

Details and Properties of the Non-Perturbative Renormalization Group

A.0.1 Evolution Equation for $W_k[B]$

To deduce Eq.(2.34) consider the partition function in presence of the regulator and a source B for the field ϕ, Eq.(2.33),

$$e^{W_k[B]} = \int \mathcal{D}\phi e^{-\hat{H}[\mathbf{J},\phi]-\Delta H_k[\phi]+\int_x B(x)\phi(x)}$$

Appying a time derivative, $\partial_t = k\partial_k$, at fixed source B yields

$$\partial_t(W_k[B])_B e^{W_k[B]} = -\frac{1}{2}\int_{x,y}\partial_t R_k(|x-y|)\int \mathcal{D}\phi\,\phi(x)\phi(y)e^{-\hat{H}[\mathbf{J},\phi]-\Delta H_k[\phi]+\int_x B(x)\phi(x)}$$

$$= -\frac{1}{2}\int_{x,y}\partial_t R_k(|x-y|)\frac{\delta^2\left(e^{W_k[B]}\right)}{\delta B(x)\delta B(y)}$$

$$= -\frac{1}{2}\int_{x,y}\partial_t R_k(|x-y|)\left(\frac{\delta^2 W_k[B]}{\delta B(x)\delta B(y)}+\frac{\delta W_k[B]}{\delta B(x)}\frac{\delta W_k[B]}{\delta B(y)}\right)e^{W_k[B]}$$

And therefore one arrives at the evolution equation for the Helmholtz free energy, Eq.(2.34):

$$\partial_t W_k[B] = -\frac{1}{2}\int_{x,y}\partial_t R_k(|x-y|)\left(\frac{\delta^2 W_k[B]}{\delta B(x)\delta B(y)}+\frac{\delta W_k[B]}{\delta B(x)}\frac{\delta W_k[B]}{\delta B(y)}\right).$$

A.0.2 Evolution Equation for $\Gamma_k[\varphi]$

Consider the definition of the effective action Eq.(2.35),

$$\Gamma_k[\varphi] + \Delta H_k[\varphi] = -W_k[B] + \int_x B(x)\varphi(x).$$

Using that

$$\partial_t(\cdot)_\varphi = \partial_t(\cdot)_B - \int_x \partial_t(\varphi(x))_B \left(\frac{\delta(\cdot)}{\delta\varphi(x)}\right)_B,$$

and

$$\left(\frac{\delta\Gamma_k[\varphi]}{\delta\varphi(x)}\right)_B = B(x) - \int_y R_k(x,y)\varphi(y)$$

allows to write:

$$\partial_t(\Gamma_k[\varphi])_\varphi = \partial_t(\Gamma_k[\varphi])_B - \int_x \partial_t(\varphi(x))_B \left(B(x) - R_k(x,y)\varphi(y) \right). \qquad \text{(A.1)}$$

But using Eq.(2.35) and Eq.(2.34) we can express $\partial_t(\Gamma_k[\varphi])_B$ as:

$$\begin{aligned}
\partial_t(\Gamma_k[\varphi])_B = {} & \frac{1}{2}\int_{x,y} \partial_t R_k(|x-y|)\left(\frac{\delta^2 W_k[B]}{\delta B(x)\delta B(y)} + \frac{\delta W_k[B]}{\delta B(x)}\frac{\delta W_k[B]}{\delta B(y)}\right) \\
& + \int_x \partial_t(\varphi(x))_B B(x) - \int_x \partial_t(\varphi(x))_B R_k(x,y)\varphi(y) \\
& - \frac{1}{2}\int_{x,y}\varphi(x)\partial_t R_k(x,y)\varphi(y). \qquad \text{(A.2)}
\end{aligned}$$

It is possible to identify the terms in Eq.(2.34) as $\frac{\delta^2 W_k[B]}{\delta B(x)\delta B(y)} = \frac{\delta\varphi(x)}{\delta B(y)}$ and $\frac{\delta W_k[B]}{\delta B(x)}\frac{\delta W_k[B]}{\delta B(y)} = \varphi(x)\varphi(y)$, so using Eq.(A.2) in Eq.(A.1), one obtains:

$$\partial_t(\Gamma_k[\varphi])_\varphi = \frac{1}{2}\int_{x,y}\partial_t R_k(x,y)\frac{\delta\varphi(x)}{\delta B(y)}$$

The remaining step is to identify what is $\frac{\delta\varphi(x)}{\delta B(y)}$ in terms of the effective action. This is done in the following manner:

$$\delta(x-y) = \frac{\delta\varphi(x)}{\delta\varphi(y)} = \frac{\delta}{\delta\varphi(y)}\frac{\delta W_k[B]}{\delta B(x)} = \int_z \frac{\delta^2 W_k[B]}{\delta B(x)\delta B(z)}\frac{\delta B(z)}{\delta\varphi(y)}$$

but from Eq.(2.35) it is straightforward to see that

$$\frac{\delta B(z)}{\delta\varphi(y)} = \frac{\delta^2\Gamma_k[\varphi]}{\delta\varphi(x)\varphi(y)} + R_k(x,y) \qquad \text{(A.3)}$$

This will imply that the flow of this generalized effective action is given by

Wetterich's equation:

$$\partial_t \Gamma_k[\varphi] = \frac{1}{2} \int_{x,y} \partial_t R_k(|x-y|) G_k[x,y;\varphi]$$

where $G_k(x,y)$ is the full propagator which satisfies

$$\int_z G_k[x,z;\varphi] \left(\frac{\delta^2 \Gamma_k}{\delta\varphi(z)\delta\varphi(y)} + R_k(z,y) \right) = \delta(x-y).$$

This expression can be written in Fourier variables as,

$$
\begin{aligned}
\partial_t \Gamma_k[\varphi] &= \frac{1}{2} \int_{x,y,q,q',Q} \partial_t R_k(Q) G_k[q,q';\varphi] e^{i(q \cdot x + q' \cdot y + Q \cdot (x-y))} \\
&= \frac{1}{2} \int_{q,q',Q} \partial_t R_k(Q) G_k[q,q';\varphi] (2\pi)^{2D} \delta(Q-q')\delta(Q+q') \\
&= \frac{1}{2} \int_Q \partial_t R_k(Q) G_k[Q;\varphi]
\end{aligned}
$$

where $G_k[Q;\varphi] \equiv G_k[Q,-Q;\varphi]$.

Appendix B

Conformal Group

It so happens that systems exhibiting a scale invariant behaviour, in general, also present conformal invariance (transformation that preserve angles). It is therefore more restrictive that just isometries plus scale invariance. Consider an infinitesimal transformations of the coordinates that only rescale the metric tensor locally,

$$g_{\mu\nu} \to g'_{\mu\nu} = \Lambda(x) g_{\mu\nu}. \tag{B.1}$$

These type of transformations leads to the standard translation and rotation (which do not yield a rescaling of the metric), and dilations which rescale the metric by a constant factor. But also, include another independent kind of transformations, called *special conformal transformation*, which consists in local dilations (rescale the metric differently depending on the position). This appendix present a general approach to conformal transformations, see for example [113].

Consider an infinitesimal change of variable of the form:

$$x^\mu \to x'^\mu = x^\mu + \varepsilon^\mu(x) \tag{B.2}$$

This change of variable would imply a change in the metric of the form:

$$\eta_{\mu\nu} \to \eta'_{\mu\nu} = \eta_{\rho\sigma} \frac{\partial x'_\rho}{\partial x_\mu} \frac{\partial x'_\sigma}{\partial x_\nu} = \eta_{\mu\nu} + \left(\frac{\partial \varepsilon_\mu}{\partial x_\nu} + \frac{\partial \varepsilon_\nu}{\partial x_\mu} \right) + \mathcal{O}(\epsilon_\mu \epsilon_\nu) \tag{B.3}$$

As stated previously, a conformal transformation preserves angles and the change in the metric implies that the transformation considered in Eq.(B.2) satisfies

$$\frac{\partial \varepsilon_\mu}{\partial x_\nu} + \frac{\partial \varepsilon_\nu}{\partial x_\mu} = h(x) \eta_{\mu\nu}, \tag{B.4}$$

which contracted with $\eta_{\mu\nu}$ yields

$$\partial_\mu \varepsilon_\mu(x) = \frac{d}{2} h(x). \tag{B.5}$$

Taking an extra derivative ∂_ρ in Eq.(B.4) yields the following relation:

$$\partial_\rho \partial_\nu \varepsilon_\mu + \partial_\rho \partial_\mu \varepsilon_\nu = \partial_\rho h(x) \eta_{\mu\nu}. \tag{B.6}$$

Considering the combination $(\text{Eq.}(\text{B.6})_{\mu\leftrightarrow\rho})$ + $(\text{Eq.}(\text{B.6})_{\nu\leftrightarrow\rho})$ − $(\text{Eq.}(\text{B.6}))$ yields:

$$2\partial_\nu \partial_\mu \varepsilon_\rho = \partial_\nu h(x) \eta_{\mu\rho} + \partial_\mu h(x) \eta_{\rho\nu} - \partial_\rho h(x) \eta_{\mu\nu} \tag{B.7}$$

which contracted with $\eta_{\mu\nu}$ and combined with Eq.(B.5) turns into

$$\partial_\rho \partial_\rho \varepsilon_\mu = \left(\frac{2}{d} - 1\right) \partial_\mu \partial_\rho \varepsilon_\rho. \tag{B.8}$$

Taking the divergence of Eq.(B.8) implies

$$(d-1)\partial_\rho \partial_\rho h(x) = 0. \tag{B.9}$$

Applying $\partial_\rho \partial_\rho$ to Eq.(B.4) and ∂_ν to Eq.(B.8) one concludes that:

$$(2-d)\partial_\mu \partial_\nu h(x) = \eta_{\mu\nu} \partial_\rho \partial_\rho h(x) \tag{B.10}$$

Combining Eq.(B.9) and Eq.(B.10) means that $h(x)$ or, equivalenty, $\partial_\nu \varepsilon_\nu$ is linear in x_μ at most.[1] So far, the constrain for a general conformal transformation if $d > 2$ takes the form of Eq.(B.11). The case $d = 2$ is to be studied separately and is out of the scope of this thesis. However, throughout the text some comments about the special case of $d = 2$ will be made. This in fact means that ε_μ is quadratic and can be written as:

$$\varepsilon_\mu(x) = a_\mu + b_{\mu\nu} x_\nu + c_{\mu\nu\rho} x_\nu x_\rho, \tag{B.11}$$

with $c_{\mu\nu\rho} = c_{\mu\rho\nu}$.

The constrains discussed so far restrict the form of conformal transformations even more. Since Eq.(B.11) holds for all x's, each power can be treated on its own.

There is no extra restriction to the x independent term. This is of course

---

[1]The term $\partial_\nu \varepsilon_\nu$ is at most linear in x_μ if $d \neq 1$ and $d \neq 2$.

the usual *translation* transformation $\varepsilon_\mu^{(T)}$:

$$\varepsilon_\mu^{(T)} = a_\mu \tag{B.12}$$

The linear term when introduced in Eq.(B.4) yields

$$b_{\mu\nu} + b_{\nu\mu} = \frac{2}{d} b_{\rho\rho} \eta_{\mu\nu}. \tag{B.13}$$

The antisymmetric part, labeled by $-2m_{\mu\nu}$, constitutes the usual *rotation* transformation $\varepsilon_\mu^{(R)} = -2m_{\mu\nu}x_\nu$. On the other hand, Eq.(B.13) implies that the symmetric part of $b_{\mu\nu}$ is equal to $\lambda\eta_{\mu\nu}$ (with $\lambda = b_{\rho\rho}/d$) which gives rise to the *dilation* transformation $\varepsilon_\mu^{(D)}$. In summary, it is

$$\varepsilon_\mu^{(R)} = -2m_{\mu\nu}x_\nu \tag{B.14}$$

and

$$\varepsilon_\mu^{(D)} = \lambda x_\mu. \tag{B.15}$$

The quadratic part will give rise to what is called the *special conformal* transformation $\varepsilon_\mu^{(SC)}$. Pluggin in the quadratic term in Eq.(B.7) restricts $c_{\mu\nu\rho}$ to be of the form:

$$c_{\mu\nu\rho} = \frac{1}{d}\left(\eta_{\mu\nu}c_{\sigma\sigma\rho} + \eta_{\mu\rho}c_{\sigma\sigma\nu} - \eta_{\nu\rho}c_{\sigma\sigma\mu}\right). \tag{B.16}$$

Defining $c_\mu = -c_{\sigma\sigma\mu}/d$, which is just a convention taken here, the expression for the quadratic term can easily be worked out to yield

$$\varepsilon_\mu^{(SC)} = (x_\nu x_\nu)c_\mu - 2(x_\nu c_\nu)x_\mu. \tag{B.17}$$

To grasp an idea of what a special conformal transformation is, one can compute x'_μ/x'^2 and discard all terms of order $\mathcal{O}(c^2)$ and higher. This gives

$$\frac{x'_\mu}{x'^2} \approx \frac{x_\mu}{x^2} - c_\mu, \tag{B.18}$$

which is nothing but an inversion (i.e. a transformation which maps x_μ into x_μ/x^2), plus an infinitesimal translation, plus another inversion. This approximate result is in fact the exact form of the *finite* special conformal transformation, with c_μ no longer infinitesimal.

Having considered the conformal transformations on coordinates, let us consider its consequences in the euclidean action, or Hamiltonian. Consider

the euclidean action of a theory written as:

$$S = \int_x \mathcal{L}(\Phi, \partial_\mu \Phi)$$

When

$$x \to x' = x^\mu + \omega_a \frac{\delta x^\mu}{\delta \omega_a},$$

the fields also change as

$$\Phi(x) \to \Phi'(x') = \Phi(x) + \omega_a \frac{\delta \mathcal{F}}{\delta \omega_a}(x)$$

or equivalently

$$\Phi'(x) = \mathcal{F}(\Phi(x)).$$

We consider linear transformations only. When the transformation considered is infinitesimal and depending on a small parameter ω_a, the transformation can be written as

$$\Phi'(x') = \Phi(x) + \omega_a \frac{\delta \mathcal{F}}{\delta \omega_a}(x)$$

which at first order in ω_a can be expressed at the same point as:

$$\Phi'(x') = \Phi(x') - \omega_a \frac{\delta x_\rho}{\delta \omega_a} \partial_\rho \Phi(x') + \omega_a \frac{\delta \mathcal{F}}{\delta \omega_a}(x'). \tag{B.19}$$

The generator of a symmetry G_a is usually defined in terms of the difference of the fields at the same point, before and after the transformation is applied. Explicitly, G_a is defined[1] by:

$$\Phi'(x) - \Phi(x) \equiv -\omega_a G_a \Phi(x) = -\omega_a \left(\frac{\delta x_\rho}{\delta \omega_a} \partial_\rho \Phi(x) - \frac{\delta \mathcal{F}}{\delta \omega_a}(x) \right) \tag{B.20}$$

For scalar fields under general conformal transformations, the fields transform as:

$$\Phi'(x') = \left| \frac{\partial x'}{\partial x} \right|^{-D_\Phi/d} \Phi(x), \tag{B.21}$$

where D_Φ is the scaling dimension of the fields. With the generators definition

---

[1]Sometimes an explicit i is introduced in the definition of the generator.

Eq.(B.20), the different transformation considered so far yield the generators[1]:

Traslations: $\qquad P_\mu = \partial_\mu.$ $\qquad$ (B.22)

Rotations: $\qquad J_{\mu\nu} = (x_\mu \partial_\nu - x_\nu \partial_\mu).$ $\qquad$ (B.23)

Dilations: $\qquad D = x_\nu \partial_\nu + D_\Phi.$ $\qquad$ (B.24)

Special Conformal: $\qquad K_\mu = x_\nu x_\nu \partial_\mu - 2x_\mu x_\nu \partial_\nu - 2D_\Phi x_\mu.$ $\qquad$ (B.25)

Putting everything together, the generators of all the conformal transformations take the form: These generators satisfy the conformal algebra which

$$\left[D, P_\mu\right] = -P_\mu, \tag{B.26}$$

$$\left[D, K_\mu\right] = K_\mu, \tag{B.27}$$

$$\left[P_\mu, K_\nu,\right] = -2(\eta_{\mu\nu} D - J_{\mu\nu}), \tag{B.28}$$

$$\left[J_{\mu\nu}, P_\rho\right] = -\eta_{\nu\rho} P_\mu + \eta_{\mu\rho} P_\nu, \tag{B.29}$$

$$\left[J_{\mu\nu}, K_\rho\right] = -\eta_{\nu\rho} K_\mu + \eta_{\mu\rho} K_\nu, \tag{B.30}$$

$$\left[J_{\mu\nu}, J_{\rho\sigma}\right] = -\eta_{\nu\rho} J_{\mu\sigma} - \eta_{\mu\sigma} J_{\nu\rho} + \eta_{\mu\rho} J_{\nu\sigma} + \eta_{\nu\sigma} J_{\mu\rho}, \tag{B.31}$$

and 0 for all the remaining commutators.

---

[1]There is an extra freedom in these definitions. For example, one could say that in the conformal case it is $\varepsilon_\mu^{(SC)} = 2(x_\nu c_\nu')x_\mu - (x_\nu x_\nu)c_\mu'$, with $c_\mu' = -c_\mu = c_{\sigma\sigma\mu}/d$. This would make the generator change in a global $-$ sign.

Appendix C

Raw Data of Critical Exponents η, ν and ω for the $O(N)$ Models up to Order $\mathcal{O}(\partial^4)$ of the Derivative Expansion

In this Appendix we present the raw data for exponents η, ν and ω computed with the derivative expansion up to order $\mathcal{O}(\partial^4)$ for various $O(N)$ models with the regulators given in Eqs.(2.30-2.32) (in the case of Θ^n regulators we present in all cases the results for $n = 3$ since for this value of n the DE is well behaved until order $\mathcal{O}(\partial^4)$ and, for $N = 1$, it turned out to be optimum at that order [12]). The $N = 1$ raw data is given in Chapter 3. As explained in that chapter, the criterion used for these raw tables is obtain the values via PMS. However, sometimes no PMS was present and therefore the philosophy of the PMS is extended an we took as value, the one that depend least on the regulator. This happened to be an inflexion point in all studied cases. These values are marked with an asterisk in the tables.

	regulator	ν	η	ω
LPA	W	$1/2$	0	0.7000
	Θ^3	$1/2$	0	0.7021
	E	$1/2$	0	0.6983
$O(\partial^2)$	W	$0.5 + 2.8 \times 10^{-8}$	5.9×10^{-8}	0.8451
	Θ^3	$0.5 + 5.9 \times 10^{-7}$	1.2×10^{-6}	0.8447
	E	$0.5 + 7.4 \times 10^{-8}$	1.3×10^{-7}	0.8446
$O(\partial^4)$	W	$0.5 + 7.0 \times 10^{-5}$	8.5×10^{-5}	0.8368
	Θ^3	$0.5 + 5.9 \times 10^{-5}$	9.7×10^{-5}	0.8344
	E	$0.5 + 8.5 \times 10^{-5}$	9.2×10^{-4}	0.8411

Table C.1: Raw data for $N = -2$ critical exponents in $d = 3$ obtained with various regulators up to order $\mathcal{O}(\partial^4)$ of the DE.

	regulator	ν	η	ω
LPA	W	0.5925	0	0.6549
	Θ^3	0.5923	0	0.6567
	E	0.5926	0	0.6535
$O(\partial^2)$	W	0.5878 *	0.0384	1.0407
	Θ^3	0.5879	0.0373	0.9431
	E	0.5878 *	0.0388	1.0489
$O(\partial^4)$	W	0.5875 *	0.0299	0.9006
	Θ^3	0.5876 *	0.0303	0.9007
	E	0.5875 *	0.0292	0.9005

Table C.2: Raw data for $N = 0$ critical exponents in $d = 3$ obtained with various regulators up to order $\mathcal{O}(\partial^4)$ of the DE. When a value of α different of PMS is employed, this is explicitly indicated.

	regulator	ν	η	ω
LPA	W	0.7099	0	0.6717
	Θ^3	0.7090	0	0.6715
	E	0.7106	0	0.6716
$O(\partial^2)$	W	0.6669	0.0474	0.7983
	Θ^3	0.6673	0.0469	0.7992
	E	0.6663	0.0480	0.7972
$O(\partial^4)$	W	0.6725	0.0361	0.7906
	Θ^3	0.6722	0.0367	0.7893
	E	0.6732	0.0350	0.7934

Table C.3: Raw data for $N = 2$ critical exponents in $d = 3$ obtained with various regulators up to order $\mathcal{O}(\partial^4)$ of the DE.

	regulator	ν	η	ω
LPA	W	0.7631	0	0.7019
	Θ^3	0.7620	0	0.7010
	E	0.7639	0	0.7026
$O(\partial^2)$	W	0.7047	0.0471	0.7541
	Θ^3	0.7054	0.0466	0.7563
	E	0.7039	0.0476	0.7516
$O(\partial^4)$	W	0.7126	0.0358	0.7681
	Θ^3	0.7122	0.0363	0.7659
	E	0.7136	0.0347	0.7729

Table C.4: Raw data for $N = 3$ critical exponents in $d = 3$ obtained with various regulators up to order $\mathcal{O}(\partial^4)$ of the DE.

	regulator	ν	η	ω
LPA	W	0.8063	0	0.7370
	Θ^3	0.8052	0	0.7354
	E	0.8071	0	0.7383
$O(\partial^2)$	W	0.7405	0.0450	0.7310
	Θ^3	0.7412	0.0445	0.7340
	E	0.7396	0.0455	0.7274
$O(\partial^4)$	W	0.7490	0.0343	0.7588
	Θ^3	0.7487	0.0348	0.7561
	E	0.7500	0.0332	0.7649

Table C.5: Raw data for $N = 4$ critical exponents in $d = 3$ obtained with various regulators up to order $\mathcal{O}(\partial^4)$ of the DE.

	regulator	ν	η	ω
LPA	W	0.8395	0	0.7706
	Θ^3	0.8385	0	0.7687
	E	0.8402	0	0.7721
$O(\partial^2)$	W	0.7731	0.0420	0.7241
	Θ^3	0.7737	0.0416	0.7275
	E	0.7722	0.0425	0.7199
$O(\partial^4)$	W	0.7808	0.0323	0.7584
	Θ^3	0.7806	0.0327	0.7558
	E	0.7815	0.0313	0.7648

Table C.6: Raw data for $N = 5$ critical exponents in $d = 3$ obtained with various regulators up to order $\mathcal{O}(\partial^4)$ of the DE.

	regulator	ν	η	ω
LPA	W	0.9194	0	0.8745
	Θ^3	0.9190	0	0.8729
	E	0.9198	0	0.8758
$O(\partial^2)$	W	0.8774	0.0276	0.7882
	Θ^3	0.8775	0.0274	0.7903
	E	0.8772	0.0279	0.7853
$O(\partial^4)$	W	0.8777	0.0222	0.8063
	Θ^3	0.8780	0.0225	0.8062
	E	0.8771	0.0218	0.8081

Table C.7: Raw data for $N = 10$ critical exponents in $d = 3$ obtained with various regulators up to order $\mathcal{O}(\partial^4)$ of the DE.

	regulator	ν	η	ω
LPA	W	0.9610	0	0.9384
	Θ^3	0.9608	0	0.9376
	E	0.9612	0	0.9391
$O(\partial^2)$	W	0.9414 *	0.0149	0.8875
	Θ^3	0.9414	0.0148	0.8880
	E	0.9414 *	0.0151	0.8867
$O(\partial^4)$	W	0.9409	0.0125	0.8875
	Θ^3	0.9411	0.0126	0.8884
	E	0.9406	0.0123	0.8863

Table C.8: Raw data for $N = 20$ critical exponents in $d = 3$ obtained with various regulators up to order $\mathcal{O}(\partial^4)$ of the DE. When a value of α different of PMS is employed, this is explicitly indicated.

194

	regulator	ν	η	ω
LPA	W	0.9925	0	0.9882
	Θ^3	0.9924	0	0.9880
	E	0.9925	0	0.9883
$O(\partial^2)$	W	0.98906	0.00308	0.9781
	Θ^3	0.98933	0.00294	0.9782 *
	E	0.98908	0.00310	0.9781
$O(\partial^4)$	W	0.98884	0.00263	0.9771
	Θ^3	0.98888	0.00264	0.9772
	E	0.98877	0.00260	0.9767

Table C.9: Raw data for $N = 100$ critical exponents in $d = 3$ obtained with various regulators up to order $\mathcal{O}(\partial^4)$ of the DE. When a value of α different of PMS is employed, this is explicitly indicated.

Appendix D

Presence of Conformal Invariance in the Cubic Model

In generic magnetic materials, the $O(N)$ symmetry is not realized microscopically because of the crystal structure. Consequently, the magnetization along certain directions may be preferred (for instance, an axis of the lattice). This may turn out to be irrelevant at a critical point, but it may also lead to another critical point describing a different universality class.

The cubic model was also studied perturbatively with the aim of extending the study of the presence of conformal invariance in different systems. We compute the scaling dimension of leading vector operators of the cubic model. We drop Einstein convention for this appendix to make notation unambiguous. This is because we sum in colour indices not only when they appear twice, but also, see the term proportion to v below in Eq.(D.1), when they appear four times. We start with the Hamiltonian:

$$H[\phi] = \int_x \left\{ \frac{1}{2} \sum_a (\nabla \phi_a)^2 + \frac{1}{2} r_o^\Lambda \sum_a \phi_a^2 + \frac{u^\Lambda}{4!} \Big(\sum_a \phi_a^2 \Big)^2 + \frac{v}{4!} \sum_a \phi_a^4 \right\}, \quad \text{(D.1)}$$

where the term $\propto v$ breaks $O(N)$ symmetry into the symmetries of the hypercube. We perturb the Hamiltonian with the following term:

$$
\begin{aligned}
H_p[\phi] = \int_x \Bigg\{ & \frac{K_1^{\Lambda,\mu}}{2} \sum_a \phi_a^2 \sum_b \phi_b \partial_\mu \Delta \phi_b \\
& + \frac{K_2^{\Lambda,\mu}}{3!} \sum_a \phi_a^3 \partial_\mu \Delta \phi_a + \frac{K_3^{\Lambda,\mu}}{2} \sum_a \phi_a^2 \sum_b \Delta \phi_b \partial_\mu \phi_b \Bigg\},
\end{aligned}
\quad \text{(D.2)}
$$

in order to analyse the possible breaking of conformal invariance at the critical point of the cubic model. We consider just these perturbations because they are

the leading integrated vector operators for this model (their scaling dimension is $3 + \mathcal{O}(\epsilon)$ at $d = 4 - \epsilon$). We will compute the scaling dimensions of K_1^μ, K_2^μ and K_3^μ at one loop at the fixed point $u \neq 0$ and $v \neq 0$. It is worth noting that there is, also, a non-renormalization theorem for a combination of these operators.

We now derive the flow equations of the K^μ couplings within the NPRG approach at zero field. For this we consider an effective action given by:

$$
\begin{aligned}
\Gamma_k[\varphi] = \int_x \Bigg\{ &\frac{1}{2} \sum_a (\nabla \varphi_a)^2 + \frac{1}{2} r_o \sum_a \varphi_a^2 + \frac{u}{4!} \Big(\sum_a \varphi_a^2 \Big)^2 + \frac{v}{4!} \sum_a \varphi_a^4 \\
&+ \frac{K_1^\mu}{2} \sum_a \varphi_a^2 \sum_b \varphi_b \partial_\mu \Delta \varphi_b + \frac{K_2^\mu}{3!} \sum_a \varphi_a^3 \partial_\mu \Delta \varphi_a + \frac{K_3^\mu}{2} \sum_a \varphi_a^2 \sum_b \Delta \varphi_b \partial_\mu \varphi_b \Bigg\}.
\end{aligned}
$$

$$(D.3)$$

To compute the flows of u, v, K_1^μ, K_2^μ and K_3^μ we need to compute the flow of $\Gamma_k^{(4)}$. $\Gamma_k^{(4)}$ can easily be shown to be:

$$
\begin{aligned}
\Gamma_{k,(n_1,n_2,n_3,n_4)}^{(4)}(p_1, p_2, p_3; \varphi) = &\frac{u}{3} \big(\delta_{n_1 n_2} \delta_{n_3 n_4} + \delta_{n_1 n_3} \delta_{n_2 n_4} + \delta_{n_1 n_4} \delta_{n_2 n_3} \big) \\
&+ v \big(\delta_{n_1 n_2} \delta_{n_1 n_3} \delta_{n_1 n_4} \big) - i K_1^\mu \big(\delta_{n_1 n_2} \delta_{n_3 n_4} + \delta_{n_1 n_3} \delta_{n_2 n_4} + \delta_{n_1 n_4} \delta_{n_2 n_3} \big) \Theta_{2,\mu} \\
&- i K_2^\mu \big(\delta_{n_1 n_2} \delta_{n_1 n_3} \delta_{n_1 n_4} \big) \Theta_{2,\mu} \\
&+ i K_3^\mu \Bigg[\big(\delta_{n_1 n_2} \delta_{n_3 n_4} + \delta_{n_1 n_3} \delta_{n_2 n_4} + \delta_{n_1 n_4} \delta_{n_2 n_3} \big) \Theta_{2,\mu} \\
&\quad + 2 \Big(\delta_{n_1 n_2} \delta_{n_3 n_4} \Theta_{1,\mu}(p_1, p_2, p_3, p_4) + \delta_{n_1 n_3} \delta_{n_2 n_4} \Theta_{1,\mu}(p_1, p_3, p_2, p_4) \\
&\quad + \delta_{n_1 n_4} \delta_{n_2 n_3} \Theta_{1,\mu}(p_1, p_4, p_2, p_3) \Big) \Bigg]
\end{aligned}
$$

$$(D.4)$$

where we introduced the momentum structures $\Theta_{1,\mu}$ and $\Theta_{2,\mu}$ defined as:

$$
\begin{aligned}
\Theta_{1,\mu}(p_1, p_2, p_3, p_4) &= (p_1 + p_2)^\mu \left[p_1 \cdot p_2 - p_3 \cdot p_4 \right], \\
\Theta_{2,\mu} &= p_1^\mu p_1^2 + p_2^\mu p_2^2 + p_3^\mu p_3^2 + p_4^\mu p_4^2,
\end{aligned}
$$

$$(D.5)$$

where $p_4 = -(p_1 + p_2 + p_3)$. At one loop, the flow of $\Gamma_k^{(4)}$ at zero field is given

by:

$$\partial_t\Gamma^{(4)}_{k,(n_1,n_2,n_3,n_4)}(p_1,p_2,p_3;\varphi) = \sum_{l,m}\int_q \partial_t R_k(q^2)G_k^2(q;\varphi)\times$$

$$\left\{ G_k(p_1+p_2+q;\varphi)\Gamma^{(4)}_{k\ (l,n_1,n_2,m)}(q,p_1,p_2;\varphi)\Gamma^{(4)}_{k\ (m,n_3,l,n_4)}(q+p_1+p_2,p_3,-q;\varphi)\right.$$

$$+ G_k(p_1+p_3+q;\varphi)\Gamma^{(4)}_{k\ (l,n_1,n_3,m)}(q,p_1,p_3;\varphi)\Gamma^{(4)}_{k\ (m,n_2,l,n_4)}(q+p_1+p_3,p_2,-q;\varphi)$$

$$\left. + G_k(p_2+p_3+q;\varphi)\Gamma^{(4)}_{k\ (l,n_2,n_3,m)}(q,p_2,p_3;\varphi)\Gamma^{(4)}_{k\ (m,n_1,l,n_4)}(q+p_2+p_3,p_1,-q;\varphi)\right\}.$$

$$\text{(D.6)}$$

D.1 Isometric Part of the Flow

Since we only want the flow to linear level on K_1^μ, K_2^μ and K_3^μ we neglect terms quadratic on these variables. We start by computing the zeroth order on K's. This gives:

$$\partial_t\Gamma^{(4),isom}_{k,(n_1,n_2,n_3,n_4)}(p_1,p_2,p_3;\varphi) = I_0 v\left(12\frac{u}{3}+3v\right)\left[\delta_{n_1n_2}\delta_{n_1n_3}\delta_{n_1n_4}\right]$$

$$+I_0\frac{u}{3}\left((N+8)\frac{u}{3}+2v\right)\left[\delta_{n_1n_2}\delta_{n_3n_4}+\delta_{n_1n_3}\delta_{n_2n_4}+\delta_{n_1n_4}\delta_{n_2n_3}\right],$$

$$\text{(D.7)}$$

where I_0 is defined the one defined in Eq.(5.9):

$$I_0 = \int_q \partial_t R_k(q^2)G_k^3(q;\varphi) \qquad \text{(D.8)}$$

D.2 Part of the Flow Proportional to K_1^μ, K_2^μ and K_3^μ

We now consider the contributions which are linear in K_1^μ, K_2^μ or K_3^μ. To do so, we project on the different structures of Eq.(D.4).

For the term proportional to K_1^μ we have:

$$\partial_t\Gamma^{(4),K_1}_{k,(n_1,n_2,n_3,n_4)}(p_1,p_2,p_3;\varphi) = -i6I_0vK_1^\mu\Theta_{2,\mu}\left[\delta_{n_1n_2}\delta_{n_1n_3}\delta_{n_1n_4}\right]$$

$$- iI_0\left((N+8)\frac{u}{3}+v\right)K_1^\mu\Theta_{2,\mu}\left[\delta_{n_1n_2}\delta_{n_3n_4}+\delta_{n_1n_3}\delta_{n_2n_4}+\delta_{n_1n_4}\delta_{n_2n_3}\right]$$

$$\text{(D.9)}$$

For the term proportional to K_2^μ we have:

$$\partial_t \Gamma^{(4),K_2}_{k,(n_1,n_2,n_3,n_4)}(p_1,p_2,p_3;\varphi) = -iI_0\left(6\frac{u}{3}+3v\right)K_2^\mu\Theta_{2,\mu}\left[\delta_{n_1n_2}\delta_{n_1n_3}\delta_{n_1n_4}\right]$$
$$- iI_0\frac{u}{3}K_2^\mu\Theta_{2,\mu}\left[\delta_{n_1n_2}\delta_{n_3n_4}+\delta_{n_1n_3}\delta_{n_2n_4}+\delta_{n_1n_4}\delta_{n_2n_3}\right]$$

(D.10)

For the term proportional to K_3^μ we have:

$$\partial_t \Gamma^{(4),K_3}_{k,(n_1,n_2,n_3,n_4)}(p_1,p_2,p_3;\varphi) = i6I_0vK_3^\mu\Theta_{2,\mu}\left[\delta_{n_1n_2}\delta_{n_1n_3}\delta_{n_1n_4}\right]$$
$$+iI_0\left((N+8)\frac{u}{3}+v\right)K_3^\mu\Theta_{2,\mu}\left[\delta_{n_1n_2}\delta_{n_3n_4}+\delta_{n_1n_3}\delta_{n_2n_4}+\delta_{n_1n_4}\delta_{n_2n_3}\right]$$
$$+2iI_0\frac{u}{3}K_3^\mu\left[(N+2)\left(\delta_{n_1n_2}\delta_{n_3n_4}\Theta_{1,\mu}(p_1,p_2,p_3,p_4)+\delta_{n_1n_3}\delta_{n_2n_4}\Theta_{1,\mu}(p_1,p_3,p_2,p_4)\right.\right.$$
$$\left.\left.+\delta_{n_1n_4}\delta_{n_2n_3}\Theta_{1,\mu}(p_1,p_4,p_2,p_3)\right)-2\Theta_{2,\mu}\left(\delta_{n_1n_2}\delta_{n_3n_4}+\delta_{n_1n_3}\delta_{n_2n_4}+\delta_{n_1n_4}\delta_{n_2n_3}\right)\right]$$
$$+2iI_0vK_3^\mu\left[\left(\delta_{n_1n_2}\delta_{n_3n_4}\Theta_{1,\mu}(p_1,p_2,p_3,p_4)+\delta_{n_1n_3}\delta_{n_2n_4}\Theta_{1,\mu}(p_1,p_3,p_2,p_4)\right.\right.$$
$$\left.\left.+\delta_{n_1n_4}\delta_{n_2n_3}\Theta_{1,\mu}(p_1,p_4,p_2,p_3)\right)-2\Theta_{2,\mu}\left(\delta_{n_1n_2}\delta_{n_3n_4}+\delta_{n_1n_3}\delta_{n_2n_4}+\delta_{n_1n_4}\delta_{n_2n_3}\right)\right].$$

(D.11)

In these expressions, all explicit dependence on the internal momenta is absent due to momentum conservation or explicit cancellation. For this reason no expansion of the propagator is needed (since it would contribute to higher order derivative terms).

Flow Equations

To isolate the flow equations we first put all external momentum equal zero and find that:

$$\partial_t u = I_0 u\left((N+8)\frac{u}{3}+2v\right),$$

(D.12)

$$\partial_t v = I_0 v\left(12\frac{u}{3}+3v\right).$$

(D.13)

These are the standard flow equations of the literature (see for example [149]). To get the flows of K_1^μ and K_3^μ we can just consider $n_1 = n_2 = 1$ and

$n_3 = n_4 = 2$ and consider the part cubic in p's, in this manner, we get that:

$$-i\partial_t K_1^\mu \Theta_{2,\mu} + i\partial_t K_3^\mu \left(\Theta_{2,\mu} + 2\Theta_{1,\mu}(p_1, p_2, p_3, p_4) \right) =$$

$$iI_0 \left\{ \left((N+8)\frac{u}{3} + v \right) \left[K_3^\mu - K_1^\mu \right] - 4\left(\frac{u}{3} + v \right) K_3^\mu - \frac{u}{3} K_2^\mu \right\} \Theta_{2,\mu}$$

$$+ 2iI_0 \left((N+2)\frac{u}{3} + v \right) K_3^\mu \Theta_{1,\mu}(p_1, p_2, p_3, p_4) = \qquad (D.14)$$

$$iI_0 \left((N+2)\frac{u}{3} + v \right) K_3^\mu \left(\Theta_{2,\mu} + 2\Theta_{1,\mu}(p_1, p_2, p_3, p_4) \right)$$

$$- iI_0 \left\{ \left((N+8)\frac{u}{3} + v \right) K_1^\mu + \frac{u}{3} K_2^\mu + \left(-2\frac{u}{3} + 4v \right) K_3^\mu \right\} \Theta_{2,\mu}$$

From this follows that the flows for K_1^μ and K_3^μ are:

$$\partial_t K_1^\mu = I_0 \left[\left((N+8)\frac{u}{3} + v \right) K_1^\mu + \frac{u}{3} K_2^\mu + \left(-2\frac{u}{3} + 4v \right) K_3^\mu \right] \qquad (D.15)$$

$$\partial_t K_3^\mu = I_0 \left((N+2)\frac{u}{3} + v \right) K_3^\mu. \qquad (D.16)$$

Finally we need to compute the flow of K_2. To do this note first that:

$$\Theta_{1,\mu}(p_1, p_2, p_2, p_3) + \Theta_{1,\mu}(p_1, p_3, p_2, p_4) + \Theta_{1,\mu}(p_1, p_4, p_2, p_3) = -\Theta_{2,\mu} \quad (D.17)$$

Putting $n_1 = n_2 = n_3 = n_4 \equiv n_0$ in the flow of $\Gamma_k^{(4)}$ (cubic in the external momentum) we get in the left hand side:

$$\partial_t \Gamma_{k,(n_0,n_0,n_0,n_0)}^{(4),\mathcal{O}(p^3)}(p_1, p_2, p_3; \varphi) = -i\left(3\partial_t K_1^\mu + \partial_t K_2^\mu - \partial_t K_3^\mu \right) \Theta_{2,\mu}, \qquad (D.18)$$

and in the right hand side:

$$\partial_t \Gamma_{k,(n_0,n_0,n_0,n_0)}^{(4),\mathcal{O}(p^3)}(p_1, p_2, p_3; \varphi) = -iI_0 \left[\left(3(N+8)\frac{u}{3} + 9v \right) K_1^\mu \right.$$
$$\left. + \left(9\frac{u}{3} + 3v \right) K_2^\mu - \left((N+8)\frac{u}{3} - 5v \right) K_3^\mu \right] \Theta_{2,\mu}. \qquad (D.19)$$

We can plug in, now, the flows of K_1^μ and K_3^μ given in Eq.(D.15) and Eq.(D.16), respectively, to isolate the flow of K_2^μ. This is:

$$\partial_t K_2^\mu = I_0 \left[6v K_1^\mu + \left(6\frac{u}{3} + 3v \right) K_2^\mu + 2v K_3^\mu \right]. \qquad (D.20)$$

Now, to find the fixed points we must consider dimensionless couplings:

$$\tilde{u} = uk^{d-4}, \qquad \tilde{v} = vk^{d-4},$$
$$\tilde{K}_1^\mu = K_1^\mu k^{d-1}, \qquad \tilde{K}_2^\mu = K_2^\mu k^{d-1}, \qquad \tilde{K}_3^\mu = K_3^\mu k^{d-1}, \tag{D.21}$$

from which the flow equations follow immediately.

Scaling dimensions

We can solve separately the isometric part of the flow and the flow of the perturbations. We first stress that there are four possible fixed point solutions, namely:

$$\left(\tilde{u}^*, \tilde{v}^*\right) = \left(0, 0\right), \tag{D.22}$$

$$\left(\tilde{u}^*, \tilde{v}^*\right) = \left(0, \frac{\epsilon}{3\tilde{I}_0}\right), \tag{D.23}$$

$$\left(\tilde{u}^*, \tilde{v}^*\right) = \left(\frac{3\epsilon}{I_0(N+8)}, 0\right) \tag{D.24}$$

and

$$\left(\tilde{u}^*, \tilde{v}^*\right) = \left(\frac{\varepsilon}{\tilde{I}_0 N}, \frac{(N-4)\varepsilon}{3\tilde{I}_0 N}\right). \tag{D.25}$$

Of course, the $\tilde{K}_i^\mu$ are vanishing at the fixed points of interest. The first of this list of fixed point is a Gaussian fixed point. The second one is a set of N decoupled Ising models. We are only interested in the fixed point solutions Eq.(D.24) and Eq.(D.25), which are the standard Wilson-Fisher fixed point and the cubic fixed point, respectively. A schematic flow diagram for this model, taken from [64], is shown in Fig.D.1 where the u coupling is named g_1 and the v coupling is named g_2.

We first consider the fixed point which breaks $O(N)$ symmetry, i.e. Eq.(D.25). This fixed point near $d = 4$ is critical for $N > 4$ and tri-critical for $N < 4$. To study the breaking of conformal invariance we compute the stability matrix for the flow of the vector couplings K_1^μ, K_2^μ and K_3^μ evaluated at the fixed point. The stability matrix $\mathcal{M}$ reads:

$$\mathcal{M} = \begin{pmatrix} 3 - \frac{\epsilon(N-4)}{3N} & \frac{\epsilon}{3N} & \epsilon\left(\frac{4}{3} - \frac{6}{N}\right) \\ \frac{2\epsilon(N-4)}{N} & 3 - \frac{2\epsilon}{N} & \frac{2\epsilon(N-4)}{3N} \\ 0 & 0 & 3 - \frac{\epsilon(N+2)}{3N} \end{pmatrix}. \tag{D.26}$$

The matrix $\mathcal{M}$ is not diagonalizable and yields the eigenvalues $\lambda_1 = 3 + \mathcal{O}(\epsilon^2)$ and $\lambda_2 = 3 - \frac{(2+N)\epsilon}{3N} + \mathcal{O}(\epsilon^2)$. These eigenvalues are $\lambda_{1,2} > 2.5$ for $N > 4$ and
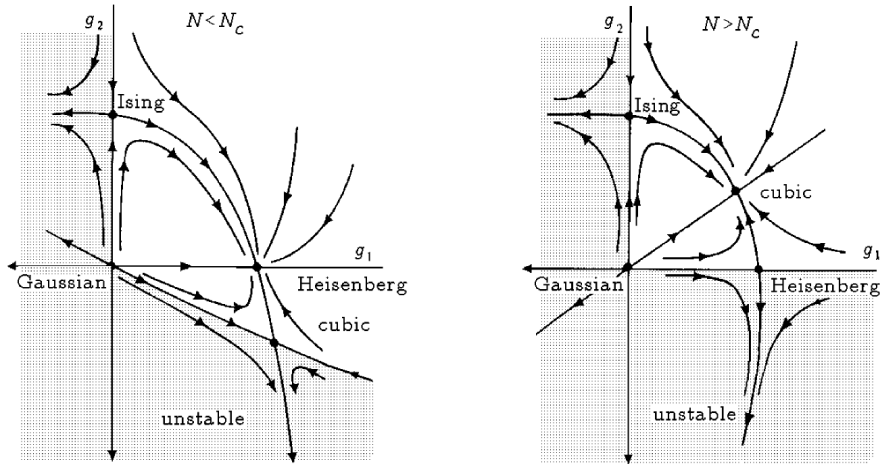
Figure D.1: Schematic representation of the RG flow diagram. Taken from [64].

based on the bound -1, according to the sufficient condition given in Chapter 4 we infer that it is conformal invariant.

Note that solving for this perturbation at the $O(N)$ fixed point [this is, Eq.(D.24)], which is the critical fixed point for $N < 4$ and tri-critical for $N > 4$ yield the eigenvalues $\lambda_1 = 3 + \mathcal{O}(\epsilon^2)$, $\lambda_2 = 3 - \frac{6\epsilon}{N+8} + \mathcal{O}(\epsilon^2)$ and $\lambda_3 = 3 - \frac{N+2}{N+8}\epsilon + \mathcal{O}(\epsilon^2)$. The first two eigenvalues are the ones persisting when K_3 is turned off, in agreement with previous calculations. We highlight that our study of Chapter 5, including the exact proof for $O(2)$, $O(3)$ and $O(4)$, assume that the microscopic model is also $O(N)$ invariant. However, if we are dealing with a microscopic theory which has the symmetries of the cubic anisotropy model, we must consider candidates for breaking the conformal symmetry which are not $O(N)$ invariant. We computed the scaling dimensions to the leading vector operators exhibiting these symmetries and find that we are also far from violating the bound -1. All eigenvalues satisfy $\lambda_{1,2,3} > 2.25$ for $N \in \{0, 1, 2, 3, 4\}$.

Appendix E

Ansatz for Γ_k at Order $\mathcal{O}(\partial^6)$ of the Derivative Expansion for the $O(N)$ Models

As described in Chapter 3, one of the limitations of the derivative expansion procedure is the growing number of independent functions. Moreover, the flow equation for each of them grows with the vertex function from which is extracted. This means that if $n > m$, typically, the flow equation for a function extracted from the vertex function $\Gamma_k^{(n)}$ is notoriously larger than the flow equation of a function extracted from the vertex function $\Gamma_k^{(m)}$. However, the increment in the computation difficulty with higher order approximations is not exclusive to the derivative expansion.

In this appendix we present a possible[1] ansatz for $\Gamma_k^{\mathcal{O}(\partial^6)}$ at order $\mathcal{O}(\partial^6)$ of the Derivative Expansion for the $O(N)$ models. This ansatz must be considered altogether with the previous ansatz for lower orders (i.e. the ansatz at order $\mathcal{O}(\partial^s)$ is $\Gamma_k = \Gamma_k^{\mathcal{O}(\partial^0)} + \cdots + \Gamma_k^{\mathcal{O}(\partial^s)}$). Omitting the subscript k for notation simplicity, the ansatz takes the form:

---

[1]An ansatz of the derivative expansion at $\mathcal{O}(\partial^s)$ is unique up to integration by parts.

$$\Gamma_k^{\mathcal{O}(\partial^6)} = \int_x \Bigg\{ X_1(\rho)\big(\partial_\mu\partial_\nu\partial_\sigma\varphi_a\big)^2 + X_2(\rho)\big(\varphi_a\partial_\mu\partial_\nu\partial_\sigma\varphi_a\big)^2 +$$

$$X_3(\rho)\partial_\sigma\rho\partial_\sigma\big(\partial_\mu\partial_\nu\varphi_a\big)^2 + X_4(\rho)\varphi_a\partial_\mu\partial_\nu\varphi_a\partial_\sigma\varphi_b\partial_\sigma\partial_\mu\partial_\nu\varphi_b +$$

$$X_5(\rho)\varphi_a\partial_\mu\partial_\nu\varphi_a\partial_\sigma\partial_\mu\varphi_b\partial_\sigma\partial_\nu\varphi_b +$$

$$X_6(\rho)\varphi_a\partial_\mu\partial_\nu\varphi_a\varphi_b\partial_\mu\partial_\sigma\varphi_b\varphi_c\partial_\nu\partial_\sigma\varphi_c +$$

$$X_7(\rho)\varphi_a\partial_\mu\partial_\nu\partial_\sigma\varphi_a\partial_\mu\varphi_b\partial_\nu\partial_\sigma\varphi_b + X_8(\rho)\big(\varphi_a\partial_\mu\partial_\nu\varphi_a\big)^2\big(\partial_\sigma\varphi_b\big)^2 +$$

$$X_9(\rho)\big(\partial_\mu\partial_\nu\varphi_a\big)^2\big(\partial_\sigma\varphi_b\big)^2 + X_{10}(\rho)\big(\partial_\sigma\big(\partial_\mu\varphi_a\big)^2\big)^2 +$$

$$X_{11}(\rho)\partial_\mu\partial_\sigma\varphi_a\partial_\nu\partial_\sigma\varphi_a\partial_\mu\varphi_b\partial_\nu\varphi_b + X_{12}(\rho)\big(\partial_\mu\partial_\nu\varphi_a\partial_\sigma\varphi_a\big)^2 +$$

$$X_{13}(\rho)\partial_\mu\partial_\nu\partial_\sigma\varphi_a\partial_\sigma\varphi_a\partial_\mu\varphi_b\partial_\nu\varphi_b + X_{14}(\rho)\partial_\mu\varphi_a\partial_\nu\partial_\sigma\varphi_a\partial_\sigma\varphi_b\partial_\mu\partial_\nu\varphi_b +$$

$$X_{15}(\rho)\partial_\mu\rho\varphi_a\partial_\mu\partial_\nu\varphi_a\partial_\nu\big(\partial_\sigma\varphi_b\big)^2 + X_{16}(\rho)\partial_\mu\partial_\nu\rho\partial_\sigma\varphi_a\partial_\mu\partial_\nu\partial_\sigma\varphi_a +$$

$$X_{17}(\rho)\partial_\mu\rho\partial_\nu\rho\partial_\mu\partial_\sigma\varphi_a\partial_\nu\partial_\sigma\varphi_a + X_{18}(\rho)\big(\varphi_a\partial_\mu\partial_\nu\varphi_a\big)^2\big(\partial_\sigma\varphi_b\big)^2$$

$$X_{19}(\rho)\big(\partial_\mu\rho\big)^2\big(\partial_\nu\partial_\sigma\varphi_a\big)^2 + X_{20}(\rho)\partial_\mu\rho\partial_\nu\varphi_a\partial_\sigma\varphi_a\varphi_b\partial_\mu\partial_\nu\partial_\sigma\varphi_b +$$

$$X_{21}(\rho)\partial_\mu\rho\varphi_a\partial_\nu\partial_\sigma\varphi_a\partial_\sigma\varphi_b\partial_\mu\partial_\nu\varphi_b +$$

$$X_{22}(\rho)\varphi_a\partial_\mu\partial_\nu\varphi_a\varphi_b\partial_\nu\partial_\sigma\varphi_b\partial_\mu\varphi_c\partial_\sigma\varphi_c +$$

$$X_{23}(\rho)\partial_\mu\rho\varphi_a\partial_\nu\partial_\sigma\varphi_a\partial_\mu\varphi_b\partial_\nu\partial_\sigma\varphi_b +$$

$$X_{24}(\rho)\partial_\mu\rho\partial_\nu\rho\partial_\sigma\rho\varphi_a\partial_\mu\partial_\nu\partial_\sigma\varphi_a + X_{25}(\rho)\partial_\mu\rho\partial_\nu\rho\varphi_a\partial_\mu\partial_\sigma\varphi_a\varphi_b\partial_\nu\partial_\sigma\varphi_b +$$

$$X_{26}(\rho)\big(\partial_\mu\rho\big)^2\big(\varphi_a\partial_\nu\partial_\sigma\varphi_a\big)^2 + X_{27}(\rho)\partial_\mu\rho\big(\partial_\nu\varphi_a\big)^2\partial_\mu\big(\partial_\sigma\varphi_a\big)^2 +$$

$$X_{28}(\rho)\partial_\mu\rho\partial_\mu\varphi_a\partial_\nu\varphi_a\partial_\nu\big(\partial_\sigma\varphi_b\big)^2 +$$

$$X_{29}(\rho)\big(\partial_\mu\varphi_a\big)^2\varphi_b\partial_\nu\partial_\sigma\varphi_b\partial_\nu\varphi_c\partial_\sigma\varphi_c + X_{30}(\rho)\partial_\mu\rho\partial_\mu\big(\partial_\nu\varphi_a\partial_\sigma\varphi_a\big)^2 +$$

$$X_{31}(\rho)\varphi_a\partial_\mu\partial_\nu\varphi_a\partial_\mu\varphi_b\partial_\sigma\varphi_b\partial_\nu\varphi_c\partial_\sigma\varphi_c +$$

$$X_{32}(\rho)\partial_\mu\rho\partial_\nu\varphi_a\partial_\sigma\varphi_a\partial_\mu\varphi_b\partial_\nu\partial_\sigma\varphi_b + X_{33}(\rho)\big(\partial_\mu\rho\big)^2\partial_\nu\rho\partial_\nu\big(\partial_\sigma\varphi_a\big)^2 +$$

$$X_{34}(\rho)\partial_\mu\rho\partial_\nu\rho\varphi_a\partial_\mu\partial_\nu\varphi_a\big(\partial_\sigma\varphi_b\big)^2 + X_{35}(\rho)\big(\partial_\mu\rho\big)^2\varphi_a\partial_\nu\partial_\sigma\varphi_a\partial_\nu\varphi_b\partial_\sigma\varphi_b +$$

$$X_{36}(\rho)\partial_\mu\rho\partial_\nu\rho\partial_\sigma\rho\partial_\mu\varphi_a\partial_\nu\partial_\sigma\varphi_a + X_{37}(\rho)\big(\partial_\mu\rho\big)^2\partial_\nu\rho\partial_\sigma\rho\varphi_a\partial_\nu\partial_\sigma\varphi_a$$

$$X_{38}(\rho)\partial_\mu\rho\partial_\nu\rho\varphi_a\partial_\nu\partial_\sigma\varphi_a\partial_\mu\varphi_b\partial_\sigma\varphi_b + X_{39}(\rho)\big(\big(\partial_\mu\varphi_a\big)^2\big)^3 +$$

$$X_{40}(\rho)\big(\partial_\mu\varphi_a\big)^2\big(\partial_\nu\varphi_b\partial_\sigma\varphi_b\big)^2 + X_{41}(\rho)\big(\partial_\mu\rho\big)^2\partial_\nu\rho\partial_\sigma\rho\partial_\nu\varphi_a\partial_\sigma\varphi_a +$$

$$X_{42}(\rho)\partial_\mu\varphi_a\partial_\nu\varphi_a\partial_\mu\varphi_b\partial_\sigma\varphi_b\partial_\nu\varphi_c\partial_\sigma\varphi_c +$$

$$X_{43}(\rho)\big(\partial_\mu\rho\big)^2\big(\big(\partial_\nu\varphi_a\big)^2\big)^2 + X_{44}(\rho)\partial_\mu\rho\partial_\nu\rho\partial_\mu\varphi_a\partial_\nu\varphi_a\big(\partial_\sigma\varphi_b\big)^2 +$$

$$X_{45}(\rho)\big(\partial_\mu\rho\big)^2\big(\partial_\nu\varphi_a\partial_\sigma\varphi_a\big)^2 + X_{46}(\rho)\partial_\mu\rho\partial_\nu\rho\partial_\mu\varphi_a\partial_\sigma\varphi_a\partial_\nu\varphi_b\partial_\sigma\varphi_b +$$

$$X_{47}(\rho)\big(\big(\partial_\mu\rho\big)^2\big)^2\big(\partial_\nu\varphi_a\big)^2 + X_{48}(\rho)\big(\big(\partial_\mu\rho\big)^2\big)^3 \Bigg\}. \tag{E.1}$$

Appendix F

Numerical Methods

We describe in this section the details of the numerical method used to determine the fixed points and critical exponents at order $\mathcal{O}(\partial^s)$ of the DE approximation within the NPRG. The general structure of the procedure can be split in three steps: 1) deriving the flow equations of each function in the ansatz for the effective action; 2) finding the fixed point which governs the critical behaviour of the system and 3) obtaining the critical exponents from the fixed point solution. This details applies to all three orders considered $s = 0$, $s = 2$ and $s = 4$ in Chapter 3 and also to the case of $s = 3$ of Chapter 5. The general procedure also applies to the study of Chapter 6, but this being so similar to the study of Chapter 3 we give just a few references for it. However, although in the different studies we were interested in finding the fixed point governing the long range physics and computing scaling dimensions, some differences arise due to the aim of each study.

F.1 Deriving Flow Equations and Truncation

In order to determine the flow equations for each of the function in the ansatze of the effective action (Eq.(3.5) and Eq.(5.44) for the studies of Chapter 3 and Chapter 5, respectively), we compute from this ansatze the general n-point vertex function $\Gamma_{k\,i_1,\ldots,i_n}^{(n)}$ and evaluate them in a homogeneous field configuration. As a rule of thumb for the DE approximation at order $\mathcal{O}(\partial^s)$, one needs to compute the flow of $\Gamma_k^{(n)}$ with n up to s. This, in turn, implies that we need to compute all n-point vertex functions up to $n = 2 + s$. Indeed, this is because, as previously explained, the flow of any $\Gamma_k^{(n)}$ involves the all vertex functions up to $\Gamma_k^{(n+2)}$.

We highlight that, when plugging in the vertex functions in the right hand

side of the flow equations for the different $\Gamma_k^{(n)}$, we can truncate the product of vertex functions *before expanding propagators* at order s, this is what we called *truncated* form of the flow equations. This is different to what was usually done in previous uses of the DE, where all terms coming from the product were taken into account leading to bigger equations (which are more complicate to handle), we call this *full* form of the flow equations. These two set of flow equations were checked to be compatible, within error bars at order $\mathcal{O}(\partial^2)$ of the $O(N)$ models and at order $\mathcal{O}(\partial^4)$ of the Ising model, see Chapter 6 for the latter. Because the difference between the two schemes are of order $\mathcal{O}(p^{s+2})$, makes the shorter and simpler set of flow equations the selected option.

Finally, matching in the left hand side and in the right hand side of the flow equations the indices and momentum structures. Allows to compute separately each of the flow equations for the different functions in the ansatz.

F.2   Finding the Fixed Point

There are two ways to go for finding the fixed point of the flow equations. The first one, which is more traceable to an experimental procedure, is to start from a microscopic theory or initial condition for $\Gamma_{k=\Lambda}$ and integrate the flow equation. One can do this for different values of the initial conditions and, in particular, vary or fine-tune one parameter. By a dichotomy procedure (which can be easily implemented by observing the flow of a certain quantity, say the derivative of the potential at zero field), one can find a parameter good enough in order to be at criticality. This is equivalent to varying the temperature and measuring the system in order to find the critical temperature T_c. The other method, which is faster and more precise, is to find the zeroes of the beta functions which requires an *a priori* sufficiently good initial condition. We will call this procedure the *root-finding* algorithm.

Since having a good enough initial condition from scratch is not simple, what we did is to to combine both approaches. The procedure implemented was then, to start with any value of N (we choose $N = 2$) and dimension d (we set from start $d = 3$ and never changed it) and start with a dichotomy procedure. This only takes a few hours if one takes a smart ansatz for the microscopic theory. After this, there is no need for doing any more dichotomy. From this point onward, one already has a good enough initial condition for a particular N and a particular d, and by means of the root-finding algorithm

we obtain a very precise fixed point solution. Now, since the equations are well behaved for non-integer values, one can take small variations of N and/or d and trace the fixed point to a new value of interest of N and d. In our particular case, we did this only for N and obtained the fixed point solution for the considered N's at $d = 3$.

We discretized the ρ variable into a grid of N_ρ points and evolved the flow equations using a fourth order Runge-Kutta with fixed step and free boundary conditions for the ρ direction. Because of the procedure used, there was no need to optimize in the time step taken, this part was merely to find a good enough fixed point solution for the root-finding part, which was implemented with a Newton-Raphson algorithm. The size of the ρ box was checked to be large enough for the predicted values to be sufficiently converged.

The normalization condition is fixed as $\tilde{Z}(\tilde{\rho}_i)|_{i=N_\rho/\chi} = 1$, where $\tilde{Z}(\tilde{\rho})$ is the dimensionless version of $Z_k(\rho)$ and $\tilde{\rho}_i$ is the value of $\tilde{\rho}$ at site i. On top of this, the size of the box L_ρ is adjusted for every N value in order for the minimum of the potential to fall always in the site $i = N_\rho/\chi$. From this definition, the value of η_k was extracted at every step of the procedure. For the study reported in Chapter 3 χ was set equal to ~ 4 and $N_\rho = 40$, for the study corresponding to Chapter 5 χ was set at ~ 3 and $N_\rho = 61$, and for the study reported in Chapter 6 χ was set to ~ 4 and $N_\rho = 100$ for regulators E_k and W_k, and χ was set to ~ 2.5 and $N_\rho = 64$ for regulators Θ_k^3 and Θ_k^4.

In the study corresponding to Chapter 3 and Chapter 6, the momentum integrals were performed using an adaptative 21 point Gauss-Kronrod quadrature rule (qags) provided in the quadpack library and ρ derivatives were approximated using a five point centered discretization. However, for the study of Chapter 5 momentum integrals were calculated by a Legendre-Gauss quadrature with 15 points in a box of size $|L_q| \equiv \frac{q_{max}}{k} = 4.2$.

Additionally, once the fixed point solution is found, the evaluation of the conformal constraint reported in Chapter 6 was performed with the same parameters and criteria used for finding the fixed point solution.

F.3 Obtaining Critical Exponents

With a very precise fixed point solution we turn to finding the critical exponents. As just mentioned, η_k is extracted from the normalization condition and is obtained simultaneously with the fixed point solution. Specifically, con-

sidering, for example, the Wetterich regulator $R_k(q^2) = Z_k q^2 r(q^2/k^2)$ with:

$$r(y) = \frac{\alpha}{e^y - 1}. \tag{F.1}$$

The factor Z_k is the field renormalization which is related to the running anomalous dimension by $\partial_t Z_k = -\eta_k Z_k$ and when approaching the fixed point η_k approaches the field anomalous dimension.

Since the critical exponents ν and ω are related to the eigenvalues of the renormalization group flow around the fixed point, after obtaining a fixed point solution we performed a linear stability analysis around it in order to compute the critical exponents ν and ω. We computed the stability matrix $\mathcal{M}$ by evaluating the beta function at points slightly away from the fixed point. Specifically, if we have $\mathcal{N}$ independent functions [for instance, for the $O(N)$ models at order $\mathcal{O}(\partial^4)$ there are 13, i.e. the function U, Z, Y, $W_1,\ldots,W_{10}$] there are $\mathcal{S} \equiv \mathcal{N} N_\rho - 1$ independent variables and so the matrix $\mathcal{M}$ is of size $\mathcal{S} \times \mathcal{S}$. The -1 corresponds to the normalization condition which removes the variable attribute that would be associated with $\tilde{Z}(\tilde{\rho}_i)|_{i=N_\rho/4}$ which was fixed to 1 because of our renormalization condition.[1] Let us call $\vec{F}$ the vector containing all independent variables [i.e. for the $O(N)$ models at order $\mathcal{O}(\partial^4)$ is $\vec{F} = (U(0), U(\rho_1), \ldots, W_{10}(\rho_{N_\rho-1}))$] and $\vec{\beta}(\vec{F})$ the associated flow equation vector. If we denote $\vec{F}^{(fp)}$ the fixed point solution, an element of the matrix $\mathcal{M}$ is, then, computed in the following form:

$$\mathcal{M}_{i,j} \equiv \frac{\beta_i(\vec{F}^{(fp)} + \vec{\delta}^{(j)}\Delta_0) - \beta_i(\vec{F}^{(fp)} - \vec{\delta}^{(j)}\Delta_0)}{2\Delta_0}, \tag{F.2}$$

where $\vec{\delta}^{(j)}$ is a vector of length $\mathcal{S}$ with the i-th component equal to the Kronecker delta δ_{ij}, and Δ_0 is a parameter whose value was set $\sim 10^{-8}$.[2] Finally, we computed the eigenvalues of the matrix $\mathcal{M}$ with the standard linear analysis subroutine *dgeev* of the *LAPACK* package for the studies of Chapter 3 and Chapter 6 and with the Arnoldi method for the study of Chapter 5. The smallest eigenvalue λ_1 is identified with ν as $\lambda_1 = -\nu^{-1}$, while the second smallest eigenvalue is simply $\lambda_2 = \omega$.

All our results have been checked against changing parameters in order to use optimal or near optimal set of parameters. The extent of the field domain

---

[1]At LPA there is just one independent function, the potential U, and the normalization condition is imposed explicitly, so there are $\mathcal{S} = N_\rho$ independent variables.

[2]In order to test our procedure, we also secured the convergence of the results on the parameter Δ_0. Additionally, we implemented variations Δ_0 depending on the actual value of the variable being varied finding the same results as for an uniform Δ_0.

considered was also varied, as well as the accuracy with which integrals were calculated.

Appendix G

Non-Renormalization Theorems

In this appendix we discuss redundant vector operators, with an emphasis on conformal invariance. Redundant operators are of the form $(\delta H/\delta\phi(x))\mathcal{O}(x)$ and they typically have short-range correlation functions[1] and, therefore, are often disregarded as uninteresting.

G.1 Redundant Operators and the Sufficient Condition for Conformal Invariance

Let us first stress that redundant operators can be ignored as possible candidates for breaking conformal invariance. On general grounds, a redundant operator, with short-range correlations can be responsible for the breaking of Ward identities of most symmetries. The existence of such an operator would have strong physical consequences because correlation functions for other fields would not display the corresponding invariance. We illustrate this in a very simple case. Consider a model with two scalar fields ϕ_1 and ϕ_2 whose dynamics is given by a general hamiltonian H (or action S) which needs not be $O(2)$-symmetric. If we perform, in the path integral of the partition function, a change of variable $\phi_i \to \phi_i + \theta\epsilon_{ij}\phi_j$ (here ϵ_{ij} is the bidimensional Levi-Civita tensor and θ an infinitesimal angle) which corresponds to an infinitesimal rotation in internal space, we obtain:

$$\int d^d x \left(\epsilon_{ij} J_i \frac{\delta W}{\delta J_j} \right) = \int d^d x \left\langle \epsilon_{ij} \phi_i \frac{\delta H}{\delta \phi_j} \right\rangle, \qquad \text{(G.1)}$$

---

[1]This implies that it is not possible to define their scaling dimension by looking at the power-law behavior of correlation functions at long distances, but their scaling dimension can be define by a stability analysis of the renormalization-group flow around the fixed point.

where J_i is a source for the field ϕ_i. The brackets in the right-hand-side represent an average over the fields with the Boltzmann distribution in presence of sources J_i for the fields ϕ_i. Of course, if the hamiltonian or action is $O(2)$ symmetric, we recover the Ward identity for rotation in internal space. However, for a generic hamiltonian H, the right-hand-side does not vanish and the $O(2)$ Ward Identity is not satisfied. Now, what is of interest for us here is that the right hand side of the previous equation is the average of a redundant operator. The operator $\epsilon_{ij}\phi_i\frac{\delta H}{\delta\phi_j}$ appearing in the right hand side of Eq.(G.1), which only has contact terms in its correlation functions, even if it is redundant, is physically important because it induces a breaking of $O(2)$ invariance, at the level of Ward identities.

To make an analogy with the strategy followed in Chapter 5 to study conformal invariance, suppose we want to prove that a model is invariant under $O(2)$ by searching for possible operators that could appear in the right hand side of Eq.(G.1). Suppose that, for some reason, we can discard the existence of such operators which are not redundant but that we have no control over redundant ones. Then, the previous example shows that we have no way to conclude on the $O(2)$ invariance of the theory. If, instead, we can discard both redundant and non-redundant operators we then conclude that the theory is indeed invariant.[1]

In spite of the previous example, the situation is entirely different in the case of conformal invariance. Assume for the moment that we find a redundant, integrated vector operator of dimension -1. Such an operator would be of the form[2] $\int d^d x (\delta\Gamma_k)/(\delta\phi(x))\mathcal{O}_\mu(x)$ where the operator $\mathcal{O}_\mu$ depends on x only through the field argument (as explained in Chapter 4, an explicit x-dependence would be inconsistent with the translational invariance of the operator Σ_μ). This operator would yield a potential violation of the Ward identity:

$$\int_x (K_\mu^x - 2D_\star^\phi x_\mu)\phi(x)\frac{\delta\Gamma_k}{\delta\phi(x)} - \frac{1}{2}\int_{x,y}\partial_t R_k(|x-y|)(x_\mu + y_\mu)G_k(x;y) = \int_x \frac{\delta\Gamma_k}{\delta\phi(x)}\mathcal{O}_\mu(x).$$
$$(G.2)$$

---

[1]It is often stated in the literature that redundant operators can be reabsorbed by a change of variables and are therefore not physically relevant. This, however, cannot be applied as such when testing whether a Ward identity is valid or not, for this would lead us to the absurd conclusion that a generic theory with two scalar fields can always be made $O(2)$-invariant by reabsorbing the redundant operator appearing in the right hand side of Eq.(G.1) through a field redefinition.

[2]We focus on the Ising case but the same discussion generalizes to other universality classes.

However, the right hand side could actually be reabsorbed in a modification of the conformal transformation of the field ϕ. At odds with the case of internal symmetries, the modified conformal transformation $\phi(x) \to \phi(x) + \epsilon_\mu[(K_\mu^x - 2D_\star^\phi x_\mu)\phi(x) - \mathcal{O}_\mu(x)]$ is non-trivial because the x-independent term $\mathcal{O}_\mu$ can not compensate the usual x-dependent variations and the bracket is therefore non zero.

Moreover, it can be shown that the modified conformal transformation, together with the usual translation, rotation, and scale transformations, satisfy the conformal algebra which means that, indeed, the system is conformal invariant. Indeed, this would be the case since non-redundant vector operator were discarded by assumption and redundant ones with scaling dimension -1 would not lead to a breaking of conformal invariance but, instead, to a modified special conformal transformation in order to make for the *correct* special conformal transformation.

G.2 Exact Scaling Dimensions of Some Redundant Operators

In this section, we show that some redundant operators have simple scaling dimensions. We can choose the microscopic Hamiltonian (or action) to be of the Ginzburg-Landau type:

$$H[\phi] = \int_x \left\{ \frac{1}{2}(\nabla\phi)^2 + \frac{1}{2}r_\Lambda \phi^2 + \frac{u_\Lambda}{4!}\phi^4 \right\}, \tag{G.3}$$

where $\int_x = \int d^d x$. In order to determine the scaling dimension of an operator, we study the evolution of the corresponding coupling under the renormalization-group flow in the vicinity of the fixed point. To this end, we add to the action a part which couples to a vector operator:

$$H_{\mathrm{V}}[\phi] = \int_x \frac{a_\Lambda^\mu}{3!}\phi^3 \partial_\mu \Delta\phi. \tag{G.4}$$

Up to integrations by parts, this operator is the same as the one considered in [128]. Moreover, it has been proved to be the most relevant integrated vector operator invariant under $\mathbb{Z}_2$ symmetry near $d = 4$ [27].

We perform an infinitesimal transformation of the integration variable:

$$\phi \to \phi - a_\Lambda^\mu/u_\Lambda \partial_\mu \Delta\phi \tag{G.5}$$

in the path integral appearing in Eq.(2.33). It is readily found that the quadratic pieces in the Hamiltonian, including the regulating term ΔH_k, are invariant under this transformation. The variation of the quartic part of the Hamiltonian compensates exactly H_V (modulo terms quadratic in a_Λ^μ). We thus find that

$$W_k[J, a_\Lambda^\mu] = W_k[J + \frac{a_\Lambda^\mu}{u_\Lambda}\partial_\mu\Delta J, 0] + \mathcal{O}(a_\Lambda^\mu a_\Lambda^\nu) \tag{G.6}$$

At the level of the effective average action, this relation implies

$$\Gamma_k[\phi, a_\Lambda^\mu] = \Gamma_k[\phi + a_\Lambda^\mu\partial_\mu\Delta\phi, 0] + \mathcal{O}(a_\Lambda^\mu a_\Lambda^\nu). \tag{G.7}$$

This last equation states that the evolution of the effective action with an infinitesimal a_Λ^μ is related to the effective action at vanishing a_Λ^μ, up to a modification of the field. This can be used in the following way. Defining the running coupling constants u_k and a_k^μ as the prefactors of, respectively, $\int_x \frac{1}{4!}\phi^4$ and $\int_x \frac{1}{3!}\phi^3\partial_\mu\Delta\phi$ in Γ_k, we obtain that a_k^μ/u_k is constant along the renormalization group flow. To obtain the scaling dimension of the vector operator, we introduce dimensionless, renormalized quantities (denoted with tilde) as

$$\tilde{x} = kx \tag{G.8}$$

$$\tilde{\phi}(\tilde{x}) = k^{-(d-2)/2}Z_k^{1/2}\phi(x), \tag{G.9}$$

where Z_k scales as $k^{-\eta}$ at the Wilson-Fisher fixed point with η the anomalous dimension. The renormalized coupling constants are thus:

$$\tilde{u}_k = k^{d-4}Z_k^{-2}u_k \tag{G.10}$$

$$\tilde{a}_k^\mu = k^{d-1}Z_k^{-2}a_k^\mu. \tag{G.11}$$

At the critical point, $\tilde{u}$ flows to a fixed point value $u_\star$. Consequently, when $k \to 0$,

$$\tilde{a}_k^\mu \sim a_\Lambda^\mu \frac{u_\star}{u_\Lambda}k^3 \tag{G.12}$$

which shows that the scaling dimension of a^μ is exactly 3.

We can also obtain this same result using another approach that does not rely on the microscopic hamiltonian, see [28]. For $O(N)$ theories, an equivalent exact eigenoperator exist with an associated eigenvalue which again has 3 (or $2n + 1$, if we change the power of the Laplacian). In [27] [see also Eq.(5.18)],

the scaling dimensions of the two vector operators of lowest dimension in an expansion in ϵ was computed and found them to be $3 + \mathcal{O}(\epsilon^2)$ and $3 - 6\epsilon/(N + 8) + \mathcal{O}(\epsilon^2)$. This result is consistent with the non-renormalization theorem proven here (the proof for the $O(N)$ case is obtained by just adding the colour index to the perturbation Eq.(G.5)). Let us stress, however, that in the $O(N)$ model the non renormalization theorem does not constraint the leading vector operator but the next-to-leading, as can be seen already at one-loop level [27] or in the analysis of Chapter 5. For other exact eigenvectors which can be obtained following the same idea see [28].

It was shown in [128] that for the Ising model there exists other redundant operators in $d = 4 - \epsilon$. In fact, all integrated vector operators of dimension up to, and including, 5 are redundant. For several of these, we were not able to determine analytically their scaling dimensions.

Appendix H

One Loop Calculation of Integrated Vector Operators with Canonical Scaling Dimension 5 (Ising Universality Class)

In this appendix we compute the scaling dimensions of all integrated vector operators having scaling dimension up to 5 at $d = 4$. At dimension $d = 4$ the fixed point is Gaussian and the scaling dimension of operators is just the canonical dimension. Fields and derivatives contribute with dimension $[k] = 1$ and there is an overall -4 due to the space integral. Therefore, with operators having scaling dimension up to 5 at $d = 4$ the effective action takes the form:

$$
\Gamma_k[\varphi] = \int_x \left\{ \frac{1}{2}(\nabla \varphi)^2 + \frac{1}{2}r_o\varphi^2 + \frac{u}{4!}\varphi^4 + \frac{a^\mu}{3!}\varphi^3 \partial_\mu \Delta \varphi + \frac{b^\mu}{5!}\varphi^5 \partial_\mu \Delta \varphi \right.
$$
$$
\left. + \frac{F_1^\mu}{3!}\varphi^3 \partial_\mu \Delta^2 \varphi + \frac{F_2^\mu}{2!}\varphi^2 \partial_\mu \Delta \varphi \Delta \varphi + \frac{F_3^\mu}{2!}\varphi^2 \partial_\nu \Delta \varphi \partial_\mu \partial_\nu \varphi \right\}. \tag{H.1}
$$

We could include a term of the form $\varphi^2(\nabla \varphi)^2$, but the reason to avoid this is that we want to compute the flow of $a^\mu, b^\mu, F_1^\mu, F_2^\mu, F_3^\mu$ around the fixed point in dimension $4 - \epsilon$ at order $\mathcal{O}(\epsilon)$, and the $\varphi^2(\nabla \varphi)^2$ term can be shown to be of order $\mathcal{O}(\epsilon^2)$. To compute the flow of $a^\mu, F_1^\mu, F_2^\mu, F_3^\mu$ we consider the exact flow of $\Gamma_k^{(4)}$ at zero field, see Eq.(5.7). The flow of b^μ is obtained from the flow of $\Gamma_k^{(6)}$ at zero field, see Eq.(5.8).

Notice that in $\partial_t R_k(q^2) = -2q^2 q^2 r(\frac{q^2}{k^2})$ the k dependence can be ignored and

we do not consider it from this point forward since it goes away once we take dimensionless variables. We compute the propagator and vertices associated with the previous expansion, which read:

$$G_k(q; \varphi) = \frac{1}{\Gamma_k^{(2)}(q; \varphi) + q^2 r(q^2)}, \qquad \Gamma_k^{(2)}(q; \varphi) = r_o + q^2, \qquad \text{(H.2)}$$

$$\Gamma_k^{(4)}(p_1, p_2, p_3; \varphi) = u - ia^\mu \Theta_{2,\mu} + iF_1^\mu \Xi_{1,\mu}$$
$$+ iF_2^\mu (\Xi_{2,\mu} - \Xi_{1,\mu}) + iF_3^\mu (\Xi_{3,\mu} - \Xi_{1,\mu}) \qquad \text{(H.3)}$$

and

$$\Gamma_k^{(6)}(p_1, p_2, p_3, p_4, p_5; \varphi) = -ib^\mu \Theta_{6,\mu}, \qquad \text{(H.4)}$$

where we introduced the independent momentum structures $\Theta_{2,\mu}$, $\Theta_{6,\mu}$, $\Xi_{1,\mu}$, $\Xi_{2,\mu}$, $\Xi_{3,\mu}$ to shorten notation. Taking $p_4 = -p_1 - p_2 - p_3$ when the sums go up to 4, this structures are defined as:

$$\Theta_2^\mu \equiv \sum_{i=1}^4 p_i^\mu p_i^2, \qquad E \equiv \sum_{i=1}^4 p_i^2,$$

$$\lambda^{\mu\nu} \equiv \sum_{i=1}^4 p_i^\mu p_i^\nu, \qquad \Xi_1^\mu \equiv \sum_{i=1}^4 p_i^\mu p_i^2 p_i^2,$$

$$\Xi_2^\mu \equiv E\Theta_2^\mu, \qquad \Xi_3^\mu \equiv \lambda_\nu^\mu \Theta_2^\nu, \qquad \text{(H.5)}$$

$$\Theta_6^\mu \equiv \sum_{i=1}^6 p_i^\mu p_i^2,$$

where we defined $p_6 = -p_1 - p_2 - p_3 - p_4 - p_5$.

We then project the flow the flows of $\Gamma_k^{(4)}$ and $\Gamma_k^{(6)}$ onto the structures appearing in the vertex functions. When doing this, because of the need to expand propagators in powers of the external momenta, the following momentum integrals appear:

$$L = \int_q \partial_t R_k(q^2) G_k^2(q^2), \qquad I_n = \int_q \partial_t R_k(q^2) G_k^3(q^2) q^{2n},$$

$$J_n = \int_q \partial_t R_k(q^2) G_k^2(q^2) G_k'(q^2) q^{2n}, \qquad K_n = \int_q \partial_t R_k(q^2) G_k^2(q^2) G_k''(q^2) q^{2n}.$$

$$\text{(H.6)}$$

These integrals satisfy the following properties:[1]

$$I_0 + 3J_1 + K_2 = 0, \tag{H.7}$$

$$\int_q h(q^2) q^\mu q^\nu = \frac{\delta^{\mu\nu}}{d} \int_q h(q^2) q^2, \tag{H.8}$$

$$\int_q h(q^2) q^\mu q^\nu q^\rho q^\sigma = \frac{\delta^{\mu\nu}\delta^{\rho\sigma} + \delta^{\mu\rho}\delta^{\nu\sigma} + \delta^{\mu\sigma}\delta^{\nu\rho}}{d(d+2)} \int_q h(q^2) q^2 q^2 \tag{H.9}$$

and

$$\int_q h(q^2) q^{\mu_1} \cdots q^{\mu_n} = 0 \qquad \text{if n is odd.} \tag{H.10}$$

The computation of the flow equations, although straightforward, is rather extensive and not very enlightening. Therefore, we just introduce the dimensionless variables

$$\begin{aligned} u = k^{4-d}\tilde{u}, \qquad a^\mu = k^{1-d}\tilde{a}^\mu, \qquad b^\mu = k^{3-2d}\tilde{b}^\mu, \\ F_1^\mu = k^{-1-d}\tilde{F}_1^\mu, \qquad F_2^\mu = k^{-1-d}\tilde{F}_2^\mu, \qquad F_3^\mu = k^{-1-d}\tilde{F}_3^\mu, \end{aligned} \tag{H.11}$$

and write down the final result. The fixed point is just $\tilde{u} = \epsilon/3I_0$ and all vector couplings set to zero. Therefore, the flow equations at order $\mathcal{O}(\epsilon)$ for the dimensionless vector couplings, around the fixed point, read:

$$\begin{aligned} \partial_t \tilde{a}^\mu &= 3\tilde{a}^\mu - \frac{L}{2}\tilde{b}^\mu - \epsilon\frac{I_1}{I_0}\tilde{F}_2^\mu + \epsilon\frac{I_1}{2I_0}\tilde{F}_2^\mu, \\ \partial_t \tilde{b}^\mu &= \left(5 + \epsilon\frac{4}{3}\right)\tilde{b}^\mu, \\ \partial_t \tilde{F}_1^\mu &= -\epsilon\left(\frac{J_0}{3I_0} - \frac{K_1}{6I_0}\right)\tilde{a}^\mu + 5\tilde{F}_1^\mu + \frac{\epsilon}{6}\tilde{F}_3^\mu, \\ \partial_t \tilde{F}_2^\mu &= -\epsilon\left(\frac{J_0}{3I_0} - \frac{K_1}{6I_0}\right)\tilde{a}^\mu + \left(5 - \epsilon\frac{2}{3}\right)\tilde{F}_2^\mu - \frac{\epsilon}{18}\tilde{F}_3^\mu, \\ \partial_t \tilde{F}_3^\mu &= \left(5 - \epsilon\frac{4}{9}\right)\tilde{F}_3^\mu. \end{aligned} \tag{H.12}$$

---

[1] The first of these properties only holds when the parameter r_o is taken to be 0. This can be done since it can be shown that this parameter is of order $\mathcal{O}(\epsilon)$.

The stability matrix for the vector couplings sector at the fixed Λ^* is simply:

$$\begin{pmatrix} 3 & -\frac{L}{2} & 0 & -\epsilon\frac{I_1}{I_0} & \epsilon\frac{I_1}{2I_0} \\ 0 & 5+\epsilon\frac{4}{3} & 0 & 0 & 0 \\ -\epsilon\frac{J_0}{3I_0}-\epsilon\frac{K_1}{6I_0} & 0 & 5 & 0 & \epsilon\frac{1}{6} \\ -\epsilon\frac{J_0}{3I_0}-\epsilon\frac{K_1}{6I_0} & 0 & 0 & 5-\epsilon\frac{2}{3} & -\epsilon\frac{1}{18} \\ 0 & 0 & 0 & 0 & 5-\epsilon\frac{4}{9} \end{pmatrix}. \qquad (H.13)$$

When computing the eigenvalues, at order $\mathcal{O}(\epsilon)$, of Λ^*, we find that these are exactly the diagonal elements. This can easily be recovered in the following way. Developing the determinant in the fifth row, then in the third column and finally in its second row we arrive at a 2×2 matrix whose off-diagonal elements are proportional to ϵ. This implies that the corrections coming from the off-diagonal terms are of order $\mathcal{O}(\epsilon^2)$ and, consequently, the remaining eigenvalues are just the diagonal elements. In summary, at order $\mathcal{O}(\epsilon)$, we have:

$$\lambda_1 = 3, \quad \lambda_2 = 5 - \epsilon\frac{2}{3}, \quad \lambda_3 = 5 - \epsilon\frac{4}{9}, \quad \lambda_4 = 5, \quad \lambda_5 = 5 + \epsilon\frac{4}{3}. \qquad (H.14)$$

The second eigenvalue found in the DE for the $O(1)$ model, see Fig.5.6, has the exact behaviour close to $d = 4$ given by the correction associated with the perturbation b^μ which scales with λ_5 (we do not show this comparison in Fig.5.6). As mentioned in Appendix G, these eigenvalues are not candidates for breaking conformal invariance because all of them are redundant. As stated in [128], the first correction of a non-redundant operator is even higher at $d = 4$. than the ones considered. In any case, this computation shows that the overall behaviour of the scaling dimension of vector operators around dimension $d = 4$, when setting $\epsilon = 1$ (i.e. $d = 3$) is far from the value -1 (this is, the coefficient of the ϵ correction is of order 1). Consequently, conformal invariance is, almost, guaranteed at all dimensions.